**Université catholique de Louvain**

Faculté des Sciences
Institute of Condensed Matter and Nanosciences
Molecules, Solids and Reactivity
Unité de Chimie organique et médicinale
Professeur J. Marchand-Brynaert

# Novel large ring bridged azetidinones: design, synthesis and biochemical evaluation against Penicillin Binding Proteins

*Dissertation présentée en vue de l'obtention du grade de docteur en sciences*

**Aline SLIWA**

Louvain-la-Neuve
2011

## JURY COMPOSITION

**Professeur Jean-François GOHY (President of jury)**
Université catholique de Louvain

**Docteur Georges DIVE**
Université de Liège

**Professeur Norbert DE KIMPE**
Universiteit Gent

**Professeur Patrice SOUMILLION**
Université catholique de Louvain

**Docteur Raphaël ROBIETTE**
Université catholique de Louvain

**Professeur Jacqueline MARCHAND-BRYNAERT (Promoter)**
Université catholique de Louvain

*Je tiens tout d'abord à exprimer ma reconnaissance à mon promoteur, le Prof. Jacqueline Marchand-Brynaert pour son accueil dans son laboratoire et pour m'avoir permis de réaliser mon doctorat dans son équipe. Merci pour sa confiance, sa disponibilité et pour la liberté accordée dans la gestion de mon travail.*

*Je tiens également à remercier le Dr. Georges Dive pour le travail réalisé, ses réponses à mes innombrables questions sur le domaine de la chimie computationnelle qui m'était peu familier, ainsi qu'à son soutien.*

*Mes remerciements s'adressent également aux membres du jury qui ont accepté de consacrer de leur temps précieux pour juger ce travail.*

*Merci à Chantal, pour son aide lors des divers problèmes administratifs et pour son éternelle bonne humeur. Merci à Sabrina pour sa gestion du laboratoire, ce qui nous permet de travailler dans de bonnes conditions.*

*Du côté des synthèses, je remercie Delphine et Chafia pour leur aide dans la synthèse de composés et intermédiaires lors de leur stage qui m'ont permis "d'apprendre à apprendre".*

*Ces remerciements s'adressent également à tous les membres du labo et du bâtiment Lavoisier, ceux qui m'ont gentiment accueilli, ont partagé mon bureau, ont supporté ma musique au labo, les nouveaux venus, avec qui j'ai passé d'agréables moments et eu de nombreux fous rires, que ce soit au labo ou en dehors: Ben, Catherine, Camille, Cécile, Cédric, Elise, Elodie, Emilie, François, Fré, Fred, Jean-Christophe, Joséphine, Julien, Nicolas, Peter, Van, Vincent, Xavier,… et ceux que j'ai forcément oublié de mentionner. Un merci particulier à Alex et Martin, votre chocolat vous attend!*

*Enfin merci à ma famille et mes parents pour leur soutien indéfectible.*

Since the discovery of Penicillin, bacteria counteract the action of antibiotics leading to a worrisome situation about antibiotics efficiency. We focused our research on the synthesis of non-traditional 1,3-bridged β-lactam embedded into macrocycles as potential inhibitors of Penicillin Binding Proteins (PBPs). As the key-step of the macrocyclization, we have selected the Ring-Closing Metathesis (RCM) reaction. 12- to 22-Membered bicyclic β-lactams were successfully synthesized by this strategy. We also unexpectedly observed *bis*-2-oxoazetidinyl macrocycles arising from a dimerization reaction under RCM conditions. Compounds from this last family revealed to be good inhibitors of the problematic methicillin-resistant *Staphylococcus aureus* (MRSA). In order to explain the biological results, the 3D structures of all the macrocycles were studied by quantum chemistry calculations, and docking experiments were also performed. Our results highlighted that the activity of the compounds is most probably related to their conformational adaptability.

The activity of our 1,3-bridged macrocycles suggests a way to design novel β-lactam antibiotics with a planar amide bond, and without a carboxylic group, a model quite different from the previous model of reactivity of "the magical drug".

| | |
|---|---|
| 6-APA | 6-aminopenicillanic acid |
| 7-ACA | 7-aminocephalosporanic acid |
| a.u. | atomic units |
| ACN | acetonitrile |
| APCI | atmospheric pressure chemical ionization |
| ASPRE | active-site serine penicillin recognizing enzymes |
| Bn | benzyl |
| Boc | *N-tert*-butoxycarbonyl |
| c.c. | cubic centimetre |
| CA | community-acquired |
| calcd. | calculated |
| CAN | ceric ammonium nitrate |
| Cbz | carbobenzyloxy |
| CCE | conformational control element |
| CI | chemical ionization |
| Cmpd | compound |
| DBU | 1,8-Diazabicyclo[5.4.0]undec-7-ene |
| DCC | dicyclohexylcarbodiimide |
| DCE | 1,2-dichloroethane |
| DCM | dichloromethane |
| DCU | *N*,*N*′-dicyclohexylurea |
| DEAD | diethyl azodicarboxylate |
| DIEA | *N*-*N*'-diisopropylethylamine |
| DMAP | 4-dimethylaminopyridine |
| DMF | *N*,*N*-dimethylformamide |
| DMSO | dimethyl sulfoxide |
| DOSY | diffusion ordered spectroscopy |
| DTNB | 5-(3-carboxy-4-nitrophenyl)disulfanyl-2-nitrobenzoic acid |
| EDCI | *N*-ethyl-*N*′-(3-dimethylaminopropyl)carbodiimide hydrochloride |
| eq | equivalent |
| ESI | electrospray ionization |
| Et | ethyl |
| EtOAc | ethyl acetate |
| GCSTESL | gradient compensated stimulated echo pulse sequence |
| GI | first generation Grubbs' catalyst |
| GII | second generation Grubbs' catalyst |
| gm., g | grams |
| h | hour |
| HA | hospital-acquired |
| HGI | first generation of Hoveyda-Grubbs' catalyst |

| | |
|---|---|
| HGII | second generation of Hoveyda-Grubbs' catalyst |
| HH | head-head |
| HMDS | hexamethyldisilazane |
| HMM | high molecular mass |
| HRMS | high resolution mass spectrometry |
| HT | head-tail |
| Hz | hertz |
| IR | infrared |
| KHMDS | potassium hexamethyldisilazide |
| LiHMDS | lithium hexamethyldisilazide |
| LMM | low molecular mass |
| m.p. | melting point |
| M.W. | molecular weight |
| Me | methyl |
| MRSA | methicillin-resistant *Staphylococcus aureus* |
| MS | mass spectrometry |
| NAG | *N*-acetylglucosamine acid |
| NAM | *N*-acetylmuramic acid |
| *n*-BuLi | *n*-butyllithium |
| NHC | N-heterocyclic carbenes |
| NMM | *N*-methylmorpholine |
| NMR | nuclear magnetic resonance |
| P | pressure |
| PBP | penicillin binding protein |
| PEG | polyethylene glycol |
| PIDA | iodobenzene diacetate |
| ppm | parts per million |
| PyBop | (benzotriazol-1-yloxy)tripyrrolidinophosphonium hexafluorophosphate |
| quant. | quantitative |
| RA | residual activity |
| RCM | ring closing metathesis |
| $R_f$ | retention factor |
| rt | room temperature |
| S2d | *N*-benzoyl-D-alanyl-thioglycolate |
| SDS-PAGE | sodium dodecyl sulfate polyacrylamide gel electrophoresis |
| sp. | species |
| subsp. | subspecies |
| TBDMS, TBS | *tert*-butyldimethylsilyl |
| t-Bu | *tert*-butyl |
| TEA | triethylamine |

| | |
|---|---|
| TFA | trifluoroacetic acid |
| THF | tetrahydrofurane |
| TLC | thin layer chromatography |
| Triton X-100 | 4-(1,1,3,3-tetramethylbutyl)phenyl-polyethylene glycol |
| TS | transition state |
| US | united states |
| WHO | world health organization |

## Table of contents


Chapter 1 - From dream to reality ..... 19

1. Assessment ..... 21

2. Beginning of the β-lactam era ..... 24

3. Major β-lactam drug classes ..... 27

3.1. Penicillins (penams) ..... 28

3.2. Cephalosporins (cephems) ..... 29

3.3. Monobactams ..... 29

3.4. Carbapenems ..... 30

4. Mode of action of β-lactam antibiotics ..... 31

4.1. History ..... 31

4.2. Target: DD-transpeptidases ..... 32

4.3. DD-transpeptidase: Serine peptidase ..... 35

5. Resistance ..... 42

5.1. Reduced outer membrane permeability and efflux pump ..... 42

5.2. Production of β-lactamases ..... 43

5.3. Production of resistant PBPs ..... 44

6. Conclusion ..... 49

7. References and notes ..... 51

Chapter 2 - Objectives and strategies ..... 55

1. Objectives ..... 57

2. Synthetic strategy ..... 60

3. Biochemical and theoretical reactivities ..... 61

4. Contents of the manuscript ..... 62

5. References and notes ..... 64

Chapter 3 - First synthetic approaches ..... 67

1. Chirons ..... 69

1.1. Structure of the chirons ..... 69

1.2. Boc chirons ..... 70

1.3. Cbz chirons ..... 73
2. Bis-acylated compounds ..... 76
2.1. From chiron **3** ..... 76
2.2. From chiron **2** ..... 77
2.3. From chiron **1** ..... 78
3. First RCM ..... 79
4. Chirons conclusions ..... 80
5. Experimental Section ..... 80
6. References and notes ..... 88
Chapter 4 - Cyclodimerization by Ring-Closing Metathesis ..... 91
1. Introduction ..... 94
2. Results and discussion ..... 97
2.1. Synthesis ..... 97
2.2. Computational chemistry ..... 103
2.3. Inhibition of R39 D,D-peptidase ..... 113
3. Conclusion ..... 115
4. Experimental Section ..... 116
4.1. General considerations ..... 116
4.2. Synthesis of compounds **6**, **7** and **8** ..... 117
4.3. Synthesis of precursors **9**, **10**, **11**, **12** and **13** ..... 120
4.4. General procedure for RCM ..... 128
4.5. General procedure for hydrogenation ..... 130
5. Acknowledgements ..... 133
6. Supplementary data ..... 134
6.1. Screening experiments with R39 ..... 134
6.2. Generation of conformers ..... 136
6.3. Grubbs adducts ..... 138
7. Addendum on methyl family ..... 139
8. Appendix on the catalyst used for metathesis ..... 143
9. References and notes ..... 149

Chapter 5 - DOSY-NMR analysis of RCM products from β-lactam precursors .... 155

1. Introduction .... 158

2. Results and discussion .... 161

3. Experimental .... 165

4. Conclusion .... 166

5. Acknowledgements .... 167

6. Supplementary material .... 167

6.1. $^{1}$H NMR chemical shift assignment .... 168

6.2. Region of the $^{1}$H DOSY-NMR spectrum of a 1:1 mixture of **HM$_{Boc2}$** and **HD$_{Boc2}$** with resolution enhancement .... 171

6.3. Region of the $^{1}$H DOSY-NMR spectrum of a 1:1 mixture of **M$_{Boc2}$** and **D$_{Boc2}$** .... 172

6.4. Region of the $^{1}$H DOSY-NMR spectrum of a 5:95 mixture of **HM$_{Boc2}$** and **HD$_{Boc2}$** .... 173

7. References and notes .... 174

Chapter 6 - Inhibition of resistant PBPs by bis-2-oxoazetidinyl macrocycles .... 177

1. Introduction .... 181

2. Results .... 183

2.1. Synthesis .... 183

2.2. Inhibition of R39, PBP2a and PBP5 .... 187

2.3. Computational chemistry .... 190

2.4. Docking .... 193

2.5. Reactivity .... 195

3. Discussion .... 200

4. Conclusion .... 201

5. Acknowledgements .... 203

6. Supplementary Information .... 203

6.1. Experimental Section .... 204

6.2. Absolute energies .... 221

6.3. Stereo view of compound **5e** in the model of R39 active site .... 224

6.4. Molecule **5f** docked as an acyl-enzyme complex in PBP2a cavity ..... 225
6.5. Experiments of temperature coefficients for amide protons ..... 227
6.6. Figures of dimers **4** and **5** ..... 228
7. References and notes ..... 230
Chapter 7 - Bis-alkyl derivatives ..... 233
1. Introduction ..... 237
2. Results and Discussion ..... 240
2.1. Synthesis ..... 240
2.2. Computational chemistry: Conformational study - heat of formation ..... 245
2.3. Reactivity versus serine enzyme models ..... 248
2.4. Inhibition of R39, PBP2a and PBP5 ..... 250
2.5. Building of the models ..... 252
3. Conclusion ..... 257
4. Experimental Section ..... 258
5. Acknowledgements ..... 277
6. Supporting Information ..... 278
6.1. Stereo view of the third model with Pen ..... 279
6.2. Pen in the third model with hydrogen atoms and hydrogen bonds ..... 280
6.3. Absolute energies of the precursors, unsaturated bicycles and saturated bicycles in the selected conformations ..... 281
6.4. Absolute energies of the transition state structures in the simple model (Figure 5) computed for the unsaturated bicycles and saturated bicycles in the selected conformations ..... 284
6.5. $^{13}$C NMR spectra of compound **10d** recorded at 125 MHz in 1,1,2,2-tetrachloroethane-$d_2$ at different temperatures ..... 286
6.6. $^{13}$C NMR spectra of compound **11d** recorded at 125 MHz in 1,1,2,2-tetrachloroethane-$d_2$ at different temperatures ..... 287
7. References and notes ..... 288
Chapter 8 - Attempts to synthesize mixed precursors ..... 291
1. Introduction ..... 293
2. N(1) position acylated and C(3)-N position alkylated ..... 294

3. N(1) position protected ..... 296
4. N(1) position silylated ..... 299
5. N(1) position alkylated ..... 301
6. Conclusion ..... 302
7. Experimental Section ..... 302
8. References and notes ..... 309
Chapter 9 - Conclusions and perspectives ..... 311
1. Conclusions ..... 313
2. Perspectives ..... 317
2.1. Cyclodimers ..... 317
2.2. Change of the side chain ..... 319
2.3. Click cyclizations ..... 321
2.4. Non β-lactam ring ..... 322
3. References and notes ..... 324
Appendix - Computational Chemistry ..... 327

# *Chapter 1 - From dream to reality*

## 1. Assessment

In 2010, the World Health Organization[1] reported that about 440 000 new cases of multidrug resistant-tuberculosis were detected, leading at least to 150 000 deaths. 69 countries had reported multi-drug resistance to tuberculosis. Each year 25 000 persons in Europe die from bacteria resistant to known antibiotics. The most important cause of antibiotic-resistant healthcare-associated infections worldwide is the methicillin-resistant *Staphylococcus aureus* (MRSA). In 2009, the European Centre for Disease Prevention and Control,[2] in its surveillance reports on antimicrobial resistance, detailed that for nine countries in Europe, 25 to 50% of isolated *Staphylococcus aureus* were resistant to methicillin (**Figure 1**).

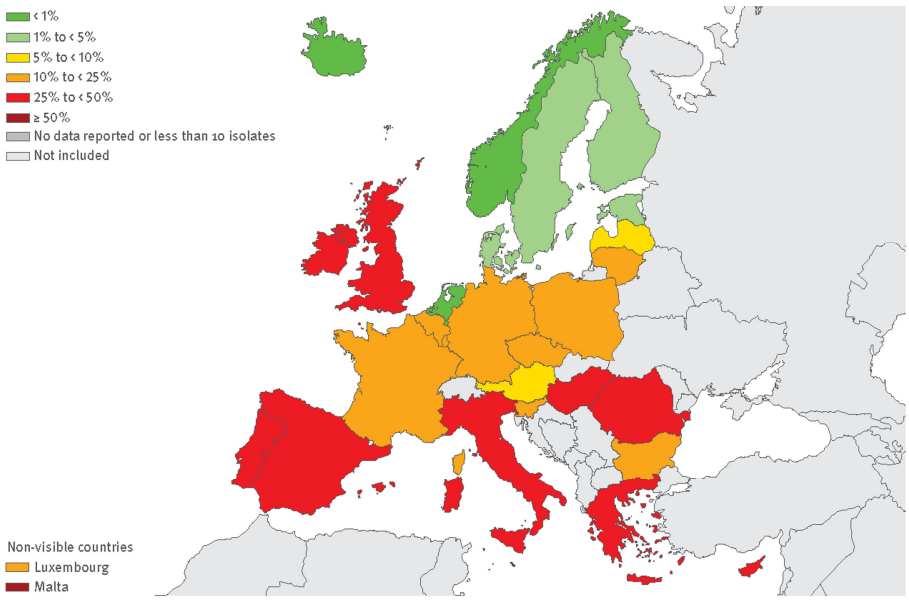


**Figure 1**. *Staphylococcus aureus*: proportion of invasive isolates resistant to methicillin (MRSA) in 2009.[2]

In 2009, was reported a new enzyme named New Delhi metallo-beta-lactamase[3] which renders bacteria resistant to the majority of β-lactam antibiotics, even to those of last generation.

These are few examples of the increasing resistance of bacteria over the recent years that lead to the worrisome situation about antibiotics.

When antibiotics were introduced in modern medicine, they were considered as magic drugs enabling to save millions of humans from potentially fatal infectious diseases like syphilis, gonorrhea, leprosy, and tuberculosis. Soon after the first steps of benzylpenicillin as a chemotherapeutic agent, bacterial resistance was reported.[4] Unfortunately, the significance of this phenomenon was not fully appreciated and since their discovery, antibiotics were used intensely and often misused, what led to the inexorable consequence of bacterial resistance. Indeed, bacteria are microorganisms with diversity and adaptability which can adjust to their environment for their survival. The antibiotic pressure, as it is called, explained the phenomenon of emergence and dispersion of mechanisms of resistance, leading to increasing selection of resistant bacteria due to the exposure to antibiotics. It consequently led to a decreasing activity of the antibiotics collection.

The following years after the discovery of benzylpenicillin, pharmaceutical industries conducted many researches in the field of antibiotics and put on the market a great number of drugs which enabled, for a time, to compete with bacteria resistance.

Drug resistance is a natural biological process, consequently the question of resistance to new generations of antibiotics is just a question of time. Humans, by the inappropriate use of antibiotics (underuse, overuse or misuse) cause a faster emergence and spread of drug-resistant pathogens.

Meanwhile, pharmaceutical industries have partially given up the fight against bacteria to work on more lucrative diseases. Nowadays the development of new antibiotics by pharmaceutical industries reaches practically to its end. If nothing is done to reverse this worrying situation, we could return to the pre-antibiotic era where many common infections led to death.

The urgency of an action to preserve the miracle-drugs was focused by the World Health Organization (WHO) by dedicating the World Health Day 2011 to antimicrobial resistance and its global spread. WHO points out the need of rational drug uses and regulations, but as it was explained, the appearance of resistance is just a matter of time. Hence even if a better use of antibiotics would extend their life expectancy, research must be carried out to find new antimicrobial drugs for the future.

Since the introduction of β-lactams as antibiotics, other structurally different classes of antibiotics were introduced as therapeutic agents.

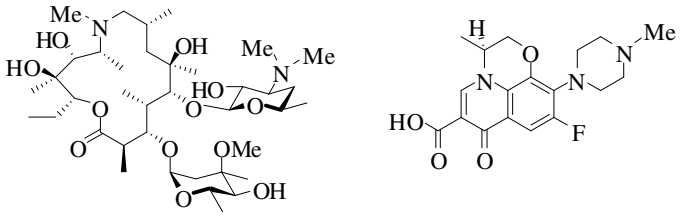


Azithromycin Levofloxacin

**Figure 2**. Structures of azithromycin and levofloxacin.

Macrolides and fluoroquinolones are the two most prescribed antibacterial agents amongst the non-β-lactam antibiotics; in **Figure 2** are presented the most sold macrolide and fluoroquinolone, respectively,

azithromycin and levofloxacin,[5] but penicillins still remain the most prescribed therapeutic class amongst antibiotics in 2010 in the United States.[6]

The focus will be done on β-lactam drugs: the discovery and rapid development of penicillin as a magical drug, the mode of action of this class of antibiotics, the startling reality of resistance to β-lactam antibiotics and some clues to develop new antibiotics for the forthcoming years.

## 2. Beginning of the β-lactam era

In his lecture, at University of Lille in December 1854, Louis Pasteur said: « In the fields of observation chance favours only the prepared mind. » This is this kind of chance that had benefited Alexander Fleming[7] and in extension which allowed the birth of the antibiotic era. Alexander Fleming described by these words[8] the discovery he made in the early September of 1928 in his laboratory of St. Mary's Hospital in London:

« While working with staphylococcus variants a number of culture-plates were set aside on the laboratory bench and examined from time to time. In the examinations these plates were necessarily exposed to the air and they became contaminated with various micro-organisms. It was noticed that around a large colony of a contaminating mould the staphylococcus colonies became transparent and were obviously undergoing lysis.

Subcultures of this mould were made and experiments conducted with a view to ascertaining something of the properties of the bacteriolytic substance which had evidently been formed in the mould culture and which had diffused into the surrounding medium. It was found that broth in which the mould had been grown at room temperature for one or two weeks had

acquired marked inhibitory, bactericidal and bacteriolytic properties to many of the more common pathogenic bacteria. »

Fleming gave to the bacteriolytic substance the name of "penicillin", which exactly corresponds to the filtrates of the broth culture of its contaminating mould, *Penicillium notatum* (which was wrongly attributed firstly to be *Penicillium rubrum*). In this article, Fleming has described the first step of "penicillin" as a therapeutic agent by evaluating the toxicity of "penicillin":

« The toxicity to animals of powerfully antibacterial mould broth filtrates appears to be very low. Twenty c.c. injected intravenously into a rabbit were not more toxic than the same quantity of broth. Half a c.c. injected intraperitoneally into a mouse weighing about 20 gm. induced no toxic symptoms. Constant irrigation of large infected surfaces in man was not accompanied by any toxic symptoms, while irrigation of the human conjunctiva every hour for a day had no irritant effect.

*In vitro* penicillin which completely inhibits the growth of staphylococci in a dilution of 1 in 600 does not interfere with leucocytic function to a greater extent than does ordinary broth. »

In this article, for the first time "penicillin" has been mentioned for a possible use in the treatment of bacterial infections. Alexander Fleming, as a bacteriologist, has found a more direct and useful application for "penicillin" by allowing the isolation on culture plates of Pfeiffer's bacillus of influenza (*Haemophilus influenzae*), by inhibiting the growth of unwanted bacteria present in culture plates. Fleming has essentially promoted "penicillin" for its use in the isolation of *Bacillus Influenzae*. In fact, at this time, Pfeiffer's bacillus was of great interest, because it was (wrongly) attributed to be the

cause of the pandemic influenza of 1918-1919, which was one of the deadliest epidemics in the world with between 50 to 100 millions dead.[9] Fleming has sent to many bacteriologists, who asked him, samples of his mould to use it as a reactant of laboratory for the isolation of Pfeiffer's bacillus. Thanks to this useful direct application of "penicillin", Fleming has preserved what revealed to be a rare variation of *Penicillium notatum*.

The second step of "penicillin" as a therapeutic agent started when Howard Walter Florey and Ernst Chain decided to investigate natural antibacterial substances from mould or bacteria. Screening the literature, they were interested by the substance discovered ten years earlier by Fleming and decided to investigate "penicillin". Florey's predecessor in the chair of pathology at the University of Oxford possessed a subculture of Fleming's mould, so the work could rapidly start. They produced, purified and tested "penicillin" as a chemotherapeutic agent on mice, rats and cats. They reported in their article of August 1940[10] the successful use of "penicillin" as a curative treatment for mice infected with *Streptococcus pyogenes*, *Staphylococcus aureus* and *Clostridium septique*. One year later, therapeutic trials on humans began and the results have been published on August 1941[11] as reported:

« Penicillin was given intravenously to five patients with staphylococcal and streptococcal infections and by mouth to one baby with a persistent staphylococcal urinary infection. It was also applied locally to four cases of eye infection. In all these cases a favourable therapeutic response was obtained. »

These first therapeutic trials on humans have been achieved only on few patients, due to the difficulty to produce "penicillin" in large quantities.

To pursue the therapeutic trials on more patients, Florey needed "penicillin" to be produced in industrial quantities. But he had to go in the United States to find a real interest for his results, enough interest to finance the mass production of the "penicillin". Actually, several pharmaceutical firms, *i.e.* Merck, Pfizer, Squibb and Lederle, and even the US government decided to start the mass production of "penicillin". In their research they found another *Penicillium* strain, *Penicillium chrysogenum*, which produced more quantity of "penicillin". They used this strain for the scaling-up. The United States, engaged in the World War II in December 1941, understood the great utility of "penicillin" in this period of trouble and its production became of national interest. Consequently, they never sent any sample to Florey, but he was very perseverant and managed to produce a quite important stock of "penicillin". Clinical trials on large scale[12] have started on both side of the ocean. The bulldozer "penicillin" was going on.

## 3. Major β-lactam drug classes

Since the discovery of "penicillin" made by Fleming, and more important its application by Florey as therapeutic agent, the search of bacteriolytic substances from natural sources has been deeply explored. A variety of structures of β-lactam antibiotics was found. Through the years, the semi-synthesis and synthesis of analogues of the natural compounds which expressed bacteriolytic properties led to an extended panel of β-lactam agents. Here are only presented the four major β-lactam drug classes with their core structure. For a long time, the research on β-lactam antibiotics was based on analogues of old compounds and it is still a strategy used to enhance the activity of drugs against multidrug resistant bacteria.

### 3.1. Penicillins (penams)

"Penicillin", as named by Fleming for the bacteriolytic substance corresponds to the filtrates of the broth culture of its contaminating mould. Few years were necessary from this discovery to isolate the active compound and even few years to determine its structure. The debate about the possible structure of penicillin ended in 1949 with its X-ray analysis.[13] The penicillin used by Florey in England, from *Penicillium notatum*, was Penicillin F and the penicillin used in the United-States, from *Penicillium chrysogenum*, revealed to be Penicillin G (**Figure 3**). Penams possess a bicyclic skeleton including a β-lactam ring fused with a thiazolidine ring.

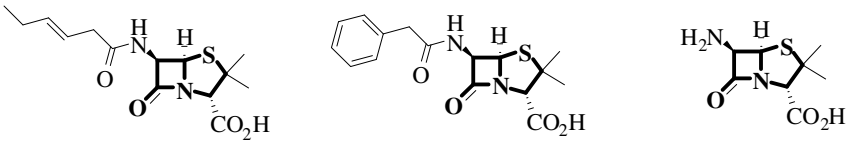


**Figure 3**. Structures of penicillins F and G and 6-APA.

In 1957, John C. Sheehan, working on the total synthesis of penicillin, isolated an intermediate of the biosynthesis of penicillin, the 6-aminopenicillanic acid (6-APA)[14] (**Figure 3**). This substance revealed to be a key compound since it allowed the semi-synthesis of a lot of compounds by adding different side chains on the 6-amino function. A variety of compounds was developed and put on the market the following years thanks to this intermediate.

### 3.2. Cephalosporins (cephems)

In 1948, from a sewer in Sardinia, Giuseppe Brotzu has isolated "cephalosporin"[15] from cultures of *Cephalosporium acremonium*. He observed that the substance produced by these cultures was active against *Salmonella typhi*, a bacterium responsible of typhoid fewer. The active compound was isolated[16] in 1956 and its structure[17] was elucidated in 1961 by Guy G. F. Newton and Edward P. Abraham (**Figure 4**).

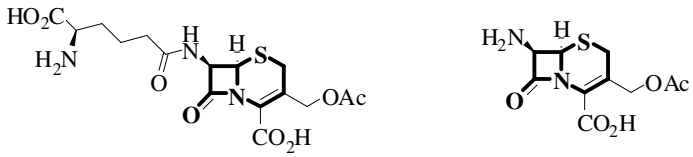


Cephalosporin C 7-ACA

**Figure 4**. Structures of cephalosporin C and 7-ACA.

Like penicillins, cephalosporins possess a β-lactam ring, but instead of being fused with a thiazolidine ring, it is fused with a dihydrothiazine ring. As for penicillin with 6-APA, the isolation of the intermediate 7-ACA, 7-aminocephalosporanic acid (**Figure 4**) allowed the development of many kinds of semi synthetic drugs.

### 3.3. Monobactams

Contrary to penicillins, monobactams are not composed of a bicyclic skeleton, they only possess a β-lactam ring. The first discovered monobactam was Nocardicin A[18] (**Figure 5**) from the fermentation broth of *Nocardia uniformis* subsp. *tsuyamenensi* in 1976. Five years later, another

monobactam was discovered from bacterial origin: Sulfazecin[19] (**Figure 5**) from *Pseudomonas acidophila*.

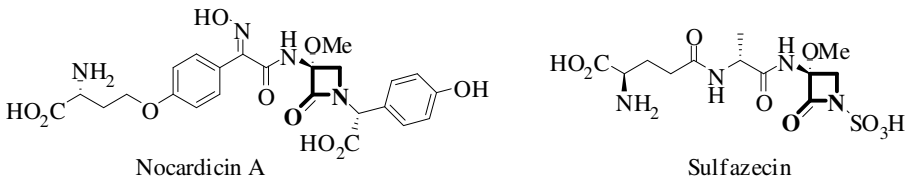


Nocardicin A Sulfazecin

**Figure 5**. Structures of nocardicin A and sulfazecin.

Research on this class of β-lactam antibiotics enabled the commercialization of a few drugs.

### 3.4. Carbapenems

Thienamycin (**Figure 6**), the first compound of the carbapenems class was discovered from a culture broth from the soil bacteria *Streptomyces cattleya* in 1976. The structure of carbapenems is very similar to penicillins: both possess a bicyclic skeleton including a β-lactam ring fused with a 5-membered ring, but instead of a thiazolidine ring for the penicillin, a pyrroline is present in carbapenems.

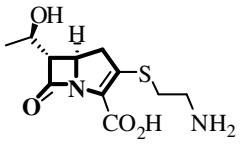


Thienamycin

**Figure 6**. Structure of thienamycin.

Due to the chemical instability of thienamycin, this substance was not employed for clinical treatment and more stable derivatives were synthesized.

## 4. Mode of action of β-lactam antibiotics

### 4.1. History

A clue to the mode of action of β-lactam antibiotics was given by the fact that the discovery of "penicillin" could not be observed as exactly described by Fleming.[20] Several researchers trying to reproduce "the discovery" reported a failure of their attempts: the mould added on *staphylococcus* did not grow, nor affect the *staphylococcus*. They found that the *staphylococcus* colonies underwent lysis only if the mould was grown previously. Penicillin does not kill adult bacteria, and as we will see later, penicillin is able to interfere in the process of growth of bacteria.

The best hypothesis on the discovery of "penicillin" is given by R. Hare[20]: the culture plates of *staphylococcus* were not incubated (voluntarily or not) and then Fleming has stacked culture plates at the edge of his bench before his departure on holidays. The top culture plate was contaminated by a mould and then it is the records of the Meteorological Office of London that could confirm the Hare's hypothesis. In a first period, the temperature was low enough for allowing the mould to grow; then the temperature rose up, enough to permit *staphylococcus* slowly growing to form colonies and afford the unexpected culture-plate observed by Fleming after he came back from holidays.

### 4.2. Target: DD-transpeptidases

The targets of β-lactam antibiotics are DD-transpeptidases, which are serine enzymes involved in the bacteria cell-wall biosynthesis. Because they are the targets of the penicillins family, these DD-transpeptidases are also called PBPs (Penicillin Binding Proteins).[21]

Both types of bacteria, gram-positive and gram-negative, possess in their cell wall a peptidoglycan layer, the difference being that in gram-negative, the peptidoglycan layer is much thinner than in gram-positive bacteria. This peptidoglycan layer confers to the cell wall the mechanical strength necessary to protect bacteria against osmotic pressure variations. The peptidoglycan units are composed of *N*-acetylglucosamine alternating with *N*-acetylmuramic acid attached to a pentapeptide chain. This pentapeptide chain is different for each bacterial strain, but it is always terminated by a D-Ala-D-Ala motif. The cross-linking of the peptidoglycan, by forming a peptide bond between two pentapeptide chains from different peptidoglycan strands, is catalyzed by the DD-transpeptidases. In **Scheme 1** is represented the cross-linking of peptidoglycan strands by a DD-transpeptidase. *N*-acetylglucosamine and *N*-acetylmuramic acid are respectively termed as NAG and NAM. The pentapeptide chain represented is the one of *Staphylococcus aureus*. In the mechanism of cross-linking, the active serine of the DD-transpeptidase attacks the carbonyl of the penultimate D-Ala of one peptidoglycan strand, resulting in the formation of an acyl-enzyme complex and the release of the terminal D-Ala amino acid. Then the terminal free amine moiety of the L-Lys-$(Gly)_5$ from the pentapeptide chain of another peptidoglycan strand attacks the acyl-enzyme complex, releasing the DD-transpeptidase and creating a peptide bond

between the two stem peptides and therefore creating a cross-linking between two strands of peptidoglycan.[21]

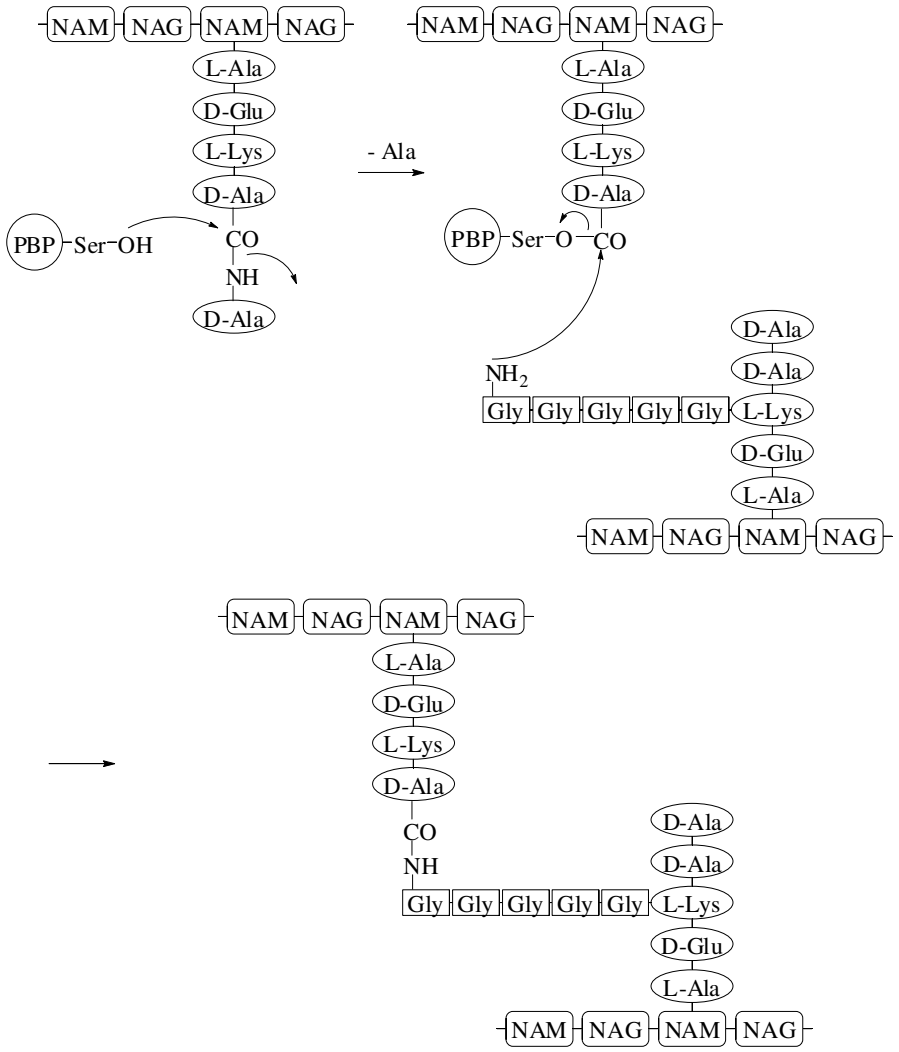


**Scheme 1**. Cross-linking of the peptidoglycan of *S. aureus* by transpeptidases.

The β-lactam antibiotic, for example Penicillin G, by mimicking the D-Ala-D-Ala moiety (**Figure 7)** present in the pentapeptide chain, is able to react with DD-transpeptidases.

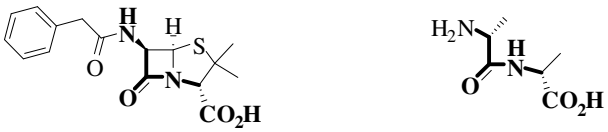


**Figure 7.** Comparison of penicillin G and D-Ala-D-Ala moiety.

A β-lactam antibiotic acts as a suicide substrate by forming a stable acyl-enzyme complex with the DD-transpeptidases (**Scheme 2**).

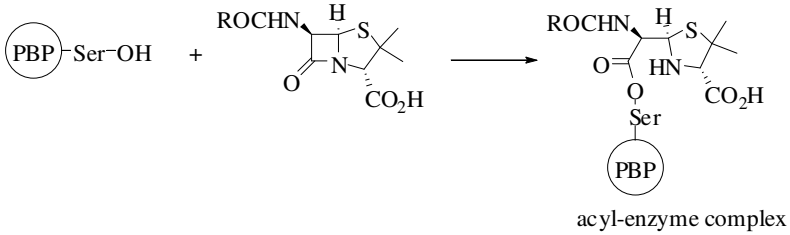


**Scheme 2.** Transpeptidase inhibition by β-lactam antibiotics.

In fact, the acyl-enzyme complex deacylates very slowly. The DD-transpeptidase is therefore blocked for a long time and cannot perform the cross-linking between the strands of peptidoglycan, leading to the inhibition of the bacteria cell wall biosynthesis. The peptidoglycan layer is consequently mechanically weaker and it results to the cell lysis due to the high osmotic pressure.

As for other serine peptidases like chymotrypsins, the reaction can be described as a three-step mechanism. **Scheme 3** represents the interaction

between the DD-transpeptidase (E) and the β-lactam antibiotic (A). $K_d$ is the dissociation constant for the reversible formation of the non-covalent Michaelis complex (E.A). $k_2$ is the rate constant for the formation of the covalent acyl-enzyme intermediate (E-A) from the Michaelis complex. $k_3$ is the rate constant for the hydrolysis of the acyl-enzyme intermediate, resulting in the formation of an inactivated product of reaction (P) and the DD-transpeptidase. The second rate constant $k_2/K_d$ represents the efficiency of the acylation.

$$E + A \underset{k_{-1}}{\overset{k_1}{\rightleftharpoons}} E.A \xrightarrow{k_2} E\text{-}A \xrightarrow[H_2O]{k_3} E + P$$

$$K_d = k_{-1}/k_1$$

**Scheme 3.** Scheme of interaction between a PBP (E) and a β-lactam antibiotic (A).

In the processing of β-lactams by transpeptidases, $k_3$ is very low (hardly ever above 0.001 $s^{-1}$)[22], and the acyl-enzyme intermediate is rapidly formed; consequently it results in an accumulation of the acyl-enzyme intermediate ($k_2/K_d >> k_3$), which leads to an inactive DD-transpeptidase.

### 4.3. DD-transpeptidase: Serine peptidase

The DD-transpeptidases catalyze the cross-linking of the peptidoglycan chains. They are named serine peptidases because they exhibit a serine residue which is central to the catalytic mechanism. The PBPs exhibit a penicillin-binding domain, which is characterized by the presence of three specific motifs: Ser-X-X-Lys, Ser(Tyr)-X-Asn and Lys(His)-Thr(Ser)-Gly-Thr(Ser) (X is any amino acid).[23] The serine of the motif Ser-X-X-Lys is the catalytic nucleophile.

When penicillin was first introduced on the market, the structure of the compound was not known, neither its mode of action. Nowadays, we dispose of more techniques to observe and understand the phenomena involved in the inhibition of bacteria growth by antibiotics. As an example, crystallographers were able in some cases to achieve X-ray crystal structures of covalent acyl-enzyme complexes between PBPs and β-lactam antibiotics. In one case, the crystal structure of a penicillin (**Figure 8**) was reported in non-covalent complex and also in covalent complex with the DD-transpeptidase of *Streptomyces* R61.[24] The penicillin used here has the particularity to include a side chain which is characteristic of the peptidoglycan of *Streptomyces* species, *i.e.* glycyl-L-α-amino-ε-pimelyl moiety.

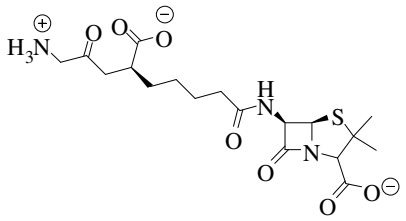

**Figure 8**. Structure of the penicillin with *Streptomyces* cell wall-specific side chain.

These crystal structures allow to nicely observe interactions between the β-lactam antibiotic and the active site involved in the DD-transpeptidase. In **Figure 9a** is presented the non-covalent DD-peptidase/β-lactam complex and in **Figure 9b** is presented the covalent complex. In dashed lines are represented the interactions between the active-site functional groups and the inhibitor. Distances for these interactions are given in Å just above those dashed lines. The Michaelis complex was obtained with an inactive enzyme. The inactivation of the enzyme results from the cross-linking of residues Lys65, Tyr159 and His108 (**Figure 9a**), supposedly attributed to the

presence of formaldehyde in the PEG solution used to store R61 DD-peptidase crystals.[25] It was assumed that this cross-linking does not perturb the active site, except that the participation of Lys65 and Tyr159 in catalysis is moderate. The non-covalent complex shows the interactions of the β-lactam with the enzyme before its inactivation and it appears that the β-lactam carbonyl is already well positioned for the attack of the catalytic nucleophile Ser62. This serine belongs to the first of the three characteristic motifs, namely Ser62-X-X-Lys65. The second motif is Tyr159-X-Asn161 and the third motif is composed by His298-Thr299-Gly300-Thr301.

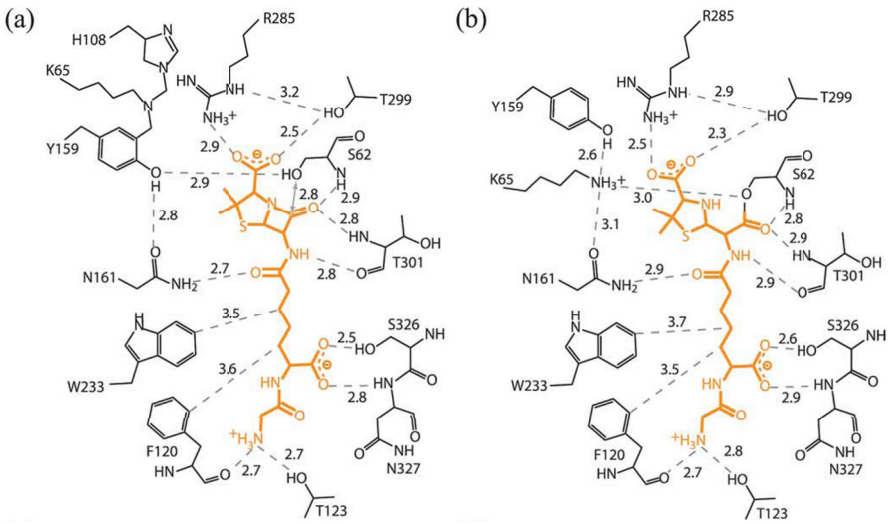


**Figure 9.** Representations of the active sites of a) the non-covalent R61 DD-peptidase/β-lactam complex b) the covalent complex.[24]

The covalent complex exhibits characteristics that several β-lactam antibiotics adopt with the active serine site as it was observed from different crystal structures of antibiotics covalently linked to PBPs. The β-lactam carbonyl oxygen is positioned in the oxyanion hole, formed in this case by the backbone amine hydrogens of Ser62 and Thr301. The carboxylate of the

thiazolidine ring is hydrogen-bonded to one or two hydroxyl group of the Lys(His)-Thr(Ser)-Gly-Thr(Ser) motif, in this case to Thr299.

There are several other interactions occurring in the good positioning of this β-lactam compound, like hydrogen interactions of Asn161 and Thr301 with the amide of the side chain; the tetramethylene motif of the side chain has hydrophobic interactions with Phe120 and Trp233 and the ammonium terminus with Phe120 and Thr123.

In a previous work,[25] the same authors have published a non-covalent complex between DD-transpeptidase of *Streptomyces* R61 and the tetrapeptide glycyl-L-α-amino-ε-pimelyl-D-Ala-D-Ala (**Figure 10**), which is a specific moiety of the peptidoglycan strand of *Streptomyces* sp.

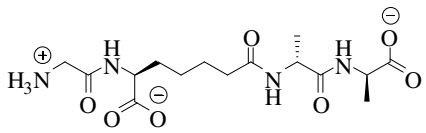

**Figure 10**. Structure of the tetrapeptide glycyl-L-α-amino-ε-pimelyl-D-Ala-D-Ala.

For the previously described penicillin (**Figure 8**) it was this glycyl-L-α-amino-ε-pimelyl moiety which was used as a peptidoglycan-mimetic side-chain. In the particular case of this penicillin, they found that the conformation of the non-covalent complex with the R61 DD-peptidase was really close to the one of the tetrapeptide (**Figure 10**), and that the penicillin and the tetrapeptide presented almost the same interactions with the enzyme. The superposition of the active site of the non-covalent complex of the penicillin (in yellow) and the tetrapeptide (in black) is shown in **Figure 11**.

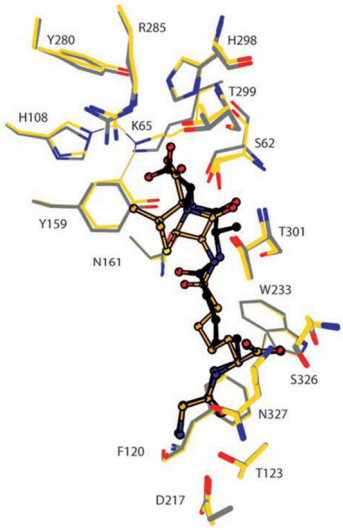


**Figure 11**. Superposition of the active site of the non-covalent complex of the penicillin and the tetrapeptide.[24]

The particularly good fitting of this penicillin with the R61 DD-peptidase is supposed to explain why the authors observed that this penicillin reacts faster (of several orders of magnitude) with the R61 DD-peptidase than other known β-lactams.

The X-ray structures of several PBPs, particularly the acyl-enzyme complexes of β-lactam antibiotics with the DD-peptidases, afforded information on PBPs and their interactions with the β-lactam antibiotics. Nevertheless, X-ray structures of several Active-site Serine Penicillin Recognizing Enzymes (ASPRE) (including PBPs and classes of β-lactamases (see section **5.2**) which are serine peptidases), did not afford direct evidences on the enzymatic mechanism.[21c] Consequently, the enzymatic mechanism of acylation still remains under discussion. There are two assumptions on the acylation sequence mechanism; it is either described

as a one-step concerted mechanism or as a two-step sequence, involving the formation of a tetrahedral intermediate. In the second hypothesis, the reaction is supposed to require a residue in the active site that could activate the nucleophile (base catalyst) or to promote the protonation the leaving group (acid catalyst).

As an example with the DD-peptidase of *Actinomadura* sp. R39, in a publication where X-ray data of a native R39 DD-peptidase and of an acyl-R39 DD-peptidase complex with nitrocefin (**Figure 12**) were reported, both two-step sequence and one-step concerted mechanisms are in agreement with the distances between the active site residues measured in crystal structures.[26]

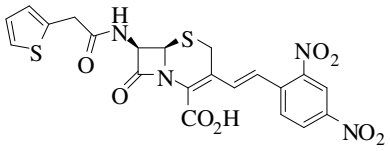


**Figure 12**. Structure of nitrocefin.

In R39 DD-peptidase, the three characteristic motifs are Ser49-X-X-Lys52, Ser298-X-Asn300 and Lys410-Thr411-Gly412-Thr413.

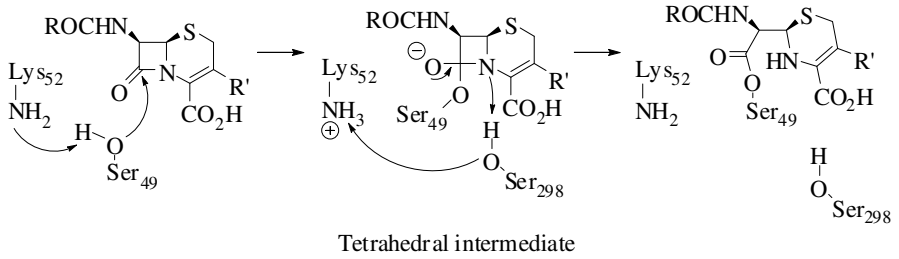


**Scheme 4**. Schematic two-step sequence mechanism with Lys52 catalyst.

In the two-step sequence, Lys52 could play the role of the base catalyst and abstract the proton from the hydroxyl of Ser49 to promote the nucleophilic attack on the carbonyl of the β-lactam. Then the proton would be back-donated to the nitrogen β-lactam via Ser298 (**Scheme 4**).

In the one-step concerted mechanism, the Ser49 nucleophilic attack is concomitant with the transfer of the proton from the hydroxyl of Ser49 to the nitrogen of Lys 52, working as a proton relay to Ser298, and the transfer of the Ser298 hydroxyl proton to the β-lactam nitrogen (**Scheme 5**).

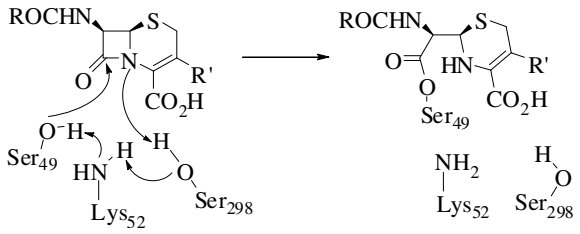


**Scheme 5**. Schematic one-step concerted mechanism.

Concerning *Streptomyces* R61, previously described, due to the fact that the inactive enzyme results from the cross-linking of residues Lys65, Tyr159 and His108 (**Figure 9a**), the authors suggest that Tyr159 could play the role of the catalytic base involved in the acyl-enzyme formation.[25]

Theoretical studies on the acylation by β-lactams of enzymatic models have been performed.[27] They are of interest since they are used to qualitatively predict the relative reactivity of compounds. Several theoretical models have been built, depending on the considered mechanism of acylation (one-step or two-step), and therefore on the amino acid residues involved. The two-step mechanism offers several possibilities, depending on

the considered catalyst. Some molecular dynamics simulations[28] studies on several models even suggested that there could be different mechanisms of acylation depending on the enzyme, and for a considered enzyme, even relying on the β-lactam antibiotic structure.

The debate on the mechanism of acylation is not ready to be closed.

## 5. Resistance

Soon after the introduction of antibiotics in the medicinal arsenal, bacteria learnt to protect themselves against antibiotics and developed several kinds of resistance. These are briefly presented below and a focus will be only done on one type of resistance, namely the production of resistant PBPs.

### 5.1. Reduced outer membrane permeability and efflux pump

First of all, an essential prerequisite for the action of antibiotics is to reach its targets and to accumulate sufficiently to act on PBPs. A type of resistance mechanism used by Gram-negative bacteria is to disable the access of the target or seriously reduce the drug concentration by a decreased antibiotic permeability and an increased antibiotic efflux. To access their target in gram-negative bacteria, antibiotics have to use porins present in the outer membrane to reach the periplasmic space; so the alteration of the outer membrane by porin deletion or modification, reduces the penetration of antibiotics in the bacterium. The reduced concentration of antibiotics in the periplasmic space can be achieved with drug efflux pumps that eject the antibiotic out of the bacterium. This type of resistance explains the broad

resistance to several kinds of antibiotics (quinolones and β-lactams) observed on Gram-negative bacteria.[29]

### 5.2. Production of β-lactamases

Another method for bacteria to resist to antibiotics is to destroy them before they reach their targets. This task is performed by β-lactamases,[29] which are soluble, excreted enzymes. They are classified into four categories. The A, C and D classes are serine peptidases and they share with DD-transpeptidases many similarities and their structures can be easily superimposed.[30] The interaction between a β-lactamase and the β-lactam antibiotic is also represented by **Scheme 3** (p35) where E here is the β-lactamase. After the formation of the acyl-enzyme complex, in the case of DD-transpeptidases the $k_3$ constant of its hydrolysis is very low and results in an accumulation of the acyl-enzyme intermediate, which leads to the inactivation of the DD-transpeptidases. But with β-lactamases, the rate constant of hydrolysis is very high and results in inactive, hydrolyzed antibiotics, while the active β-lactamases are recovered with a high turn-over. As an example, when the substrate is a penicillin, the hydrolysis of the acyl-enzyme complex leads to the inactive penicilloic acid. (**Scheme 6**)

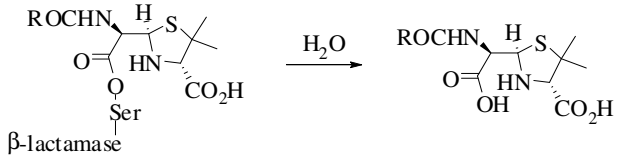


**Scheme 6**. Hydrolysis of the acyl-enzyme complex leading to the inactive penicilloic acid.

The last class of β-lactamases is the class B of metallo-β-lactamases. Unlike the other classes, the class B enzymes are not serine peptidases, and require a zinc-ion to catalyze the hydrolysis of the β-lactam ring.

### 5.3. Production of resistant PBPs

Resistant PBPs are PBPs which present a low affinity with the antibiotics. Even in this kind of resistance, bacteria have several strategies to produce resistant PBPs: they could acquire an additional PBP which has a low affinity with antibiotics, they could over-express an initially present PBP with low-affinity, or they could modify the initial PBP, for example by mutations.

There are two categories of PBPs, according to their molecular weight; the low molecular mass (LMM) PBPs, which were not reported to present a resistance to antibiotics, and the high molecular mass (HMM) PBPs.[23] Instead of reviewing all the resistant PBPs, we will focus on one resistant PBP which is related to the most important cause of antibiotic-resistant healthcare-associated infections worldwide, *i.e.* the methicillin-resistant *Staphylococcus aureus* (MRSA).

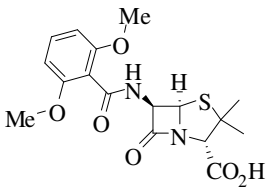


Methicillin

**Figure 13**. Structure of methicillin.

After the introduction of benzylpenicillin, strains of *Staphylococcus aureus* appeared to be resistant by the production of β-lactamases. To counteract this phenomenon, methicillin (**Figure 13**) was introduced as a drug.[31] But soon after, strains of methicillin-resistant *Staphylococcus aureus* were found in hospitals.[32] Initially, MRSA were associated with hospital care (HA-MRSA), but now we are also exposed to community-acquired MRSA (CA-MRSA).

HA-MRSA are highly resistant, virtually to all β-lactams. Vancomycin, a glycopeptide, is often used as the last chance to fight HA-MRSA, but as usually, strains of *Staphylococcus aureus* resistant to vancomycin and methicillin started to appear.[33] Nowadays, CA-MRSA is sensitive to more antibiotics than HA-MRSA, but anyway it is important to develop new antibiotics against MRSA before the problem get even worse, and therefore, it is important to know from what the resistance comes from.

The resistance of MRSA is due to the presence of a low-affinity PBP named PBP2a. This PBP is an additional PBP, not found in the native *Staphylococcus aureus.* There are four native PBPs which are β-lactam susceptible. When the transpeptidases activity of these native PBPs is hindered by β-lactam antibiotics, PBP2a takes care of the transpeptidase activity necessary to the synthesis of the peptidoglycan. As a low-affinity PBP, PBP2a reacts slowly with β-lactam antibiotics. Two causes are responsible for this low reactivity. First, there is a low affinity between PBP2a and β-lactams, with elevated dissociation constants ($K_d$, **Scheme 3**, p35) and second, the enzyme acylation rate is slow (low $k_2$).[34]

Clues on the structural explanations of resistance of PBP2a came from the crystal structures of PBP2a.[35] X-ray data of a native PBP2a and of an acyl-PBP2a complex with nitrocefin (**Figure 12**, p40) were obtained. The comparison of the native and nitrocefin-acyl complex allowed hypothesis on the structural changes involved in the resistant protein.

The **Figure 14a** shows the active site of the acyl-enzyme complex between nitrocefin and PBP2a. The nitrocefin is represented in sticks with purple carbons.

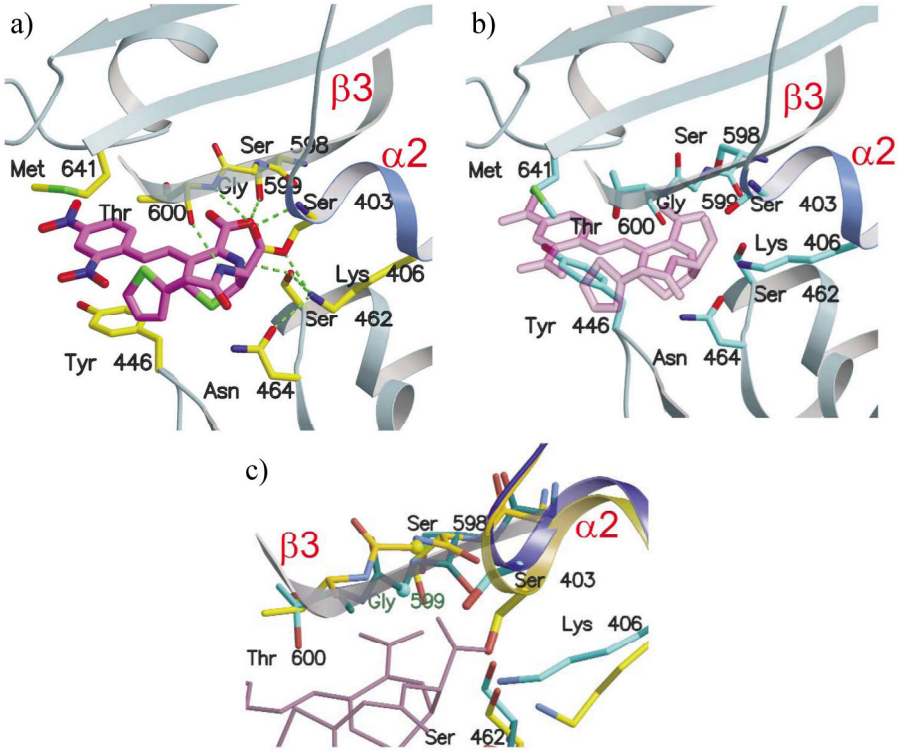


**Figure 14**. Representations of the active sites a) of the acyl-enzyme complex between nitrocefin and PBP2a b) of the native PBP2a c) of the native PBP2a superposed with PBP2a bound with nitrocefin. [35]

The **Figure 14b** is the active site of the native PBP2a. Nitrocefin, in translucent sticks, is represented in the same position than in the acyl-enzyme complex, allowing comparisons. The **Figure 14c** allows a better comparison with the superposition of the active site of the native PBP2a (in blue) and the active site with bound nitrocefin (in yellow). Nitrocefin is also represented in purple stick. It is clearly visible that the active site Ser403, in the native form, is not well positioned for the nucleophilic attack on the β-lactam. To allow this nucleophilic attack, the active site needs to perform some conformational changes in the strand β3 and also in the helix α2. In fact, for nucleophilic attack, the Oγ of Ser 403 has even to move of 1.8 Å (1.1 and 1.4 Å respectively for Cα and Cβ). The β3 sheet has to twist to accommodate with the α2 helix (and so Ser403) and avoid some steric clash. The conformational changes of PBP2a upon acylation were corroborated by circular dichroism measurements.[34]

The distortions of the active site, needed to allow the acylation with β-lactam antibiotics, were suggested to cost energy and therefore to be responsible for the resistance of PBP2a towards β-lactam antibiotics.

The native active site of PBP2a (without a bound antibiotic) appears relatively closed and must open, with conformational changes, to bind substrates, *i.e.* β-lactam antibiotics or peptidoglycan strands. Indeed, by circular dichroism measurements, it was also observed that binding with peptidoglycan fragments is accompanied with changes of PBP2a conformation.[36] In the presence of a peptidoglycan synthetic surrogate, it was reported that there is an increased acylation of β-lactam antibiotics, and therefore an easier enzyme inhibition, suggesting that PBP2a activity could be stimulated allosterically by peptidoglycan.[37] The interaction of

peptidoglycan with an allosteric site of PBP2a would facilitate the opening of the active site and enable the entry of β-lactams.

Ceftaroline fomasil, one of the latest cephalosporin developed by the pharmaceutical industry, is active against MRSA. Ceftaroline fosamil is the prodrug of the active metabolite ceftaroline (**Figure 15**).

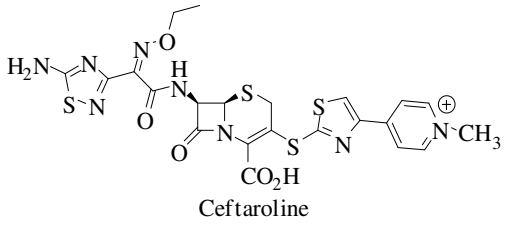


**Figure 15**. Structure of ceftaroline.

This drug is active against PBP2a because it appears that it is able to trigger the conformational changes, in the same way as peptidoglycan does open the active site. It seems that ceftaroline is able to bind to the allosteric site of PBP2a, enabling the access of the active site of PBP2a and therefore allowing the inhibition of the DD-transpeptidase activity. As previously seen, the efficiency of the acylation is given by the second order rate constant $k_2/K_d$ (**Scheme 3**, p35). When the concentration of the peptidoglycan synthetic surrogate increases, nitrocefin (as an example of a low inhibitor of PBP2a) shows a decrease of $K_d$ value and an increase of $k_2$ value, meaning a better inhibition of PBP2a. The second order rate constant $k_2/K_d$ increases from $19 \pm 3$ $M^{-1}$ $s^{-1}$ to $515 \pm 100$ $M^{-1}$ $s^{-1}$ when the amount of peptidoglycan synthetic surrogate increases. On the contrary, the effect of the peptidoglycan synthetic surrogate on the activity of ceftaroline was not significant ($k_2/K_d$ increases from $(2.4 \pm 0.1) \times 10^4$ $M^{-1}$ $s^{-1}$ to $(6.5 \pm 0.1) \times 10^4$ $M^{-1}$ $s^{-1}$ when the amount of peptidoglycan synthetic surrogate increases). It

would indicate that ceftaroline binds efficiently the allosteric site of PBP2a, and consequently open the active site allowing the inhibition of the DD-transpeptidase activity by ceftaroline.[38]

Interestingly, when comparing the efficiency of acylation of nitrocefin and ceftaroline (or other β-lactam antibiotics which are better inhibitors of PBP2a than nitrocefin),[37,38] it appears that the efficiency of acylation is essentially related to a significantly reduced value of $K_d$ for the good inhibitors ((190 ± 25) x $10^3$ nM for nitrocefin and 340 ± 40 nM for ceftaroline), whereas the acylation rate $k_2$ was unchanged.

The increase of interactions between PBP2a and β-lactam antibiotics should give lower values of $K_d$ and therefore improve the efficiency of acylation. The crystal structure of PBP2a should allow to design efficient β-lactam antibiotics by increasing the interactions with PBP2a and therefore improving the pre-acylation binding.

## 6. Conclusion

Since the discovery and the initial uses of penicillin as a therapeutic agent, things have evolved. Following the years of the discovery of penicillin, the screening of natural sources for the search of bacteriolytic substances was intensive and enabled the discovery of several families of antibiotics. Even if the phenomenon of resistance appeared, it was not considered exactly to its true worth, believing that technology and modern medicine would win against infectious diseases. A known citation, attributed to the Surgeon General of the United States of America, William Stewart, in 1967, states: « it is time to close the book on infectious diseases ». Even if in fact this exact quote could be an urban legend,[39] this opinion was shared by

many specialists of this time. Another example of optimism was given by the Nobel laureate Sir Macfarlane Burnet: « the most likely forecast about the future of infectious disease is that it will be very dull »,[40] and as a consequence, the pharmaceutical industries began to disinterest the area of antibiotics to other more lucrative diseases. But the miracle drugs began to fail and the phenomenon of resistance became widespread and led to this worrying situation, even if public does not really realized it. Actually, people seem to have forgotten the price of infectious diseases paid by previous generations. Even if the public is not conscious of this, the problem is yet more important than they think, and they could be surprised to learn that, in 2005, in the United States MRSA was responsible of more deaths than AIDS (18 650 compared to 16 000).[41]

Some strategies can be used to slow down the development of antimicrobial resistance, like enhancing the infection control and prevention, a rational use and the regulation of drugs, especially in the animal husbandry which is the most important consumer of antibiotics. But precautious measures will only delay the phenomena of resistance and the real urgency is the search of novel antibiotics.

When penicillins were firstly used as medicinal drugs, their structures and even their mode of action were unknown. After the discovery of their structures, their activity was attributed to the strain of the four-membered ring (azetidin-2-one) and the pyramidalization of the nitrogen atom, which increases the reactivity towards nucleophilic attack by serine-peptidases. Research in the following years after the discovery was dedicated to the homologues of the natural products and to enhance the properties aforementioned. However, science evolved, and a better design and evaluation of new compounds are now possible. New compounds still containing a β-lactam could be designed. Crystal structures allowed to know

the residues involved in the active site of the PBP, to understand and apprehend the interactions happening between the PBP and the β-lactam antibiotic. Theoretical studies, with models established in concordance with the crystal structure, allowed to evaluate qualitatively the reactivity of designed compounds. Docking can predict the binding orientation of potential drugs within the active site of PBPs. The reactivity of a compound during the acylation step can be evaluated, using several theoretical models which have been validated. This became possible due to the fast improvement of the calculation power of computers and developments in computational chemistry. Even if all the parameters are not known yet (as for example, no direct information on the step of acylation from crystal structures, and absence of consensus on the sequence step of this mechanism, or for the PBP2a, the real implication of the opening of the active site), there were considerable progresses in the understanding of the enzyme processing, and the phenomena of resistance, which allow to think that the resulting design of new compounds would lead to efficient antibiotics in the future.

## 7. References and notes

[1] http://www.who.int/en/

[2] http://ecdc.europa.eu/en/Pages/home.aspx

[3] Yong, D.; Toleman, M. A.; Giske, C. G.; Cho, H. S.; Sundman, K.; Lee, K.; Walsh, T. R. *Antimicrob. Agents Chemother.* **2009**, *53*, 5046-5054.

[4] Abraham, E. P.; Chain, E. *Nature* **1940**, *146*, 837.

[5] Walsh, C. *Nat. Rev. Microbiol.* **2003**, *1*, 65-69.

[6] The Use of Medicines in the United States: Review of 2010, IMS Institute for Healthcare Informatics

[7] Macfarlane G. in *Alexander Fleming: the man and the myth*, Chatto & Windus, London, 1984.

[8] Fleming, A. *Brit. J. Exp. Pathol*. **1929**, *10*, 226-236.

[9] Johnson, N.P.; Mueller, J. *Bull Hist Med.* **2002** Spring, *76(1)*, 105-115.

[10] Chain, E.; Florey, H. W.; Gardner, A. D.; Heatley, N. G.; Jennings, M. A.; Orr-Ewing, J.; Sanders, A. G. *Lancet* **1940**, *236*, 226-228.

[11] Abraham, E. P.; Chain, E.; Fletcher, C. M.; Gardner, A. D.; Heatley, N. G.; Jennings, M. A.; Florey, H. W. *Lancet* **1941**, *238*, 177-189.

[12] (a) Florey, M. E.; Florey, H. W. *Lancet* **1943**, *241*, 387-397; (b) Bodenham, D. C. *Lancet* **1943**, *242*, 725-728.

[13] Hodgkin, D. C. *Advancement Sci.* **1949**, *6*, 85-9.

[14] Sheehan, J. C. *J. Am. Chem. Soc.* **1957**, *79*, 1262-1263.

[15] Brotzu, G. *Lavori Inst. Igiene Cagliari* **1948**, 1-11.

[16] Newton, G. G. F.; Abraham, E. P. *Biochem. J.* **1956**, *62*, 651-658.

[17] (a) Abraham, E. P.; Newton, G. G. F. *Biochem. J.* **1961**, *79*, 377-393; (b) Hodgkin, D. C.; Maslen E. N. *Biochem. J.* **1961**, *79*, 393-402.

[18] Aoki, H.; Sakai, H.-I.; Kohsaka, M.; Konomi, T.; Hosoda, J.; Kubochi, Y.; Iguchi, E.; Imanaka H. *J. Antibiot.* **1976**, *29*, 492-500.

[19] Asai, M.; Haibara, K.; Muroi, M.; Kintaka K.; Kishi, T. *J. Antibiot.* **1981**, *34*, 621-627.

[20] Hare, R. in *The birth of penicillin*, George Allen and Unwin, London, 1970.

[21] (a) Walsh, C. *Nature* **2000**, *406*, 775-781; (b) Hubschwerlen, C. in *Comprehensive Medicinal Chemistry*, 2nd ed., (Eds: J. B.

Taylor, D. J. Triggle), Elsevier, Oxford, UK, 2007, chapter 7.17, pp. 479-517; (c) Zapun, A.; Contreras-Martel, C.; Vernet, T. *FEMS Microbiol. Rev.* **2008**, *32*, 361-385.

[22] Matagne, A.; Lamotte-Brasseur, J.; Frère, J.-M. *Biochem J.* **1998**, *330*, 581-598.

[23] Sauvage, E.; Kerff, F; Terrak, M.; Ayala, J. A.; Charlier, P. *FEMS Microbiol. Rev.* **2008**, *32*, 234-258.

[24] Silvaggi, N. R.; Josephine, H. R.; Kuzin, A. P.; Nagarajan, R.; Pratt, R. F.; Kelly, J. A. *J. Mol. Biol.* **2005**, *345*, 521-533.

[25] McDonough, M. A.; Anderson, J. W.; Silvaggi, N. R.; Pratt, R. F.; Knox, J. R.; Kelly, J. A. *J. Mol. Biol.* **2002**, *322*, 111-122.

[26] Sauvage, E.; Herman, R.; Petrella, S.; Duez, C.; Bouillenne, F.; Frère, J.-M.; Charlier, P. *J. Biol. Chem.* **2005**, *280*, 31249-31256.

[27] Lopez, R.; Menendez, M. I.; Diaz, N.; Suarez, D.; Campomanes, P.; Ardura, D.; Sordo, T. L. *Curr. Org. Chem.* **2006**, *10*, 805-821.

[28] Oliva, M.; Dideberg, O.; Field, M. J. *Proteins* **2003**, *53*, 88-100.

[29] Fischer, J. F.; Meroueh, S. O.; Mobashery, S. *Chem. Rev.* **2005**, *105*, 395-424.

[30] (a) Fonzé, E.; Vermeire, M.; Nguyen-Distèche, M.; Brasseur, R.; Charlier, P. *J. Biol. Chem.* **1999**, *274*, 21853-21860; (b) Davies, C.; White, S. W.; Nicholas, R. A. *J. Biol. Chem.* **2001**, *276*, 616-623.

[31] Fairbrother, R. W.; Taylor, G. *Lancet* **1961**, *7175*, 473-476.

[32] Jevons, M. P.; Coe, A. W.; Parker, M. T. *Lancet* **1963**, *281*, 904-907.

[33] (a) Hiramatsu, K.; Hanaki, H.; Ino, T.; Yabuta, K.; Oguri, T.; Tenover, F. C. *J. Antimicrob. Chemother.* **1997**, *40*, 135-136; (b) Weigel, L. M.; Clewell, D. B.; Gill, S. R.; Clark, N. C.; McDougal,

L. K.; Flannagan, S. E.; Kolonay, J. F.; Shetty, J.; Killgore, G. E.; Tenover, F. C. *Science* **2003**, *302*, 1569-1571.

[34] Fuda, C.; Suvorov, M.; Vakulenko, S. B.; Mobashery, S. *J. Biol. Chem.* **2004**, *279*, 40802-40806.

[35] Lim, D.; Strynadka, N. C. J. *Nat. Struct. Biol.* **2002**, *9*, 870-876.

[36] Fuda, C.; Hesek, D.; Lee, M.; Morio, K.; Nowak, T.; Mobashery, S. *J. Am. Chem. Soc.* **2005**, *127*, 2056-2057.

[37] Fuda, C.; Hesek, D.; Lee, M.; Heilmayer, W.; Novak, R.; Vakulenko, S. B.; Mobashery, S. *J. Biol. Chem.* **2006**, *281*, 10035-10041.

[38] Villegas-Estrada, A.; Lee, M.; Hesek, D.; Vakulenko, V. B.; Mobashery, S. *J. Am. Chem. Soc.* **2008**, *130*, 9212-9213.

[39] Spellberg, B. *Clin Infect Dis.* **2008**, *47*, 294.

[40] Burnet, F. MacFarlane; White, D. O. in *The natural history of infectious disease* (4th ed.), London: Cambridge University Press, 1972.

[41] Klevens, R. M.; Morrison, M. A.; Nadle, J.; Petit, S.; Gershman, K.; Ray, S.; Harrison, L. H.; Lynfield, R.; Dumyati, G.; Townes, J. M.; Craig, A. S.; Zell, E. R.; Fosheim, G. E.; McDougal, L. K.; Carey, R. B.; Fridkin, S. K. *JAMA*, **2007**, *298*, 1763-1771.

# *Chapter 2 - Objectives and strategies*

## 1. Objectives

The project takes place in the context of the rise of bacterial resistance and the need of novel antibiotics. The search will be focused on irreversible inhibitors (or acylating molecules) of penicillin binding proteins (PBPs).

The β-lactam moiety, from the early antibiotics, can still be efficient in the fight against bacterial resistance and be used as structural base of new antibiotics with some structural adaptations, as proven with ceftaroline fomasil,[1] one of the latest cephalosporin developed and which exhibits an extended activity against gram-positive bacteria including MRSA.

Initially, the activity of β-lactam antibiotics was attributed to the strain of the four-membered ring[2] and the pyramidalization of the nitrogen atom.

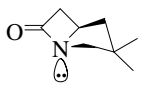

**Figure 1**. Pyramidalization of the nitrogen atom.

In strained bicyclic structures, substituents of the amide of 2-azetidinone are not in the same plane (**Figure 1**), and it results in a twisted amide with reduced electron delocalization (**Scheme 1**).

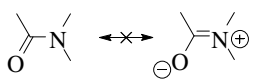

**Scheme 1**. Lack of amide resonance.

It was widely considered that the high reactivity of the β-lactam antibiotics towards nucleophilic attack by serine-peptidases is due to this lack of amide resonance[3] in the 2-azetidinone ring. It is the reason of the search on novel β-lactam antibiotics which has been extensively conducted on strained 1,4-fused bicyclic structures with an aim to improve the so-called "acylating power" of the twisted amide motif of the 2-azetidinone ring.[4] But this long-established model of reactivity seems to be over-evaluated since there is still no clear relationship between these structural characteristics and the biological activity. Studies have shown that strained β-lactam systems are not necessarily better antibiotics and that the contribution of the factors of the previous model of reactivity was not proven.[5]

Our laboratory explored another model of reactivity by preparing 1,3-bridged bicyclic β-lactam compounds with a large ring instead of strained 1,4-fused bicyclic structures. In this unusual approach, the aim was to decrease the activation barrier of the 2-azetidinone N-C(O) bond cleavage by increasing the conformational adaptability of the macrocyclic structure that would be involved in the reorganization of the atoms during the acyl-enzyme covalent complex formation.

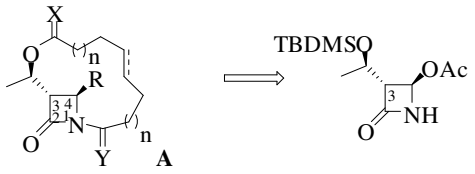


R = H, *n*-Pr, OAc
X = Y = O ; X = Y = H,H ; X = O and Y = H,H
TBDMS = *tert*-butyldimethylsilyl

**Figure 2**. 1,3-bridged bicyclic β-lactams **A** synthesized during the PhD thesis of Allan Urbach.

This hypothesis has been previously exploited in the PhD thesis of Allan Urbach for the preparation of 1,3-bridged bicyclic β-lactams **A**, derived from acetoxy-azetidinone, a commercial and common precursor of thienamycin derivatives (**Figure 2**).[6]

Several 12- and 13-membered rings were synthesized and evaluated as potential inhibitors of PBPs. However, these compounds were only modest inhibitors of PBPs. The low activities could be explained (at least partially) by the lack of accessibility of the α-face of the molecules for the nucleophile serine attack, the α-face being hindered by the folding of the ring. Therefore, to pursue our research on novel, non-traditional, bicyclic β-lactams, we decided to change the absolute stereochemistry on C(3). Due to constraints of synthesis (a more rapid access to chirons), we have decided to make compounds structurally related to the cephalosporin and penicillin families with an amino side chain on C(3) (**Figure 3**).

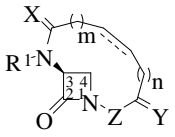


**B**

X = O ; H,H
Y = O ; H,H
$R^1$ = COR, H, Me
Z = O, -

**Figure 3**. Target molecules **B**.

To sum up, the novel β-lactams synthesized, in a view to inhibit the PBPs, are bicyclic azetidinones endowed with the following features:

- the C(3) absolute configuration of penicillins
- an amino substituent at C(3)

- a macrocycle connecting the positions C(3)-N and N(1) with various lengths of the bicycle
- functionalizations on the macrocycle including carbonyls, or HC=CH double bond are possible.

This inversion of absolute configuration on C(3) should position the bicycle on the β-face of the azetidinone ring and consequently make the serine nucleophilic attack easier on the α-face during the processing of the tested compounds by PBPs.

## 2. Synthetic strategy

The **Scheme 2** reports the synthetic strategy which will be employed for the synthesis of the 1,3-bridged bicycles **B**.

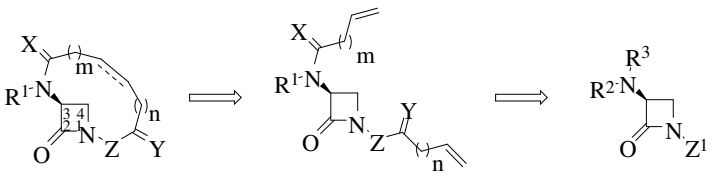


**B** **C** **D**

X = O ; H,H
Y = O ; H,H
$R^1$ = COR, H, Me
$R^2$ = COR
$R^3$ = H, Me
Z = O, -
$Z^1$ = OH, H

**Scheme 2**. Retrosynthetic strategy.

The Ring Closing Metathesis (RCM) reaction is chosen as the key-step for the synthesis of the 1,3-bridged bicycles **B**. The precursors are chiral

azetidin-2-ones **C** equipped with ω-alkenoyl or ω-alkenyl chains on the positions N(1) and C(3)-N, deriving from chirons **D**.

Theoretical studies will be performed to investigate the feasibility of the RCM reaction on the precursors **C**, and consequently on the difficulty in forming the 1,3-bridged bicycles **B**.

## 3. Biochemical and theoretical reactivities

The inhibition potential of the synthesized compounds will be tested against R39 D,D-peptidase,[7] which is a commonly used model for bacterial enzymes. These evaluations are performed by Dr. Astrid Zervosen. All the compounds will be evaluated against PBP2a, the PBP responsible of the resistance of MRSA and also against another example of high-molecular-weight D,D-peptidase responsible for bacterial resistance, PBP5 from *Enterococcus faecium*.[8] These evaluations are performed by Dr. Ana Amoroso and Olivier Verlaine.

The reactivity of the synthesized β-lactams will be evaluated into a model of PBP cavity (**Figure 4**) at the RHF/MINI-1' level of theory.

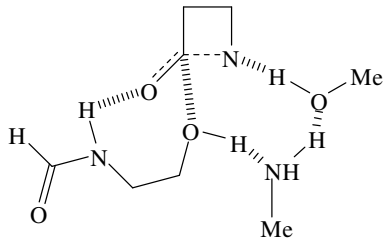


**Figure 4.** Model of concerted nucleophilic attack on the β-lactam ring.

The considered model is a model of concerted nucleophilic attack on the β-lactam ring. In this model, the nucleophilic serine is mimicked by a 2-formylamino-1-ethanol interacting with a methylamine working as a proton relay to a methanol molecule which, *in fine*, transfers a H atom to the β-lactam nitrogen. The formamide moiety mimicks the oxyanion hole stabilization.[9] This model has been validated in many cases as a representative one of the R39 reactive entities by docking the penicillin G and cephalosporin transition states in the R39 crystallographic structure. These theoretical studies are performed by Dr. G. Dive.

To estimate the potential acylating power of the synthesized β-lactam, an elaborate model of R39 active site representing the three conserved motifs of the PBPs family will be built by computational chemistry.

Some docking experiments of the most active compounds into the R39 and PBP2a crystallographic structures will be also performed by Dr. E. Sauvage.

## 4. Contents of the manuscript

The context of the thesis and the objectives have been presented in Chapters 1 and 2, respectively. To follow up, the main part of our experimental work is written in the form of articles, published or submitted.

The Chapter 3 summarizes the initial synthetic approaches towards β-lactamic chirons and the first assays of acylation and RCM reactions.

The Chapter 4 describes the synthesis of three series of *bis*-acylated β-lactamic precursors and presents the problem encountered with the RCM

reaction, *i.e.* the cyclodimerization which was the preferred outcome. (article)

The Chapter 5 presents an elegant method to discriminate between cyclomonomer and cyclodimers of the previous chapter, *i.e.* DOSY-NMR method. (article)

The Chapter 6 focuses on an in-depth study of one family of *bis*-2-oxoazetidinyl cyclodimers which exhibit interesting biological activities against PBP2a. (article)

The Chapter 7 describes the synthesis of two series of *bis*-alkylated precursors and resultant cyclized products. (article)

The Chapter 8 introduces attempts to synthesize mixed compounds, with one acyl chain and one alkyl chain.

The Chapter 9 gathers the conclusions and perspectives.

Compounds of Chapters 4, 6 and 7 were biologically evaluated against R39, and compounds of Chapters 6 and 7 were also evaluated against PBP2a of MRSA and PBP5 of resistant *E. faecium*.

Theoretical studies in Chapter 4 were performed to understand the highly preferred outcome of cyclodimerization.

In Chapter 6, quantum chemistry calculations were performed to study the 3D structures of all the dimers. Using an elaborate model of R39 active site, the reactivity of one cyclodimer was analyzed. Docking experiments of the same cyclodimer into the R39 and PBP2a crystallographic structures were performed.

In Chapter 7, *ab initio* calculations were performed to estimate the reactivity of 1,3-bridged β-lactams by the determination of the energy barrier of a concerted nucleophilic attack and lactam ring-opening process into a

simple model of PBP cavity (**Figure 4**). Very elaborate reactivity models of the R39 active site have been built to analyze the reactivity of the synthesized compounds. The construction of the elaborate model of R39 active site used in Chapter 6 is detailed in this chapter.

In the appendix is presented a simple introduction to computational chemistry to explain the methods, which are not familiar for all chemists.

## 5. References and notes

[1] Biek, D.; Critchley, I. A., Riccobene, T. A., Thye, D. A. *J. Antimicrob. Chemother.* **2010**, *65*, Suppl 4: iv9-16.

[2] Strominger, J. L. *Antibiotics* **1967**, *1*, 705-713

[3] Woodward, R. B. in *The Chemistry of Penicillin* (Eds. H. T. Clarke, J. R. Johnson et R. Robinson), Princeton University Press, Princeton, New Jersey, 1949, chapter 15, pp. 440-454.

[4] (a) Alcaide, B.; Aragoncillo, C.; Almendros, P. in *Comprehensive Heterocyclic Chemistry III* (Ed.: C. Stevens), Elsevier, Oxford, 2008, vol. 2, chapter 2.02, pp. 111-171; (b) Marchand-Brynaert, J.; Brulé, C. in *Comprehensive Heterocyclic Chemistry III* (Ed.: C. Stevens), Elsevier, Oxford, 2008, vol. 2, chapter 2.03, pp. 173-237.

[5] (a) Proctor, P.; Gensmantel, N. P.; Page, M. I. *J. Chem. Soc. Perkin Trans. II* **1982**, 1185-1192; (b) Page, M. I. *Acc. Chem. Res.* **1984**, *17*, 144-151.

[6] (a) Urbach, A.; Dive, G.; Marchand-Brynaert, J. *Eur. J. Org. Chem.* **2009**, *11*, 1757-1770; (b) Urbach, A.; Dive, G.; Tinant, B.; Duval, V.; Marchand-Brynaert, J. *Eur. J. Med. Chem.* **2009**, *44*, 2071-2080.

[7] (a) Sauvage, E.; Herman, R.; Petrella, S.; Duez, C.; Bouillenne, F.; Frère, J. M.; Charlier, P. *J. Biol. Chem.* **2005**, *280*, 31249-31256; (b) Sauvage, E.; Powell, A. J.; Heilemann, J.; Josephine, H. R.; Charlier, P.; Davies, C.; Pratt, R. F. *J. Mol. Biol.* **2008**, *381*, 383-393.

[8] Sauvage, E.; Kerff, F.; Fonzé, E.; Herman, R.; Schoot, B.; Marquette, J.-P.; Taburet, Y.; Prevost, D.; Dumas, J.; Leonard, G.; Stefanic, P.; Coyette, J.; Charlier, P. *Cell. Mol. Life Sci.* **2002**, *59*, 1223-1232.

[9] Dive, G.; Dehareng, D. *Int. J. Quant. Chem.* **1999**, *73*, 161-174.

# *Chapter 3 - First synthetic approaches*

# 1. Chirons

## 1.1. Structure of the chirons

The starting point for the access to the desired 1,3-bridged bicycles was the synthesis of (*S*)-3-amino-2-azetidinone and (*S*)-3-amino-1-hydroxy-2-azetidinone. Concerning the side chain on the amino substituent at C(3), we chose the *tert*-butyloxycarbonyl and benzyloxycarbonyl groups, which are protecting groups that could be easily removed by TFA hydrolysis and hydrogenolysis, respectively. Therefore, (*S*)-*tert*-butyl 2-oxoazetidin-3-ylcarbamate **1**, (*S*)-*tert*-butyl 1-hydroxy-2-oxoazetidin-3-ylcarbamate **2**, (*S*)-benzyl 2-oxoazetidin-3-ylcarbamate **3** and (*S*)-benzyl 1-hydroxy-2-oxoazetidin-3-ylcarbamate **4** were our first targets (**Figure 1**).

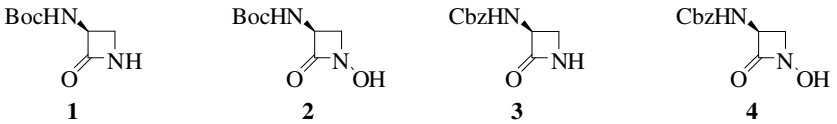


**1** **2** **3** **4**

**Figure 1**. Structures of the first targets.

The first synthesis of 2-azetidinone was reported by Staudinger in 1907.[1] The elucidation of the structure of penicillin increased the interest for the β-lactam moiety, due to its biological activity. 2-Azetidinones are also used as intermediates in organic chemistry. This is why the synthesis of 2-azetidinones has been widely discussed, and many strategies were developed to access the β-lactam nucleus: intramolecular cyclizations, [2 + 2] cycloadditions, rearrangement of another ring or insertion of metal carbenoids are the main strategies of syntheses of β-lactams described in many reviews dedicated to this subject.[2]

To have a rapid access to the starting chirons, protocols from the literature (as such, or modified) and combinations of standard protocols were used to synthesize them.

### 1.2. Boc chirons

Different syntheses of chiron **1** are reported in the literature. It can be obtained by degradation of the commercially available 6-APA, which 6-amino function was previously acylated with the Boc protecting group (**Scheme 1**).[3]

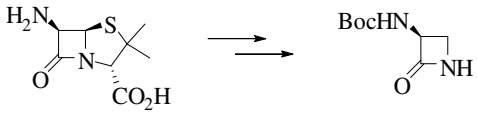


6-APA **1**

**Scheme 1**. Degradation of 6-APA into chiron **1**.

The obtention of chiron **1** is also described by a [2 + 2] cycloaddition. The treatment of chiral hydrazone **5** with aminoketene **7**, generated via the glycine derivative **6**, afforded azetidinone **8**, which following steps of protection and deprotection led to chiron **1** (**Scheme 2**).[4] Another [2 + 2] cycloaddition was reported to provide chiron **1**. Treatment of imine **9** with the chiral ketene generated in situ from carboxylic acid chloride **10** and triethylamine, afforded the β-lactam **11**. Subsequent steps of deprotection led to chiron **1** (**Scheme 3**).[5]

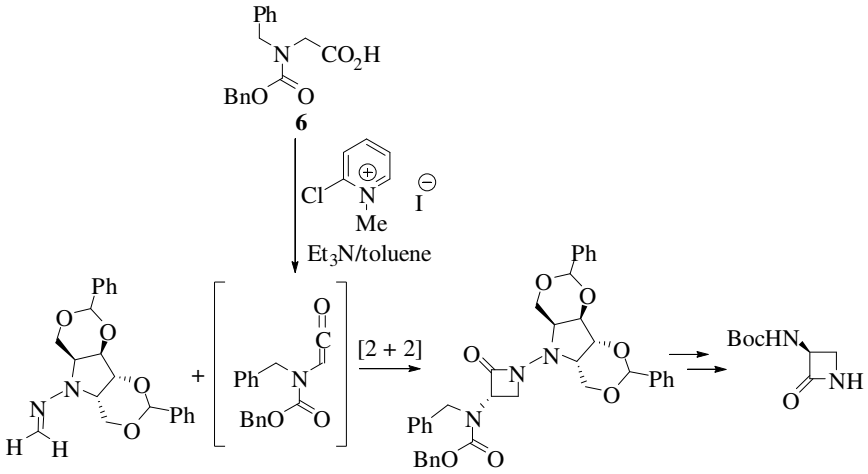


**Scheme 2**

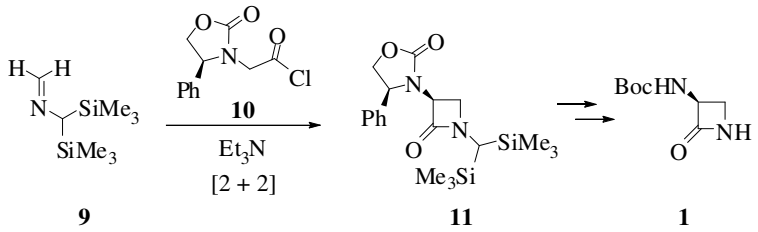


**Scheme 3**. Synthesis of chiron **1** by [2 + 2] cycloadditions.

Chiron **1** can also be obtained by intramolecular cyclization. In one of this kind of synthesis, one intermediate, (*S*)-*tert*-butyl 1-(benzyloxy)-2-oxoazetidin-3-ylcarbamate **14** is of interest because it allows access to both chirons **1** and **2**.[6] Consequently we used this synthetic strategy.

The commercially available Boc-L-serine **12** was converted into the corresponding hydroxamate **13** by a coupling reaction involving O-benzylhydroxylamine and the coupling reagent DCC. The intramolecular cyclization of **13** was performed with the method proposed by Miller, with the use of $PPh_3$, $Et_3N$ and $CCl_4$ (**Scheme 4**).[6] The use of $CBr_4$ and both

$CBr_4$/imidazole, instead of the toxic $CCl_4$ were also tested. The use of $CBr_4$/imidazole in THF afforded **14** in good yield (70%), but in high quantity, the use of $CBr_4$, which was sublimed before its utilization, was not convenient. The scaling-up of the coupling reaction (65 mmol) and the intramolecular cyclization (27 mmol) was easily performed and allowed a rapid access to high quantity of compound **14**.

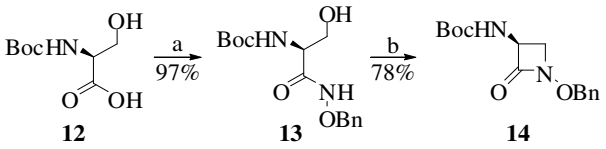


**12** **13** **14**

**Scheme 4**. Synthesis of compound **14**. Reagents and conditions: (a) DCC, $NH_2OBn$, THF, 0 °C to rt; (b) $PPh_3$, $CCl_4$, TEA, $CH_3CN$, 0 °C to rt.

Catalytic hydrogenation of compound **14** in the presence of Pd/C gave the compound **2** in quantitative yield (**Scheme 5**). Miller reported the subsequent synthesis of compound **1** by N-O reduction of chiron **2** with titanium trichloride, affording **1** in good yield.[7] However the possible direct O-benzyl cleavage with derivatives of compound **14** was reported to occur by hydrogenation in presence of Raney nickel[8], and since this method allowed to obtain chiron **1** directly from compound **14** in quantitative yield, it was the method employed to access to chiron **1** (**Scheme 5**).

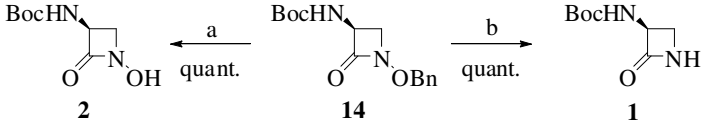


**2** **14** **1**

**Scheme 5**. Synthesis of chirons **1** and **2**. Reagents and conditions: (a) $H_2$, Pd/C, MeOH, rt; (b) $H_2$, Raney-Ni, MeOH, rt.

Moreover, the synthesis of chiron **2** in quantitative yield was performed on small quantities (0.5 mmol) of starting material **14**, but in higher quantities, the reaction was not quantitative and requires an arduous purification. Compound **2** is not stable: the rearrangement of *N*-hydroxy-β-lactam into isoxazolidin-5-one **15** has been observed under basic or acid media, or by heating (**Scheme 6**).[9] Thus the quality of the catalyst is important because it could contain more or less quantity of residual acid, depending on the supplier. Purification by column chromatography on silica gel, that is slightly acidic, could also lead to partial rearrangement of chiron **2**.

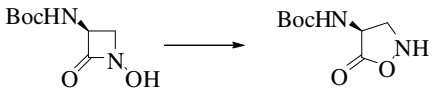


**2** **15**

**Scheme 6**. Rearrangement of compound **2** into compound **15**.

### 1.3. Cbz chirons

(*S*)-benzyl 1-(benzyloxy)-2-oxoazetidin-3-ylcarbamate **16**, equivalent of compound **14** with the Cbz side-chain, is accessible with the same method applied for the synthesis of **14**,[6,10] from the protected Cbz-L-serine.[11] However the direct access to chiron **4** from **16** is not possible since both Cbz and Bn group are cleaved by catalytic hydrogenation in presence of Pd/C (**Scheme 7**).

Moreover, the compound issued from the hydrogenolysis of both protecting groups was reported as an unstable compound, from which the attempts of N-acylation were not conclusive.[12]

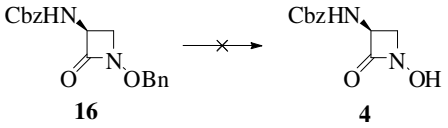


**Scheme 7**. Not conclusive synthesis of compound **4** from compound **16**.

In this same publication, the authors reported the synthesis of compound **4** from D-cycloserine in 34% overall yield (**Scheme 8**).

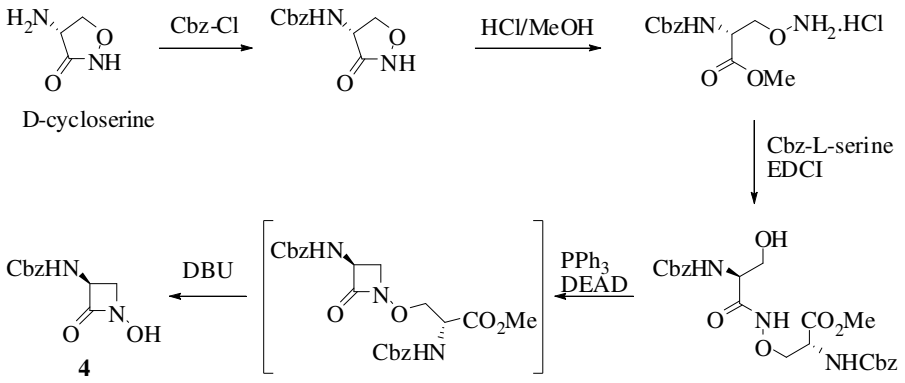


**Scheme 8**. Synthesis of chiron **4**.

As described later (see section **3**, p79), the first test on the RCM reaction with a bis-acylated derivative of chiron **2**, led only to degradation of the reactant. We supposed that this problem could be related to the presence in the compound of the O-acyl hydroxamate function, susceptible to complex the RCM catalysts. So we decided to temporarily abandon the synthesis of (*S*)-3-amino-1-hydroxy-2-azetidinone chirons **2** and **4**.

(*S*)-benzyl 2-oxoazetidin-3-ylcarbamate **3**, equivalent of compound **1**, with the Cbz side-chain, is the last chiron that we wanted to synthesize.

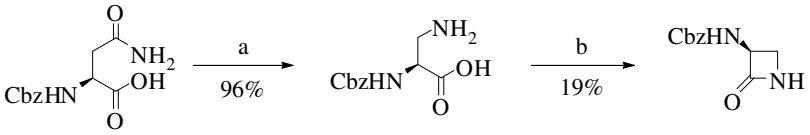


**17** **18** **3**

**Scheme 9**. Synthesis of chiron **3**. Reagents and conditions: (a) iodobenzene diacetate, EtOAc/MeCN/$H_2O$, rt; (b) $CH_3SO_2Cl$, $NaHCO_3$, $CH_3CN$, reflux.

Compound **18** was obtained, in nearly quantitative yield, by Hoffman-type rearrangement of commercially available N-(benzyloxycarbonyl)-L-asparagine **17**, using a hypervalent iodine reagent.[13] The mechanism of this reaction is presented in **Scheme 10**. The isocyanate intermediate **20**, obtained after the rearrangement of the PIDA (iodosobenzene diacetate) adduct **19**, is hydrolyzed by the co-solvent water.

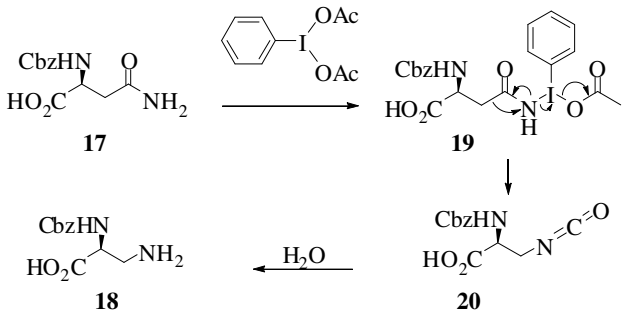


**Scheme 10**. Mechanism of formation of compound **18**.

Compound **18** was subsequently cyclized with the use of mesyl chloride to give the β-lactam **3** in low yield (**Scheme 9**).[14] DCC and PyBop, other activating reagents, were tested but no reaction occurred. Mukayiama's reactant[15] worked but led to small yield as mesyl chloride. The low yield could be due to a problem of low solubility of compound **18** in $CH_3CN$ and a

problem of competition between the carboxylic acid and the amine functions.

## 2. Bis-acylated compounds

### 2.1. From chiron 3

The chiron **3** was mono-acylated at N(1) position regioselectively under mild conditions giving compound **21** in good yield.[16] An attempt to obtain compound **22** directly from chiron **3** was carried out with double quantities of pyridine and 4-pentenoyl chloride, but only mono-acylation occurred. Therefore the use of a strong base is necessary to deprotonate the carbamate. Treatment of compound **21** with *n*-BuLi and 4-pentenoyl chloride afforded the bis-acylated compound **22** in low yield (**Scheme 11**).

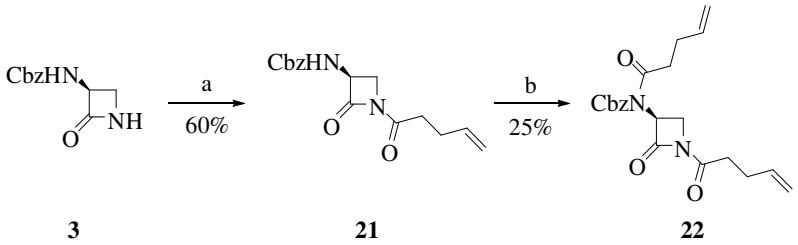


**3** **21** **22**

**Scheme 11**. Synthesis of *bis*-acylated **22**. Reagents and conditions: (a) 4-pentenoyl chloride, pyridine, $CH_2Cl_2$, rt; (b) 4-pentenoyl chloride, *n*-BuLi, THF, -78 °C to rt.

The available quantity of chiron **3** did not allow us to perform other experiments. Therefore to not waste more time, we decided to abandon the synthesis of bis-acyl derivatives of chiron **3** and to concentrate our efforts on the chirons with the Boc protecting group.

### 2.2. From chiron 2

With the same method applied to the mono-acylation of chiron **3**, we mono-acylated chiron **2**, giving compound **23** in moderate yield (36%) (**Scheme 12**). An optimization was performed (**Table 1**) and compound **23** was obtained in nearly quantitative yield (94%), with the use of triethylamine and 4-pentenoyl chloride in presence of DMAP.[17]

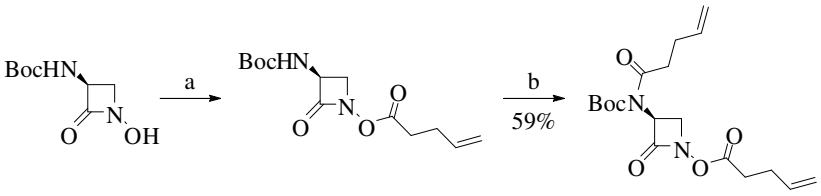


**Scheme 12**. Synthesis of *bis*-acylated **24**. Reagents and conditions: (a) 4-pentenoyl chloride, base; (b) 4-pentenoyl chloride, *n*-BuLi, THF, -78 °C to rt.

The low yield observed with pyridine could be explained by the fact that chiron **2** is not stable and that the rearrangement occurs before acylation. This phenomenon of rearrangement is exacerbated at reflux, explaining that no compound **23** was detected.

**Table 1**

Acylation of chiron **2** to compound **23**.

| Base | Pentenoyl chloride | Solvent | Time | T (°C) | Yield (%) |
|---|---|---|---|---|---|
| Pyridine (2 eq) | 2 eq | $CH_2Cl_2$ | 48 h | rt | 36 |
| Pyridine (2 eq) | 2 eq | $CH_2Cl_2$ | 48 h | reflux | 0 |
| Pyridine (1.1 eq) | 1.1 eq | $CH_2Cl_2$ | 24 h | rt | 45 |
| $Et_3N$ (1.1 eq) /DMAP (cat) | 1.2 eq | $CH_3CN$ | 45 min | rt | 94 |

The bis-acylated compound **24** was obtained by treatment of the compound **23** with 4-pentenoyl chloride in the presence of butyl lithium (**Scheme 12**).

### 2.3. From chiron 1

The compound **1** was mono-acylated at N(1) position, with the same method employed to mono-acylate the chiron **3**, affording compound **25** in 89% yield (**Scheme 13**).

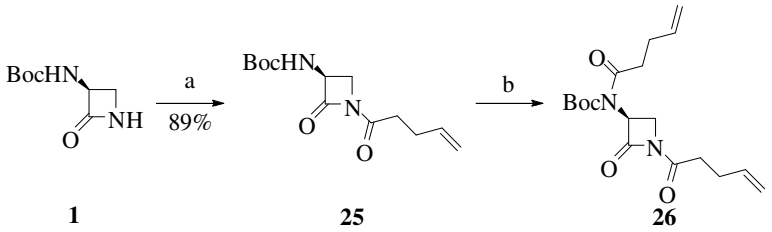


**1** **25** **26**

**Scheme 13**. Synthesis of *bis*-acylated **26**. Reagents and conditions: (a) 4-pentenoyl chloride, pyridine, $CH_2Cl_2$, rt; (b) 4-pentenoyl chloride, base, THF.

**Table 2**

Acylation of compound **25** to compound **26**.

| Base (1.1 eq) | T (°C) | Time with base | Yield (%) |
|---|---|---|---|
| *n*- BuLi | -78 | 1 h | 28 |
| *n*- BuLi | -78 | 30 min | 40 |
| KHMDS | -78 | 45 min | traces |
| KHMDS | -78 | 30 min | 7 |
| KHMDS | -30 | 30 min | 0 |
| LiHMDS | -78 | 1 h | 23 |
| LiHMDS | -78 | 45 min | 44 |
| LiHMDS | -78 | 30 min | 95 |

Several attempts were performed to find the best conditions to carry out the second acylation (**Table 2**), which revealed that the use of LiHMDS as base at -78 °C, with 30 min between the addition of LiHMDS and 4-pentenoyl chloride, allowed to recover compound **26** in 95% yield.

From this table, we can see that when the base is let with compound **25** a too long time before the addition of 4-pentenoyl chloride, the yield of **26** diminishes. It is explained by the fact that deprotonated carbamate of compound **25** could acylate another β-lactam compound, leading to open β-lactam ring side products.

With the same conditions developed for the second acylation, we can directly synthesize compound **26** from chiron **1** with double quantities of LiHMDS and 4-pentenoyl chloride in 61% yield.

## 3. First RCM

Ring closing metathesis reaction was carried out on the bis-acylated compound **24**, in presence of second generation Grubbs catalyst (5 mol%) in dichloromethane at room temperature. After 12 h, there was no more starting material, but unfortunately only degradation of compound **24** was observed (**Scheme 14**).

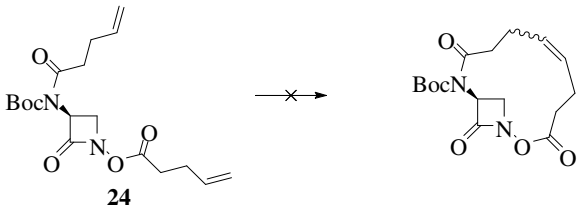


**Scheme 14**. Trial of RCM reaction on compound **24**. Reagents and conditions: Grubbs II catalyst (5 mol%), $CH_2Cl_2$, rt.

## 4. Chirons conclusions

The first result on the RCM of the derivative of chiron **2** was not encouraging. The failure could be linked to the O-acyl hydroxamate moiety. Therefore taking into account the problem of producing high quantities of chiron **2** with the hydroxamic acid, we decided to abandon the investigations on the derivatives of (*S*)-3-amino-1-hydroxy-2-azetidinone chirons **2** and **4**.

Due to the low efficiency of the cyclization step to obtain the chiron **3**, we also decided to stop the synthesis of this chiron and its derivatives.

Synthesis of derivatives of chiron **1** was continued and RCM reactions were tried on the bis-acylated compounds issued from chiron **1**. These experiments are reported in the next chapter.

## 5. Experimental Section

Experiments were performed under argon atmosphere in flame-dried glassware. All solvents, including anhydrous solvents, and reagents were purchased from Acros Organics, Alfa Aesar, Fluka, Sigma-Aldrich or VWR, and used without any further purification. TLC analyses were performed on aluminium plates coated with silica gel $60F_{254}$ (Merck) and visualized with a $KMnO_4$ solution and UV (254 nm) detection and column chromatography was performed on silica gel (40-63 or 63-200 μm) purchased from Rocc. Melting points (mp) were determined on a Büchi B-540 apparatus calibrated with caffeine, vanillin, and phenacetin. $[\alpha]_D$ were measured on a Perkin-Elmer 241 MC or 343 polarimeter, at 20 °C, in $CHCl_3$. Concentrations are given in g/100 mL. Nuclear magnetic resonance ($^1H$ and $^{13}C$) spectra were recorded at 300 MHz for proton and 75 MHz for carbon (Bruker Avance 300) or 500 MHz for proton and 125 MHz for carbon (Bruker Avance 500)

using deuterated chloroform ($CDCl_3$) or deuterated DMSO ($(CD_3)_2SO$). Chemical shifts are reported in ppm relative to residual $CHCl_3$ in $CDCl_3$ (7.26 and 77.16 ppm) or residual $(CHD_2)(CD_3)SO$ in $(CD_3)_2SO$ (2.50 ppm). NMR coupling constants (*J*) are reported in Hertz. Infrared (IR) spectra were recorded using a FTIR-8400S Shimadzu apparatus. Products were analyzed as thin films deposited on a Se-Zn crystal by evaporation from $CH_2Cl_2$ solutions. Low resolution mass spectra were obtained using a ThermoFinnigan LCQ Quantum spectrometer or using a FinniganMat TSQ7000. High Resolution Mass Spectrometry (HRMS) analyses were performed at the University of Mons Hainaut (Belgium).

*(S)-tert-butyl 2-oxoazetidin-3-ylcarbamate* (**1**).

A modified procedure from literature was used.[8]

Compound **14** (1.00 g, 3.42 mmol) dissolved in methanol (40 mL) was placed under $H_2$ at rt in the presence of Raney-Ni (50% in water) catalyst for 12 h. The mixture was then filtered through a pad of Celite and concentrated under reduced pressure to provide **1** as a white solid (0.64 g, 100%), which was used without further purification. $R_f$=0.58 (EtOAc); $^1$H NMR (300 MHz, $CDCl_3$): δ=6.13-5.96 (br s, 1H, N*H* β-lactam), 5.31-5.20 (br d, *J*=6.7 Hz, 1H, N*H*-Boc), 4.83 and 4.59 (2 br s, 1H, rotamers, C*H* β-lactam), 3.65-3.54 (m, 1H, C$H_2$ β-lactam), 3.36-3.30 (dd, *J*=2.6, 5.5 Hz, 1H, C$H_2$ β-lactam), 1.44 ppm (s, 9H, Boc); MS (ESI) *m/z*: 209 $[M + Na]^+$.

Spectral data are concordant to those reported in the literature.[7,18]

*(S)-tert-butyl 1-hydroxy-2-oxoazetidin-3-ylcarbamate* (**2**).

A modified procedure from literature was used.[7]

To a stirred solution of **14** (150 mg, 0.51 mmol) in methanol (15 mL) were added 10 mg of 10% Pd/C. After being stirred under an hydrogen

atmosphere for 3 h at room temperature, the mixture was filtered through a short pad of Celite and concentrated under reduced pressure to provide **2** as a white solid (103 mg, 100%), which was used without further purification. $^1$H NMR (300 MHz, $CDCl_3$): δ=5.78-5.67 (br d, *J*=7.4 Hz, 1H, N*H*-Boc), 4.71-4.50 (m, 1H, C*H* β-lactam), 3.92-3.83 (m, 1H, C$H_2$ β-lactam), 3.67-3.50 (m, 1H, C$H_2$ β-lactam), 1.43 ppm (s, 9H, Boc); MS (APCI) *m*/*z*: 203 $[M + H]^+$. Spectral data are concordant to those reported in the literature.[7]

*(S)-benzyl 2-oxoazetidin-3-ylcarbamate* (**3**).

A modified procedure from literature was used.[14]

To a stirred suspension of $NaHCO_3$ (146 mg, 1.74 mmol) in MeCN (20 mL) at reflux was added methanesulfonyl chloride (34 μL, 0.43 mmol), followed by the portionwise addition of the compound **18** (90 mg, 0.38 mmol) over 4 h. After 16 h under reflux, the solid was removed by filtration at 60 °C and the resulting clear reaction mixture concentrated under reduced pressure. The residue was purified by flash column chromatography (EtOAc), to provide **3** as a white solid (16 mg, 19%). $^1$H NMR (300 MHz, $CDCl_3$): δ=7.40-7.29 (m, 5H, Ph), 5.95 (br s, 1H, N*H* β-lactam), 5.59-5.45 (br d, *J*=7.1 Hz ,1H, N*H*-Cbz), 5.12 (s, 2H, C$H_2$ Cbz), 4.90-4.82 (m, 1H, C*H* β-lactam), 3.65-3.55 (m, 1H, C$H_2$ β-lactam), 3.39-3.32 ppm (m, 1H, C$H_2$ β-lactam).

Spectral data are concordant to those reported in the literature.[14]

*(S)-tert-butyl 1-(benzyloxyamino)-3-hydroxy-1-oxopropan-2-ylcarbamate* (**13**).

A modified procedure from literature was used.[6,10]

A solution of *N*,*N*-dicyclohexylcarbodiimide (DCC) (14.09 g, 68.31 mmol) in THF (50 mL) was added dropwise, at 0 °C, into a well-stirred solution of

Boc-L-serine **12** (13.35 g, 65.05 mmol) and *O*-(phenylmethyl)hydroxylamine (7.57 mL, 65.05 mmol) in THF (600 mL). The reaction mixture was stirred for 1 h at 0 °C and overnight at room temperature. The obtained white precipitate (DCU) solution was separated by filtration and the resulting clear reaction mixture concentrated under reduced pressure. After addition of $Et_2O$, the precipitate was filtered, washed with $Et_2O$ and dried under reduced pressure to provide **13** as a white solid (19.58 g, 97%). $R_f$=0.32 (hexane/EtOAc 3/7); $^1$H NMR (300 MHz, $CDCl_3$): δ=9.29 (br s, 1H, N*H*-OBn), 7.43-7.33 (m, 5H, Ph), 5.59-5.49 (br d, *J*=5.9 Hz,1H, N*H*-Boc), 4.91 (s, 2H, C$H_2$ Bn), 4.13-3.96 (m, 2H, C*H* and one H C$H_2$-OH), 3.64-3.59 (m, 1H, one H C$H_2$-OH), 1.42 ppm (s, 9H, Boc); $^{13}$C (75 MHz, $CDCl_3$): δ=169.2 (*C*=O-NH-O), 156.3 (*C*=O Boc), 135.0 (*C*quat Ph), 129.4 (2C Ph), 129.0 (Ph), 128.7 (2C Ph), 81.0 (*C*quat t-Bu), 78.5 (*C*$H_2$ Bn), 62.6 (*C*$H_2$-OH), 52.9 (*C*H), 28.4 (3*C*$H_3$) ppm; MS (ESI) *m*/*z*: 309 [M - H]$^-$.

Spectral data are concordant to those reported in the literature.[6]

*(S)-tert-butyl 1-(benzyloxy)-2-oxoazetidin-3-ylcarbamate* (**14**).

A modified procedure from literature was used.[6,10]

A solution of $PPh_3$ (7.90 g, 30.13 mmol) in dry MeCN (124 mL) was added dropwise, at 0 °C and under an inert atmosphere, to a stirred solution of **13** (8.50 g, 27.39 mmol) in dry MeCN (75 mL), containing $CCl_4$ (2.91 mL, 30.13 mmol) and anhydrous triethylamine (5.73 mL, 41.08 mmol). The resulting clear reaction mixture was stirred for 2 h at 0 °C and overnight at room temperature. After completion of the reaction, the obtained white precipitate was separated by filtration and the resulting clear reaction mixture concentrated under reduced pressure. The residue was redissolved with EtOAc (150 mL), washed with a saturated $NH_4Cl$ solution (2 x 100

mL) and brine (150 mL). After drying over $MgSO_4$ and removing the solvent under reduced pressure, the residue was purified by flash column chromatography (hexane/EtOAc 3/2), to provide **14** as a white solid (6.21 g, 78%). $R_f$=0.38 (hexane/EtOAc 3/2); $^1$H NMR (300 MHz, $CDCl_3$): δ=7.43-7.36 (m, 5H, Ph), 5.06-4.95 (m, 3H, C$H_2$ OBn and N*H*-Boc), 4.53 (br s, 1H, C*H* β-lactam), 3.56-3.46 (m, 1H, C$H_2$ β-lactam), 3.23-3.19 (dd, *J*=2.2, 4.7 Hz, 1H, C$H_2$ β-lactam), 1.42 ppm (s, 9H, Boc); $^{13}$C (75 MHz, $CDCl_3$): δ=163.0 (*C*=O β-lactam), 155.0 (*C*=O Boc), 134.7 (*C*quat Ph), 129.1 (2C Ph), 129.0 (Ph), 128.6 (2C Ph), 80.2 (*C*quat t-Bu), 77.7 (*C*$H_2$ Bn), 54.2 (*C*H β-lactam), 53.3 (*C*$H_2$ β-lactam), 28.2 (3*C*$H_3$) ppm.

Spectral data are concordant to those reported in the literature.[6]

*(S)-3-amino-2-(benzyloxycarbonylamino)propanoic acid* (**18**).

A modified procedure from literature was used.[13]

A slurry of N-(benzyloxycarbonyl)-L-asparagine **17** (5.00 g, 18.8 mmol) and iodosobenzene diacetate (7.26 g, 22.5 mmol) in EtOAc (46 mL), MeCN (48 mL) and water (24 mL) was cooled at 10 °C and stirred for 30 min. The mixture was then warmed to rt and stirred overnight. The reaction mixture was cooled to 5 °C and then the precipitate was filtered, washed with EtOAc (200 mL) and dried under reduced pressure to provide **18** as a white solid (4.32 g, 96%); $^1$H NMR (300 MHz, $(CD_3)_2SO$/TFA): δ=7.92 (br s, 3H, N$H_3^+$), 7.74-7.68 (d, *J*=8.6 Hz, 1H, N*H*-Cbz), 7.39-7.28 (m, 5H, Ph), 5.07 (s, 2H, C$H_2$ Cbz), 4.35-4.25 (m, 1H, C*H*), 3.31-3.18 (m, 1H, C$H_2$-$NH_3^+$), 3.08-2.95 ppm (m, 1H, C$H_2$-$NH_3^+$).

Spectral data are concordant to those reported in the literature.[13]

*(S)-benzyl 2-oxo-1-pent-4-enoylazetidin-3-ylcarbamate* (**21**).

A modified procedure from literature was used.[16]

To a stirred solution of β-lactam **3** (100 mg, 0.45 mmol) in dry $CH_2Cl_2$ (4 mL) were added pyridine (74 μL, 0.91 mmol) and 4-pentenoyl chloride (101 μL, 0.91 mmol). The mixture was stirred for 24 h at room temperature and then diluted with $CH_2Cl_2$ (20 mL) and the organic layer was washed with HCl 2 M solution (25 mL), a saturated $NaHCO_3$ solution (25 mL) and brine (25 mL). After drying over $MgSO_4$ and removing the solvent under reduced pressure, the residue was purified by flash column chromatography (hexane/EtOAc 3/2), to provide **21** as a white solid (83 mg, 60%). $R_f$=0.60 (hexane/EtOAc 1/1); m.p. 68.0-68.8 °C; $[\alpha]_D^{20}$ +17.2 (*c* 3.0, $CHCl_3$); $^1$H NMR (300 MHz, $CDCl_3$): δ=7.37-7.28 (m, 5H, Ph), 5.90-5.74 (m, 1H, C*H*=$CH_2$), 5.63-5.54 (br d, *J*=7.6 Hz, 1H, N*H*-Cbz), 5.16-4.97 (m, 4H, C$H_2$ Cbz and CH=C$H_2$), 4.72-4.64 (m, 1H, C*H* β-lactam), 3.90-3.82 (m, 1H, C$H_2$ β-lactam), 3.70-3.63 (dd, *J*=3.9, 7.6 Hz, 1H, C$H_2$ β-lactam), 2.92-2.74 (m, 2H, C$H_2$-C=O acyl chain), 2.47-2.36 ppm (m, 2H, C$H_2$-CH=$CH_2$); $^{13}$C (75 MHz, $CDCl_3$): δ=170.6 (*C*=O acyl chain), 164.8 (*C*=O β-lactam), 155.4 (*C*=O Boc), 136.4 (*C*H=$CH_2$), 135.6 (*C*quat Ph), 128.8 (2C Ph), 128.6 (Ph), 128.4 (2C Ph), 115.9 (CH=*C*$H_2$), 67.7 (*C*$H_2$ Cbz), 56.8 (*C*H β-lactam), 45.3 (*C*$H_2$ β-lactam), 36.0 (*C*$H_2$-C=O acyl chain), 27.9 (*C*$H_2$-CH=$CH_2$) ppm; IR: ν=3338-3334, 3068, 2974-2918, 1793, 1693, 1679, 1525 $cm^{-1}$; MS (ESI) *m/z*: 325 $[M + Na]^+$, 303 $[M + H]^+$; HRMS (ESI): calcd. for $C_{16}H_{18}N_2O_4Na$ $[M + Na]^+$ 325.1164, found 325.1163.

*(S)-benzyl 2-oxo-1-pent-4-enoylazetidin-3-yl(pent-4-enoyl)carbamate* (**22**).

A stirred solution of compound **21** (50 mg, 0.16 mmol) in anhydrous THF (1 mL) was cooled to -78 °C. n-BuLi 2.5N in hexane (73 μL, 0.18 mmol) was

slowly added and the mixture was stirred for 45 minutes. 4-Pentenoyl chloride (20 μL, 0.18 mmol) was then added by syringe and the mixture was stirred for another hour. The mixture was then warmed to rt over 4 h and then quenched with saturated $NH_4Cl$ (5 mL). The resulting mixture was extracted with EtOAc (2 x 5 mL) and the organic layers were washed with a saturated $NaHCO_3$ solution (10 mL) and brine (10 mL). After drying over $MgSO_4$ and removing the solvent under reduced pressure, the residue was purified by flash column chromatography (hexane/EtOAc 4/1), to provide **22** as a pale-yellow oil (16 mg, 25%). $R_f$=0.50 (hexane/EtOAc 4/1); $[\alpha]_D^{20}$ +9.5 (*c* 1.6, $CHCl_3$); $^1$H NMR (300 MHz, $CDCl_3$): δ=7.42-7.32 (m, 5H, Ph), 5.88-5.70 (m, 3H, 2C*H*=$CH_2$ and C*H* β-lactam), 5.26-5.18 (m, 2H, C$H_2$ Cbz), 5.10-4.97 (m, 4H, 2CH=C$H_2$), 3.85-3.78 (m, 1H, C$H_2$ β-lactam), 3.61-3.55 (dd, *J*=4.1, 7.2 Hz, 1H, C$H_2$ β-lactam), 3.05-2.98 (m, 2H, C$H_2$-C=O acyl chain), 2.73-2.46 (m, 2H, C$H_2$-C=O acyl chain), 2.43-2.28 ppm (m, 4H, 2C$H_2$-CH=$CH_2$); $^{13}$C (125 MHz, $CDCl_3$): δ=174.7 (*C*=O acyl chain), 170.4 (*C*=O acyl chain), 163.8 (*C*=O β-lactam), 152.6 (*C*=O Cbz), 136.6 (*C*H=$CH_2$), 136.5 (*C*H=$CH_2$), 133.7 (*C*quat Ph), 129.4 (Ph), 129.2 (2C Ph), 129.1 (2C Ph), 115.8 (2CH=*C*$H_2$), 70.2 (*C*$H_2$ Cbz), 57.1 (*C*H β-lactam), 43.8 (*C*$H_2$ β-lactam), 37.5 (*C*$H_2$-C=O acyl chain), 35.7 (*C*$H_2$-C=O acyl chain), 28.8 (*C*$H_2$-CH=$CH_2$), 27.8 (*C*$H_2$-CH=$CH_2$) ppm; IR: ν=2918, 1799, 1749, 1703 $cm^{-1}$; MS (ESI) *m/z*: 407 $[M + Na]^+$; HRMS (ESI): calcd. for $C_{21}H_{24}N_2O_5Na$ $[M + Na]^+$ 407.1583, found 407.1587.

*(S)-3-(tert-butoxycarbonylamino)-2-oxoazetidin-1-yl pent-4-enoate* (**23**).

To a stirred solution of β-lactam **2** (100 mg, 0.49 mmol) in dry MeCN (7 mL) were added a catalytic amount of DMAP, anhydrous triethylamine (76 μL, 0.544 mmol) and 4-pentenoyl chloride (66 μL, 0.59 mmol). The mixture

was stirred for 1 hour at room temperature and then concentrated under reduced pressure. The residue was redissolved with $CH_2Cl_2$ (25 mL) and the organic layer was washed with a saturated $NH_4Cl$ solution (25 mL), a saturated $NaHCO_3$ solution (25 mL) and brine (25 mL). The organic layer was dried over $MgSO_4$ and the solvent was removed under reduced pressure to provide **20** as a pale-yellow oil (132 mg, 94%). $R_f$=0.69 (hexane/EtOAc 3/2); $[\alpha]_D^{20}$ +15.7 (*c* 4.7, $CHCl_3$); $^1$H NMR (300 MHz, $CDCl_3$): δ=5.88-5.72 (m, 1H, C*H*=$CH_2$), 5.34-5.24 (br d, *J*=7.1 Hz, 1H, N*H*-Boc), 5.13-5.01 (m, 2H + 0.3H, rotamer, CH=C$H_2$ and C*H* β-lactam), 4.90-4.81 (br s, 0.7H, rotamer, C*H* β-lactam), 4.01-3.94 (m, 1H, C$H_2$ β-lactam), 3.64-3.61 (dd, *J*=2.4, 4.5 Hz, 1H, C$H_2$ β-lactam), 2.57-2.48 (m, 2H, C$H_2$-C=O acyl chain), 2.46-2.36 (m, 2H, C$H_2$-CH=$CH_2$), 1.43 ppm (s, 9H, Boc); $^{13}$C (75 MHz, $CDCl_3$): δ=170.1 (*C*=O acyl chain), 163.7 (*C*=O β-lactam), 155.0 (*C*=O Boc), 135.5 (*C*H=$CH_2$), 116.6 (CH=*C*$H_2$), 81.0 (*C*quat Boc), 55.5 (*C*$H_2$ β-lactam), 54.3 (*C*H β-lactam), 30.7 (*C*$H_2$-C=O acyl chain), 28.4 (*C*$H_2$-CH=$CH_2$), 28.3 (3*C*$H_3$) ppm; IR: ν=3346, 2980-2922, 1801, 1772, 1685, 1535 $cm^{-1}$; MS (ESI) *m/z*: 307 $[M + Na]^+$; HRMS (ESI): calcd. for $C_{13}H_{20}N_2O_5Na$ $[M + Na]^+$ 307.1270, found 307.1275.

*(S)-3-(N-(tert-butoxycarbonyl)pent-4-enamido)-2-oxoazetidin-1-yl pent-4-enoate* (**24**).

Compound **24** was synthesized according to the procedure described for the synthesis of compound **22** from compound **20** (100 mg, 0.35 mmol) but the mixture was stirred only 15 min between the addition of n-BuLi and 4-pentenoyl chloride. Flash column chromatography (hexane/EtOAc 5/1) provided **24** as a colourless oil (75 mg, 59%). $R_f$=0.38 (hexane/EtOAc 4/1); $[\alpha]_D^{20}$ +11.2 (*c* 3.4, $CHCl_3$); $^1$H NMR (300 MHz, $CDCl_3$): δ=5.90-5.74 (m, 2H, 2C*H*=$CH_2$), 5.73-5.69 (dd, *J*=3.0, 5.7 Hz, 1H, C*H* β-lactam) 5.13-4.96

(m, 4H, 2CH=C$H_2$), 3.98-3.94 (dd, *J*=4.1, 5.7 Hz, 1H, C$H_2$ β-lactam), 3.76-3.71 (dd, *J*=3.1, 3.9 Hz, 1H, C$H_2$ β-lactam), 3.06-2.88 (td, *J*=2.9, 7.5 Hz, 2H, C$H_2$-C=O-O), 2.59-2.49 (m, 2H, C$H_2$-C=O), 2.47-2.34 (m, 4H, 2C$H_2$-CH=$CH_2$), 1.54 ppm (s, 9H, Boc); $^{13}$C (75 MHz, $CDCl_3$): δ=175.1 ($CH_2$-*C*=O-O), 170.1 ($CH_2$-*C*=O), 163.8 (*C*=O β-lactam), 151.4 (*C*=O Boc), 137.0 (*C*H=$CH_2$), 135.6 (*C*H=$CH_2$), 116.6 (CH=*C*$H_2$), 115.6 (CH=*C*$H_2$), 85.7 (*C*quat Boc), 55.0 (*C*H β-lactam), 52.2 (*C*$H_2$ β-lactam), 37.7 (*C*$H_2$-C=O-O), 30.8 (*C*$H_2$-C=O), 29.0 (*C*$H_2$-CH=$CH_2$), 28.5 (*C*$H_2$-CH=$CH_2$), 28.0 (3*C*$H_3$) ppm; IR: ν=2978-2932, 1809, 1782, 1743, 1705, 1643 cm$^{-1}$; MS (ESI) *m*/*z*: 389 $[M + Na]^+$, 289 $[M + H - CO_2 - C_4H_8]^+$; HRMS (ESI): calcd. for $C_{18}H_{26}N_2O_6Na$ $[M + Na]^+$ 389.1689, found 389.1686.

*(S)-tert-butyl 2-oxo-1-pent-4-enoylazetidin-3-ylcarbamate* (**25**).

Synthesis and structural data are reported in the next chapter (Chapter 4, section **4.3**, p120, the compound is therein named **10a**).

*(S)-tert-butyl 2-oxo-1-pent-4-enoylazetidin-3-yl(pent-4-enoyl)carbamate* (**26**).

Synthesis and structural data are reported in the next chapter (Chapter 4, section **4.3**, p120, the compound is therein named **9a**).

## 6. References and notes

[1] Staudinger, H. *Justus Liebigs Ann. Chem.* **1907**, *356*, 51-123.

[2] (a) Van der Steen, F. H.; Van Koten, G. *Tetrahedron* **1991**, *47*, 7503-7524; (b) Singh, G. S.; D'hooghe, M.; De Kimpe, N. in *Comprehensive Heterocyclic Chemistry III* (Ed.: C. Stevens),

Elsevier, Oxford, **2008**, vol. 2, chapter 2.01, pp. 1-110; (c) Brandi, A.; Cicchi, S.; Cordero, F. M. *Chem. Rev.* **2008**, *108*, 3988-4035; (d) Aranda, M. T.; Pérez-Faginas, P.; González-Muñiz R. *Curr. Org. Synth.* **2009**, *6*, 325-341.

[3] Pfaendler, H. R.; Hoppe, H. *Heterocycles* **1985**, *23*, 265-272.

[4] Martin-Zamora, E.; Ferrete, A.; Llera, J. M.; Munoz, J. M.; Pappalardo, R. R.; Fernandez, R.; Lassaletta, J. M. *Chem. Eur. J.* **2004**, *10*, 6111-6129.

[5] Palomo, C.; Aizpurua, J. M.; Legido, M.; Galarza, R. *Chem. Comm.* **1997**, 233-234.

[6] Miller, M. J.; Mattingly, P. G.; Morrison, M. A.; Kerwin, J. F., Jr. *J. Am. Chem. Soc.* **1980**, *102*, 7026-7032.

[7] Mattingly, P. G.; Miller, M. J. *J. Org. Chem.* **1980**, *45*, 411-415.

[8] (a) Qabar, M. N.; Kahn, M. *Tetrahedron Lett.* **1996**, *37*, 965-968; (b) Kiyota, H.; Takai, T.; Saitoh, M.; Nakayama, O.; Oritani, T.; Kuwahara, S. *Tetrahedron Lett.* **2004**, *45*, 8191-8194; (c) Kiyota, H.; Takai, T.; Shimasaki, Y.; Saitoh, M.; Nakayama, O.; Takada, T.; Kuwahara, S. *Synthesis*, **2007**, *16*, 2471-2380.

[9] (a) Hirose, T.; Chiba, K.; Mishio, S.; Nakano, J.; Uno, H. *Heterocycles* **1982**, *19*, 1019-1022; (b) Baldwin, J. E.; Adlington, R. M.; Birch, D. J. *Tetrahedron Lett.* **1985**, *26*, 5931-5934; (b) Zercher, C. K.; Miller, M. J. *Tetrahedron Lett.* **1989**, *30*, 7009-7012

[10] Strazzolini, P.; Dall'Arche, M. G.; Zossi, M.; Pavsler, A. *Eur. J. Org. Chem.* **2004**, 4710-4716.

[11] Scheurer A.; Mosset P.; Bauer W.; Saalfrank R. W. *Eur. J. Org. Chem*. **2001**, 3067-3074.

[12] Gordon, E. M.; Ondetti, M. A.; Pluscec, J.; Cimarusti, C. M.; Bonner, D. P.; Sykes, R. B. *J. Am. Chem. Soc.* **1982**, *104*, 6053-6060.

[13] (a) Chhabra, S. R.; Mahajan, A.; Chan, W. C. *J. Org. Chem*. **2002**, *67*, 4017-4029; (b) Zhang, L.; Kauffman, G. S.; Pesti, J. A.; Yin, J. *J. Org. Chem*. **1997**, *62*, 6918-6920.

[14] (a) Lall, M. S.; Ramtohul, Y. K.; James, M. N. G.; Vederas, J. C. *J. Org. Chem.* **2002**, *67*, 1536-1547; (b) Loewe, M. F.; Cvetovich, R. J.; Hazen, G. G. *Tetrahedron Lett.* **1991**, *32*, 2299-2302.

[15] Mukaiyama, T.; Usui, M.; Saigo K. *Chem. Lett.* **1976**, *5*, 49-50.

[16] Urbach, A.; Dive, G.; Tinant, B.; Duval, V.; Marchand-Brynaert, J. *Eur. J. Med. Chem.* **2009**, *44*, 2071-2080.

[17] Matsuda, A.; Shinozaki, M.; Suzuki, M.; Watanabe, K.; Miyasaka, T. *Synthesis* **1986**, 385-386

[18] Floyd, D. M.; Fritz, A. W.; Pluscec, J.; Weaver, E. R.; Cimarusti, C. M. *J. Org. Chem.* **1982**, *47*, 5160-5167.

# *Chapter 4 - Cyclodimerization by Ring-Closing Metathesis*

The paper was published in *Tetrahedron* **2010**, *66*, 9519-9527.

***Title***

Cyclodimerization by Ring-Closing Metathesis: synthesis, computational and biological evaluation of novel *bis*-azetidinyl-macrocycles.

***Authors***

Aline Sliwa,[a] Georges Dive,[b] Jean-Louis Habib Jiwan[a] and Jacqueline Marchand-Brynaert[a,*]

***Affiliations***

[a] Institute of Condensed Matter and Nanosciences, Université catholique de Louvain, Place Louis Pasteur 1, B-1348 Louvain-la-Neuve, Belgium

[b] Centre d'ingénierie des Protéines, Université de Liège, Bâtiment B6, Allée du 6 Août, 4000 Sart-Tilman (Liège), Belgium

* Corresponding author. Tel.: +32 (0)10 47 27 40; fax: +32 (0)10 47 41 68; e-mail: jacqueline.marchand@uclouvain.be

***Keywords***

RCM; β-lactams; Cyclodimers; B3LYP calculations; R39 inhibitors

***Abstract***

During our research on novel, non-traditional, bicyclic β-lactams as potential inhibitors of Penicillin Binding Proteins (PBPs), we focused on the synthesis of 1,3-bridged 2-azetidinones by RCM reaction from 1,3-*bis*-ω-alkenoyl-3(*S*)-amino-2-azetidinone precursors. Submitting the precursors to RCM, we faced an unexpected problem: cyclodimerization was the preferred outcome. This peculiar reactivity, explained by a computational study, led to unprecedented bis-azetidinyl macrocycles acting as potent inhibitors of R39 D,D-peptidase, a bacterial model enzyme for PBPs.

## 1. Introduction

Ring-closing metathesis (RCM) of α,ω-dienes is nowadays a very common reaction used for the construction of medium-sized and macrocyclic organic compounds. Its wide scope and use as the key step in numerous total syntheses of complex target molecules have been reviewed[1] recently. The thermodynamic and kinetic aspects of the RCM and related reactions catalyzed by ruthenium-carbene complexes have been discussed as well.[2]

Despite an increasing amount of technical reports, there are still no clear rules available for planning a new RCM synthesis: different catalysts and loading, different substrate concentrations, addition and reaction times, different solvents, additives and temperatures have to be tested for maximizing the yield of the desired cyclic product. Beside the experimental conditions, the ring size to be formed, the substrate structure, its substitution pattern, steric and conformational factors will also influence the outcome of the reaction, *i.e.* the product E/Z ratio, the formation of isomerized or/and

oligomerized by-products. In general, oligomerization is considered detrimental to the RCM reaction[2] and the corresponding products are neither isolated nor characterized. But in few cases, dimers, and in particular cyclic dimers, are highly desired products.[3] Recently, a double-centered catalyst has been designed to favor the dimer ring-closing metathesis reaction,[4] and the competitive pathways leading to the cyclic monomer and dimer have been theoretically studied with 1,7-octadiene as model substrate.[5]

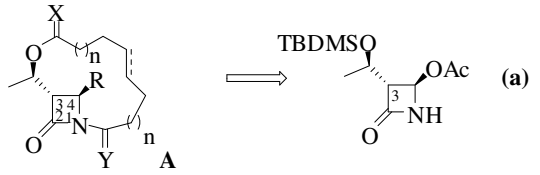


R = H, n-Pr, OAc
X = Y = O ; X = Y = H,H ; X = O and Y = H,H
TBDMS = tert-butyldimethylsilyl

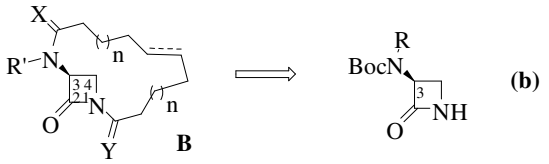


R' = Boc, H, Me ; R = H, Me
X = Y = O

**Figure 1**. Two Families of 1,3-bridged 2-azetidinones.

We have previously applied the RCM reaction for the preparation of 1,3-bridged bicyclic β-lactams **A** (*i.e.* 2-azetidinones) derived from the commercial acetoxy-azetidinone used as the chiral precursor of carbapenem antibiotics[6] (**Figure 1**, Eq. (a)). Series of compounds featuring 12 and 13-membered rings (including HC=CH double bond or the reduced motif) have been obtained and evaluated as potential inhibitors of Penicillin Binding Proteins (PBPs). The weak activities recorded were attributed, among other factors, to the steric effect of the macrocycles which hinders the so-called α-

face of the azetidinone ring and thus might prevent nucleophilic attack by the active serine of PBPs. This hypothesis derives from a theoretical investigation of the reactivity of the bridged azetidinones **A** when processed into a model of serine peptidase active site.[6] To further our research on novel, non-traditional, bicyclic β-lactams, we have focused on 1,3-bridged compounds **B** derived from 3-amino-2-azetidinone featuring the amino substituent and the chirality of penicillins and cephalosporins at the C(3) carbon (**Figure 1**, Eq. (b)). This inversion of configuration regarding the carbapenem chiron (see Eq. (a)) should position the macrocycle above the β-face of the azetidinone ring and consequently make the serine nucleophilic attack easier on the α-face during the processing of molecules **B** by PBPs.

In this article, we describe our synthetic efforts toward the target molecules **B** belonging to the *bis*-acylated family (X = Y = O). From the 3-amino-2-azetidinone chiron, three series of RCM precursors have been prepared (R' = Boc, H or Me) varying by the length of the ω-alkenoyl chain fixed on the N(1) and N-C(3) atoms. Surprisingly, under RCM conditions, the isolated products were all cases but one the cyclic dimers instead of the expected cyclic monomers **B**. These observations stimulated a theoretical investigation of the possible cyclization reactions. Our study highlights the dramatic effect of accessible conformations and flexibility of precursors on the intra- or intermolecular ring closure, particularly when the substrates possess amide, imide and carbamate functions.

The inhibition potential of our compounds (precursors and RCM products) has been tested against R39 D,D-peptidase which is a commonly used model for bacterial enzymes.

## 2. Results and discussion

### 2.1. Synthesis

The RCM reaction was chosen as the key-step for the synthesis of 1,3-bridged bicycles **B**, a strategy which has already been successfully used for the preparation of 1,3-bridged derivatives **A**.[6] The precursors are chiral azetidin-2-ones **C** equipped with ω-alkenoyl chains on the positions N(1) and C(3)-N (**Figure 2**). The starting chirons, *i.e.* (*S*)-3-(t-butyloxycarbonyl)amino-2-azetidinone and (*S*)-3-N-methyl(t-butyloxycarbonyl)amino-2-azetidinone, derive from commercially available Boc-L-serine and Boc-Me-L-serine, respectively.

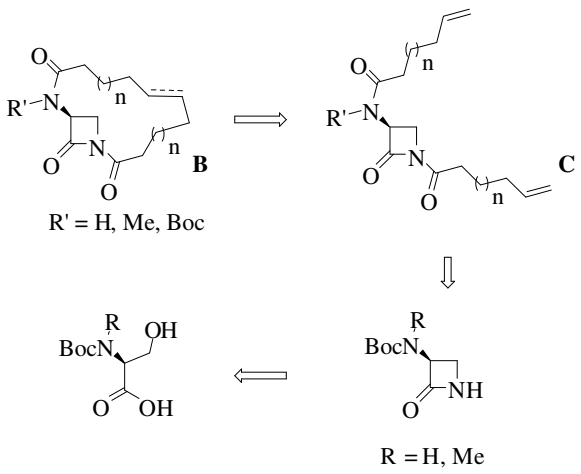


**Figure 2**. General RCM strategy.

Boc-L-serine **1** was converted, in nearly quantitative yield, into the corresponding hydroxamate **2**, employing O-benzylhydroxylamine and DCC.[7] Intramolecular cyclization was performed with the method proposed by Miller,[7] in the presence of $PPh_3$ and $CCl_4$, and afforded the β-lactam **3** in

78% yield. Subsequent hydrogenation in the presence of Raney nickel[8] gave the desired chiron **4**[9] in quantitative yield (**Scheme 1**). In the first attempt to obtain the corresponding N-Me chiron **8**, we considered the direct methylation[10] of **3** into the desired intermediate **7**. This reaction proceeded with 62% yield at the mmol scale, but the scaling-up was not successful. So we developed a similar route toward the N-Me derivatives as for the N-H derivatives, starting from Boc-Me-L-serine **5**. This compound was converted into hydroxamate **6** employing EDCI in 91% yield. The β-lactam **7** was obtained in 82% yield and subsequent hydrogenation afforded the chiron **8** in 64% yield.

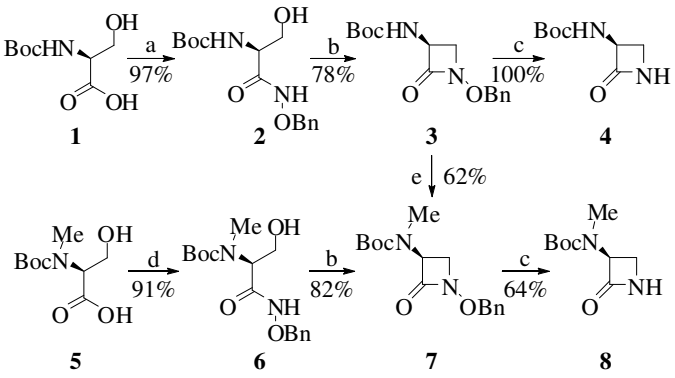


**Scheme 1**. Synthesis of chirons **4** and **8**. Reagents and conditions: (a) DCC, $NH_2OBn$, THF, 0 °C to rt; (b) $PPh_3$, $CCl_4$, TEA, $CH_3CN$, 0 °C to rt; (c) $H_2$, Raney-Ni, MeOH, rt; (d) EDCI, $NH_2OBn$, $CH_2Cl_2$, 0 °C to rt; (e) $Me_2SO_4$, LiHMDS, THF, -78 °C to rt.

The N-Boc *bis*-acylated monocyclic azetidinones **9a-c** were obtained in one step by treatment of the chiron **4** with 2 equivalents of alkenoyl chlorides in the presence of 2 equivalents of lithium hexamethyldisilazide (**Scheme 2**). 4-pentenoyl chloride (n = 0) is commercially available, while 5-hexenoyl chloride (n = 1) and 6-heptenoyl chloride (n = 2) have been

previously synthesized starting from the corresponding commercial carboxylic acid.[11]

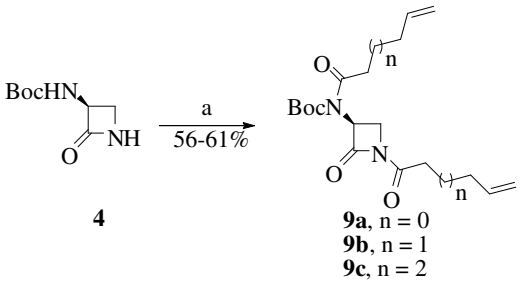


**Scheme 2.** Synthesis of *bis*-acylated **9**. Reagents and conditions: (a) alkenoyl chloride, LiHMDS, THF, -78 °C to rt.

For the preparation of N-H and N-Me *bis*-acylated precursors, a three-step sequence was used (**Scheme 3**). The chiron **4** was mono-acylated at the N(1) position regioselectively under mild conditions giving the series of compounds **10a-c**. Then, the Boc protecting group was removed with trifluoroacetic acid and the free amine function was acylated with the alkenoyl chlorides affording the series of compounds **12a-c**. Similarly, the chiron **8** was mono-acylated (compounds **11a-c**), N-deprotected and acylated again to produce the N-Me precursors **13a-c**.

The first attempts at RCM were performed on *bis*-acylated compounds with n = 0 (*i.e.* **9a**, **12a** and **13a**) with the view to forming 12-membered macrocycles, under standard reaction conditions ($CH_2Cl_2$, 40 °C, 5 mM) in the presence of second generation Grubbs catalyst (5 mol%). Conversion was not observed in any case. To prevent the possible deactivation of the Ru-catalyst by the formation of a stable chelated alkylidene ring, we tried to use Ti(O*i*Pr$_4$)[12] as an additive, without success. Increasing the temperature (DCE, 80 °C), with or without Ti(O*i*Pr$_4$), only led to the degradation of the starting material.

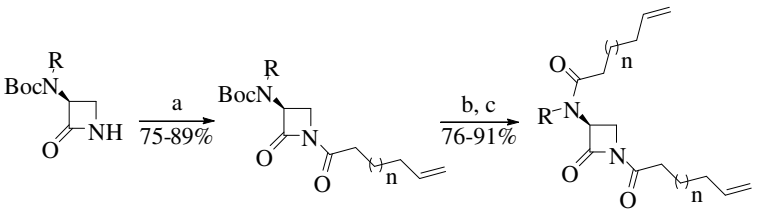


**4**, R = H
**8**, R = Me

**10a**, R = H, n = 0
**10b**, R = H, n = 1
**10c**, R = H, n = 2
**11a**, R = Me, n = 0
**11b**, R = Me, n = 1
**11c**, R = Me, n = 2

**12a**, R = H, n = 0
**12b**, R = H, n = 1
**12c**, R = H, n = 2
**13a**, R = Me, n = 0
**13b**, R = Me, n = 1
**13c**, R = Me, n = 2

**Scheme 3**. Synthesis of bis-acylated **12-13**. Reagents and conditions: (a) alkenoyl chloride, pyridine, $CH_2Cl_2$, rt; (b) TFA, $CH_2Cl_2$, 0 °C to rt; (c) alkenoyl chloride, TEA, $CH_2Cl_2$, 0 °C to rt.

Next, RCM reactions were tested on compounds with n = 1 (*i.e.* **9b**, **12b** and **13b**) leading in principle to 14-membered macrocycles, under the same standard conditions previously described. In each case, monitoring the reaction by TLC showed apparently the progressive formation of a single product over a time period of 24 h. After several chromatographies, products were isolated with moderate yields (35-44%). Products obtained from **9b**, **12b** and **13b** are named **15b**, **16b** and **17b** (**Figure 3**), respectively. Their structural assignment proved to be an unexpectedly difficult problem: the $^{1}H$ and $^{13}C$ NMR spectra were not well resolved,[2] most probably due to the presence of several rotamers, stereoisomers (mixtures of E/Z olefins), regioisomers (HH and HT dimers) and possible contamination by lower homologs (double bond migration and cyclization with the formal extrusion of one or two $CH_2$ groups). The $^{13}C$ NMR spectra just showed the disappearance of the terminal olefin bonds and the preservation of the β-lactam ring, with the presence of the typical signals of C(3) and C(4) (**Table 1**, entries 2, 4 and 6). In fact, mass spectrometry (MS) turned out to be the appropriate tool for accurate structural determination. Spectra were recorded

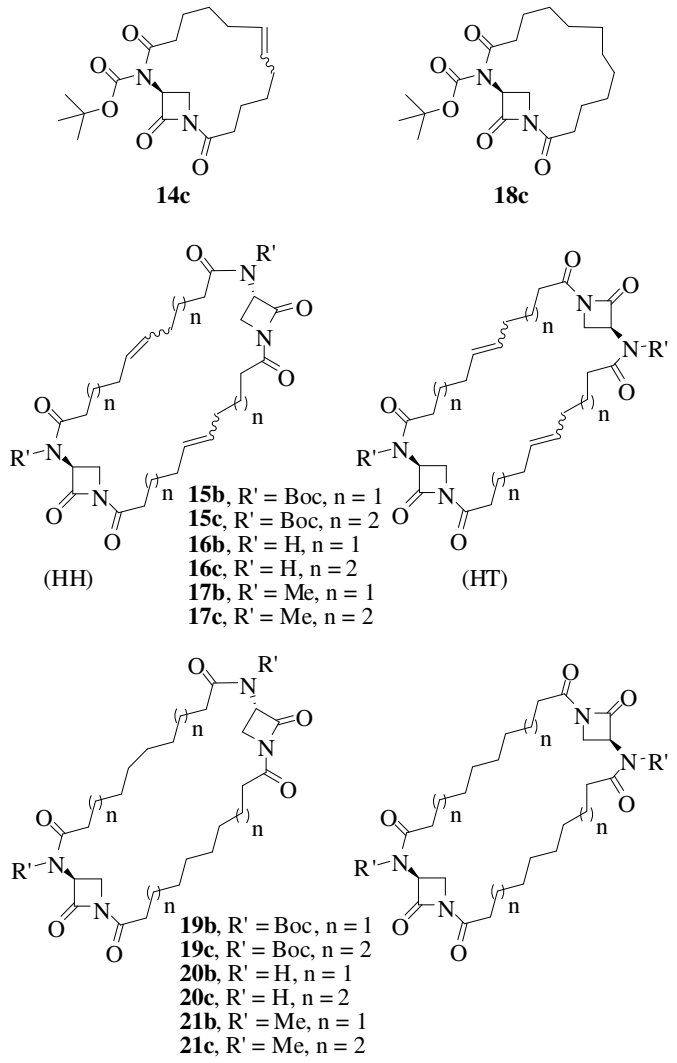


**Figure 3**. Compounds synthesized by RCM.

in electrospray ionization (ESI) and atmospheric pressure chemical ionization (APCI) modes for comparison. All the isolated compounds were cyclic dimers, most probably a mixture of head-head (HH) and head-tail (HT) isomers, as drawn in the **Figure 3**. ESI is a soft ionization method but well-known to favor the formation of dimeric adducts during the evaporation step.

Moreover, ionization by formation of $Na^+$ or $K^+$ adducts is also frequently observed. These adducts can be monomeric or dimeric. In our case, as observed during the analysis of the *bis*-acylated precursors, formation of dimeric $Na^+$ adducts was the major ionization process in ESI. So for the compounds issued of the RCM, we could not be sure that we really observe a cyclodimer compound in complex with $Na^+$ or two cyclomonomer compounds in complex with $Na^+$. To confirm, we applied a somewhat harder method of ionization, APCI not known to favor formation of adducts, which showed that the compounds are really the cyclodimers (**Table 1**). Moreover, the analysis of the ESI spectra allowed us to detect the presence, in relatively weak abundance, of lower homologs (double bond migration and cyclization with the formal extrusion of one $CH_2$ group).

The RCM reactions were finally tested on compounds with n = 2 (*i.e.* **9c**, **12c** and **13c**) in the same standard conditions as previously. 16-Membered cyclomonomers are expected, but as previously for compounds with n = 1, the reactions afforded the cyclodimers **15c**, **16c** and **17c** respectively in modest yields (10-30%) (**Table 1** and **Figure 3**). Surprisingly, in one case (starting material **9c**), the macrocyclic monomer **14c** was also obtained (**Table 1** and **Figure 3**), but in low yield (9%).

The monomer **14c** and the series of cyclodimers **15b-c**, **16b-c** and **17b-c** were subjected to catalytic hydrogenation to produce the corresponding saturated macrocycles **18c** and **19b-c**, **20b-c** and **21b-c** respectively (**Figure 3**).

*Bis*-acylated precursors with n = 0 did not cyclize at all: neither the cyclomonomers nor the cyclodimers could be detected. *Bis*-acylated precursors with n = 1 gave cyclodimers but did not cyclize into the monomers, therefore we suspected that the length of the carbon chain bearing the olefin was too short to afford the 14-sized macrocycle. On the

other hand, the formation of compound **14c**, proves that the chain length is long enough to produce the 16-sized cyclic product, even if the dimerization remains the preferred process. We set out to find reaction conditions to promote the formation of cyclomonomer derived from **12c** (n = 2). There are numerous parameters that could influence the outcome of the RCM, and there are no pre-established conditions which would guarantee the successful production of a desired compound. We have tested several parameters, such as the choice of the catalyst, the solvent, the temperature, the concentration and the reaction time.[2]

First and second generation Grubbs or Hoveyda-Grubbs and Neolyst M2 catalysts were tested but in all cases, they only afforded the cyclodimer **20c** (n = 2). Carrying out the RCM reactions at room temperature also produced the cyclodimer. It is known that increasing the reaction temperature can control the product distribution (monomer versus dimer) in RCM macrocyclization.[13] But in our case, the RCM reaction in refluxing DCE afforded only the cyclodimer, just faster than at room temperature. Decreasing the concentration of the reaction, from 5 mM to 1 mM, or using the "infinite dilution" conditions[14] led to a lower yield of the cyclodimer; the desired cyclomonomer was never detected. The results of these various attempts seems to point toward intrinsic structural parameters governing the outcome of our RCM reactions. In the next section we describe *ab initio* calculations that explain our results.

### 2.2. Computational chemistry

The almost exclusive formation of macrocyclic dimers instead of cyclic monomers under RCM conditions is rarely mentioned in previous

literature and thus deserves to be examined from the theoretical point of view.

**Table 1**

Selected structural data of cyclic dimers and monomer.

| Entry | Compound | $^{13}C$ $C_4$; $C_3$; C=C (ppm) | Isolated Yield[a] (%) |
|---|---|---|---|
| 1 | **14c** | 44.6<br>59.7<br>130.6 and 131.1 | 9[b] |
| 2 | **15b** | 43.7-43.8<br>57.5-57.8<br>129.9-130.2-130.5-131.6 | 44 |
| 3 | **15c** | 43.8-43.9<br>57.2-57.4<br>130.3-130.5-130.6-130.7 | 10[b] |
| 4 | **16b** | 46.0<br>55.7<br>130.8-131.5 | 35 |
| 5 | **16c** | 45.1-45.4<br>55.2-55.6<br>130.0-130.6-130.8-130.9 | 28 |
| 6 | **17b** | 43.1<br>61.8-63.0<br>130.4-130.7-131.0-131.4 | 43 |
| 7 | **17c** | 43.1-43.2<br>62.5-63.1<br>130.2-130.4-130.5-130.6 | 40 |

[a] Conversion (80-90%). Crude yields (50-60%). Analysis of crude mixtures by TLC, MS and NMR: oligomers, isomerized starting materials and β-lactam degradation compounds were observed as side-products. Several column chromatographies are necessary to clear out the catalyst.

[b] Very low isolated yields because major fraction is a mixture of **14c** and **15c**.

**Table 1** (continued)

| Entry | Compound | MS ESI *m/z*<br>Relative Abundance | MS APCI *m/z*<br>$[M+H]^+$ |
|---|---|---|---|
| 1 | **14c** | 401 (69) $[M+Na]^+$<br>301 (100) (401-$CO_2$ & $C_4H_8$) | 379.22275<br>($C_{20}H_{31}O_5N_2$) |
| 2 | **15b** | 723 (100) $[M+Na]^+$<br>709 (13) (723-$CH_2$)<br>623 (48) (723-$CO_2$ & $C_4H_8$)<br>523 (68) (723-2($CO_2$ & $C_4H_8$)) | 701.37449<br>($C_{36}H_{53}O_{10}N_4$) |
| 3 | **15c** | 779 (100) $[M+Na]^+$<br>765 (10) (779-$CH_2$)<br>679 (37) (779-$CO_2$ & $C_4H_8$)<br>579 (33) (779-2($CO_2$ & $C_4H_8$)) | 757.43682<br>($C_{40}H_{61}O_{10}N_4$) |
| 4 | **16b** | 523 (100) $[M+Na]^+$<br>509 (11) (523-$CH_2$) | 501.26999<br>($C_{26}H_{37}O_6N_4$) |
| 5 | **16c** | 579 (100) $[M+Na]^+$<br>565 (35) (579-$CH_2$)<br>551 (7) (579-$C_2H_4$) | 557.33287<br>($C_{30}H_{45}O_6N_4$) |
| 6 | **17b** | 551 (100) $[M+Na]^+$<br>537 (14) (551-$CH_2$) | 529.30170<br>($C_{28}H_{41}O_6N_4$) |
| 7 | **17c** | 607 (100) $[M+Na]^+$<br>593 (38) (607-$CH_2$) | 585.36407<br>($C_{32}H_{49}O_6N_4$) |

The geometry of all the molecules has been fully optimized at the B3LYP level using 6-31G basis set with added polarization functions.[15] All the calculations have been performed with the Gaussian 03 program.[16] For the Grubbs adducts, the basis sets LanL2MB and Lan2DZ, minimal and double ζ functions for the first row and Los Alamos effective core potential on the other atoms, have been used with the same B3LYP functional.[17]

The precursors have been studied (*bis*-acylated azetidinones **9** (N-Boc), **12** (N-H) and **13** (N-Me)) taking into account several factors which could have an incidence on the formation of the cyclic monomer (see Supplementary data): the tautomeric amide forms, the cis or trans geometry

of the amide functions, the conformations of the $\omega$-alkenoyl chains leading to a cycle located up or down with respect to the β-lactam plane in a range of 5-10 kcal/mol. In all cases, the OH-tautomers are less stable than the standard amide in a range of 10-20 kcal/mol. In the same way, the trans amide and the conformation *anti* of the two carbonyls of the imide are preferred. The *syn* and *anti* conformations are respectively noted *i* and *ii* (**Figure 4** and **Table 2**). The conformational space is strongly influenced by the interaction between the two imide carbonyls which tend to move off.

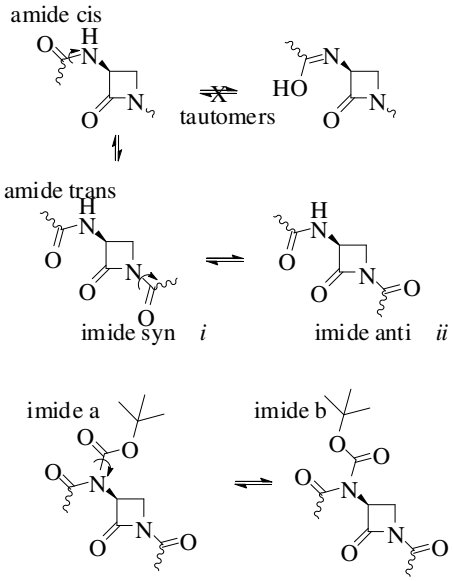


**Figure 4**. Degrees of rotation.

The trans-cis rotation barrier depends on the substituent of the amide nitrogen. The decreasing values going from N-H, N-Me and N-Boc are 20.49, 16.86 and 3.50 kcal/mol. A great number of minima could be localized in a large energy range (20 kcal/mol). The ring size also has an incidence on the conformation related to the number of $CH_2$ on both sides of

the double bond. In order to sweep a common conformational space for all the substituted molecules **9**, **12** and **13**, four conformations (amide cis or trans; imide carbonyls in conformation *i* or *ii*) have been searched and located. In the case of the N-Boc substitution, an additional degree of freedom has to be taken into account: the conformation with the two Boc carbonyls *syn* and *anti* noted a and b (**Figure 4** and **Table 2**). Last, several conformations of the 14- and 16-membered rings under the β-lactam plane have been located. They are less stable than the up conformations (*i.e.* above the β-lactam plane) with a mean energy difference of 4 kcal/mol for **9c** and 10 kcal/mol for the **9b**.

The heats of formation of the cyclic monomers have been calculated with respect to the parent conformation of the open precursor: all the values are positive (**Table 2**). **Figure 5** summarizes, on the same graph, for the compound **14c** (n = 2) the relative energies of the precursor **9c**/cyclic monomer in the selected conformations and also the respective heat of formation. Most of the time, the amide trans conformations are the most stable ones. **Figure 6** illustrates the conformational diversity for compound **14c** with 4 conformers represented. It can be noted that the heat of formation of the N-Boc substituted molecules is higher for the 12-membered ring (**9a** precursor) than for the 14- and 16-membered rings (**9b** and **9c** precursors).

In order to investigate the incidence of the conformations on the cycle formation, the two possible intermediates of the Grubbs catalyst first step addition have been computed for **9c**, **12c**, **9b** and **12b** (see Supplementary data). In N-H series, some adducts generated with both functions amide and imide in the cis or trans conformation have a favorable orientation for the ring closing into monomer.

**Table 2**

Relative energies of the precursors/cyclic monomers in the selected conformations and also the respective heat of formation resulting from the cyclisation of the **9** (N-Boc), **12** (N-H) and **13** (N-Me) precursors.

| Precursor | Geometry | Relative Energy of Open Precursors (kcal/mol) | | Relative Energy of Monomers (kcal/mol) | |
|---|---|---|---|---|---|
| | | *i* | *ii* | *i* | *ii* |
| **12a** | Amide cis | 10.21 | 4.94 | 4.19 | 0.00 |
| | Amide trans | 5.18 | 0.00 | 9.17 | 0.89 |
| **12b** | Amide cis | 10.33 | 4.77 | 4.95 | 7.12 |
| | Amide trans | 5.95 | 0.00 | 5.56 | 0.00 |
| **12c** | Amide cis | 10.22 | 4.77 | 10.26 | 1.88 |
| | Amide trans | 4.88 | 0.00 | 5.00 | 0.00 |
| **13a** | Amide cis | 8.16 | 2.84 | 18.58 | 0.00 |
| | Amide trans | 6.03 | 0.00 | 9.80 | 4.30 |
| **13b** | Amide cis | 8.59 | 3.01 | 6.67 | 0.00 |
| | Amide trans | 6.53 | 0.00 | 9.45 | 2.97 |
| **13c** | Amide cis | 0.00 | 6.47 | 8.68 | 0.21 |
| | Amide trans | 9.05 | 3.66 | 5.35 | 0.00 |
| **9a** | Amide cis a | 17.09 | 11.80 | 0.99 | 9.53 |
| | Amide cis b | 13.63 | 8.46 | 2.89 | 6.18 |
| **9a** | Amide trans a | 6.19 | 0.88 | 3.77 | 0.99 |
| | Amide trans b | 6.75 | 0.00 | 3.83 | 0.00 |
| **9b** | Amide cis a | 8.45 | 3.56 | 11.38 | 2.99 |
| | Amide cis b | 5.04 | 0.26 | 8.12 | 11.23 |
| **9b** | Amide trans a | 5.51 | 0.45 | 6.93 | 0.50 |
| | Amide trans b | 5.96 | 0.00 | 6.30 | 0.00 |
| **9c**[a] | Amide cis a | 15.32 | 10.81 | 15.73 | 8.17 |
| | Amide cis b | 11.96 | 7.54 | 12.40 | 4.92 |
| **9c**[a] | Amide trans a | 5.54 | 1.02 | 5.46 | 0.42 |
| | Amide trans b | 5.03 | 0.00 | 5.03 | 0.00 |

**Table 2** (continued)

| Precursor | Geometry | Heat of Formation of Monomers (kcal/mol) | |
|---|---|---|---|
| | | *i* | *ii* |
| **12a** | Amide cis | 8.63 | 9.71 |
| | Amide trans | 18.65 | 15.54 |
| **12b** | Amide cis | 7.47 | 15.20 |
| | Amide trans | 12.45 | 12.85 |
| **12c** | Amide cis | 8.53 | 5.56 |
| | Amide trans | 8.57 | 8.45 |
| **13a** | Amide cis | 22.55 | 9.29 |
| | Amide trans | 15.90 | 16.43 |
| **13b** | Amide cis | 7.26 | 6.17 |
| | Amide trans | 12.09 | 12.15 |
| **13c** | Amide cis | 20.70 | 5.78 |
| | Amide trans | 8.32 | 8.36 |
| **9a** | Amide cis a | 0.21 | 14.03 |
| | Amide cis b | 5.57 | 14.02 |
| **9a** | Amide trans a | 13.89 | 16.42 |
| | Amide trans b | 13.39 | 16.31 |
| **9b** | Amide cis a | 6.47 | 2.96 |
| | Amide cis b | 6.61 | 14.50 |
| **9b** | Amide trans a | 4.96 | 3.59 |
| | Amide trans b | 3.87 | 3.53 |
| **9c**[a] | Amide cis a | 8.16 | 5.11 |
| | Amide cis b | 8.20 | 5.13 |
| **9c**[a] | Amide trans a | 7.67 | 7.15 |
| | Amide trans b | 7.75 | 7.75 |

[a] Led to compound **14c**

But, only the cis amide conformation allows the introduction of the N-Boc substituent due to steric hindrance. This spatial orientation which is constrained by the N-Boc substituent can be related to the appearance of **14c** as RCM monomer product along with the dimers. **Figure 7** illustrates the

optimized geometry of the **9c** adduct with the N-C(3)-arm linked to the Ru atom.

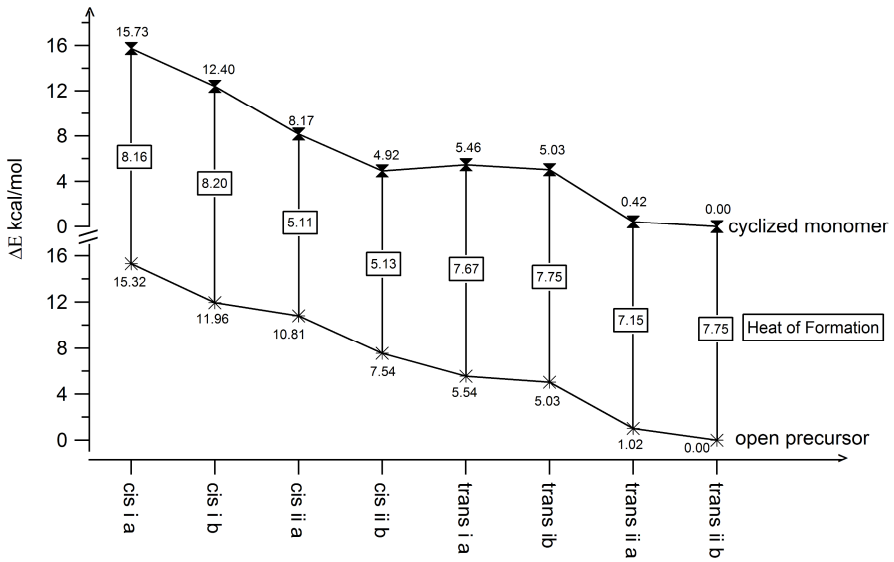


**Figure 5**. Relative energies of precursor/cyclic monomer in the selected conformations and heats of formation for **14c**.

In order to explain the preferential formation of dimers, the search of different conformations has been investigated. For the three sizes of the ring, two isomers of the β-lactam can be located giving rise to a head-head (HH) or head-tail (HT) arrangement in the macrocycle (see **Figure 3**). Moreover, an additional factor has to be considered, mainly for the N-H substitution, due to the formation of intramolecular H bonds which significantly stabilize some conformations. Again, with the conformation cis/trans of the amide and *syn*/*anti* imide orientation, a lot of conformations have been found which are not necessarily geometrically related going from N-H to N-Boc substitutions.

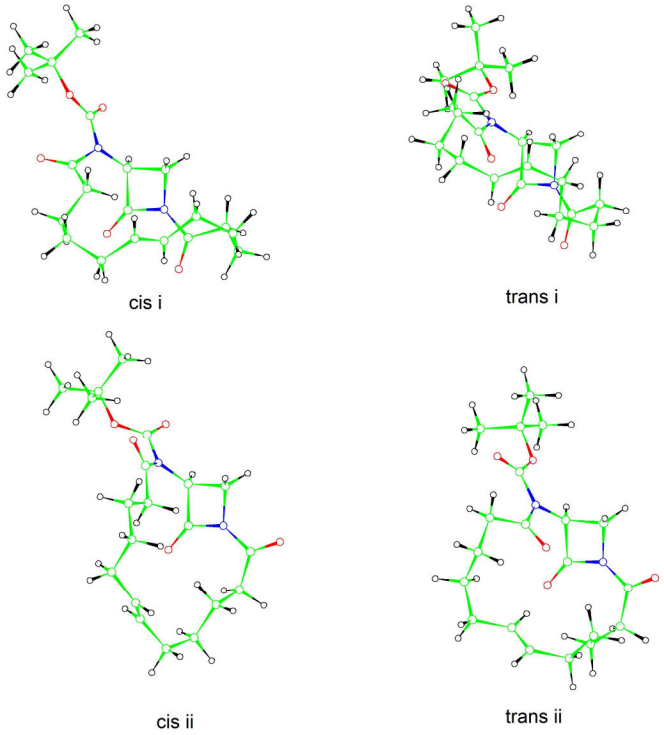


**Figure 6**. Four conformers of compound **14c**, in geometry b.

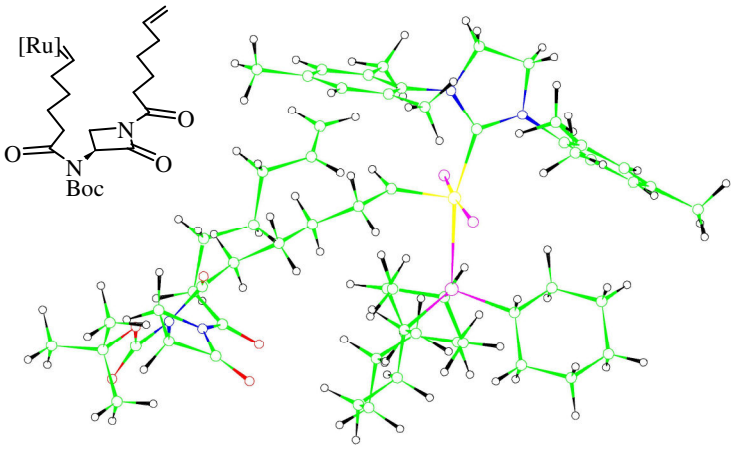


**Figure 7**. Optimized geometry of the **9c** adduct.

As an example, **Figure 8** illustrates the most stable conformer of compounds **15c** (HT) and **16c** (HH).

The energy range is large and superior to 20 kcal/mol. In most of the cases, the trans conformation of the two amides is more stable than other combinations cis/trans or cis/cis. For this spatial disposition, a complete homogenous set of conformers has been located. Most of the time, the HT isomers are more stable than the HH ones. As for the monomers, the heat of formation has been calculated with respect to the open precursor (**Table 3**). In many cases, the heat of formation of dimer is negative or slightly positive with an energy demand lower than the one required for the cyclic monomer formation (see **Table 2**). Remarkably, the heat of formation of **15c** corresponds to the highest positive value (9.13 kcal/mol) of the selected conformers, higher than the one of the cyclic monomer **14c** which is experimentally also observed (7.75 kcal/mol).

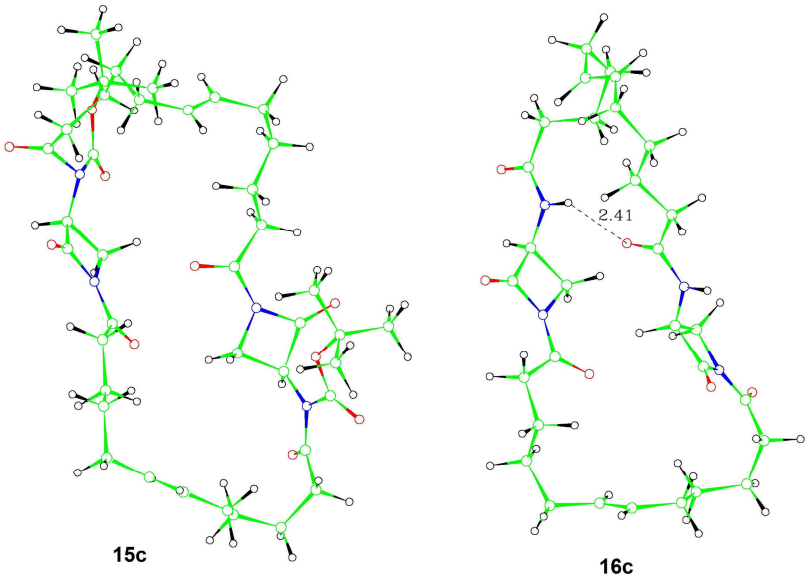


**Figure 8**. Most stable conformer of compounds **15c** (HT) and **16c** (HH).

**Table 3**

Heat of formation of macrocyclic dimers for selected compounds.

| Precursor | Product | ΔE (HH-HT) (kcal/mol) | Heat of Formation (kcal/mol) |
|---|---|---|---|
| **12a** | - | 2.23 | -1.11 |
| **13a** | - | 4.09 | 1.75 |
| **9a** | - | 10.37 | 6.55 |
| **12b** | **16b** | 9.59 | -5.66 |
| **13b** | **17b** | -1.13 | 3.76 |
| **9b** | **15b** | -1.74 | -8.06 |
| **12c** | **16c** | -2.43 | -1.81 |
| **13c** | **17c** | 3.09 | 4.99 |
| **9c** | **15c** | 5.35 | 9.13 |

### 2.3. Inhibition of R39 D,D-peptidase

All bis-acylated compounds, precursors and cyclic products, were tested against Actinomadura R39,[18] a model serine-enzyme of low molecular weight D,D-peptidases, usually considered for a preliminary screening of penicillin-like compounds. R39 and the tested azetidinones (100 μM) were incubated (1 h, 25 °C) together. After preincubation, the residual activity (RA) was determined by observing the hydrolysis of the thiolester substrate,[19] in the presence of DTNB, catalyzed by the non inhibited enzyme. The results are given in **Table 4** as percentages (%) of initial activity. The activity in the absence of inhibitors is set at 100% and low values indicate very active compounds as the bacterial enzyme has been inhibited by the tested compound and consequently cannot hydrolyze its reporter substrate. A tested compound is considered as a "hit" (*i.e.* potential inhibitor) for a RA < 80%.

**Table 4**

Evaluation of azetidinones against R39 D,D-peptidase.

| Entry | Compound | RA (%) | Entry | Compound | RA (%) |
|---|---|---|---|---|---|
| 1 | **9a** | 82 ± 5 | 13 | **15c** | 4 ± 3 |
| 2 | **9b** | 87 ± 1 | 14 | **16b** | 4 ± 8 |
| 3 | **9c** | 96 ± 3 | 15 | **16c** | 0 |
| 4 | **12a** | >100 | 16 | **17b** | 93 ± 5 |
| 5 | **12b** | 17 ± 9 | 17 | **17c** | 43 ± 3 |
| 6 | **12c** | 23 ± 0 | 18 | **19b** | 101 ± 8 |
| 7 | **13a** | >100 | 19 | **19c** | 103 ± 5 |
| 8 | **13b** | 103 ± 3 | 20 | **20b** | 2 |
| 9 | **13c** | 95 ± 7 | 21 | **20c** | 0 |
| 10 | **14c** | 0 | 22 | **21b** | 88 ± 7 |
| 11 | **18c** | 14 ± 10 | 23 | **21c** | 39 ± 0 |
| 12 | **15b** | 111 ± 2 | 24 | **PenG** | 0[20] |

Amongst the precursors (non cyclized compounds: **Table 4**, entries 1-9), two molecules are good inhibitors of R39, namely **12b** and **12c** (N-H family, entries 5-6). The cyclomonomers **14c/18c** (entries 10-11) also inhibited efficiently R39 despite the fact that the molecules are still N-Boc protected. Unfortunately, the corresponding N-H derivatives were not accessible for testing because the TFA treatment of **14c** and **18c** (for Boc cleavage) gave a mixture of deprotected β-lactams and hydrolyzed products. Surprisingly, the cyclodimers (entries 12-23) are generally more active than their respective precursors and some of them showed very good inhibition potential, *i.e.* **16b-c** (entries 14-15), and **20b-c** (entries 20-21); these correspond to the N-H (deprotected) derivatives. It is worth noting that all these non-traditional inhibitors are quite lipophilic compounds, devoid of the carboxylic function usually found in penicillins and related antibiotics.

## 3. Conclusion

The RCM reaction applied to azetidinone substrates featuring amide and imide functions led almost exclusively to macrocyclic dimers instead of the cyclomonomers. These unexpected results are in fact in good agreement with the computed heats of formation of the dimers and monomers respectively. Our theoretical investigation has highlighted the dramatic importance of the conformational flexibility of the substrates and products on the RCM reaction. Interestingly, in the only case where the dimer (*i.e.* **15c**) was predicted to be slightly less favoured than the corresponding monomer (*i.e.* **14c**), both products were experimentally observed.

The biological activity results collected with our compounds using the R39 serine-enzyme are promising. The novel bicyclic β-lactams **14c** and **18c** are good inhibitors of this D,D-peptidase while their precursor **9c** is not active. Also, the *bis*-azetidinyl macrocycles **15c**, **16b**, **16c**, **20b**, and **20c** have shown remarkable inhibitory effect.

Since the azetidinone moieties are not activated by the traditional angular strain leading to "twisted" amide functions like in penicillins,[21] the activity should be attributed, amongst other factors, to the flexibility of the substrates (a lot of conformers are possible) allowing their adjustment into the enzymic pocket and their easy conformational rearrangement during the processing by the active site serine residue. Moreover, the most active compounds are those with R' = H (**16b-c**, **20b-c**) comparatively to the corresponding N-substituted derivatives with R' = Me (**17b-c**, **21b-c**) and R' = Boc (**15b**, **19b-c**), most probably for steric reasons, and the activity does not seem to be so much dependent on the preferred head-tail or head-head dimeric structures.

Work is in progress for producing preferably bicyclic azetidinones related to the structures **14c/18c**, *i.e.* cyclomonomers. In case of difficult

macrocyclizations, a novel auxiliary has been recently developed as conformational control element (CCE) favoring the appropriate conformation toward the desired RCM reaction.[22] Since this elegant strategy is not readily applicable to our precursors **9**, **12** and **13**, we are now investigating the corresponding *bis*-alkylated derivatives which show an increase of the freedom degrees for the side-chains rotations.

## 4. Experimental Section

### 4.1. General considerations

Experiments were performed under argon atmosphere in flame-dried glassware. All solvents, including anhydrous solvents, and reagents were purchased from Acros Organics, Alfa Aesar, Fluka, Sigma-Aldrich or VWR, and used without any further purification. TLC analyses were performed on aluminium plates coated with silica gel $60F_{254}$ (Merck) and visualized with a $KMnO_4$ solution and UV (254 nm) detection and column chromatography was performed on silica gel (40-63 or 63-200 μm) purchased from Rocc. Melting points (mp) were determined on a Büchi B-540 apparatus calibrated with caffeine, vanillin, and phenacetin. $[\alpha]_D$ were measured on Perkin-Elmer 241 MC polarimeter, at 20 °C, in $CHCl_3$. Concentrations are given in g/100 mL. Nuclear magnetic resonance ($^1H$ and $^{13}C$) spectra were recorded at 300 MHz for proton and 75 MHz for carbon (Bruker Avance 300) or 500 MHz for proton and 125 MHz for carbon (Bruker Avance 500) using deuterated chloroform ($CDCl_3$) or deuterated methanol ($CD_3OD$). Chemical shifts are reported in ppm relative to residual $CHCl_3$ in $CDCl_3$ (7.26 and 77.16 ppm) or residual $CHD_2OD$ in $CD_3OD$ (3.31 and 49.00 ppm). NMR coupling constants (*J*) are reported in Hertz. Infrared (IR) spectra were recorded using

FTIR-8400S Shimadzu apparatus. Products were analyzed as thin films deposited on a Se-Zn crystal by evaporation from $CH_2Cl_2$ solutions. For precursors, mono-acylated and bis-acylated compounds High Resolution Mass Spectrometry (HRMS) analyses were performed at the University of Mons Hainaut (Belgium) or at the University College London (UK). For compounds issued from RCM, low and high resolution mass spectrometry were performed at UCL on LTQ-Orbitrap-XL equipment. For compounds **14**-**21**, only the $^{13}C$ NMR spectra are given. Originally, experimental details for compounds **6**, **7**, **8**, **18** to **21**, structural data for compounds **6** to **8**, **9a-b** to **13a-b**, **18c**, **19b-c** to **21b-c** were in the Supplementary data, here they were added directly to the experimental section.

### 4.2. Synthesis of compounds 6, 7 and 8

*(S)-tert-butyl 1-(benzyloxyamino)-3-hydroxy-1-oxopropan-2-yl(methyl) carbamate* (**6**).

*N*-Ethyl-*N*′-(3-dimethylaminopropyl)carbodiimide hydrochloride (EDCI) (1.31 g, 6.84 mmol) was added portion-wise, at 0 °C, into a well-stirred solution of Boc-*N*-Methyl-L-serine (1.00 g, 4.56 mmol) and *O*-(phenylmethyl)hydroxylamine (0.80 mL, 6.84 mmol) in $CH_2Cl_2$ (40 mL), and the reaction mixture was stirred for 1 h at 0 °C and overnight at room temperature. The solution was washed with water (40 mL) and brine (40 mL). After drying over $MgSO_4$ and removing the solvent under reduced pressure, the residue was purified by flash column chromatography (hexane/EtOAc 1/1), to provide **6** as a colourless oil (1.34 g, 91%). $R_f$=0.37 (hexane/EtOAc 3/7); $[\alpha]_D^{20}$ -64.9 (*c* 1.1, $CHCl_3$); $^1H$ NMR (300 MHz, $CDCl_3$): δ=9.35 and 8.86 (2 br s, 1H), 7.36 (m, 5H), 4.89 (s, 2H), 4.50 (br s,

1H), 3.97 (br s, 1H), 3.81 (br s, 1H), 2.82 (s, 3H), 1.41 ppm (s, 9H); $^{13}C$ (75 MHz, $CDCl_3$): δ=168.2, 156.9, 135.0, 129.3, 128.9, 128.7, 81.3, 78.5, 60.5, 57.4, 31.8, 28.4 ppm; IR: ν=3437-3229, 2974-2854, 1666 $cm^{-1}$; HRMS (ESI): calcd. for $C_{16}H_{24}N_2O_5Na$ $[M + Na]^+$ 347.1583, found 347.1579.

*(S)-tert-butyl 1-(benzyloxy)-2-oxoazetidin-3-yl(methyl)carbamate* (**7**).

Path A: A solution of $PPh_3$ (0.91 g, 3.47 mmol) in dry $CH_3CN$ (14 mL) was added dropwise, at 0 °C and under an inert atmosphere, to a stirred solution of **6** (1.02 g, 3.16 mmol) in dry $CH_3CN$ (9 mL), containing $CCl_4$ (0.33 mL, 3.47 mmol) and anhydrous triethylamine (0.66 mL, 4.74 mmol). The resultant clear reaction mixture was stirred for 2 h at 0 °C and overnight at room temperature. After completion of the reaction, the obtained white precipitate was separated by filtration and the resulting clear reaction mixture concentrated under reduced pressure. The residue was redissolved with EtOAc (30 mL), washed with a saturated $NH_4Cl$ solution (2x20 mL) and brine (30 mL). After drying over $MgSO_4$ and removing the solvent under reduced pressure, the residue was purified by flash column chromatography (hexane/EtOAc 4/1), to provide **7** as a colourless solid (0.79 g, 82%).

Path B: A stirred solution of β-lactam **3** (100 mg, 0.34 mmol) in anhydrous THF (1 mL) was cooled to -78 °C. LiHMDS 1N in hexane (0.34 mL, 0.34 mmol) was slowly added and the mixture was stirred for 30 minutes. Dimethyl sulfate (0.05 mL, 0.51 mmol) was then added by syringe and the mixture was stirred for another 30 minutes. The mixture was then warmed to rt and stirred additionally for 20 h. The reaction was quenched with 30% $NH_4OH$ (1 mL) and the stirring was continued for an additional hour. The resulting mixture was diluted with EtOAc (15 mL) and water (15 mL). The organic layer was washed with brine (20 mL), dried over $MgSO_4$ and

concentrated under reduced pressure. The residue was purified by flash column chromatography (hexane/EtOAc 4/1), to provide **7** as a colourless solid (65 mg, 62%). $R_f$=0.48 (hexane/EtOAc 3/2); m.p. 64.5-65.6 °C; $[\alpha]_D^{20}$ +0.2 (*c* 3.6, $CHCl_3$); $^1$H NMR (500 MHz, $CDCl_3$): δ=7.42-7.37 (m, 5H), 5.15 and 4.78 (2 br s, 1H, rotamers), 4.96 (s, 2H), 3.45 (m, 1H), 3.16 (br s, 1H), 2.69 (br s, 3H), 1.42 ppm (s, 9H); $^{13}$C (125 MHz, $CDCl_3$): δ=162.7, 155.1-154.6 (rotamers), 135.0, 129.3, 128.8, 81.2-80.9 (rotamers), 77.9, 59.7-58.8 (rotamers), 51.6-51.1 (rotamers), 31.1-30.5 (rotamers), 28.3 ppm; IR: ν=2976, 1778, 1693 cm$^{-1}$; HRMS (ESI): calcd. for $C_{16}H_{22}N_2O_4Na$ [M + Na]$^+$ 329.1477, found 329.1474.

*(S)-tert-butyl methyl(2-oxoazetidin-3-yl)carbamate* (**8**).

Compound **7** (0.24 g, 0.78 mmol) dissolved in methanol (8 mL) was placed under $H_2$ (1 atm) at rt in the presence of Raney-Ni (50% in water) catalyst for 7 h. Then the mixture was filtered through a pad of Celite and concentrated under reduced pressure. The residue was purified by flash column chromatography (EtOAc), to provide **8** as a colourless solid (100 mg, 64%). $R_f$=0.5 (EtOAc); m.p. 92.8-93.6 °C; $[\alpha]_D^{20}$ -4.2 (*c* 3.0, $CHCl_3$); $^1$H NMR (300 MHz, $CDCl_3$): δ=6.34 (br s, 1H), 5.34 and 5.00 (2 br s, 1H, rotamers), 3.51 (m, 1H), 3.32 (dd, *J*=2.6, 5.6 Hz, 1H), 2.87 (s, 3H), 1.43 ppm (s, 9H); $^{13}$C (75 MHz, $CDCl_3$): δ=168.4, 155.0-154.8 (rotamers), 81.1-80.8 (rotamers), 65.3-64.6 (rotamers), 42.4-41.7, (rotamers) 32.0-31.4 (rotamers), 28.3 ppm; IR: ν=3504-3278, 2976-2905, 1755, 1681 cm$^{-1}$; HRMS (ESI): calcd. for $C_9H_{16}N_2O_3Na$ [M + Na]$^+$ 223.1059, found 223.1063.

### 4.3. Synthesis of precursors 9, 10, 11, 12 and 13

*(S)-tert-butyl hept-6-enoyl(1-hept-6-enoyl-2-oxoazetidin-3-yl)carbamate* (**9c**).

A stirred solution of β-lactam **4** (300 mg, 1.61 mmol) in anhydrous THF (11 mL) was cooled to -78 °C. LiHMDS 1N in hexane (3.54 mL, 3.54 mmol) was slowly added and the mixture was stirred for 30 minutes. 6-Heptenoyl chloride (592 mg, 3.54 mmol) was then added by syringe and the mixture was stirred for another 30 minutes. The mixture was then warmed to rt over 4 h and then quenched with saturated $NH_4Cl$ (20 mL). The resulting mixture was extracted with EtOAc (2 x 20 mL) and the organic layers were washed with a saturated $NaHCO_3$ solution (50 mL) and brine (50 mL). After drying over $MgSO_4$ and removing the solvent under reduced pressure, the residue was purified by flash column chromatography (hexane/EtOAc 4/1), to provide **9c** as a pale-yellow oil (366 mg, 56%). $R_f$=0.58 (hexane/EtOAc 4/1); $[\alpha]_D^{20}$ +1.4 (*c* 3.0, $CHCl_3$); $^1$H NMR (300 MHz, $CDCl_3$): δ=5.86-5.72 (m, 3H), 5.03-4.92 (m, 4H), 3.83 (m, 1H), 3.61 (dd, *J*=4.2, 7.1 Hz, 1H), 2.88 (m, 2H), 2.73 (m, 2H), 2.07 (m, 4H), 1.74-1.60 (m, 4H), 1.51 (s, 9H), 1.48-1.38 ppm (m, 4H); $^{13}$C (75 MHz, $CDCl_3$): δ=175.5, 171.2, 164.5, 151.2, 138.5, 138.4, 114.8 (2C), 85.6, 56.9, 43.9, 38.2, 36.5, 33.6, 33.5, 28.4, 27.9 (2C), 24.4, 23.5 ppm; IR: ν=3076-2860, 1798, 1747, 1697 $cm^{-1}$; HRMS (ESI): calcd. for $C_{22}H_{34}N_2O_5Na$ $[M + Na]^+$ 429.2365, found 429.2382.

*(S)-tert-butyl 2-oxo-1-pent-4-enoylazetidin-3-yl(pent-4-enoyl)carbamate* (**9a**).

Compound **9a** was synthesized according to the procedure described for the synthesis of compound **9c** from β-lactam **4** (80 mg, 0.43 mmol) and 4-pentenoyl chloride. Flash column chromatography (hexane/EtOAc 4/1)

provided **9a** as a pale-yellow oil (92 mg, 61%). $R_f$=0.59 (hexane/EtOAc 3/2); $[\alpha]_D^{20}$ +3.2 (*c* 5.3, $CHCl_3$); $^1$H NMR (300 MHz, $CDCl_3$): δ=5.90-5.74 (m, 3H), 5.12-4.99 (m, 4H), 3.84 (m, 1H), 3.62 (dd, *J*=4.2, 7.1 Hz, 1H), 2.99 (m, 2H), 2.84 (m, 2H), 2.41 (m, 4H), 1.51 ppm (s, 9H); $^{13}$C (75 MHz, $CDCl_3$): δ=174.8, 170.5, 164.4, 151.2, 136.9, 136.5, 116.0, 115.8, 85.8, 56.9, 43.9, 37.6, 35.9, 28.9, 28.0 (2C) ppm; IR: ν=3078-2851, 1798, 1745, 1697 $cm^{-1}$; HRMS (ESI): calcd. for $C_{18}H_{26}N_2O_5Na$ $[M + Na]^+$ 373.1739, found 373.1744.

*(S)-tert-butyl hex-5-enoyl(1-hex-5-enoyl-2-oxoazetidin-3-yl)carbamate* (**9b**).
Compound **9b** was synthesized according to the procedure described for the synthesis of compound **9c** from β-lactam **4** (300 mg, 1.61 mmol) and 5-hexenoyl chloride. Flash column chromatography (hexane/EtOAc 4/1) provided **9b** as a pale-yellow oil (359 mg, 59%). $R_f$=0.41 (hexane/EtOAc 4/1); $[\alpha]_D^{20}$ +2.0 (*c* 3.1, $CHCl_3$); $^1$H NMR (300 MHz, $CDCl_3$): δ=5.86-5.71 (m, 3H), 5.07-4.96 (m, 4H), 3.83 (m, 1H), 3.61 (dd, *J*=4.2, 7.1 Hz, 1H), 2.87 (m, 2H), 2.74 (m, 2H), 2.11 (m, 4H), 1.83-1.69 (m, 4H), 1.51 ppm (s, 9H); $^{13}$C (75 MHz, $CDCl_3$): δ=175.4, 171.2, 164.4, 151.2, 137.9, 137.8, 115.5, 115.4, 85.7, 56.9, 43.8, 37.6, 35.9, 33.1 (2C), 28.0, 24.0, 23.2 ppm; IR: ν=3076-2935, 1798, 1747, 1693 $cm^{-1}$; HRMS (ESI): calcd. for $C_{20}H_{30}N_2O_5Na$ $[M + Na]^+$ 401.2052, found 401.2047.

*(S)-tert-butyl 1-hept-6-enoyl-2-oxoazetidin-3-ylcarbamate* (**10c**).
To a stirred solution of β-lactam **4** (427 mg, 2.29 mmol) in dry $CH_2Cl_2$ (19 mL) were added pyridine (0.37 mL, 4.59 mmol) and 6-heptenoyl chloride (673 mg, 4.59 mmol). The mixture was stirred for 24 h at room temperature and then diluted with $CH_2Cl_2$ (30 mL) and the organic layer was washed with

HCl 2 M solution (50 mL), a saturated $NaHCO_3$ solution (50 mL) and brine (50 mL). After drying over $MgSO_4$ and removing the solvent under reduced pressure, the residue was purified by flash column chromatography (hexane/EtOAc 4/1), to provide **10c** as a colourless solid (523 mg, 77%). $R_f$=0.45 (hexane/EtOAc 3/2); m.p. 92.9-93.6 °C; $[\alpha]_D^{20}$ +11.3 (*c* 2.6, $CHCl_3$); $^1$H NMR (300 MHz, $CDCl_3$): δ=5.78 (m, 1H), 5.17 (d, *J*=7.6 Hz, 1H), 5.03-4.92 (m, 2H), 4.66 and 4.44 (2 br s, 1H, rotamers), 3.86 (m, 1H), 3.64 (dd, *J*=3.9, 7.6 Hz, 1H), 2.72 (m, 2H), 2.07 (m, 2H), 1.67 (m, 2H), 1.49-1.40 ppm (m, 11H); $^{13}$C (75 MHz, $CDCl_3$): δ=171.3, 165.2, 154.7, 138.5, 114.8, 81.2, 56.6, 45.6, 36.6, 33.5, 28.4, 28.3, 23.5 ppm; IR: ν=3354, 2976-2864, 1796, 1689, 1518 $cm^{-1}$; HRMS (ESI): calcd. for $C_{15}H_{24}N_2O_4Na$ $[M + Na]^+$ 319.1634, found 319.1636.

*(S)-tert-butyl 2-oxo-1-pent-4-enoylazetidin-3-ylcarbamate* (**10a**).

Compound **10a** was synthesized according to the procedure described for the synthesis of compound **10c** from β-lactam **4** (270 mg, 1.45 mmol) and 4-pentenoyl chloride. Flash column chromatography (hexane/EtOAc 4/1) provided **10a** as a colourless solid (348 mg, 89%). $R_f$=0.74 (hexane/EtOAc 1/1); m.p. 98.8-99.4 °C; $[\alpha]_D^{20}$ +13.8 (*c* 3.1, $CHCl_3$); $^1$H NMR (300 MHz, $CDCl_3$): δ=5.83 (m, 1H), 5.40 and 5.17 (br s and br d, *J*=6.5Hz, 1H, rotamers), 5.08 (m, 1H), 5.00 (m, 1H), 4.67 and 4.46 (2 br s, 1H, rotamers), 3.87 (m, 1H), 3.65 (dd, *J*=3.8, 7.4 Hz, 1H), 2.83 (m, 2H), 2.41 (m, 2H), 1.44 ppm (s, 9H); $^{13}$C (75 MHz, $CDCl_3$): δ=170.6, 165.2, 154.7, 136.5, 115.9, 81.3, 56.7, 45.6, 36.0, 28.3, 27.9 ppm; IR: ν=3356, 2978-2933, 1796, 1693, 1518 $cm^{-1}$; HRMS (ESI): calcd. for $C_{13}H_{20}N_2O_4Na$ $[M + Na]^+$ 291.1321, found 291.1328.

*(S)-tert-butyl 1-hex-5-enoyl-2-oxoazetidin-3-ylcarbamate* (**10b**).

Compound **10b** was synthesized according to the procedure described for the synthesis of compound **10c** from β-lactam **4** (200 mg, 1.07 mmol) and 5-hexenoyl chloride. Flash column chromatography (hexane/EtOAc 4/1) provided **10b** as a colourless solid (243 mg, 80%). $R_f$=0.50 (hexane/EtOAc 3/2); m.p. 93.3-94.1 °C; $[\alpha]_D^{20}$ +12.3 (*c* 3.0, $CHCl_3$); $^1$H NMR (300 MHz, $CDCl_3$): δ=5.77 (m, 1H), 5.19 (br d, *J*=7.3 Hz, 1H), 5.06-4.96 (m, 2H), 4.66 and 4.44 (2 br s, 1H, rotamers), 3.86 (m, 1H), 3.64 (dd, *J*=3.8, 7.4 Hz, 1H), 2.73 (m, 2H), 2.11 (m, 2H), 1.76 (m, 2H), 1.43 ppm (s, 9H); $^{13}$C (75 MHz, $CDCl_3$): δ=171.2, 165.2, 154.6, 137.8, 115.5, 81.2, 56.6, 45.6, 36.0, 33.1, 28.3, 23.2 ppm; IR: ν=3354, 2976-2934, 1794, 1690, 1518 cm$^{-1}$; HRMS (ESI): calcd. for $C_{14}H_{22}N_2O_4Na$ $[M + Na]^+$ 305.1477, found 305.1483.

*(S)-tert-butyl 1-hept-6-enoyl-2-oxoazetidin-3-yl(methyl)carbamate* (**11c**).

Compound **11c** was synthesized according to the procedure described above for the synthesis of compound **10c** from β-lactam **8** (250 mg, 1.24 mmol) and 6-heptenoyl chloride and the mixture was put under reflux for 24 h. Flash column chromatography (hexane/EtOAc 4/1) provided **11c** as a colourless oil (336 mg, 87%). $R_f$=0.53 (hexane/EtOAc 3/2); $[\alpha]_D^{20}$ +11.5 (*c* 5.0, $CHCl_3$); $^1$H NMR (300 MHz, $CDCl_3$): δ=5.76 (m, 1H), 5.06-4.91 (m, 2H+0.5H, rotamer), 4.60 (br s, 0.5H, rotamer), 3.80 (m, 1H), 3.61 (dd, *J*=3.9, 7.5 Hz, 1H), 2.92 (br s, 3H), 2.71 (br s, 2H), 2.05 (m, 2H), 1.66 (m, 2H), 1.43 ppm (br s, 11H); $^{13}$C (75 MHz, $CDCl_3$): δ=171.3, 164.9, 154.9-154.3 (rotamers), 138.4, 114.8, 82.1-81.4 (rotamers), 63.7-62.9 (rotamers), 44.4-43.2 (rotamers), 36.5, 35.2-33.5 (rotamers), 33.5, 28.3, 28.2, 23.5 ppm; IR: ν=2976-2864, 1794, 1693, 1639 cm$^{-1}$; HRMS (ESI): calcd. for $C_{16}H_{26}N_2O_4Na$ $[M + Na]^+$ 333.1790, found 333.1796.

*(S)-tert-butyl methyl(2-oxo-1-pent-4-enoylazetidin-3-yl)carbamate* (**11a**).

Compound **11a** was synthesized according to the procedure described for the synthesis of compound **10c** from β-lactam **8** (100 mg, 0.50 mmol) and 4-pentenoyl chloride. Flash column chromatography (hexane/EtOAc 4/1) provided **11a** as a pale-yellow oil (105 mg, 75%). $R_f$=0.46 (hexane/EtOAc 3/2); $[\alpha]_D^{20}$ +15.3 (*c* 3.3, $CHCl_3$); $^1$H NMR (500 MHz, $CDCl_3$): δ=5.82 (m, 1H), 5.07 (m, 1H+0.5H, rotamer), 5.00 (m, 1H), 4.61 (br s, 0.5H, rotamer), 3.82 (m, 1H), 3.63 (dd, *J*=3.8, 7.5 Hz, 1H), 2.95-2.83 (m, 5H), 2.41 (m, 2H), 1.43 ppm (s, 9H); $^{13}$C (125 MHz, $CDCl_3$): δ=170.6, 164.9, 154.9-154.2 (rotamers), 136.5, 116.0, 82.1-81.4 (rotamers), 63.8-62.9 (rotamers), 44.4-43.2 (rotamers), 36.0, 35.2-33.4 (rotamers), 28.2, 28.0 ppm; IR: ν=3001-2922, 1790, 1705 $cm^{-1}$; HRMS (ESI): calcd. for $C_{14}H_{22}N_2O_4Na$ $[M + Na]^+$ 305.1477, found 305.1469.

*(S)-tert-butyl 1-hex-5-enoyl-2-oxoazetidin-3-yl(methyl)carbamate* (**11b**).

Compound **11b** was synthesized according to the procedure described for the synthesis of compound **10c** from β-lactam **8** (255 mg, 1.27 mmol) and 5-hexenoyl chloride and the mixture was refluxed for 24 h. Flash column chromatography (hexane/EtOAc 4/1) provided **11b** as a colourless oil (325 mg, 86%). $R_f$=0.47 (hexane/EtOAc 3/2); $[\alpha]_D^{20}$ +12.4 (*c* 3.0, $CHCl_3$); $^1$H NMR (300 MHz, $CDCl_3$): δ=5.77 (m, 1H), 5.05-4.95 (br m, 2H+0.5H, rotamer), 4.61 (br s, 0.5H, rotamer), 3.81 (m, 1H), 3.62 (dd, *J*=3.9, 7.4 Hz, 1H), 2.93 (br s, 3H), 2.73 (br s, 2H), 2.11 (m, 2H), 1.76 (m, 2H), 1.43 ppm (s, 9H); $^{13}$C (125 MHz, $CDCl_3$): δ=171.2, 164.9, 154.9-154.2 (rotamers), 137.7, 115.5, 82.1-81.4 (rotamers), 63.7-62.9 (rotamers), 44.4-43.2 (rotamers), 36.0, 35.2-33.3 (rotamers), 33.1, 28.2, 23.2 ppm; IR: ν=2970-

2852, 1794, 1705 $cm^{-1}$; HRMS (ESI): calcd. for $C_{15}H_{24}N_2O_4Na$ $[M + Na]^+$ 319.1634, found 319.1646.

*(S)-N-(1-hept-6-enoyl-2-oxoazetidin-3-yl)hept-6-enamide* (**12c**).

Trifluoroacetic acid (0.75 mL, 10.12 mmol) was added to **10c** (150 mg, 0.51 mmol) dissolved in $CH_2Cl_2$ (5 mL) at 0 °C. The mixture was warmed to room temperature and stirred for 2 h. Concentration of the reaction solution afforded the crude trifluoroacetate salt as a viscous oil. Then 6-heptenoyl chloride (111 mg, 0.76 mmol) was added to a stirred solution of the crude trifluoroacetate salt and triethylamine (0.21 mL, 1.58 mmol) in $CH_2Cl_2$ (5 mL) cooled at 0 °C. The mixture was then warmed to rt and stirred overnight. The mixture was then diluted with $CH_2Cl_2$ (25 mL), and sequentially washed with HCl 2 M solution (30 mL), a saturated $NaHCO_3$ solution (30 mL) and brine (40 mL). After drying over $MgSO_4$ and removing the solvent under reduced pressure, the residue was purified by flash column chromatography (hexane/EtOAc 3/2), to provide **12c** as a colourless solid (129 mg, 83%). $R_f$=0.34 (hexane/EtOAc 1/1); m.p. 97.2-98.5 °C; $[\alpha]_D^{20}$ +13.4 (*c* 3.0, $CHCl_3$); $^1$H NMR (300 MHz, $CDCl_3$): δ=6.21 (d, *J*=7.0 Hz, 1H), 5.77 (m, 2H), 5.03-4.92 (m, 4H), 4.70 (td, *J*=3.9, 6.9 Hz, 1H), 3.85 (m, 1H), 3.66 (dd, *J*=3.9, 7.4 Hz, 1H), 2.72 (m, 2H), 2.24 (t, *J*=7.5 Hz, 2H), 2.10-2.02 (m, 4H), 1.72-1.59 (m, 4H), 1.50-1.36 ppm (m, 4H); $^{13}$C (75 MHz, $CDCl_3$): δ=173.6, 171.3, 164.7, 138.4, 138.3, 115.0, 114.8, 55.8, 45.0, 36.5, 35.8, 33.5 (2C), 28.4 (2C), 24.8, 23.5 ppm; IR: ν=3290, 3080-2852, 1797, 1780, 1693, 1651, 1537 $cm^{-1}$; HRMS (ESI): calcd. for $C_{17}H_{26}N_2O_3Na$ $[M + Na]^+$ 329.1841, found 329.1846.

*(S)-N-(2-oxo-1-pent-4-enoylazetidin-3-yl)pent-4-enamide* (**12a**).

Compound **12a** was synthesized according to the procedure described for the synthesis of compound **12c** from β-lactam **10a** (121 mg, 0.45 mmol) and 4-pentenoyl chloride. Flash column chromatography (hexane/EtOAc 3/2) provided **12a** as a colourless solid (95 mg, 84%). $R_f$=0.32 (hexane/EtOAc 1/1); m.p. 114.9-115.7 °C; $[\alpha]_D^{20}$ +20.7 (*c* 2.5, $CHCl_3$); $^1$H NMR (300 MHz, $CDCl_3$): δ=6.38 (d, *J*=7.0 Hz, 1H), 5.81 (m, 2H), 5.10-4.98 (m, 4H), 4.70 (td, J=4.0, 7.0 Hz, 1H), 3.85 (m, 1H), 3.66 (dd, *J*=4.0, 7.4 Hz, 1H), 2.82 (m, 2H), 2.44-2.30 ppm (m, 6H); $^{13}$C (75 MHz, $CDCl_3$): δ=173.0, 170.6, 164.7, 136.5, 136.4, 116.2, 115.9, 55.9, 44.9, 35.9, 35.1, 29.2, 27.9 ppm; IR: ν=3313-3298, 3059-2852, 1796, 1697, 1659, 1641, 1531 cm$^{-1}$; HRMS (ESI): calcd. for $C_{13}H_{18}N_2O_3Na$ $[M + Na]^+$ 273.1215, found 273.1214.

*(S)-N-(1-hex-5-enoyl-2-oxoazetidin-3-yl)hex-5-enamide* (**12b**).

Compound **12b** was synthesized according to the procedure described above for the synthesis of compound **12c** from β-lactam **10b** (191 mg, 0.68 mmol) and 5-hexenoyl chloride. Flash column chromatography (hexane/EtOAc 3/2) provided **12b** as a colourless solid (163 mg, 87%). $R_f$=0.39 (hexane/EtOAc 1/1); m.p. 88.7-89.6 °C; $[\alpha]_D^{20}$ +14.6 (*c* 2.75, $CHCl_3$); $^1$H NMR (300 MHz, $CDCl_3$): δ=6.18 (d, *J*=7.0 Hz, 1H), 5.76 (m, 2H), 5.05-4.96 (m, 4H), 4.71 (td, J=3.9, 7.4 Hz, 1H), 3.86 (m, 1H), 3.66 (m, 1H), 2.73 (td, *J*=3.8, 7.4 Hz, 2H), 2.24 (m, 2H), 2.10 (m, 4H), 1.75 ppm (m, 4H); $^{13}$C (75 MHz, $CDCl_3$): δ=173.5, 171.3, 164.7, 137.8, 137.6, 115.7, 115.5, 55.8, 45.0, 36.0, 35.0, 33.1, 33.0, 24.2, 23.2 ppm; IR: ν=3329-3298, 3057-2852, 1797, 1697, 1661, 1643, 1531 cm$^{-1}$; HRMS (ESI): calcd. for $C_{15}H_{22}N_2O_3Na$ $[M + Na]^+$ 301.1528, found 301.1535.

*(S)-N-(1-hept-6-enoyl-2-oxoazetidin-3-yl)-N-(methyl)hept-6-enamide* (**13c**).
Compound **13c** was synthesized according to the procedure described above for the synthesis of compound **12c** from β-lactam **11c** (336 mg, 1.08 mmol) and 6-heptenoyl chloride. Flash column chromatography (hexane/EtOAc 3/2) provided **13c** as a colourless oil (263 mg, 76%). $R_f$=0.28 (hexane/EtOAc 3/2); $[\alpha]_D^{20}$ +13.3 (*c* 3.5, $CHCl_3$); $^1$H NMR (300 MHz, $CDCl_3$): δ=5.77 (m, 2H), 5.02-4.89 (m, 5H), 3.81 (m, 1H), 3.63 (dd, *J*=3.9, 7.4 Hz, 1H), 3.05 (s, 3H), 2.73 (m, 2H), 2.34 (m, 2H), 2.06 (m, 4H), 1.66 (m, 4H), 1.43 ppm (m, 4H); $^{13}$C (75 MHz, $CDCl_3$): δ=173.8, 171.3, 164.4, 138.5, 138.4, 114.9, 114.8, 62.9, 43.1, 36.5, 35.4, 33.6, 33.5, 33.4, 28.6, 28.4, 24.1, 23.5 ppm; IR: ν=3074-2858, 1790, 1738, 1703, 1651 $cm^{-1}$; HRMS (CI): calcd. for $C_{18}H_{29}N_2O_3$ $[M + H]^+$ 321.21782, found 321.21822.

*(S)-N-methyl-N-(2-oxo-1-pent-4-enoylazetidin-3-yl)pent-4-enamide* (**13a**).
Compound **13a** was synthesized according to the procedure described for the synthesis of compound **12c** from β-lactam **11a** (150 mg, 0.53 mmol) and 4-pentenoyl chloride. Flash column chromatography (hexane/EtOAc 3/2) provided **13a** as a colourless solid (127 mg, 91%). $R_f$=0.31 (hexane/EtOAc 1/1); m.p. 39.8-40.5 °C; $[\alpha]_D^{20}$ +19.0 (*c* 3.0, $CHCl_3$); $^1$H NMR (300 MHz, $CDCl_3$): δ=5.83 (m, 2H), 5.10-4.97 (m, 4H), 4.92 (dd, *J*=3.9, 6.6 Hz, 1H), 3.82 (m, 1H), 3.64 (dd, *J*=3.9, 7.4 Hz, 1H), 3.06 (s, 3H), 2.83 (m, 2H), 2.47-2.37 ppm (m, 6H); $^{13}$C (75 MHz, $CDCl_3$): δ=173.1, 170.6, 164.3, 137.0, 136.6, 115.8, 115.7, 62.9, 43.1, 35.9, 35.4, 32.8, 28.7, 28.0 ppm; IR: ν=3076-2852, 1790, 1697, 1651 $cm^{-1}$; HRMS (ESI): calcd. for $C_{14}H_{20}N_2O_3Na$ $[M + Na]^+$ 287.1372, found 287.1385.

*(S)-N-(1-hex-5-enoyl-2-oxoazetidin-3-yl)-N-methylhex-5-enamide* (**13b**).

Compound **13b** was synthesized according to the procedure described above for the synthesis of compound **12c** from β-lactam **11b** (326 mg, 1.10 mmol) and 5-hexenoyl chloride. Flash column chromatography (hexane/EtOAc 3/2) provided **12b** as a colourless oil (255 mg, 79%). $R_f$=0.34 (hexane/EtOAc 1/1); $[\alpha]_D^{20}$ +14.3 (*c* 4.1, $CHCl_3$); $^1$H NMR (300 MHz, $CDCl_3$): δ=5.77 (m, 2H), 5.05-4.95 (m, 4H), 4.91 (dd, *J*=3.9, 6.5 Hz, 1H), 3.81 (m, 1H), 3.64 (dd, *J*=3.9, 7.4 Hz, 1H), 3.04 (s, 3H), 2.74 (m, 2H), 2.34 (m, 2H), 2.10 (m, 4H), 1.75 ppm (m, 4H); $^{13}$C (75 MHz, $CDCl_3$): δ=173.7, 171.3, 164.3, 137.9, 137.8, 115.5, 115.4, 62.9, 43.1, 36.0, 35.4, 33.1 (2C), 32.6, 23.6, 23.2 ppm; IR: ν=3076-2851, 1790, 1697, 1651 $cm^{-1}$; HRMS (CI): calcd. for $C_{16}H_{25}N_2O_3$ $[M + H]^+$ 293.18652, found 293.18725.

### 4.4. General procedure for RCM

Grubbs catalyst (second generation) (0.05 eq.) was added to a stirred solution of β-lactam (1 eq.) in dry $CH_2Cl_2$ (5 mM) and the solution was stirred at reflux under argon for 4 h. Then a second addition of Grubbs catalyst (0.05 eq.) was made and then reaction was additionally stirred at reflux for 20 h. Then the solvent was removed under reduced pressure and the crude product purified thrice by column chromatography (hexane/EtOAc), to provide products as pale-brown oils.

*(S)-tert-butyl 2,13,16-trioxo-1,14-diazabicyclo[13.1.1]heptadec-7-ene-14-carboxylate* (**14c**).

Yield: 9% (43 mg from 1.22 mmol of **9c**). $R_f$=0.51 (hexane/EtOAc 7/3); $[\alpha]_D^{20}$ -32.4 (*c* 2.8, $CHCl_3$); $^{13}$C (125 MHz, $CDCl_3$): δ=176.6, 172.6, 164.2,

151.3, 131.1, 130.6, 85.4, 59.7, 44.6, 38.3, 38.2, 32.1, 31.5, 30.5, 28.9, 28.1, 24.8, 22.7 ppm; IR: ν=2976-2854, 1799, 1738, 1697 $cm^{-1}$; HRMS (ESI): calcd. for $C_{20}H_{30}N_2O_5Na$ $[M + Na]^+$ 401.20469, found 401.20442.

*Compound* (**15b**).

Yield: 44% (229 mg from 1.47 mmol of **9b**). $R_f$=0.53 (hexane/EtOAc 3/2); $[\alpha]_D^{20}$ -9.1 (*c* 3.0, $CHCl_3$); $^{13}C$ (75 MHz, $CDCl_3$): δ=175.7, 175.4, 171.4, 164.1, 163.9, 151.4, 151.3, 85.5, 85.1, 57.8, 57.5, 43.8, 43.7, 37.7, 37.4, 34.8, 31.9, 31.8, 31.7, 31.5, 28.0, 24.5, 22.6 ppm; IR: ν=2970-2853, 1797, 1744, 1701 $cm^{-1}$; HRMS (ESI): calcd. for $C_{36}H_{52}N_4O_{10}Na$ $[M + Na]^+$ 723.35756, found 723.35643.

*Compound* (**15c**).

Yield: 10% (46 mg from 1.22 mmol of **9c**). $R_f$=0.45 (hexane/EtOAc 7/3); $[\alpha]_D^{20}$ +5.8 (*c* 4.4, $CHCl_3$); $^{13}C$ (125 MHz, $CDCl_3$): δ=175.6, 175.5, 171.5, 171.4, 164.5, 164.4, 151.4, 151.3, 130.7, 130.6, 130.5, 130.3, 85.5, 57.4, 57.2, 43.9, 43.8, 38.4, 38.2, 36.5, 32.3, 32.2, 32.1, 28.8, 28.7, 28.0, 24.1, 24.0, 23.7, 23.4 ppm; IR: ν=2928-2856, 1799, 1742, 1697 $cm^{-1}$; HRMS (ESI): calcd. for $C_{40}H_{60}N_4O_{10}Na$ $[M + Na]^+$ 779.42017, found 779.41947.

*Compound* (**16b**).

Yield: 35% (30 mg from 0.34 mmol of **12b**). $R_f$=0.32 (EtOAc); $[\alpha]_D^{20}$ -15.6 (*c* 2.2, $CHCl_3$); $^{13}C$ (75 MHz, $CDCl_3$): δ=174.4, 171.0, 165.8, 131.5, 130.8, 55.7, 46.0, 35.4, 34.5, 31.8, 31.6, 24.3, 22.0 ppm; IR: ν=3387-3284, 2930-2906, 1784, 1693, 1676, 1655, 1527 $cm^{-1}$; HRMS (ESI): calcd. for $C_{26}H_{36}N_4O_6Na$ $[M + Na]^+$ 523.25271, found 523.25171.

*Compound* (**16c**).

Yield: 28% (46 mg from 0.42 mmol of **12c**). $R_f$=0.48 (EtOAc); $[\alpha]_D^{20}$ +13.3 (*c* 2.4, $CHCl_3$); $^{13}C$ (125 MHz, $CDCl_3$): δ=174.2, 173.8, 172.4, 171.7, 165.5, 164.9, 130.9, 130.8, 130.6, 130.0, 55.6, 55.2, 45.4, 45.1, 36.8, 36.5, 36.3, 36.1, 31.9, 31.8, 31.7, 28.4, 28.3, 28.2, 28.1, 24.7, 24.4, 23.3, 22.8 ppm; IR: ν=3323, 2926, 2854, 1796, 1697, 1678, 1533 $cm^{-1}$; HRMS (ESI): calcd. for $C_{30}H_{44}N_4O_6Na$ $[M + Na]^+$ 579.31531, found 579.31433.

*Compound* (**17b**).

Yield: 43% (78 mg from 0.69 mmol of **13b**). $R_f$=0.46 (EtOAc); $[\alpha]_D^{20}$ -10.7 (*c* 1.1, $CHCl_3$); $^{13}C$ (125 MHz, $CDCl_3$): δ=174.1, 171.4, 164.5, 131.4, 130.9, 130.6, 130.4, 63.0, 61.9, 43.1, 36.0, 35.4, 35.2, 35.1, 32.5, 31.9, 31.6, 31.4, 24.1, 24.0, 23.4, 22.8 ppm; IR: ν=2976-2851, 1790, 1695, 1651 $cm^{-1}$; HRMS (ESI): calcd. for $C_{28}H_{40}N_4O_6Na$ $[M + Na]^+$ 551.28401, found 551.28341.

*Compound* (**17c**).

Yield: 40% (20 mg from 0.17 mmol of **13c**). $R_f$=0.47 (EtOAc); $[\alpha]_D^{20}$ -9.1 (*c* 3.0, $CHCl_3$); $^{13}C$ (125 MHz, $CDCl_3$): δ=174.0, 173.9, 171.6, 164.5, 164.4, 130.6, 130.5, 130.4, 130.2, 63.1, 62.5, 43.2, 43.1, 36.6, 36.5, 33.6, 33.5, 33.4, 32.3, 32.1, 32.0, 29.2, 29.0, 28.9, 28.8, 23.9, 23.8, 23.6, 23.5 ppm; IR: ν=3003-2851, 1786, 1736, 1716 $cm^{-1}$; HRMS (ESI): calcd. for $C_{32}H_{48}N_4O_6Na$ $[M + Na]^+$ 607.34661, found 607.34582.

### 4.5. General procedure for hydrogenation

To a stirred solution of compound obtained by RCM (1 eq.) in methanol (0.03 M) was added 10% Pd/C (0.05 eq.). After being stirred under

hydrogen atmosphere (P = 1 atm) for 3 h at room temperature, the mixture was filtered through a short pad of Celite and concentrated under reduced pressure. The residue was purified by column chromatography (hexane/EtOAc), to provide products as colourless oils.

*(S)-tert-butyl 2,13,16-trioxo-1,14-diazabicyclo[13.1.1]heptadecane-14-carboxylate* (**18c**).

Yield: 68% (30 mg from 43 mg of **14c**). $R_f$=0.29 (hexane/EtOAc 4/1); $[\alpha]_D^{20}$ -6.3 (*c* 2.2, $CHCl_3$); $^{13}C$ (125 MHz, $CDCl_3$): δ=176.5, 172.9, 164.3, 151.4, 85.3, 59.5, 44.3, 38.2, 37.0, 28.4, 28.3, 28.1, 27.7, 27.5, 26.6, 26.5, 25.7, 23.0 ppm; IR: ν=2976-2854, 1798, 1743, 1697 $cm^{-1}$; MS (ESI) *m/z* (%): 403 (57) $[M + Na]^+$, 783 (100) $[2M + Na]^+$; MS (APCI) *m/z* (%): 381 (67) $[M + H]^+$, 281 (100) (381-$CO_2$ & $C_4H_8$); HRMS (ESI): calcd. for $C_{20}H_{32}N_2O_5Na$ $[M + Na]^+$ 403.22034, found 403.22019.

*Compound* (**19b**).

Yield: 70% (36 mg from 51 mg of **15b**). $R_f$=0.53 (hexane/EtOAc 3/2); $[\alpha]_D^{20}$ -16.8 (*c* 2.7, $CHCl_3$); $^{13}C$ (75 MHz, $CDCl_3$): δ=175.7, 172.0, 171.9, 164.1, 164.0, 151.4, 85.4, 58.3, 58.1, 43.7, 43.6, 38.5, 38.1, 36.5, 36.4, 29.2, 28.8, 28.7, 28.6, 28.4, 28.0, 27.9, 24.8, 24.6, 24.3 ppm; IR: ν=2978-2856, 1797, 1744, 1697 $cm^{-1}$; MS (ESI) *m/z* (%): 727 (91) $[M + Na]^+$, 713 (10) (727 - $CH_2$), 627 (81) (727 - $CO_2$ & $C_4H_8$), 527 (100) (727 - 2($CO_2$ & $C_4H_8$)); MS (APCI) *m/z* (%): 705 $[M + H]^+$; HRMS (ESI): calcd. for $C_{36}H_{56}N_4O_{10}Na$ $[M + Na]^+$ 727.38886, found 727.38811.

*Compound* (**19c**).

Yield: 35% (28 mg from 80 mg of **15c**). $R_f$=0.44 (hexane/EtOAc 7/3); $[\alpha]_D^{20}$ -14.4 (*c* 1.9, $CHCl_3$); $^{13}C$ (125 MHz, $CDCl_3$): δ=175.7, 171.8, 164.2, 164.1,

151.3, 85.5, 57.9, 57.8, 43.7, 43.6, 38.4, 38.3, 38.2, 36.6, 36.5, 29.3, 29.2, 29.1, 29.0, 28.9, 28.8, 28.7, 28.0, 24.7, 24.4, 24.2 ppm; IR: ν=2976-2854, 1797, 1745, 1697 $cm^{-1}$; MS (ESI) *m/z* (%): 783 (100) $[M + Na]^+$, 769 (82) (783 - $CH_2$), 755 (32) (783 - $C_2H_4$), 683 (37) (783 - $CO_2$ & $C_4H_8$), 583 (24) (783 - 2($CO_2$ & $C_4H_8$)); MS (APCI) *m/z* (%): 761 $[M + H]^+$; HRMS (ESI): calcd. for $C_{40}H_{64}N_4O_{10}Na$ $[M + Na]^+$ 783.45147, found 783.45063.

*Compound* (**20b**).

Yield: 48% (20 mg from 41 mg of **16b**). $R_f$=0.41 (EtOAc/MeOH 98/2); $[\alpha]_D^{20}$ -22.1 (*c* 1.2, $CHCl_3$); $^{13}C$ (125 MHz, $CD_3OD$): δ=176.8, 173.4, 166.8, 57.1, 56.9, 45.7, 45.4, 37.2, 37.1, 36.3, 36.1, 29.9, 29.6, 29.5, 29.4, 26.4, 26.3, 25.3, 25.2 ppm; IR: ν=3313, 2928, 2856, 1796, 1697, 1670, 1655, 1535 $cm^{-1}$; MS (ESI) *m/z* (%): 527 (100) $[M + Na]^+$, 513 (18) (527 - $CH_2$); MS (APCI) *m/z* (%): 505 $[M + H]^+$; HRMS (ESI): calcd. for $C_{26}H_{40}N_4O_6Na$ $[M + Na]^+$ 527.28401, found 527.28333.

*Compound* (**20c**).

Yield: 60% (30 mg from 50 mg of **16c**). $R_f$=0.43 (EtOAc); $[\alpha]_D^{20}$ -11.6 (*c* 2.2, $CHCl_3$); $^{13}C$ (125 MHz, $CDCl_3$): δ=174.1, 174.0, 171.8, 165.1, 164.8, 55.9, 55.8, 45.2, 45.0, 36.5, 36.4, 35.9, 35.8, 28.6, 28.5, 28.4, 28.2, 25.1, 24.0 ppm; IR: ν=3358-3068, 2926, 2852, 1796, 1693, 1682, 1533 $cm^{-1}$; MS (ESI) *m/z* (%): 583 (100) $[M + Na]^+$, 569 (14) (583 - $CH_2$); MS (APCI) *m/z* (%): 561 $[M + H]^+$; HRMS (ESI): calcd. for $C_{30}H_{48}N_4O_6Na$ $[M + Na]^+$ 583.34661, found 583.34579.

*Compound* (**21b**).

Yield: 70% (28 mg from 39 mg of **17b**). $R_f$=0.24 (EtOAc); $[\alpha]_D^{20}$ -13.6 (*c* 2.7, $CHCl_3$); $^{13}C$ (125 MHz, $CDCl_3$): δ=173.9, 172.1, 171.9, 164.2, 64.2,

63.2, 43.4, 43.3, 36.7, 36.5, 33.5, 33.0, 29.0, 28.7, 28.6, 28.5, 28.3, 24.6, 24.5, 24.3 ppm; IR: ν=2928, 2854, 1792, 1693, 1651 $cm^{-1}$; MS (ESI) *m/z* (%): 555 (100) $[M + Na]^+$; MS (APCI) *m/z* (%): 533 $[M + H]^+$; HRMS (ESI): calcd. for $C_{28}H_{44}N_4O_6Na$ $[M + Na]^+$ 555.31531, found 555.31421.

*Compound* (**21c**).

Yield: 24% (12 mg from 48 mg of **17c**). $R_f$=0.43 (EtOAc); $[\alpha]_D^{20}$ -9.6 (*c* 1.1, $CHCl_3$); $^{13}C$ (125 MHz, $CDCl_3$): δ=174.0, 171.9, 164.3, 63.6, 63.1, 43.3, 36.6, 36.5, 36.2, 35.6, 33.6, 33.4, 29.8, 29.5, 29.3, 29.2, 29.1, 29.0, 28.8, 24.5, 24.4, 24.3 ppm; IR: ν=2924, 2852, 1794, 1697, 1655 $cm^{-1}$; MS (ESI) *m/z* (%): 611 (100) $[M + Na]^+$, 597 (25) (611 - $CH_2$); MS (APCI) *m/z* (%): 589 $[M + H]^+$; HRMS (ESI): calcd. for $C_{32}H_{52}N_4O_6Na$ $[M + Na]^+$ 611.37791, found 611.37680.

## 5. Acknowledgements

This work was supported by the Interuniversity Attraction Pole (IAP P6/19 PROFUSA), F.R.S.-FNRS, UCL and ULg (computational facilities). G. D. and J. M.-B. are senior research associates of the F.R.S.-FNRS (Belgium). J.-L. H. J. thanks the Belgian National Fund for Scientific Research (FNRS) (FRFC 2.4555.08), the Special Fund for Research (FSR) and the faculty of medicine of UCL for financial support on this research (LTQ-Orbitrap). Dr. Astrid Zervosen is acknowledged for the R39 testing. Ir. Raoul Rozenberg, Dr. Cécile Le Duff and Dr. Marie-France Hérent have contributed to the structural analysis.

## 6. Supplementary data

The Supplementary data includes NMR spectra of all new compounds, ESI and APCI mass spectra for compounds **14c**, **15b-c** to **17b-c**, generation of conformers, graphics of relative energies of precursors/cyclic monomers, heat of formation for precursors **9a-c**, **12a-c** and **13a-c**, and testing protocol *vs* R39. Supplementary data related to this article can be found online at doi:10.1016/j.tet.2010.10.015. Relevant material of the Supplementary data is added below, *i.e.* screening experiments with R39, generation of conformers and Grubbs adducts.

### 6.1. Screening experiments with R39

All assays with R39 have been done in microtiter plates 96-well. The residual activity (RA) was determined after preincubation of the PBP in the presence of inhibitors. Therefore the initial rate of hydrolysis of 1mM substrate (S2d) in the presence of 1mM DTNB was determined by monitoring the increase of absorbance at 412 nm (DTNB: $\varepsilon[\Delta\varepsilon] = 13600\ M^{-1}\ s^{-1}$). The rate of spontaneous hydrolysis of S2d in the presence of the inhibitors was also determined in absence of the enzyme. All assays have been done three times. The determination of RA of R39 in absence of inhibitors has been done six times on each plate.

Assays have been done under the following conditions: 20 mM of the testing compounds have been solved in DMF. Finally 7.5 μL of the solution have been used in the assay. The final concentration of the compounds in the assays was 1 mM or 100 μM. The final concentration of

DMF in the assays was 5% (1 mM compound) or 0.25% (100 µM compound).

Preincubation has been done under the following conditions (volume: 127 µl): 3.5 nM R39 was incubated in the presence of inhibitors in 10 mM sodium phosphate buffer (pH 7.2) with 100 mM NaCl, 100 mM D-alanine, 0.01 mg/ml BSA and 0.01% Triton for 60 min at 25 °C. The determination of the RA was done by addition of S2d in the presence of DTNB (volume: 23 µl) as described above using a microtiter plate reader power wave.

Discussion: In order to study the maximum of compounds in a short time assay conditions have been developed that allow us to use 96-well micro titer plates for the realization of the assays. A preincubation of the testing compounds with R39 of 1 hour was realized, in order to detect also slow binding inhibitors. After the preincubation the residual activity RA of PBP was determined by observing the hydrolysis of the thiolester S2d catalyzed by the non-inhibited enzyme. A tested compound was considered as an inhibitor if RA was < 80%. In order to detect false positives, the assays have been done in the presence of 0.01% Triton-X-100. As described in literature promiscuous inhibitors (false positives) are slow binding, non-competitive inhibitors. In order to avoid a detailed kinetic research it is possible to identify such compounds by realizing assays in the presence of Triton-X-100. Promiscuous inhibitors show no inhibition in the presence of Triton-X-100.

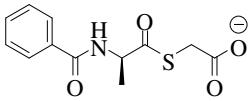

**Figure 9**. N-benzoyl-D-alanyl-thioglycolate (S2d).

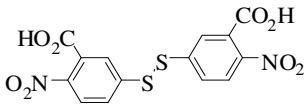

**Figure 10**. 5-(3-Carboxy-4-nitrophenyl)disulfanyl-2-nitrobenzoic acid (DTNB).

### 6.2. Generation of conformers

Generation of precursor, monomer and dimer conformers: an optimized geometry is the starting point submitted to a dynamics simulation at 300 K. The chosen force field is Amber,[23] with a relative dielectric constant set to 1. The programs used are Insight-Discover[24] running on a Pentium 4 3.4 GHz under Unix Debian. From this sampling, several conformers are reoptimized at the B3LYP/6-31G(d) level. Depending on the numerous combinations of parameters, such as the relative orientation of the carbonyls and the different conformations of the cycle due to the $CH_2$-$CH_2$ disposition, a subset of 4 conformers has been retained to compare their relative energies and heats of formation.

Conformers with the 14- and 16-membered cycles under the β-lactam ring: in this table, the relative energies are calculated for the open precursors and monocyclic molecules, and also with respect to the corresponding conformer, with the cycle above the β-lactam ring. For both molecules in the 4 conformations, the "up" disposition is more stable than

the "down" one, the energy differences being greater for **9b** than **9c** (**Table 5**).

**Table 5**

Relative energies of the precursors/cyclic monomers in the selected conformations with the cycle above the β-lactam ring, and comparison with "up" monomers.

| Precursor | Geometry | Relative Energy of open precursors (kcal/mol) | Relative Energy of "down" monomers (kcal/mol) | Relative Energy in comparison with "up" monomers (kcal/mol) |
|---|---|---|---|---|
| **9b** | Amide cis *i* a | 5.85 | 7.21 | 6.87 |
| | Amide cis *i* b | 4.30 | 5.64 | 8.57 |
| | Amide cis *ii* a | 2.55 | 2.01 | 10.07 |
| | Amide cis *ii* b | 0.00 | 0.00 | 8.06 |
| **9c** | Amide cis *i* a | 6.85 | 9.66 | 1.92 |
| | Amide cis *i* b | 4.99 | 7.53 | 3.12 |
| | Amide cis *ii* a | 2.61 | 4.90 | 4.72 |
| | Amide cis *ii* b | 0.00 | 0.00 | 3.06 |

Tautomeric forms: in the same way than in the previous table, the relative energies of **12b** and **12c** are also calculated with respect to the standard amide bond. In all cases, the tautomeric conformers are not the more stable (**Table 6**).

**Table 6**

Relative energies of the tautomeric form and comparison with the amide form.

| Precursor | Geometry | | Relative Energy of tautomeric form (kcal/mol) | Relative Energy in comparison with amide form (kcal/mol) |
|---|---|---|---|---|
| **12b** | Open | cis *i* | 7.02 | 8.03 |
| | precursor | cis *ii* | 7.36 | 13.93 |
| | | trans *i* | 4.42 | 9.82 |
| | | trans *ii* | 0.00 | 11.35 |
| | Monomer | cis *i* | 7.25 | 12.76 |
| | | cis *ii* | 0.00 | 3.33 |
| | | trans *i* | 13.90 | 18.80 |
| | | trans *ii* | 10.79 | 21.25 |
| **12c** | Open | trans *i* | 4.44 | 11.21 |
| | precursor | trans *ii* | 0.00 | 11.66 |
| | Monomer | cis *i* | 11.59 | 12.46 |
| | | cis *ii* | 4.50 | 13.75 |
| | | trans *i* | 3.65 | 9.77 |
| | | trans *ii* | 0.00 | 11.13 |

### 6.3. Grubbs adducts

Several attempts to generate the Grubbs's first step adducts have been performed at the B3LYP level using the double ζ basis set of the Los Alamos effective core potential. Minima have been located for both types of link between the Ru atom and the ethylenic fragment either located on the C(3) of the β-lactam (left) or on the N(1) imide chain (right) in the case of compound **12b**. With the amide cis and the imide *syn*, both adducts present the *a priori* favourable conformation. The C(3) linked Ru conformer is more stable than the N(1) imide substitution. The energy difference is less than 0.7 kcal (negligeable). The second pair of conformers concerns the *syn* imide

arrangement coupled with the trans amide orientation. The C(3) conformer is 1.9 kcal more stable. In both cases, the second ethylenic fragment is not oriented to the Ru. These results reinforce the proprension of such compounds to generate dimers.

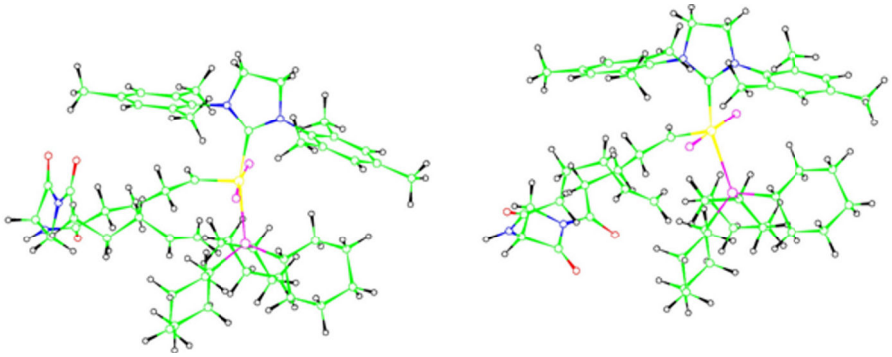

**Figure 11**. Amide cis and the imide *syn*.

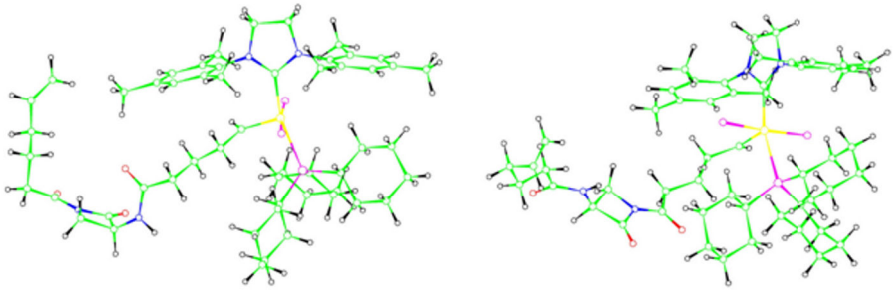

**Figure 12**. Amide trans and the imide *syn*.

## 7. Addendum on methyl family

This section was not present in the publication and describes previous results on the methyl family.

As a first strategy to obtain the N-Me family, we considered the synthesis of compound **7** from compound **3** (**Scheme 4**).

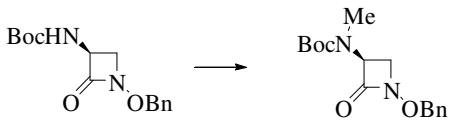


**3** **7**

**Scheme 4**. N-methylation of amide **3**.

Several attempts were performed, to find the best conditions to carry out the methylation (**Table 7**), which revealed to be the use of LiHMDS in the presence of dimethyl sulfate, giving compound **7** in 62% yield.[10]

**Table 7**

Methylation of amide **3**.

| Base | Reagent | Time | T | Yield (%) |
|---|---|---|---|---|
| NaH (1.1 eq)[25] | MeI (4 eq) | 12 h | 0 °C to rt | 0 |
| KOH (1 eq)[26] | MeI (20 eq) | 12 h | 0 °C to rt | 0 |
| KHMDS (1 eq)[27] | MeI (10 eq) | 12 h | -78 °C to rt | 16 |
| KHMDS (1 eq) | $Me_2SO_4$ (1.5 eq) | 48 h | -78 °C to rt | 35 |
| LiHMDS (1 eq) | $Me_2SO_4$ (1.5 eq) | 24 h | -78 °C to rt | 62 |

As said previously, the scaling-up was not successful. Then we tried to synthesize Boc-Me-L-serine **5** from Boc-L-serine **1**. The direct methylation of compound **1** to compound **5** failed, the reaction leading to both N-methylation and O-methylation (**Scheme 5**).

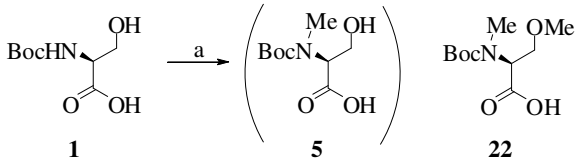


**1** **5** **22**

**Scheme 5**. Synthesis of compound **22**. Reagents and conditions: (a) NaH, MeI, THF, 0 °C.

To avoid the O-alkylation, we carried out the N-methylation on the commercially available compound **23**, derivative of Boc-L-serine, for which the hydroxyl function is protected with a benzyl group. This experiment was performed with the method proposed by Cheung and Benoiton[28] in the presence of NaH and MeI at 0 °C during 24h and afforded compound **24** in 59% yield. Catalytic hydrogenation of compound **24** in the presence of $Pd(OH)_2/C$ gave the compound **5** in quantitative yield (**Scheme 6**).[29]

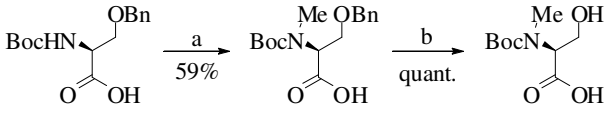


**23** **24** **5**

**Scheme 6**. Synthesis of compound **5**. Reagents and conditions: (a) NaH, MeI, THF, 0 °C; (b) $H_2$, $Pd(OH)_2/C$, MeOH, rt.

The N-methylation of compound **23** afforded compound **24** with medium yield, and this reaction was not easily performed in high scale.

Therefore to spare time, we decided to buy compound **5**, even if this compound is quite expensive (68 € for 1 g). Boc-Me-L-serine **5** was converted into the corresponding hydroxamate **6** by a coupling reaction with O-benzylhydroxylamine (**Scheme 7**).

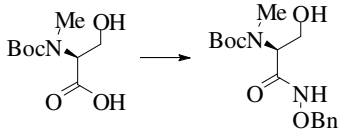


**5** **6**

**Scheme 7**. Synthesis of hydroxamate **6**.

We needed several attempts to reach the optimal conditions for the coupling reaction (**Table 8**), namely the use of EDCI as coupling reagent in $CH_2Cl_2$ as previously described.

**Table 8**

Synthesis of hydroxamate **6**.

| Coupling reagent | $NH_2OBn$ | Solvent | Yield (%) |
|---|---|---|---|
| DCC (1.05 eq) | 1 eq | THF | 44 |
| DCC (1.05 eq)/DMAP (cat) | 1 eq | THF | 53 |
| EDCI (1.3 eq)/ DMAP (cat) | 1 eq | $CH_2Cl_2$ | 65 |
| EDCI (1.3 eq)/ NMM (1.3 eq) | 1.3 eq | $CH_2Cl_2$ | 55 |
| EDCI (1.3 eq) | 1 eq | $CH_2Cl_2$ | 72 |
| EDCI (1.5 eq) | 1.5 eq | $CH_2Cl_2$ | 91 |

Then intramolecular cyclization of compound **6** was performed with the method proposed by Miller et al. to obtain compound **7** (**Scheme 8**).[7]

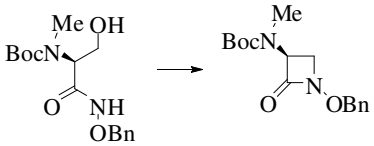


**6** **7**

**Scheme 8**. Cyclization of hydroxamate **6**.

Several attempts were performed to find the best conditions to carry out the intramolecular cyclization (**Table 9**), which revealed to be the use of TEA, $PPh_3$ and $CCl_4$ in $CH_3CN$ as previously described.

**Table 9**

Cyclization of hydroxamate **6**.

| $CX_4$ | TEA | $PPh_3$ | Solvent | Yield (%) |
|---|---|---|---|---|
| $CBr_4$ (2 eq) /imidazole (2eq) | 2 eq | 2 eq | THF | 48 |
| $CCl_4$ (1.1 eq) | 1.5 eq | 1.1 eq | THF | 0 |
| $CCl_4$ (1.1 eq) | 1.5 eq | 1.1 eq | THF/$CH_3CN$ (1/1) | 56 |
| $CCl_4$ (1.1 eq) | 1.5 eq | 1.1 eq | $CH_3CN$ | 82 |

The synthesis of chiron **8** and the mono- and bis-acylated compounds (**11a-c** and **13a-c**) of methyl family were synthesized as described and did not necessitate optimizations.

## 8. Appendix on the catalyst used for metathesis

In the attempts to obtain a cyclomonomer, several metathesis catalysts were tested. In order to evaluate different parameters such as temperature, solvent, concentration or time, we selected ruthenium catalysts that are commercially available.

The synthesis of medium or large sized rings from acyclic diene precursors by Ring-Closing metathesis reaction (**Scheme 9**) became a common process with the introduction of ruthenium catalysts.

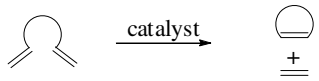


**Scheme 9**. Ring-Closing Metathesis reaction.

In fact, ruthenium catalysts, instead of the early titanium, tungsten or molybdenum catalysts, are tolerant to many functional groups. In **Table 10** is represented the functional group tolerance of metal metathesis catalysts.[30] Ruthenium catalysts react preferentially with olefins instead of other functions. These catalysts are stable in presence of air atmosphere and moisture unlike the other catalysts. Consequently, many studies were performed for the development of well-defined ruthenium catalyst.

**Table 10**

Functional group tolerance of transition metal olefin metathesis catalysts.

| Titanium | Tungsten | Molybdenum | Ruthenium | |
|---|---|---|---|---|
| Acids | Acids | Acids | Olefins | Increasing |
| Alcohols, water | Alcohols, water | Alcohols, water | Acids | Reactivity |
| Aldehydes | Aldehydes | Aldehydes | Alcohols, water | ↑ |
| Ketones | Ketones | Olefins | Aldehydes | |
| Esters, Amides | Olefins | Ketones | Ketones | |
| Olefins | Esters, Amides | Esters, Amides | Esters, Amides | |

During their prospect on ruthenium alkylidene complexes, Grubbs and co-workers synthesized the pre-catalyst GI (**Figure 13**) which is now known as first generation Grubbs' catalyst. The easy synthesis of this catalyst, even on large scale, allowed its commercialization and therefore its widespread use in organic synthesis.

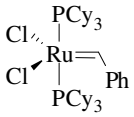


GI

**Figure 13**. Structure of GI catalyst.

Mechanistic studies were performed, allowing a better comprehension and a better design on the catalyst activity. Two mechanisms were studied, one is an associative pathway and the second one is a dissociative pathway (**Scheme 10**). Experimental studies indicate that the dissociative pathway, with phosphine dissociation preceding olefin binding, is favored.[31]

In the studies that lead to the synthesis of GI, it was established that the activity of the $(PR_3)_2X_2Ru{=}CHR^1$ catalyst is highly dependent of the ligand R and the halide X.[32] It was described that the activity increased with larger and more electron donating phosphines ($PPh_3$ << $PiPr_2Ph$ < $PCy_2Ph$ < $PiPr_3$ < $PCy_3$) and with smaller and more electron withdrawing halogens (I < Br < Cl).

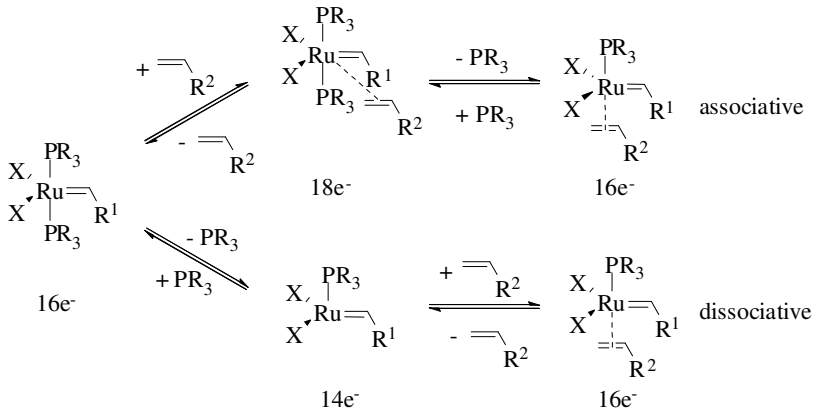


**Scheme 10**. Associative and dissociative pathways of $(PR_3)_2X_2Ru{=}CHR^1$.

Considering the ligands, the electron donating ability of phosphines stabilizes the $14e^-$ intermediate. Moreover the steric bulk of the ligands helps in the dissociation of one phosphine by destabilizing the bis(phosphine) complex. Less bulky phosphines are too strongly coordinated to the metal, and bulkier phosphines than $PCy_3$ lead to unstable complexes.

Considering the halogens, the problem could be related to the steric bulk from Cl to I. The more bulky halogens could increase the crowding at the ruthenium center, and therefore could disfavor the olefin coordination on the metal.

A problem encountered with the GI catalyst is its short lifetime. Studies on decomposition of catalysts showed that substituted alkylidenes were decomposed by a bimolecular mechanism involving the loss of a phosphine.[33] Since the first step in the metathesis reaction is the dissociation of a phosphine, any method to enhance the loss of a phosphine ligand would also increase the decomposition rate of the catalyst.

The next improvement in the development of ruthenium catalyst was the introduction of N-heterocyclic carbenes (NHC) ligands. Inspired by the work of Hermann,[34] who firstly introduced NHC ligands in ruthenium catalyst, many groups proposed catalysts with one NHC ligand and one phosphine. Grubbs developed compound GII (**Figure 14**), which is now known as second generation Grubbs' catalyst.[35]

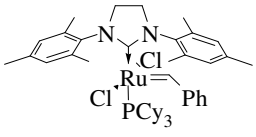


GII

**Figure 14**. Structure of GII catalyst.

This catalyst exhibits a high olefin metathesis activity and a better thermal activity compared to GI. Compared to phosphine, NHC ligands are stronger σ-donors and are less labiles. NHCs are neutral compounds with a divalent carbon occupied by six electrons in its valence shell, thus the singlet electronic state with $\sigma^2$ configuration is favored. The empty $p_\pi$ orbitals are in fact stabilized by the $p_\pi$ donation of the adjacent nitrogen atoms. It is leading to the strong σ-donor and low π-acceptor properties of NHCs (**Figure 15**).[36]

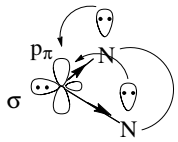


**Figure 15**. σ-donor property of NHC ligand.

The design of this type of catalyst was to enhance the dissociation of the more labile phosphine $PCy_3$, and to increase the stability of the $14e^-$ species with the σ-donor properties and steric protection to the metal center by the bulky NHC ligand. In fact steric properties of phosphines and NHC ligands are very different. In the case of phosphine ligands, the substituents point away of the metal, forming a "cone", for NHCs, the substituents point toward the metal, forming a "fence" (**Figure 16**).[37]

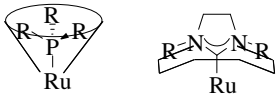


**Figure 16**. Comparison of $PR_3$ and NHC ligands.

But as proven by mechanistic studies[31a] the increase of activity of the catalysts containing a NHC ligand was not due to enhanced dissociation of the phosphine: in fact the rate of formation of the $14e^-$ species was $10^2$ times

slower compared to the first generation catalyst. The high activity is due to the fact that this second generation catalysts present an enhanced preference for the coordination with olefinic substrates instead of phosphines.

The first and second generation of Hoveyda-Grubbs' catalysts[38] (**Figure 17**) are analogues of first and second generation of Grubbs's catalyst, but an O-chelating benzylidene moiety was used instead of a leaving phosphine. Compared to Grubbs' catalysts, Hoveyda-Grubbs' catalysts are highly recyclable and the purification by flash chromatography is easier.

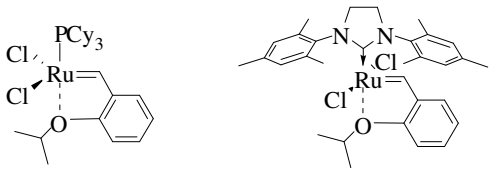


HGI HGII

**Figure 17**. Structures of HGI and HGII catalysts.

With the Schrock catalyst, the four catalysts described above are the most employed in organic synthesis.

Additionally, the last tried catalyst was Neolyst M2 (**Figure 18**). It is a ruthenium-indenylidene complexe developed by Nolan.[39]

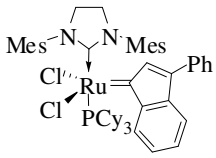


Neolyst M2

**Figure 18**. Structure of Neolyst M2 catalyst.

The indenylidene complexes are known to be more resistant to harsh reaction conditions than the benzylidene analogues.[40] Using higher temperatures, it was expected that conformers allowing the monocyclization would be present in solution. But in our case, it did not work.

To overcome the problem on conformational flexibility, the substrate was changed to *bis*-alkylated precursors (Chapter 7).

## 9. References and notes


[1] (a) Gradillas, A.; Pérez-Castells, *J. Angew. Chem. Int. Ed.* **2006**, *45*, 6086-6101; (b) Conrad, J. C.; Fogg, D. E. *Curr. Org. Chem.* **2006**, *10*, 185-202; (c) Majumdar, K. C.; Rahaman, H.; Roy, B. *Curr. Org. Chem.* **2007**, *11*, 1339-1365; (d) Clavier, H.; Grela, K.; Kirshning, A.; Mauduit, M.; Nolan, S. P. *Angew. Chem. Int. Ed.* **2007**, *46*, 6786-6801; (e) Nicolaou, K. C.; Bulger, P. G.; Sarlah, D. *Angew. Chem. Int. Ed.* **2005**, *44*, 4490-4527; (f) Brik, A. *Adv. Synth. Catal.* **2008**, *350*, 1661-1675.

[2] (a) Monfette, S.; Fogg, D. E. *Chem. Rev.* **2009**, *109*, 3783-3816; (b) Monfette, S.; Crane, A. K.; Duarte Silva, J. A.; Facey, G. A.; dos Santos, E. N.; Araujo, M. H.; Fogg, D. E. *Inorg. Chim. Acta* **2010**, *363*, 481-486.

[3] (a) Creighton, C. J.; Leo, G. C.; Du, Y.; Reitz, A. B. *Bioorg. Med. Chem.* **2004**, *12*, 4375-4385; (b) Chen, G.; Kirschning, A. *Chem. Eur. J.* **2002**, *8*, 2717-2729.

[4] (a) Tzur, E.; Ben-Asuly, A.; Diesendruck, C. E.; Goldberg, I.; Lemcoff, N. G. *Angew. Chem. Int. Ed.* **2008**, *47*, 6422-6425; (b) Diesendruck, C. E.; Ben-Asuly, A.; Goldberg, I.; Lemcoff, N. G. *Chim. Oggi* **2010**, *28*, 15-18.

[5] Pandian, S.; Hillier, I. H.; Vincent, M. A.; Burton, N. A.; Ashworth, I. W.; Nelson, D. J.; Percy, J. M.; Rinaudo, G. *Chem. Phys. Lett.* **2009**, *476*, 37-40.

[6] (a) Urbach, A.; Dive, G.; Marchand-Brynaert, J. *Eur. J. Org. Chem.* **2009**, *11*, 1757-1770; (b) Urbach, A.; Dive, G.; Tinant, B.; Duval, V.; Marchand-Brynaert, J. *Eur. J. Med. Chem.* **2009**, *44*, 2071-2080.

[7] Miller, M. J.; Mattingly, P. G.; Morrison, M. A.; Kerwin, J. F., Jr. *J. Am. Chem. Soc.* **1980**, *102*, 7026-7032.

[8] Qabar, M. N.; Kahn, M. *Tetrahedron Lett.* **1996**, *37*, 965-968.

[9] Structural description given by Mattingly, P. G.; Miller, M. J. *J. Org. Chem.* **1980**, *45*, 410-415.

[10] Prashad, M.; Har, D.; Hu, B.; Kim, H.-Y.; Repic, O.; Blacklock, T. J. *Org. Lett.* **2003**, *5*, 125-128.

[11] (a) Ahrendt, K. A.; Williams, R. M. *Org. Let.* **2004**, *24*, 4539-4541; (b) Gaul, C.; Njardarson, J. T.; Shan, D.; Dorn, D. C.; Wu, K.; Tong, W. P.; Huang, X.; Moore, M. A. S.; Danishefsky, S. J. *J. Am. Chem. Soc.* **2004**, *126*, 11326-11337.

[12] Fürstner, A.; Langemann, K. J. Am. Chem. Soc. 1997, 119, 9130-9136.

[13] Yamamoto, K.; Biswas, K.; Gaul, C.; Danishefsky, S. *Tetrahedron Lett.* **2003**, *44*, 3297-3299.

[14] (a) Knops, P.; Sendhoff, N.; Mekelburger, B.; Voegtle, F. *Top. Curr. Chem.* **1991**, *161*, 1-36; (b) Illumani, G.; Mandolini, L. *Acc. Chem. Res.* **1981**, *14*, 95-102.

[15] Francl, M. M.; Pietro, W. J.; Hehre, W. J.; Binkley, J. S.; DeFrees, D. J.; Pople, J. A.; Gordon, M. S. *J. Chem. Phys.* **1982**, *77*, 3654-3666.

[16] Frisch, M. J.; Trucks, G. W.; Schlegel, H. B.; Scuseria, G. E.; Robb, M. A.; Cheeseman, J. R.; Montgomery, J. A., Jr.; Vreven, T.; Kudin, K. N.; Burant, J. C.; Millam, J. M.; Iyengar, S. S.; Tomasi, J.; Barone, V.; Mennucci, B.; Cossi, M.; Scalmani, G.; Rega, N.; Petersson, G. A.; Nakatsuji, H.; Hada, M.; Ehara, M.; Toyota, K.; Fukuda, R.; Hasegawa, J.; Ishida, M.; Nakajima, T.; Honda, Y.; Kitao, O.; Nakai, H.; Klene, M.; Li, X.; Knox, J. E.; Hratchian, H. P.; Cross, J. B.; Adamo, C.; Jaramillo, J.; Gomperts, R.; Stratmann, R. E.; Yazyev, O.; Austin, A. J.; Cammi, R.; Pomelli, C.; Ochterski, J. W.; Ayala, P. Y.; Morokuma, K.; Voth, G. A.; Salvador, P.; Dannenberg, J. J.; Zakrzewski, V. G.; Dapprich, S.; Daniels, A. D.; Strain, M. C.; Farkas, O.; Malick, D. K.; Rabuck, A. D.; Raghavachari, K.; Foresman, J. B.; Ortiz, J. V.; Cui, Q.; Baboul, A. G.; Clifford, S.; Cioslowski, J.; Stefanov, B. B.; Liu, G.; Liashenko, A.; Piskorz, P.; Komaromi, I.; Martin, R. L.; Fox, D. J.; Keith, T.; Al-Laham, M. A.; Peng, C. Y.; Nanayakkara, A.; Challacombe, M.; Gill, P. M. W.; Johnson, B.; Chen, W.; Wong, M. W.; Gonzalez, C.; Pople, J. A. *Gaussian 03*, *Revision D.02*; Gaussian: Wallingford CT, 2004.

[17] Dunning, T. H., Jr.; Hay, P. J. In *Modern Theoretical Chemistry*; Schaefer, H. F., III, Ed.; PLENUM: New York, NY, 1976; Vol. 3, pp 1-28.

[18] Sauvage, E.; Herman, R.; Petrella, S.; Duez, C.; Bouillenne, F.; Frère, J.-M.; Charlier, P. *J. Biol. Chem.* **2005**, *280*, 31249-31256.

[19] (a) Schwyzer, R.; Hurlimann, C.; Coenzyle, C. *Helv. Chim. Acta* **1954**, *37*, 155-166; (b) Adam, M.; Damblon, C.; Plaitin, B.; Christiaens, L.; Frère, J.-M. *Biochem. J.* **1990**, *270*, 525-529.

[20] Zervosen, A.; Lu, W.-P.; Chen, Z.; White, R. E.; Demuth, T. P., Jr.; Frère, J.-M. *Antimicrob. Agents Chemother.* **2004**, *48*, 961-969.

[21] (a) Woodward, R. B. *Phil. Trans. R. Soc. Lond.(B)* **1980**, *289*, 239-250; (b) Cohen, N. C. *J. Med. Chem.* **1983**, *26*, 259-264; (c) Bruton, G. *Bioorg. Med. Chem. Lett.* **1993**, *3*, 2329-2332.

[22] El-azizi, Y.; Schmitzer, A.; Collins, S. K. *Angew. Chem. Int. Ed.* **2006**, *45*, 968-973.

[23] (a) Weiner, P. K.; Kollman, P. A. *J. Comput. Chem.* **1981**, *2*, 287-303; (b) Weiner, S. J.; Kollman, P. A.; Nguyen, D. T.; Case, D. A. *J. Comput. Chem.* **1986**, *7*, 230-252.

[24] Programs Insight and Discover, Accelrys Software Inc., www.accelrys.com

[25] Kells, K. W.; Ncube, A.; Chong, J. M. *Tetrahedron* **2004**, *60*, 2247-2257.

[26] Sammes, P. G.; Smith, S. *J. Chem. Soc. Perkin Trans. I* **1984**, 2415-2419.

[27] Hara, S.; Makino, K.; Hamada, Y. *Tetrahedron* **2004**, *60*, 8031-8035.

[28] Cheung, S. T.; Benoiton, N. L. *Can. J. Chem.* **1977**, *55*, 906-910.

[29] Pinet, E.; Cavelier, F.; Verducci, J.; Girault, G.; Dubart, L.; Haraux, F; Sigalat, C.; André, F. *Biochemistry* **1996**, *35*, 12804-12811.

[30] Trnka, T. M.; Grubbs, *Acc. Chem. Res.* **2001**, *34*, 18-29.

[31] (a) Sanford, M. S.; Ulman, M.; Grubbs, R. H. *J. Am. Chem. Soc.* **2001**, *123*, 749-750; (b) Sanford, M. S.; Love, J. A.; Grubbs, R. H. *J. Am. Chem. Soc.* **2001**, *123*, 6543-6554.

[32] Dias, E. L.; Nguyen, S. T.; Grubbs, R. H. *J. Am. Chem. Soc.* **1997**, *119*, 3887-3897.

[33] Ulman, M.; Grubbs, R. H. *J. Org. Chem.* **1999**, *64*, 7202-7207.

[34] (a) Herrmann, W. A.; Köcher, C. *Angew. Chem. Int. Ed.* **1997**, *36*, 2162-2187; (b) Weskamp, T.; Schattenmann, W. C.; Spiegler, M.; Herrmann, W. A. *Angew. Chem. Int. Ed.* **1998**, *37*, 2490-2493.

[35] Scholl, M.; Ding, S.; Lee, C. W.; Grubbs, R. H. *Org. Lett.* **1999**, *1*, 953-956.

[36] Bourissou, D.; Guerret, O.; Gabbaï, F. P.; Bertrand, G. *Chem. Rev.* **2000**, *100*, 39-91.

[37] Glorius, F. *Top Organomet. Chem.* **2007**, *21*, 1-20.

[38] (a) Kingsbury, J. S.; Harrity, J. P. A.; Bonitatebus, P. J.; Hoveyda, A. H. *J. Am. Chem. Soc.* **1999**, *121*, 791-799; (b) Gessler, S.; Randl, S.; Blechert, S. *Tetrahedron Lett.* **2000**, *41*, 9973-9976.

[39] Jafarpour, L.; Schanz, H.-J.; Stevens, E. D.; Nolan, S. P. *Organometallics* **1999**, *18*, 5416-5419.

[40] (a) Clavier, H.; Petersen, J. L.; Nolan, S. P. *J. Organomet. Chem.* **2006**, *691*, 5444 -5477; (b) Clavier, H.; Nolan, S. P. *Chem. Eur. J.* **2007**, *13*, 8029-8036.

# *Chapter 5 - DOSY-NMR analysis of RCM products from β-lactam precursors*

The paper was accepted in *Magnetic Resonance in Chemistry*.

***Title***

DOSY-NMR analysis of ring closing metathesis (RCM) products from β-lactam precursors.

***Authors***

Aline Sliwa,[a] Jacqueline Marchand-Brynaert[a,*] and Michel Luhmer[b,*]

***Affiliations***

[a] Institute of Condensed Matter and Nanosciences, Université catholique de Louvain, Place Louis Pasteur 1, B-1348 Louvain-la-Neuve, Belgium

[b] Laboratoire de Résonance Magnétique Nucléaire Haute Résolution, Université Libre de Bruxelles, Avenue F.D. Roosevelt 50, CP160/08, B-1050 Brussels, Belgium

* Corresponding authors. Tel.: +32 (0)10 47 27 40; fax: +32 (0)10 47 41 68 (J.M.-B.); tel.: +32 (0)26 50 66 37; fax: +32 (0)26 50 66 42 (M.L.). E-mail addresses: jacqueline.marchand@uclouvain.be (J. Marchand-Brynaert), mluhmer@ulb.ac.be (M. Luhmer).

***Keywords***

NMR; $^{1}$H; DOSY; β-lactams; RCM; Cyclodimers

***Abstract***

The discrimination between cyclomonomers and various oligomers formed during a Ring Closing Metathesis (RCM) process is not an easy task. Their $^{1}$H NMR patterns are often very similar and the use of mass spectrometry techniques is usually recommended. Here we show that the DOSY-NMR method is a reliable tool to help in the identification of cyclomonomers versus cyclodimers, by comparing the translational diffusion coefficient of the compounds issued from RCM reactions with the diffusion coefficient of their respective precursors.

## 1. Introduction

Ring-Closing Metathesis (RCM) of α,ω-dienes is one of the most powerful tool to synthesize medium-sized and macrocyclic organic compounds. RCM is nowadays usually employed in many syntheses of complex target compounds.[1] A major limitation to the formation of intramolecular ring-closed products is the occurrence of side products from intermolecular oligomerization. Recently, in the course of a research dedicated to non-traditional β-lactams as potential inhibitors of Penicillin Binding Proteins (PBPs), we tried to synthesize 1,3-bridged 2-azetidinones via RCM as the key-step for macrocyclization.[2] However, it was found that the reaction, performed in the presence of second generation Grubbs' catalyst, mainly yields cyclodimers. In a single case the desired cyclomonomer was obtained together with the cyclodimer (R = Boc, n = 2) (**Figure 1**). The identification of the reaction products was not straightforward. Indeed, $^{1}$H and $^{13}$C NMR data were inconclusive due to their huge complexity, most probably resulting from the presence of

stereoisomers (E/Z stereochemistry of the C=C double bonds), regioisomers (head-to-head and head-to-tail dimers) and rotamers around the amide/imide/carbamate linkages (**Figure 1**). Two different ionization techniques were needed for the characterization of the products by mass spectrometry. Electrospray ionization (ESI) of the precursors (**Figure 2**) yielded base peaks corresponding to dimeric $Na^+$ adducts. Hence, in the case of compounds issued from RCM, it was impossible to discriminate between 1:1 complexes of a cyclodimer with $Na^+$ and 2:1 complexes of cyclomonomers with $Na^+$. Atmospheric pressure chemical ionization (APCI), a method which is known to disfavour adducts formation, was therefore applied and enabled to finally solve the problem. However, the interpretation of these APCI mass spectra was not straightforward due to several fragmentations giving the major peaks.

Diffusion Ordered Spectroscopy (DOSY)[3] is an NMR method capable to discriminate molecules according to their translational diffusion coefficient, which is inversely proportional to their size. DOSY is frequently used in supramolecular or transition-metal chemistry, for instance.[4] Recently, it has been reported that $^1H$ DOSY-NMR may provide evidence for oligomers formation in RCM chemistry.[5] The present note further illustrates the potency of DOSY experiments for solving problems in RCM chemistry, such as the discrimination between cyclomonomer and cyclodimer formation. It also validates our previous conclusions based on APCI mass spectrometry.[2]

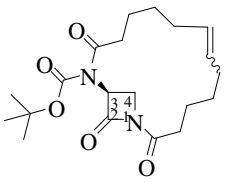

**$M_{Boc2}$**, R = Boc, n = 2; M.W. = 378.46

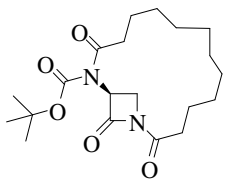

**$HM_{Boc2}$**, R = Boc, n = 2; M.W. = 380.48

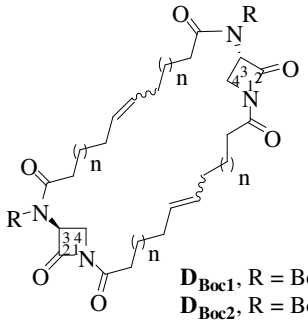

and/or

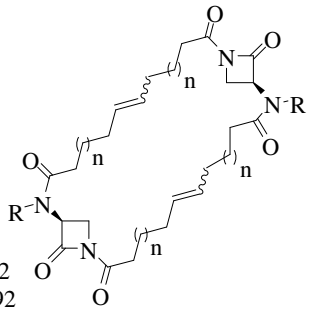

**$D_{Boc1}$**, R = Boc, n = 1; M.W. = 700.82
**$D_{Boc2}$**, R = Boc, n = 2 ; M.W. = 756.92
**$D_{H1}$**, R = H, n = 1; M.W. = 500.26
**$D_{H2}$**, R = H, n = 2; M.W. = 556.32
**$D_{Me1}$**, R = Me, n = 1; M.W. = 528.64
**$D_{Me2}$**, R = Me, n = 2; M.W. = 584.74

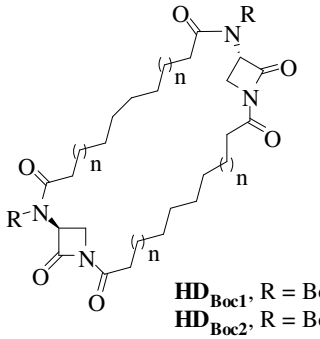

and/or

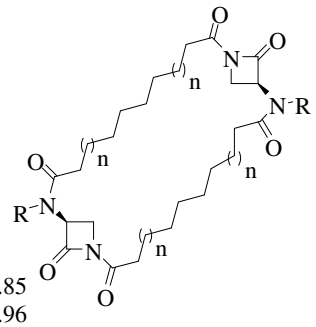

**$HD_{Boc1}$**, R = Boc, n = 1; M.W. = 704.85
**$HD_{Boc2}$**, R = Boc, n = 2; M.W. = 760.96
**$HD_{H1}$**, R = H, n = 1; M.W. = 504.62
**$HD_{H2}$**, R = H, n = 2; M.W. = 560.73
**$HD_{Me1}$**, R = Me, n = 1; M.W. = 532.67
**$HD_{Me2}$**, R = Me, n = 2; M.W. = 588.78

**Figure 1**. Compounds issued from RCM and their hydrogenated derivatives with their molecular weight ($g.mol^{-1}$).

## 2. Results and discussion

In the following description, the precursors are named **P** (**Figure 2**), the cyclomonomers **M** and the cyclodimers **D**. The reaction products after hydrogenation are named **HM** and **HD** for monomer and dimer respectively (**Figure 1**). The DOSY-NMR experiments were conducted at 25 °C and 14.1 T (600 MHz for $^{1}$H) using deuterated chloroform as solvent. Experimental details on sample preparation and NMR measurements are provided in the experimental section.

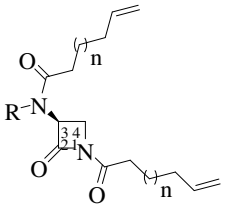

**$P_{Boc1}$**, R = Boc, n = 1; M.W. = 378.46
**$P_{Boc2}$**, R = Boc, n = 2; M.W. = 406.52
**$P_{H1}$**, R = H, n = 1; M.W. = 278.35
**$P_{H2}$**, R = H, n = 2; M.W. = 306.40
**$P_{Me1}$**, R = Me, n = 1; M.W. = 292.37
**$P_{Me2}$**, R = Me, n = 2; M.W. = 320.43

**Figure 2**. Precursors of RCM with their molecular weight (g.mol$^{-1}$).

A table of $^{1}$H NMR chemical shifts of protons H-3, H-4a,b, CH=CH$_{(2)}$ and N-R (R = H, Me, Boc), for the compounds depicted in **Figure 1** and **2**, is given as Supplementary material (p168). Representative spectra of reduced cyclodimers and **$HM_{Boc2}$** monomer are also provided (see online version of Supplementary material).

The system for which the cyclomonomer could be obtained (R = Boc, n = 2) was studied first in order to assess whether DOSY-NMR can provide evidence of cyclodimer formation. For this purpose, DOSY analyses were conducted on a 1:1 mixture of **$M_{Boc2}$** and **$D_{Boc2}$** as well as on 1:1 and 5:95 mixtures of **$HM_{Boc2}$** and **$HD_{Boc2}$**. The region of the DOSY spectrum showing the signals of the β-lactam ring(s) is presented in **Figure 3** for the 1:1 mixture of **$HM_{Boc2}$** and **$HD_{Boc2}$**.[6]

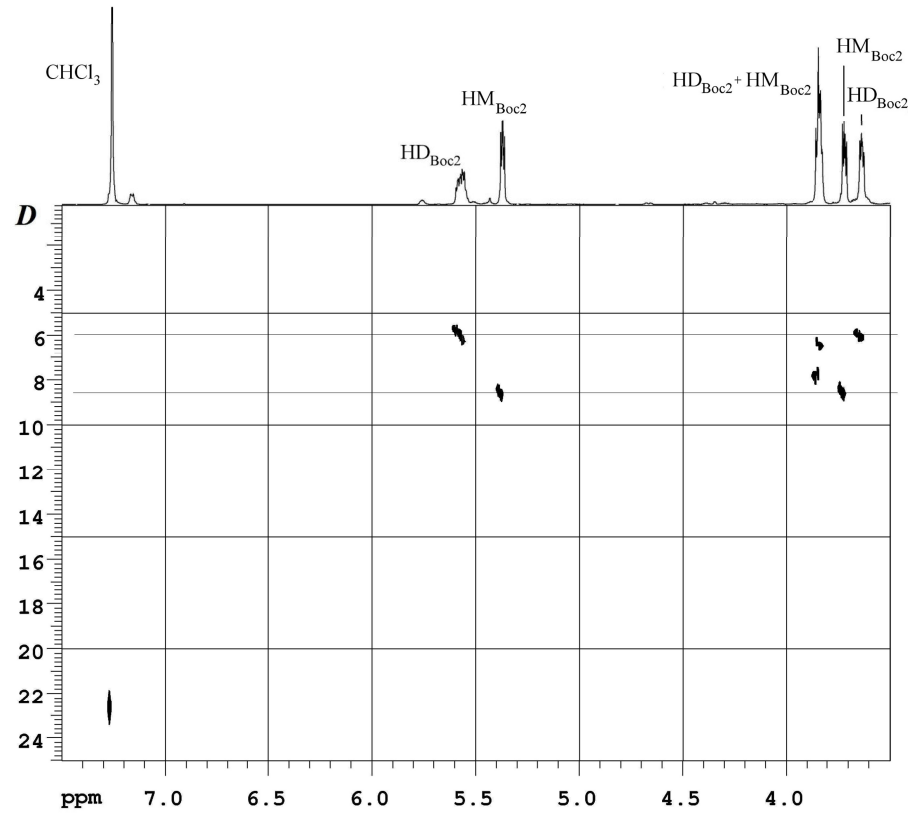


**Figure 3**. Region of the $^{1}$H DOSY-NMR spectrum of a 1:1 mixture of $\mathbf{HM_{Boc2}}$ and $\mathbf{HD_{Boc2}}$ in $CDCl_3$ (600 MHz, 298 K). The diffusion scale is given in $10^{-10}$ $m^2s^{-1}$.

Clearly, DOSY-NMR enables to discriminate between the dimer $\mathbf{HD_{Boc2}}$, which exhibits the smallest diffusion coefficient (D ~ $5.8\times10^{-10}$ $m^2s^{-1}$ in **Figure 3**), and the monomer $\mathbf{HM_{Boc2}}$ (D ~ $8.6\times10^{-10}$ $m^2s^{-1}$). Signal overlap is known to impede accurate DOSY analysis and this is also illustrated in **Figure 3**. Indeed, intermediate diffusion coefficients are determined from the massif of signals observed at 3.85 ppm.[7] Similar results were obtained for the 1:1 mixture of $\mathbf{M_{Boc2}}$ and $\mathbf{D_{Boc2}}$ but additional signals overlaps were observed.[8] Interestingly, the analysis of the 5:95 mixture of $\mathbf{HM_{Boc2}}$ and

**$HD_{Boc2}$** indicates that DOSY-NMR is effective for revealing the presence of a small amount of cyclomonomer (p173 in Supplementary material).

Next, we examined the possibility of unambiguously assigning the monomeric or dimeric structure of RCM products by comparison of their diffusion coefficients with the diffusion coefficient of the corresponding precursor. Our assumption was that the diffusion coefficients of the cyclomonomer and its precursor should be similar. In contrast, the diffusion coefficient of the cyclodimer is expected to be significantly smaller than the diffusion coefficient of its precursor. DOSY experiments were systematically carried out on all of the precursors and, because their $^1$H NMR spectra are better resolved, on all of the hydrogenated RCM products. The diffusion coefficient (*D*) of each compound was determined by using the methylene proton resonances of the β-lactam (H-4a,b).[9] To minimize systematic errors, residual $CHCl_3$ was used as an internal reference and the results are reported as relative diffusion coefficients ($D_R = D_{H\text{-}4}/D_{CHCl3}$). For the system R = Boc and n = 2, $D_R$ is somewhat higher for the cyclomonomer than for the precursor (**Figure 4**). This is likely due to the fact that the precursor is a more extended and flexible molecule and this translates into a larger average hydrodynamic radius. In contrast, $D_R$ is significantly smaller for the cyclodimer than for the precursor. The non-hydrogenated forms were also studied for this system and, as expected, the results are not significantly different. The DOSY technique clearly shows that all the other products issued from RCM are not cyclomonomers. Indeed, their diffusion coefficient is much smaller than the diffusion coefficient of their respective precursor. The diffusion coefficient of these RCM products is actually similar to the diffusion coefficient determined for the dimer **$HD_{Boc2}$**.

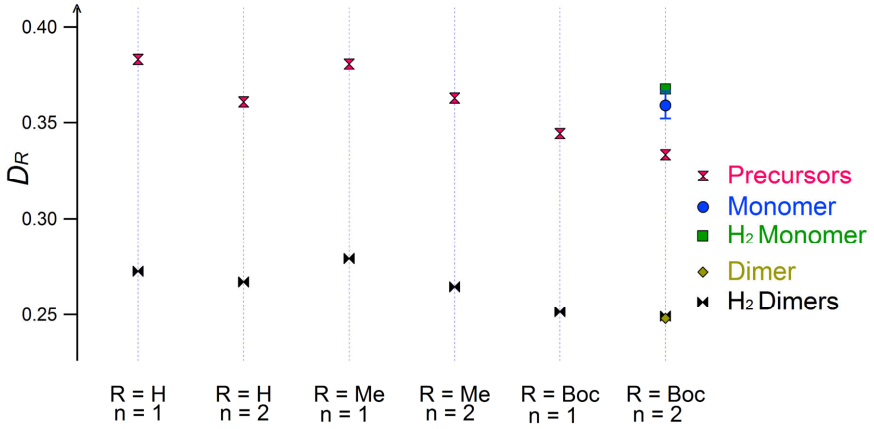


**Figure 4.** Relative diffusion coefficients ($D_R = D_{H\text{-}4}/D_{CHCl3}$) determined at 298 K for the various systems under study. The average diffusion coefficient of residual $CHCl_3$ was measured to be $23.7\times10^{-10}$ $m^2s^{-1}$; the confidence interval shown for $\mathbf{M_{Boc2}}$ corresponds to an error of 2% (see experimental section). The data for $\mathbf{D_{Boc2}}$ and $\mathbf{HD_{Boc2}}$ are almost superimposed.

This is nicely illustrated in **Figure 5** where the relative diffusion coefficients are shown as a function of the inverse molecular weight. Two families of compounds are clearly visible. The first family, with the highest diffusion coefficients, is the precursor family. The diffusion data determined for the cyclomonomers $\mathbf{M_{Boc2}}$ and $\mathbf{HM_{Boc2}}$ are somewhat higher and this is likely due to a more compact average 3D-structure, as suggested above. The relative diffusion coefficients of the other RCM products are lower and form the second family corresponding to cyclodimers. This qualitative analysis allowed to distinguish unambiguously cyclomonomers from cyclodimers, by comparing the translational diffusion coefficient of the compounds issued from RCM with the diffusion coefficient of their respective precursors. A deeper analysis, correlating the molecular weight with the diffusion coefficient,[10] is not feasible because the range of masses spans less than a factor of two, and more increasing repetitive units should be required.

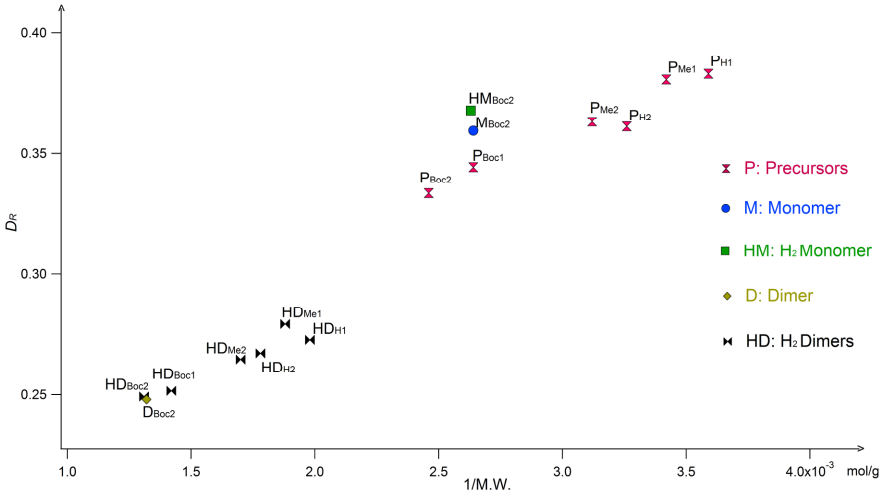


**Figure 5.** Representation of the relative diffusion coefficients as a function of 1/*M.W.*

## 3. Experimental

The samples were prepared by dissolving 5 or 9 mg of compound in 600 µL of $CDCl_3$ (9 mg were used for $\mathbf{P_{Boc1}}$ and $\mathbf{HD_{Boc1}}$) and the solutions were transferred in 5 mm NMR tubes equipped with a valve (Wilmad 535-LPV-7 low pressure/vacuum NMR tubes).

The NMR measurements were conducted at 25 °C and 14.1 T (600 MHz for $^1$H). The DOSY experiments were carried out using a convection-corrected Gradient Compensated STimulated Echo pulse sequence (GCSTESL_cc from the VNMRJ pulse sequence library; spin-lock was not used) and the following acquisition parameters: diffusion delay 90 ms, 20 values of gradient strength ranging between approximately 2 G cm$^{-1}$ and 40 G cm$^{-1}$, acquisition time 2 s, relaxation delay 3 s, 8 steady-state (dummy) scans and 16 repetitions. Unless otherwise stated, the free

induction decays were apodized with exponential multiplication (lb = 0.5 Hz) and zero-filling was applied before Fourier transform (fn = 128k). Diffusion coefficients and DOSY displays were obtained using the VNMRJ diffusion processing package. Residual $CHCl_3$ was used as an internal reference for chemical shift calibration (7.26 ppm) as well as for relative diffusion coefficient data measurements. Calibration of the gradient strength for absolute diffusion coefficient data reporting was completed by using a sample of pure water in a coaxial insert for which the diffusion coefficient was set to $22.99\times10^{-10}$ $m^2s^{-1}$.[11] The average value of the diffusion coefficient of $CHCl_3$ (statistics on 17 independent measurements) is then found to be $23.7\times10^{-10}$ $m^2s^{-1}$, which is in excellent agreement with the value reported by Lafitte et al. ($23.66\times10^{-10}$ $m^2s^{-1}$).[12] The standard deviation is $0.6\times10^{-10}$ $m^2s^{-1}$; the error on the diffusion coefficient measurements is thus estimated to be of the order of 2%.

## 4. Conclusion

In conclusion, DOSY-NMR is a valuable technique for the characterization of RCM reaction products. It enables to discriminate between cyclomonomer and/or cyclodimer formation just by comparing the translational diffusion coefficient of the reaction product(s) with the diffusion coefficient of the precursor. Indeed, the structural assignment of isolated $\mathbf{HM_{Boc2}}$ and $\mathbf{HD_{Boc2}}$ could not be made on the basis of their $^1$H NMR chemical shifts because their respective patterns are expected to be very close, even for the two regioisomeric dimers (head-to-head and head-to-tail). Moreover, in the case of molecules featuring several amide and related functions, rotamers of the same species could give rise to different $^1$H NMR signals. The DOSY method, as illustrated in **Figure 5**, is unambiguous.

Moreover, it enables to detect the presence of small amounts of minor products to the extent that they respectively possess at least one non-overlapping $^1$H NMR signal. Since the azetidinone protons clearly offer this possibility, DOSY experiments allow rapid and safe analyses of RCM crude mixtures from β-lactam precursors of the herein described family, independently of the possible presence of isomers and/or rotamers.

## 5. Acknowledgements

This work was supported by the Interuniversity Attraction Pole (IAP P6/19 PROFUSA), F.R.S.-FNRS, UCL and ULB. J.M.-B. is senior research associate of the F.R.S.-FNRS (Belgium).

## 6. Supplementary material

Supplementary data associated with this article can be found in the online version. Relevant material of the Supplementary material is added below, *i.e.* the $^1$H NMR chemical shift assignment of $\mathbf{M_{Boc2}}$, $\mathbf{D_{Boc2}}$, all precursors and hydrogenated RCM products, the region of the $^1$H DOSY-NMR spectrum of a 1:1 mixture of $\mathbf{HM_{Boc2}}$ and $\mathbf{HD_{Boc2}}$ in $CDCl_3$ with resolution enhancement, the region of the $^1$H DOSY-NMR spectrum of a 1:1 mixture of $\mathbf{M_{Boc2}}$ and $\mathbf{D_{Boc2}}$ in $CDCl_3$ and the region of the $^1$H DOSY-NMR spectrum of a 5:95 mixture of $\mathbf{HM_{Boc2}}$ and $\mathbf{HD_{Boc2}}$. Additionally to the relevant material presented below, representative spectra can be found in the online version of Supplementary material.

### 6.1. $^1$H NMR chemical shift assignment

$^1$H NMR chemical shifts (δ, ppm) of $\mathbf{M_{Boc2}}$, $\mathbf{D_{Boc2}}$, all precursors and hydrogenated RCM products (multiplicities, J values in Hz and integrations are given in parentheses, ° indicate overlapping signals).

| | $\mathbf{P_{Boc1}}$ | $\mathbf{P_{Boc2}}$ |
|---|---|---|
| H-3 | 5.71-5.86 (m°, 1H) | 5.72-5.86 (m°, 1H) |
| H-4a,b | 3.81-3.85 (m, 1H) | 3.80-3.85 (m, 1H) |
| | 3.61 (dd, 4.2, 7.1 Hz, 1H) | 3.61 (dd, 4.2, 7.1 Hz, 1H) |
| HC=CH$_2$ | 5.71-5.86 (m°, 2H) | 5.72-5.86 (m°, 2H) |
| | 4.96-5.07 (m, 4H) | 4.92-5.03 (m, 4H) |
| R (Boc, H or Me) | 1.51 (s, 9H) | 1.51 (s, 9H) |
| CH$_2$ acyl chain | 2.85-2.90 (m, 2H) | 2.85-2.90 (m, 2H) |
| | 2.71-2.76 (m, 2H) | 2.71-2.76 (m, 2H) |
| | 2.06-2.16 (m, 4H) | 2.03-2.11 (m, 4H) |
| | 1.69-1.83 (m, 4H) | 1.60-1.74 (m, 4H) |
| | | 1.38-1.48 (m, 4H) |
| | $\mathbf{P_{Me1}}$ | $\mathbf{P_{Me2}}$ |
| H-3 | 4.91 (dd, 3.9, 6.5 Hz, 1H) | 4.89-5.02 (m°, 1H) |
| H-4a,b | 3.79-3.84 (m, 1H) | 3.79-3.83 (m, 1H) |
| | 3.64 (dd, 3.9, 7.4 Hz, 1H) | 3.63 (dd, 3.9, 7.4 Hz, 1H) |
| HC=CH$_2$ | 5.70-5.84 (m, 2H) | 5.71-5.84 (m, 2H) |
| | 4.95-5.05 (m, 4H) | 4.89-5.02 (m°, 4H) |
| R (Boc, H or Me) | 3.04 (s, 3H) | 3.05 (s, 3H) |
| CH$_2$ acyl chain | 2.71-2.77 (m, 2H) | 2.70-2.76 (m, 2H) |
| | 2.31-2.36 (m, 2H) | 2.31-2.36 (m, 2H) |
| | 2.06-2.15 (m, 4H) | 2.03-2.10 (m, 4H) |
| | 1.69-1.81 (m, 4H) | 1.59-1.72 (m, 4H) |
| | | 1.37-1.49 (m, 4H) |

| | $\mathbf{P_{H1}}$ | $\mathbf{P_{H2}}$ |
|---|---|---|
| H-3 | 4.71 (td, 3.9, 7.4 Hz, 1H) | 4.70 (td, 3.9, 6.9 Hz, 1H) |
| H-4a,b | 3.84-3.88 (m, 1H) | 3.83-3.88 (m, 1H) |
| | 3.65-3.68 (m, 1H) | 3.66 (dd, 3.9, 7.4 Hz, 1H) |
| $HC=CH_{(2)}$ | 5.69-5.85 (m, 2H) | 5.70-5.85 (m, 2H) |
| | 4.96-5.05 (m, 4H) | 4.92-5.03 (m, 4H) |
| R (Boc, H or Me) | 6.18 (d, 7.0 Hz, 1H) | 6.21 (d, 7.0 Hz, 1H) |
| $CH_2$ acyl chain | 2.73 (td, 3.8, 7.4 Hz, 2H) | 2.64-2.81 (m, 2H) |
| | 2.21-2.29 (m, 2H) | 2.24 (t, 7.5 Hz, 2H) |
| | 2.05-2.15 (m, 4H) | 2.02-2.10 (m, 4H) |
| | 1.69-1.82 (m, 4H) | 1.59-1.72 (m, 4H) |
| | | 1.36-1.50 (m, 4H) |
| | $\mathbf{M_{Boc2}}$ | $\mathbf{D_{Boc2}}$ |
| H-3 | 5.34-5.45 (m°, 1H) | 5.71-5.76 (m, 2H) |
| H-4a,b | 3.81-3.85 (m, 1H) | 3.80-3.86 (m, 2H) |
| | 3.71-3.74 (m, 1H) | 3.59-3.65 ( m, 2H) |
| $HC=CH_{(2)}$ | 5.60-5.70 (m, 1H) | 5.33-5.41 (m, 4H) |
| | 5.34-5.45 (m°, 1H) | |
| R (Boc, H or Me) | 1.25-2.33 (m°, 9H) | 1.51-1.68 (m°, 18H) |
| $CH_2$ acyl chain | 2.90-2.99 (m, 1H) | 2.63-2.91 (m, 8H) |
| | 2.66-2.82 (m,2H) | 1.96-2.10 (m, 8H) |
| | 1.25-2.33 (m°, 13H) | 1.51-1.68 (m°, 8H) |
| | | 1.35-1.47 (m, 8H) |
| | $\mathbf{HM_{Boc2}}$ | |
| H-3 | 5.36-5.38 (m,1H) | |
| H-4a,b | 3.82-3.86 (m, 1H) | |
| | 3.70-3.72 (m, 1H) | |
| R (Boc, H or Me) | 1.55 (s, 9H) | |
| $CH_2$ acyl chain | 3.08-3.13 (m, 1H) | |
| | 2.72-2.84 (m, 2H) | |
| | 2.30-2.36 (m, 1H) | |
| | 1.67-1.95 (m, 4H) | |
| | 1.21-1.45 (m, 12H) | |

| | **$HD_{Boc1}$** | **$HD_{Boc2}$** |
|---|---|---|
| H-3 | 5.48-5.77 (m, 2H) | 5.53-5.77 (m, 2H) |
| H-4a,b | 3.80-3.85 (m, 2H) | 3.82-3.85 (m, 2H) |
| | 3.61-3.65 (m, 2H) | 3.62-3.64 (m, 2H) |
| R (Boc, H or Me) | 1.50-1.77 (m°, 18H) | 1.51-1.75 (m°, 18H) |
| $CH_2$ acyl chain | 2.52-2.92 (m, 8H) | 2.57-2.86 (m, 8H) |
| | 1.50-1.77 (m°, 8H) | 1.51-1.75 (m°, 10H) |
| | 1.24-1.43 (m, 16H) | 1.24-1.39 (m, 22H) |
| | **$HD_{Me1}$** | **$HD_{Me2}$** |
| H-3 | 4.37-5.37 (m, 2H) | 4.70-5.31 (m, 2H) |
| H-4a,b | 3.79-3.99 (m, 2H) | 3.80-3.99 (m, 2H) |
| | 3.63-3.73 (m, 2H) | 3.64-3.74 (m, 2H) |
| R (Boc, H or Me) | 2.70-3.12 (m°, 6H) | 2.51-3.08 (m°, 6H) |
| $CH_2$ acyl chain | 2.70-3.12 (m°, 2H) | 2.51-3.08 (m°, 4H) |
| | 2.27-2.38 (m, 6H) | 2.32-2.37 (m, 4H) |
| | 1.55-1.80 (m, 8H) | 1.56-1.77 (m, 8H) |
| | 1.24-1.40 (m, 16H) | 1.22-1.40 (m, 24H) |
| | **$HD_{H1}$** | **$HD_{H2}$** |
| H-3 | 4.78-4.96 (m, 2H) | 4.72-4.79 (m, 2H) |
| H-4a,b | 3.86-3.95 (m, 2H) | 3.85-3.89 (m, 2H) |
| | 3.62-3.69 (m, 2H) | 3.64-3.71 (m, 2H) |
| R (Boc, H or Me) | 6.45-6.52 (m, 2H) | 6.49-6.67 (m, 2H) |
| $CH_2$ acyl chain | 2.21-2.29 (m, 4H) | 2.57-2.84 (m, 4H) |
| | 1.61-1.77 (m, 8H) | 2.18-2.32 (m, 4H) |
| | 1.25-1.41 (m, 16H) | 1.56-1.81 (m, 10H) |
| | | 1.22-1.44 (m, 22H) |

### 6.2. Region of the $^{1}$H DOSY-NMR spectrum of a 1:1 mixture of $HM_{Boc2}$ and $HD_{Boc2}$ with resolution enhancement

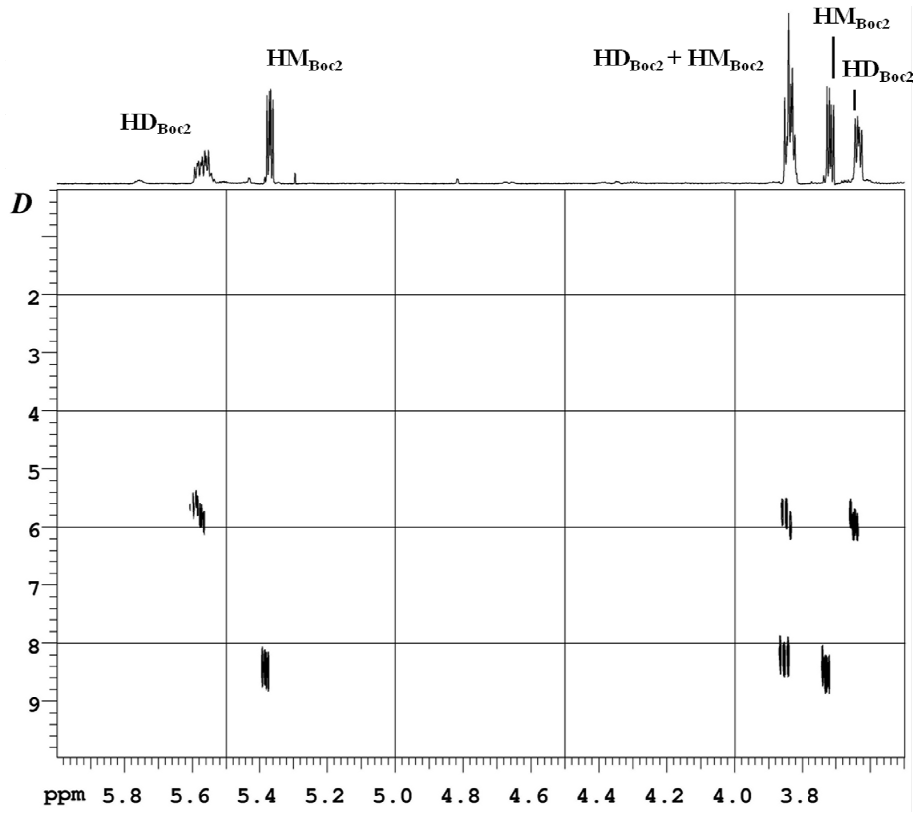


The diffusion scale is given in $10^{-10}$ $m^2s^{-1}$.

### 6.3. Region of the $^{1}$H DOSY-NMR spectrum of a 1:1 mixture of $M_{Boc2}$ and $D_{Boc2}$

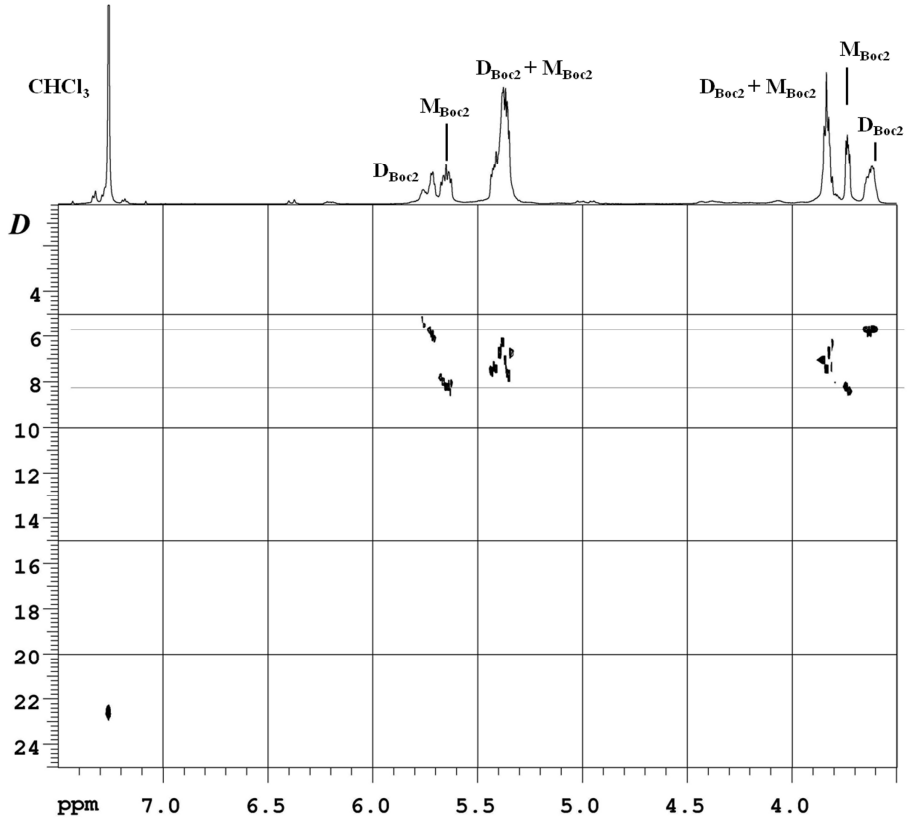


The diffusion scale is given in $10^{-10}$ $m^2s^{-1}$.

### 6.4. Region of the $^{1}$H DOSY-NMR spectrum of a 5:95 mixture of $HM_{Boc2}$ and $HD_{Boc2}$

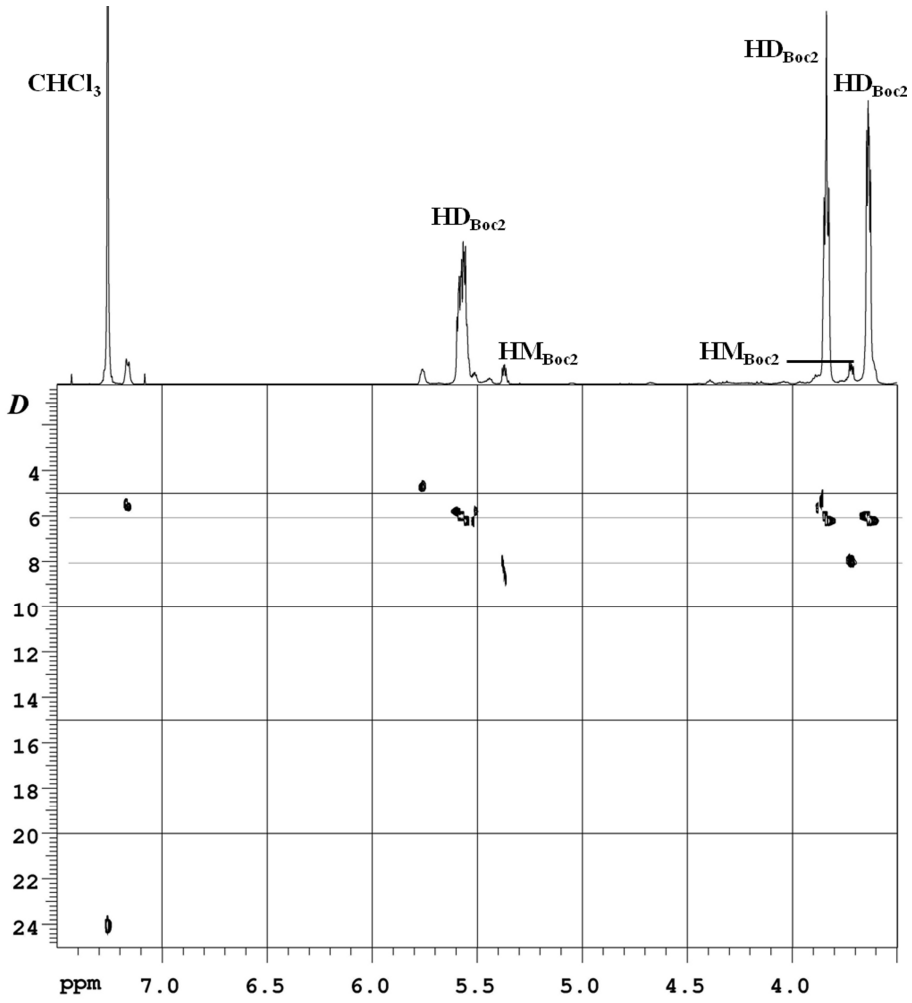


The diffusion scale is given in $10^{-10}$ $m^2s^{-1}$.

Despite the fact that the NMR signals of the cyclomonomer **$HM_{Boc2}$** are weak, they are easily detected in the DOSY spectrum.

The signal next to the residual peak of $CHCl_3$ is a residue of Grubb's catalyst.

## 7. References and notes

[1] (a) Cossy, J.; Arseniyadis, S.; Meyer, C. in *Metathesis in Natural Product Synthesis: Strategies, Substrates and Catalysts*, Wiley-VCH: Weinheim, Germany, 2010; (b) Monfette, S.; Fogg, D. E. *Chem. Rev.* **2009**, *109*, 3783-3816; (c) Majumdar, K. C.; Rahaman, H.; Roy, B. *Curr. Org. Chem.* **2007**, *11*, 1339-1365; (d) Arisawa, M.; Nishida, A.; Nakagawa, M. *J. Organomet. Chem.* **2006**, *691*, 5109-5121; (e) Gradillas, A.; Pérez-Castells, J. *Angew. Chem. Int. Ed.* **2006**, *45*, 6086-6101.

[2] Sliwa, A.; Dive, G.; Habib Jiwan, J.-L.; Marchand-Brynaert, J. *Tetrahedron* **2010**, *66*, 9519-9527.

[3] Johnson, C. S. *Prog. Nucl. Magn. Reson. Spectrosc.* **1999**, *34*, 203-256.

[4] (a) Cohen, Y.; Avram, L.; Frish, L. *Angew. Chem. Int. Ed.* **2005**, *44*, 520-554; (b) Pregosin, P. S.; Kumar, P. G. A.; Fernandez, I. *Chem. Rev.* **2005**, *105*, 2977-2998.

[5] Monfette, S.; Crane, A. K.; Duarte Silva, J. A.; Facey, G. A.; dos Santos, E. N.; Araujo, M. H.; Fogg, D. E. *Inorg. Chim. Acta* **2010**, *363*, 481-486.

[6] The region of the β-lactam ring resonances shows limited signal overlap and was therefore selected for analysis (H-3, H-4a,b: see p168 in Supplementary material).

[7] One H-4 proton of each β-lactam ring of the dimer and one H-4 proton of the monomer give overlapping signals at 3.85 ppm. It is noteworthy that apozidation for resolution enhancement enables better determination of the diffusion coefficients from these signals (p171 in Supplementary material).

[8] Besides the overlap observed with the mixture **$HM_{Boc2}$/$HD_{Boc2}$**, olefinic protons from **$M_{Boc2}$** and **$D_{Boc2}$** also give overlapping signals and there is also a small overlap of the H-3 signals from **$M_{Boc2}$** and **$D_{Boc2}$**. (p172 in Supplementary material).

[9] The H-4a,b signals of the β-lactamic methylene group always appear as two independent multiplets between 3.6 and 3.9 ppm and do not overlap with other signals. The average of the diffusion coefficients determined from the H-4a,b signals was used for the calculation of $D_R$. In contrast, the H-3 signal is not convenient because its chemical shift is significantly dependent on the R-substituent and is also affected by the presence of rotamers and mixtures of head-to-head and head-to-tail isomers generating several peaks (see table of $^1$H NMR chemical shifts p168 and representative spectra given in online Supplementary material).

[10] (a) Augé, S.; Schmit, P.-O.; Crutchfield, C. A.; Islam, M. T.; Harris, D. J.; Durand, E.; Clemancey, M.; Quoineaud, A.-A.; Lancelin, J.-M.; Prigent, Y.; Taulelle, F.; Delsuc, M.-A. *J. Phys. Chem. B* **2009**, *113*, 1914-1918; (b) Floquet, S.; Brun, S.; Lemonnier, J.-F.; Henry, M.; Delsuc, M.-A.; Prigent, Y.; Cadot, E.; Taulelle, F. *J. Am. Chem. Soc*. **2009**, *131*, 17254-17259.

[11] (a) Mills, R. *J. Phys. Chem.* **1973**, *77*, 685-688; (b) Kato, H.; Saito, T.; Nabeshima, M.; Shimada, K.; Kinugasasee, S. *J. Magn. Reson.* **2006**, *180*, 266-273.

[12] Lafitte, V. G. H.; Aliev, A. E.; Horton, P. N.; Hursthouse, M. B.; Hailes, H. C. *Chem. Commun.* **2006**, *20*, 2173-2175.

# *Chapter 6 - Inhibition of resistant PBPs by bis-2-oxoazetidinyl macrocycles*

The paper was accepted in *Medicinal Chemistry Communications*.

***Title***

Unprecedented inhibition of resistant Penicillin Binding Proteins by *bis*-2-oxoazetidinyl macrocycles.

***Authors***

Aline Sliwa,[a] Georges Dive,[b] Astrid Zervosen,[c] Olivier Verlaine,[b] Eric Sauvage[b] and Jacqueline Marchand-Brynaert[a,*]

***Affiliations***

[a] Institute of Condensed Matter and Nanosciences (IMCN), Molecules, Solids and Reactivity (MOST), Université catholique de Louvain, Bâtiment Lavoisier, Place Louis Pasteur L4.01.02, 1348 Louvain-la-Neuve, Belgium E-mail: jacqueline.marchand@uclouvain.be; Fax: +32 (0)10 47 41 68; Phone: +32 (0)10 47 27 40

[b] Centre d'ingénierie des Protéines (CIP), Université de Liège, Bâtiment B6, Allée de la Chimie, 4000 Sart-Tilman (Liège), Belgium

[c] Centre de Recherches du Cyclotron, B30, Université de Liège, Allée du 6 août 8, Sart Tilman, B-4000 Liège, Belgium

Electronic Supplementary Information (ESI) includes: Experimental procedures, characterization data, copies of $^{13}C$ NMR spectra, experiments

of temperature coefficients for amide protons, protocols of biochemical evaluation, information on computational chemistry, acyl-enzyme modeling, absolute energies and figures of compounds **4** and **5**.

***Abstract***

Since the discovery of Penicillin, bacteria counteract the action of antibiotics leading to a worrisome situation about antibiotics efficiency. During our research on non-traditional 1,3-bridged β-lactams embedded into macrocycles as potential inhibitors of Penicillin Binding Proteins (PBPs), we unexpectedly synthesized *bis*-2-oxoazetidinyl macrocycles arising from a dimerization reaction under ring closing metathesis (RCM) conditions. These molecules revealed to be good inhibitors of the D,D-peptidase from *Actinomadura* R39, which is commonly used as model of PBPs. To pursue the research on this type of novel compounds, a complete family of cyclodimers **4** and **5** was synthesized and evaluated against R39, and high molecular weight DD-peptidases: PBP2a of methicillin-resistant *Staphylococcus aureus* and PBP5 of resistant *Enterococcus faecium*. Some *bis*-2-oxoazetidinyl macrocycles exhibited very promising activities against PBP2a. In order to explain the biological results, docking experiments of one cyclodimer (**5e**) into the R39 and PBP2a crystallographic structures were performed. The 3D structures of all the dimers were studied by quantum chemistry calculations and the reactivity of one cyclodimer (**5e**) was evaluated using an elaborated model of R39 active site. Our results highlighted that the activity of the compounds is most probably related to their conformational adaptability, depending of the size of the macrocycle and their geometrical constraints induced by intramolecular H bonds.

## 1. Introduction

The introduction of penicillins (*i.e.* the β-lactam antibiotics) into the health care system is one of the most important contribution to the medical science of the 20th century. However a consequence of the large use of antibiotics was the emergence of resistant bacteria. Mechanical strength of the bacterial cell wall is conferred by an essential cross-linked biopolymer, which final step of biosynthesis is the transpeptidation of peptidoglycan strands catalyzed by D,D-peptidase enzymes. β-Lactam antibiotics, by inhibiting these D,D-peptidases also called penicillin-binding proteins (PBPs), disable the normal cross-linking of peptidoglycan and leave the bacteria sensitive to cell lysis.[1] Structural modifications of the original PBPs[2] is one of the mechanisms of bacterial resistance[1] and a major example of such phenomenon is the methicillin-resistant *Staphylococcus aureus* (MRSA). In this pathogen, responsible for nosocomial infections in hospitals, the resistance to β-lactam antibiotics is conferred by the expression of a novel PBP with very low β-lactam affinity, named PBP2a.[3] To face the growing resistance towards existing β-lactam antibiotics, the development of new compounds is required.

Recently, in the course of our research on non-traditional β-lactams (*i.e.* 2-azetidinones) as potential inhibitors of PBPs, we attempted to synthesize large ring 1,3-bridged 2-azetidinones **B** *via* ring-closing metathesis (RCM) of precursors **A** as the key-step for macrocyclization.[4] However, we observed that a cyclodimerization giving the *bis*-2-oxoazetidinyl macrocycles **C** was the preferred outcome; the desired cyclomonomer **B** was obtained in a single case (R = Boc and n = 2) as the minor RCM product (**Figure 1**). Nevertheless, the inhibition potential of the

β-lactam precursors **A** and RCM products **C** was tested against R39, a low molecular weight D,D-peptidase[5] which is commonly used as a model of bacterial serine-enzymes. Compounds from three families, differing in the nature of the N-C(3) substituent (R = Boc, Me, H) have been evaluated.

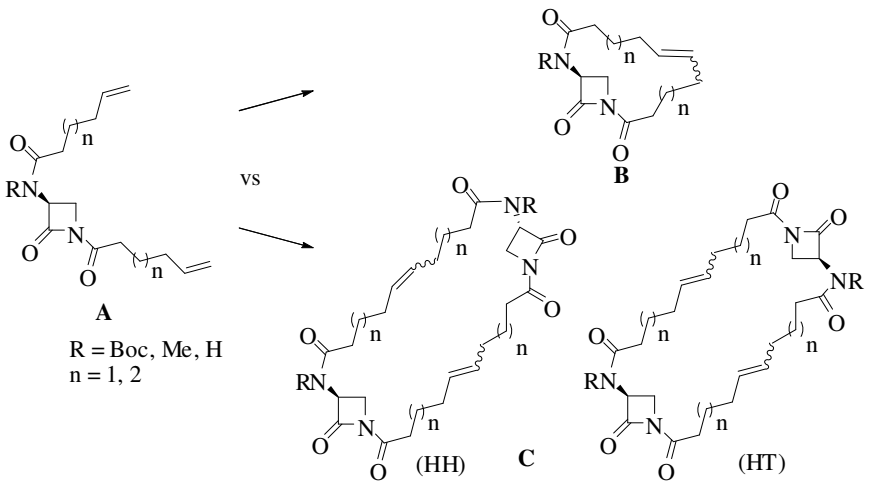


**Figure 1**. Cyclic monomer versus cyclic dimer.

The precursors **A** of the N-H family (R = H) were good inhibitors of R39 and surprisingly, the cyclodimers **C** of the N-H family were even more active than their respective precursors, some of them showing a very good inhibition potential. In order to study more deeply the activity of this series of molecules, non-symmetrical precursors and the corresponding dimers were synthesized, and evaluated against R39, PBP2a and PBP5, another example of high-molecular-weight D,D-peptidase responsible for bacterial resistance of *Enterococcus faecium*.[6] Some *bis*-2-oxoazetidinyl macrocycles showed promising activities against PBP2a. Non-cyclic dimers were also synthesized to determine if the unique activity of these compounds was due to the geometry of the macrocycle or to the presence of two β-lactam rings.

The 3D structures of all compounds have been studied by quantum chemistry calculations. Molecule **5e** was modelled as an acyl-enzyme into the R39 and PBP2a active sites.

## 2. Results

### 2.1. Synthesis

Starting from the chiron **1**,[4] *i.e.* (S)-3-(t-butyloxycarbonyl)amino-2-azetidinone, N(1) mono-acylated β-lactams **2a-c** were prepared regioselectively employing pyridine and alkenoyl chlorides.

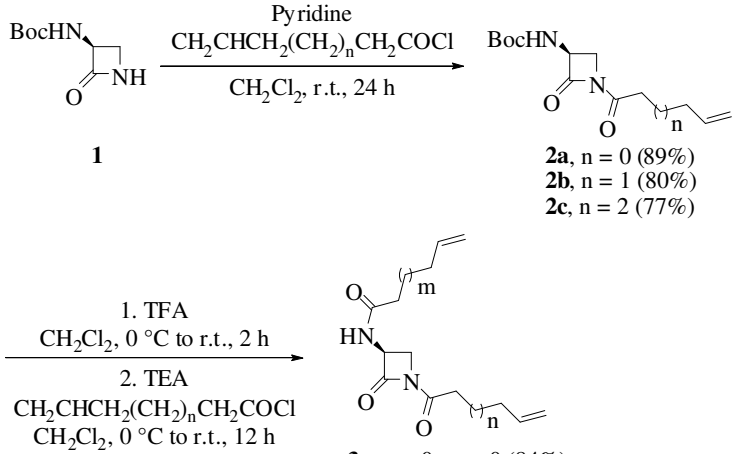


**Scheme 1**. Synthesis of *bis*-acylated precursors **3**.

The *bis*-acylated precursors **3a-i** were then prepared in two steps. The Boc protecting group was removed in the presence of trifluoroacetic acid and the resulting free amine function was acylated with the appropriate alkenoyl chloride using triethylamine as base (**Scheme 1**). Mono- (**2**) and *bis*-acylated products (**3**) were isolated in high yields after chromatography.

Among the symmetrical precursors (n = m = 0, 1, 2), **3a** could not be cyclized (24-membered cyclic dimer not accessible), while ring closing metathesis (RCM) reaction performed on **3e** and **3i** under standard conditions ($CH_2Cl_2$, 40 °C, 5 mM) in the presence of second generation Grubbs' catalyst (2 x 5 mol%), afforded 28-membered (**4e**) and 32-membered (**4i**) cyclic dimers (probably mixtures of head-head (HH) and head-tail (HT) regioisomers) in modest yields (35% and 28%, respectively). As previously reported,[4] *ab initio* calculations have suggested the presence of intramolecular H bonds in these cyclic dimers, stabilizing particular conformations of the macrocycle that could explain why the cyclic dimers with R ≠ H (*i.e.* R = Boc, Me) were not as good inhibitors of R39 D,D-peptidase as the N-H derivatives. In order to study the possible incidence on the biological activity of the length of the two branches of the cyclic dimers, all the non-symmetrical dimers were similarly prepared. Thus the RCM reaction of **3b**, **3c**, **3d**, **3f**, **3g** and **3h** led respectively to the macrocycles **4b** (26-membered), **4c** (28-membered), **4d** (26-membered), **4f** (30-membered), **4g** (28-membered), and **4h** (30-membered), with yields ranging from 31% to 57% (**Scheme 2**). Then the dimers were submitted to catalytic hydrogenation in presence of Pd/C to afford the corresponding saturated macrocycles **5b-i** (**Scheme 2**).

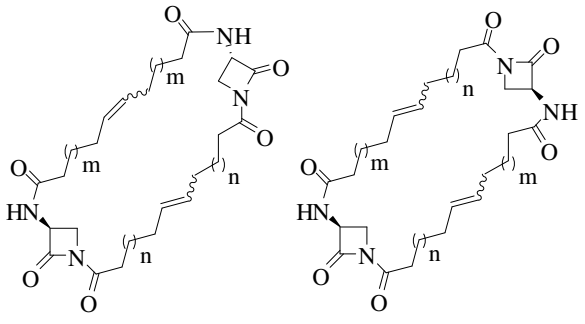

(HH) (HT)

**4b**, n = 0, m = 1 (35%)
**4c**, n = 0, m = 2 (33%)
**4d**, n = 1, m = 0 (21%)
**4e**, n = 1, m = 1 (35%)
**4f**, n = 1, m = 2 (57%)
**4g**, n = 2, m = 0 (41%)
**4h**, n = 2, m = 1 (31%)
**4i**, n = 2, m = 2 (28%)

$H_2$, Pd/C | MeOH, 3 h, r.t.

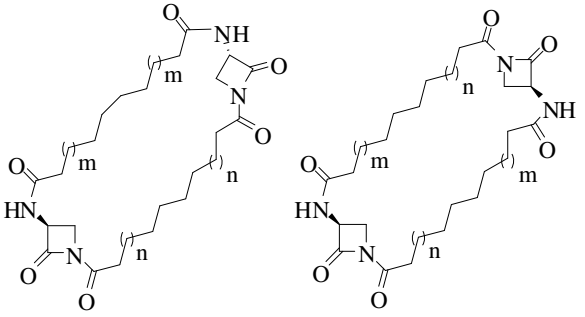

**5b**, n = 0, m = 1 (48%)
**5c**, n = 0, m = 2 (52%)
**5d**, n = 1, m = 0 (22%)
**5e**, n= 1 , m = 1 (48%)
**5f**, n = 1, m = 2 (63%)
**5g**, n = 2, m = 0 (60%)
**5h**, n = 2, m = 1 (36%)
**5i**, n = 2 , m = 2 (60%)

**Scheme 2**. Symmetrical and non-symmetrical cyclic dimers.

Two non cyclic dimers were considered as reference compounds for comparison of the biochemical results. Their precursors **6** and **9**, structurally related to the β-lactam **3c** (n = 0 and m = 2) were prepared by using the same

sequence of reactions as depicted before in **Scheme 1**. Starting from the mono-acylated compound **2a,** the Boc protecting group was removed and the amine function was acylated with heptanoyl chloride and triethylamine giving the *bis*-acylated β-lactam **6** in 80% yield. Mono-acylation of the chiron **1** in presence of pyridine and valeroyl chloride (40% yield), followed by Boc deprotection and amine function acylation with hept-6-enoyl chloride and triethylamine afforded **9** in 86% yield.

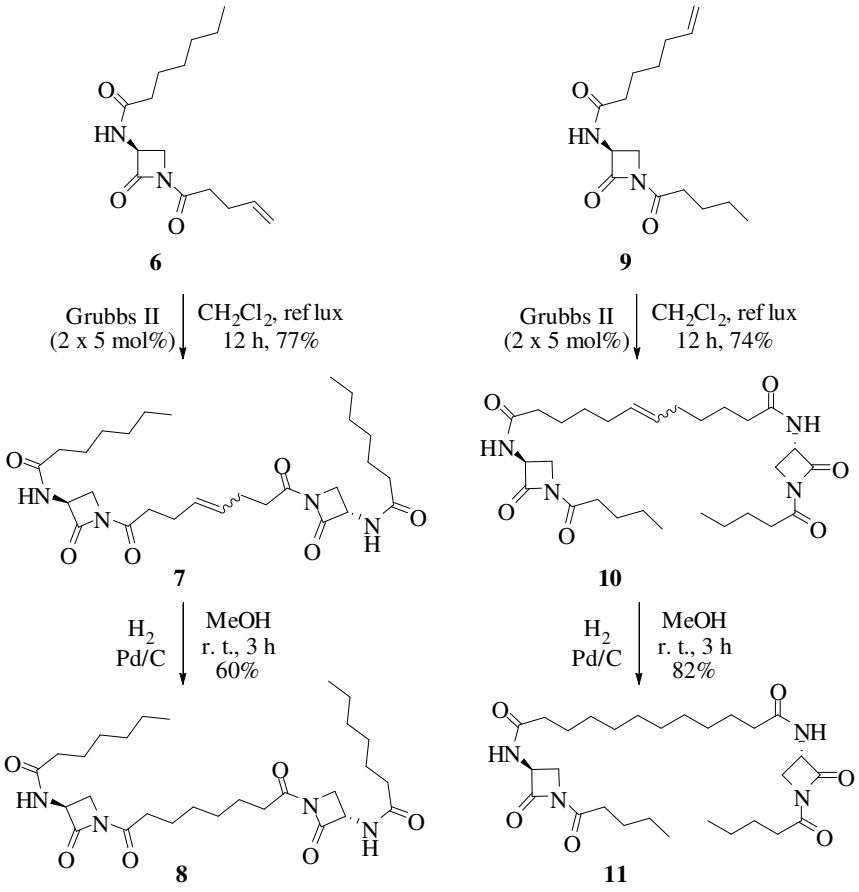


**Scheme 3**. Non-cyclic dimers.

Cross metathesis of precursors **6** and **9** gave the respective non-cyclic dimers **7** and **10** in good yields, and catalytic hydrogenation led to the corresponding saturated products **8** and **11** (**Scheme 3**).

The accurate structural analysis of the RCM products **4** is a very difficult task due to the presence of non-separable isomers: (i) head-head (HH) and head-tail (HT) regioisomers, (ii) E and Z stereoisomers because of the uncontrolled configuration of the C=C double bonds. Additionally, the presence of conformers makes the NMR analyses quite complicated (see Experimental section in Supplementary Information). Using Mass Spectroscopy, we could observe in some cases contamination products issued from double bond migration (in precursors) leading *in fine* to dimers **4** with the formal extrusion of one $CH_2$ unit. To avoid this contamination we performed the RCM reactions in the presence of 1,4-benzoquinone,[7] but without achieving the complete disappearance of the lower homologues.

### 2.2. Inhibition of R39, PBP2a and PBP5

All *bis*-acylated β-lactams, precursors (*i.e.* **3**, **6** and **9**) and dimers (*i.e.* **4**, **5**, **7**, **8**, **10** and **11**), were evaluated for their potential inhibition effect on bacterial serine enzymes.

The D,D peptidase from *Actinomadura* R39[5] is usually considered for a preliminary screening of penicillin-like compounds. R39 and the tested azetidinone (100 μM) were incubated together (1 h, 25 °C). After preincubation the residual activity (RA) of the enzyme was determined by measuring the hydrolysis rate of the thiolester substrate S2d (*i.e.* N-benzoyl-D-Alanyl-thioglycolate),[8] in the presence of Ellman's reagent (for labeling

the formed thiol), by monitoring the increase of absorbance at 412 nm. The results are given in **Table 1** as percentages (%) of residual activity. The activity in the absence of inhibitor is set at 100% and therefore low values indicate very active compounds, since the enzyme has been inhibited by the tested compound and consequently cannot hydrolyze its substrate. A tested compound is considered as a "hit" (*i.e.* potential inhibitor of interest) for a RA value below 80%.

Except one product amongst the precursors (entry 1, *i.e*. compound **3a**), all the other precursors and dimers inhibited R39, and the dimers were generally more active than their precursors.

Then all the compounds were evaluated against two high-molecular-weight D,D-peptidases responsible for bacterial resistance to β-lactam antibiotics: PBP2a from *S. aureus* and PBP5 from *E. faecium.* PBPs and the tested azetidinone (1 mM) were incubated together (4 h, 30 °C). Then fluorescein-labelled ampicillin[9] was added to detect the residual activity (RA). In this protocol, the tested compounds were supposed to be able of acylating the PBPs (to give stable acyl-enzyme intermediates), and the residual activity of PBPs is determined by the amount of covalent PBP-ampicillin complexes formed, as measured by fluorescence spectroscopy after denaturation and SDS-PAGE separation of the acylated enzymes from the reagent band.

Only a small activity against PBP5 was detected for two precursors (entries 1 and 7) and two saturated cyclic dimers (entries 18 and 24). Several products exhibited a small to moderate activity against PBP2a (entries 1, 6, 7, 9, 11, 14, 18, 20, 21, 24, 25 and 28) but amongst the hydrogenated non-symmetrical cyclic dimers, three compounds, namely **5c**, **5f** and **5g** (entries 19, 22 and 23) showed a very good inhibition potential.

**Table 1**

Results of the inhibition experiments with R39, PBP2a and PBP5.

| Entry | Cmpd | R39 RA (%) | PBP5 RA (%) | PBP2a RA (%) | Size cycle |
|---|---|---|---|---|---|
| 1 | **3a** | >100 | 79 | 72 | |
| 2 | **3b** | 14 ± 3 | 93 | 98 | |
| 3 | **3c** | 14 ± 11 | 89 | 91 | |
| 4 | **3d** | 39 ± 12 | 100 | 99 | |
| 5 | **3e** | 17 ± 9 | 100 | 90 | |
| 6 | **3f** | 21 ± 27 | 85 | 74 | |
| 7 | **3g** | 50 ± 3 | 77 | 72 | |
| 8 | **3h** | 15 ± 3 | 82 | 86 | |
| 9 | **3i** | 23 ± 0 | 81 | 80 | |
| 10 | **4b** | 2 ± 1 | 92 | 91 | 26 |
| 11 | **4c** | 3 ± 1 | 95 | 73 | 28 |
| 12 | **4d** | 9 ± 1 | 86 | 84 | 26 |
| 13 | **4e** | 4 ± 8 | 90 | 94 | 28 |
| 14 | **4f** | 1 ± 2 | 98 | 78 | 30 |
| 15 | **4g** | 2 ± 2 | 96 | 100 | 28 |
| 16 | **4h** | 3 ± 1 | 100 | 100 | 30 |
| 17 | **4i** | 0 | 89 | 84 | 32 |
| 18 | **5b** | 2 ± 1 | 70 | 70 | 26 |
| 19 | **5c** | 0 | 100 | 29 | 28 |
| 20 | **5d** | 0 | 100 | 55 | 26 |
| 21 | **5e** | 2 | 90 | 70 | 28 |
| 22 | **5f** | 1 ± 1 | 100 | 22 | 30 |
| 23 | **5g** | 0 ± 3 | 100 | 33 | 28 |
| 24 | **5h** | 2 ± 1 | 72 | 63 | 30 |
| 25 | **5i** | 0 | 95 | 61 | 32 |
| 26 | **6** | 6 ± 0 | 100 | 92 | |
| 27 | **7** | 0 | 100 | 100 | |
| 28 | **8** | 10 ± 4 | 99 | 74 | |
| 29 | **9** | 5 ± 2 | 100 | 97 | |
| 30 | **10** | 5 ± 2 | 89 | 90 | |
| 31 | **11** | 3 ± 4 | 90 | 89 | |

None of the non-cyclic dimers had a significant activity on PBP2a, therefore the activity could not be correlated simply to the presence of two β-lactam rings. We hypothesized that geometrical factors imposed by the macrocycles should be determining.

### 2.3. Computational chemistry

The geometry of all the molecules has been fully optimized at the B3LYP level[10] using the 6-31G(d) basis set.[11] A great number of local minima could be trapped for precursors **3**. Four conformations of the precursors referred to as « *i* », « *ii* », « *iii* », « *iv* » have been located (**Figure 2**). The C(3) amide function exhibits the trans geometry in all cases;[4] the conformers result from rotations around the C(3)-N and N(1)-CO bonds.

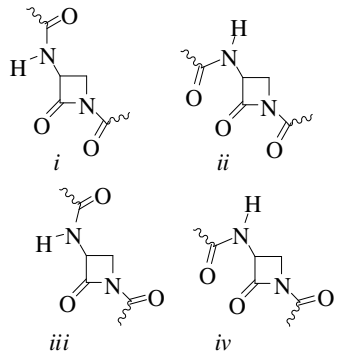


**Figure 2**. Conformations *i*, *ii*, *iii* and *iv* of the precursors.

The four conformations lie in the same range of stability, the relative energies being less than 7 kcal/mole; the *iii* conformation is always the most stable one (**Table 2**) (all absolute energies of the precursors in the selected conformations are given in the Supplementary Information).

**Table 2**

Relative energies of the precursors in the selected conformations.

| Compound | Relative Energy of Open Precursors (kcal/mol) | | | |
|---|---|---|---|---|
| | *i* | *ii* | *iii* | *iv* |
| **3a** | 4.73 | 5.50 | 0.00 | 0.33 |
| **3b** | 4.61 | 6.84 | 0.00 | 1.52 |
| **3c** | 4.71 | 5.64 | 0.00 | 0.40 |
| **3d** | 5.11 | 5.60 | 0.00 | 0.10 |
| **3e** | 4.82 | 6.27 | 0.00 | 0.91 |
| **3f** | 4.62 | 5.64 | 0.00 | 0.13 |
| **3g** | 4.80 | 5.51 | 0.00 | 0.07 |
| **3h** | 4.57 | 5.53 | 0.00 | 0.13 |
| **3i** | 4.88 | 5.71 | 0.00 | 0.37 |

A lot of conformers can exist for the dimers **4** (only the *trans* C=C configuration has been considered). Two conformations of the β-lactam can be located giving rise to a head-head (HH) or head-tail (HT) arrangement in the macrocycle. There are as many stable HT conformers (*i.e.* **4c**, **4d**, **4e**, **4g**) as stable HH conformers (*i.e.* **4b**, **4f**, **4h**, **4i**).

The heats of formation of the dimers have been calculated with respect to the most stable conformation of their respective open precursor which is the *iii* conformation (**Table 3**) (all absolute energies of the HH and HT conformers are given in the Supplementary Information). The heat of formation of the most stable conformers is negative or slightly positive. For saturated compounds **5** (**Table 3**), the conformations often remain in the same local minima as for the unsaturated ones and their relative energies are slightly modified.

**Table 3**

Relative energies and heat of formation of HH and HT unsaturated dimers and relative energies of HH and HT saturated dimers.

| Unsaturated Dimer | Relative Energy of HH Unsaturated Dimer (kcal/mol) | Heat of formation of HH Unsaturated Dimer (kcal/mol) | Relative Energy of HT Unsaturated Dimer (kcal/mol) | Heat of formation of HT Unsaturated Dimer (kcal/mol) |
|---|---|---|---|---|
| **4b** | 0.00 | 1.13 | 5.30 | 6.43 |
| **4c** | 14.00 | 14.24 | 0.00 | 0.24 |
| **4d** | 19.06 | 17.65 | 0.00 | -1.40 |
| **4e** | 9.59 | 3.93 | 0.00 | -5.66 |
| **4f** | 0.00 | 2.32 | 7.36 | 9.68 |
| **4g** | 14.21 | 17.22 | 0.00 | 3.01 |
| **4h** | 0.00 | 11.08 | 1.85 | 12.93 |
| **4i** | 0.00 | -1.81 | 2.43 | 0.62 |

**Table 3** (continued)

| Saturated Dimer | Relative Energy of HH Saturated Dimer (kcal/mol) | Relative Energy of HT Saturated Dimer (kcal/mol) |
|---|---|---|
| **5b** | 0.00 | 6.93 |
| **5c** | 8.61 | 0.00 |
| **5d** | 12.39 | 0.00 |
| **5e** | 8.70 | 0.00 |
| **5f** | 0.00 | 8.26 |
| **5g** | 14.62 | 0.00 |
| **5h** | 0.00 | 0.43 |
| **5i** | 0.00 | 1.52 |

### 2.4. Docking

All the cyclodimers display high activities against R39, while some saturated cyclodimers have good activities against PBP2a. So we focused on the saturated cyclodimers **5** to understand their activities.

The molecule **5e** has been docked as an acyl-enzyme complex in the R39 (**Figure 3a**) and PBP2a (**Figure 3b**) cavities. This symmetrical cyclodimer, featuring a medium activity against PBP2a, has been selected as a representative compound of the whole series **5**.

a)

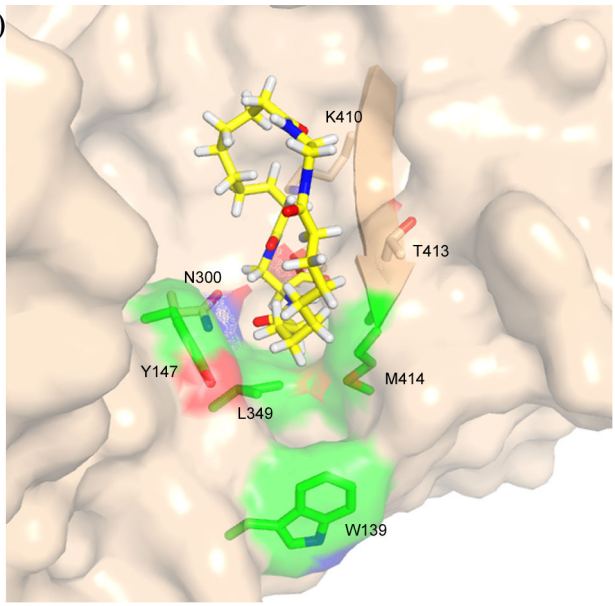

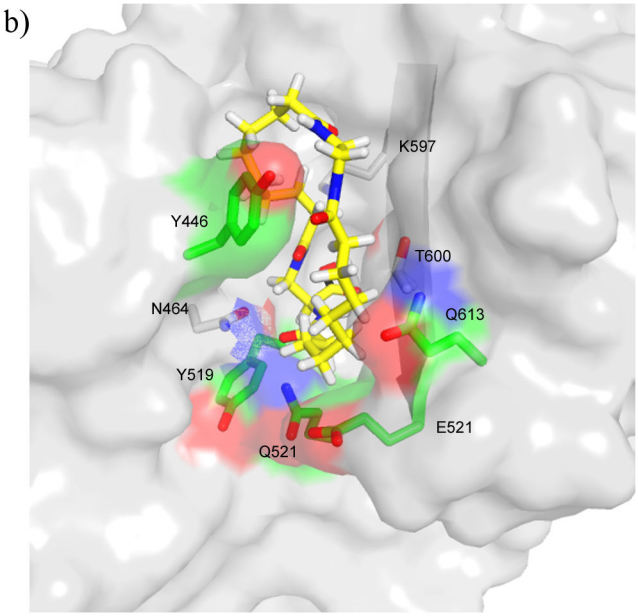


**Figure 3**. a) Acyl-enzyme complex between **5e** and R39. b) Acyl-enzyme complex between **5e** and PBP2a. Legend: Residues surrounding the alkyl chain of the macrocycle in the bottom of the active site are highlighted with carbon atoms coloured green, nitrogen blue and oxygen red. The carbon atoms of **5e** are coloured yellow and hydrogen white. The active serine is hidden by the ligand.

Using the crystal structures of complexes of R39 and PBP2a[3c] with β-lactam antibiotics as templates, **5e** was docked into their respective active sites, conserving the main interactions found in the X-ray structures. The HH conformer has been considered, according to the reactivity model (see below). As expected, **5e** adapted perfectly to the geometrical constraints of the R39 cavity (RA of **5e** versus R39 = 2%). The acyl-enzyme model showed that the alkyl chain of the macrocycle can run into a mainly hydrophobic cavity that normally receives the side chain of the D-α-aminopimelic acid, one of the aminoacid constituting the pentapeptide substrate. Consistently with the measured activity (RA = 70% versus

PBP2a), **5e** fitted quite well into the PBP2a cavity although the cavity is narrower than in R39 (**Figure 3**). The residues of PBP2a surrounding the alkyl chain of the macrocycle are not hydrophobic. The flexibility of the macrocycle **5f**, the most active non-symmetrical dimer versus PBP2a, allowed the docking of both HH and HT isomers in the active site as acyl-enzymes. The docking in the PBP2a active site highlighted the possibility for the whole macrocycle to completely fill the cavity with the closed lactam cycle sandwiched between Tyr446 and Met641 (the figures of macrocycle 5f of both HH and HT isomers docked as an acyl-enzyme complex in the PBP2a cavity are given in Supplementary Information, p225).

The explanation of the difference between non-resistant and penicillin-resistant PBP's activity remains an open question. The main feature could be related to the access to the nucleophilic serine of resistant PBPs which is more ploughed in than the R39 one. So we hypothesized that the conformational flexibility of the *bis*-2-oxoazetidinyl macrocycles could favor their insertion into the "closed" conformation of PBP2a.

The significant differences in the biological results between unsaturated (**4**) and the corresponding saturated macrocycles (**5**) could also be due to conformational features.

### 2.5. Reactivity

To go a step further, the potential acylating power of the *bis*-2-oxoazetidinyl macrocycle **5e** (HH dimer) has been estimated by computational chemistry. The reaction considered is the concerted β-lactam ring opening by nucleophilic attack of the active serine residue. The location of the transition state (TS) structure has been performed with an elaborated model of R39 active site representing the three conserved motifs of the PBPs

family, as reported from the X-ray data.[5] The first motif is composed of the nucleophilic serine Ser49 and the following amino acids Asn50, Met51 and Lys52. The second and third motifs are formed by Ser298, Asn299 and Asn300, and Lys410, Thr411, Gly412 and Thr413, respectively. The TS structure has been fully optimized in all the directions given by the degrees of freedom at the RHF/MINI-1' level[12] (216 atoms, 632 basis functions) (**Figure 4**) (The stereo view corresponding to **Figure 4** is given in Supplementary Information). At this equilibrium structure, Ser49, Lys52 and Ser298 side-chains form a pseudo-8-membered ring with the C(2)-N(1) bond of one β-lactam ring in order to transfer the Oγ hydrogen to the β-lactam N(1) via the Lys amino group.

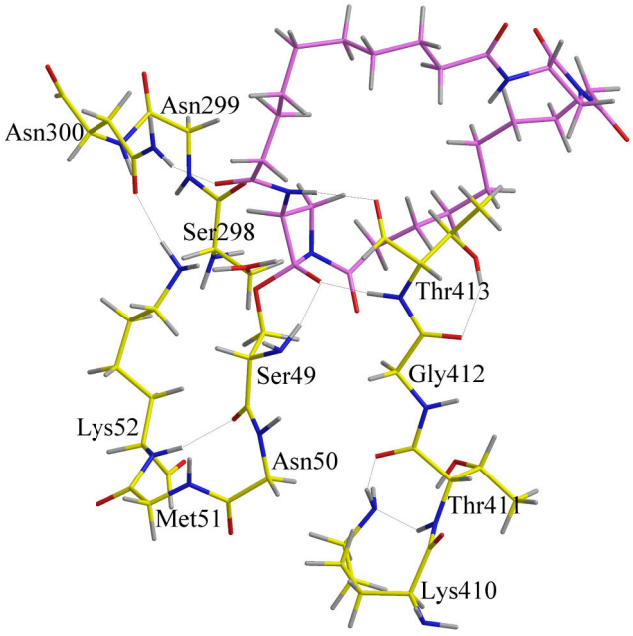


**Figure 4**. Compound **5e** at the transition state in the model of R39 active site. Legend: C of **5e** are purple, others in yellow, H are in grey, O in red, N in blue, hydrogen bonds are in thin sticks.

Similarly to the docking, to be well orientated into the model (and hence into the active site), the carbonyl of the amide on position C(3)-N has to rise below the 4-membered ring and the acyl chain of the macrocycle has to expand to the right upper corner C(4) of the processed β-lactam. This precise type of conformation of one β-lactam ring has been chosen for the representation of compounds **5c**, **5f** and **5g** depicted in **Figure 5** (all figures of compounds **4b-i** and **5b**, **5d-i** are given in the Supplementary Information). This type of arrangement was the used one for the docking of compound **5e**.

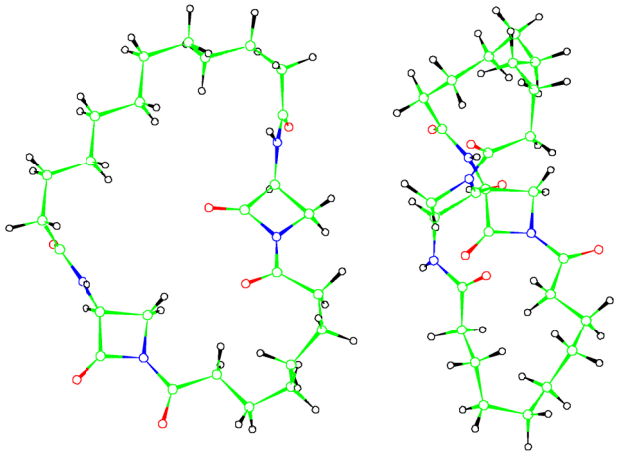

**5c** HH ΔE = 15.57 **5c** HT ΔE = 6.96

**5f** HH ΔE = 0.00 **5f** HT ΔE = 8.26

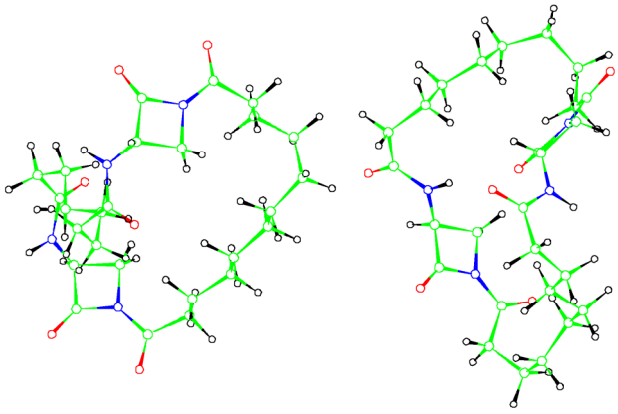

**5g** HH ΔE = 22.94 **5g** HT ΔE = 8.32

**Figure 5**. Representative conformers of **5c**, **5f** and **5g**. Relative energies are given in kcal/mol.

Depending on the size of the cycle growing from 26 to 32 bonds, the "pitch of screw" has a great incidence on the conformation either in the HH or HT arrangement. For some molecules, a conformation where the acyl chain of the macrocycle is more orientated towards the carbonyl C(2) of one β-lactam ring, is localized for **4/5c**, **4/5d** and **4/5e** HT geometries. This could be related to the non adequacy of this conformation to accommodate the active site. The molecules **4/5c**, **4/5e** and **4/5g** containing the same number of methylene units (28-membered ring) are interesting as they can adopt an active-site compatible geometry in their HH arrangement (**Figure 5** and **Figure 6**). In the case of **4/5i** (32-membered ring), the conformation looks like the same in HH and HT arrangements. All the optimized geometries are local minima. What is remarkable is the ability of some molecules to adapt their conformation to the active site. An example is detailed with compound **5e**. The HT geometry is the most stable with regard to the HH(1) one which is 8.70 kcal less stable. A modification of the geometry has been applied to dock this molecule into R39 as well for the localisation of the TS structure in

the theoretical model. Starting from these two different geometries, a reoptimization at the B3LYP/6-31G(d) level leads to two other local minima HH(2) (from docking) and HH(3) (from theoretical model) with relative energies of 9.51 kcal and 14.73 kcal (**Figure 6**). The biological results could be related to the conformational adaptability of the compounds which is a tenuous equilibrium between the size of the cycle and the geometric constraints imposed by its conformation.

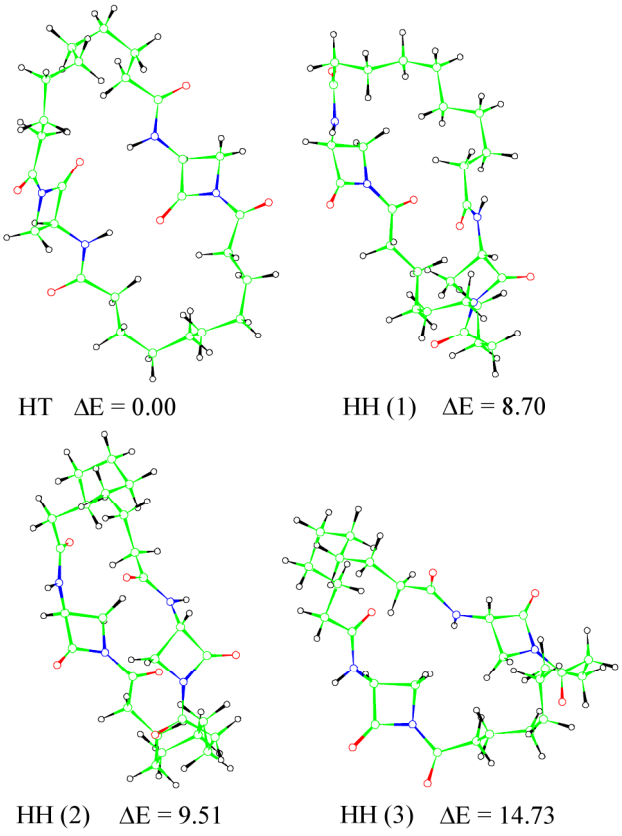


**Figure 6**. Conformers of **5e**. Relative energies are given in kcal/mol.

## 3. Discussion

All the dimers **4/5** exhibit a high activity against a non-resistant PBP (R39) and solely some saturated cyclodimers **5** show a good activity against a resistant PBP (PBP2a). The fine analysis of the behaviour of the *bis*-2-oxoazetidinyl macrocycles **4/5** is a problem of huge complexity, for a lot of reasons. The RCM reaction affords most probably a distribution of HH and HT regioisomers, as well as mixtures of E/Z olefins. For the hydrogenated compounds **5** the problem of E/Z geometry has been suppressed, but there are still HH and HT isomers for which the distribution product is not known. For each regioisomer, several conformations exist. The conformers are more or less stabilized and present different geometrical constraints due to the presence in the cyclodimers of intramolecular H bonds. Proton NMR experiments were performed in order to determine if the amide protons of cyclic dimers were involved in intramolecular H-bond. One amide proton of **5c** exhibited a different behaviour compared to the non-cyclic dimer **11**, which supported the involvement of one intramolecular hydrogen bond in the cyclic dimer (results are given in Supplementary Information, p227).

Using a model of R39 active site, we have determined the geometrical requirements necessary to form the transition state of the acyl-enzyme complex: (i) the macrocyclic chain has to expand to the right upper corner C(4) of the processed β-lactam; (ii) the carbonyl of the amide on position C(3)-N has to rise below the β-lactam ring to allow the interaction with the NH of Asn300 amino acid residue.

This model of reactivity could also be applied to the case of PBP2a that shares with R39 the same three conserved motifs into the catalytic cavity. The differences are to be found at the entry, and at the bottom of the respective cavities.[3,5] Globally, the active serine of PBP2a is less accessible, because it is more buried into the active site.

Amongst the saturated cyclodimers **5**, because of the intramolecular H bonds, compounds are more or less distorted and some of them look like a screw. This structural feature is more pronounced for the non-symmetrical dimers regarding the symmetrical ones of the same sizes. As a matter of fact, the best activities were recruited for the "non-symmetrical" compounds (**5c**, **5d**, **5f**, **5g**).

The poor activity (or the absence of activity) of all the dimers **4/5** against PBP5 could not be rationalized. Ceftobiprole, a cephalosporin derivative with high affinity for PBP2a of MRSA, is not similarly active against PBP5 of *E. faecium*. The role of the antibiotics side-chains (at positions 7 on the β-lactam ring and 3 on the fused six-membered ring) on their specificity is not yet elucidated.[13] These chains are supposed to contribute to the good positioning of the β-lactam carbonyl versus the active serine of the target PBP. In particular, the different chains fixed on the cephalosporin fused ring (ceftobiprole and ceftazidime, for example) could behave as a "lever arm" inducing an unpredictable inhibition pattern against the set of PBPs.[14] So, it is not surprising that our compounds show different affinities for PBP2a and PBP5.

## 4. Conclusion

Nowadays, the mode of action of non-resistant and resistant PBPs, at the molecular level, is not fully understood. The comprehension of molecular interactions between proteins and small molecules relies on complementary studies based on experimental (measured activities, X-ray structures) and theoretical data (modeling, docking experiments), making the foundation of structure-based drug design.[15]

Herein we have disclosed a novel family of β-lactam compounds able to acylate PBPs, namely the *bis*-2-oxoazetidinyl macrocycles. 26- to 32-Membered *bis*-2-oxoazetidinyl macrocycles devoid of side-chain (R = H) are synthesized using the RCM reaction as key-step for cyclodimerization. All the compounds are good inhibitors of R39; some saturated macrocycles reveal very promising activities against PBP2a of MRSA while the corresponding linear dimers are inactive confirming that the activity is not imputable to the presence of two β-lactam cores in the molecules. The structure of our novel inhibitors is totally different from penicillins or cephalosporins, and abolishes the traditional dogma linked to the β-lactam antibiotics, such as the requirement of a 5 or 6-membered cycle fused to the N(1)-C(4) atoms of the β-lactam ring, and the presence of a carboxylic function on this fused ring.

Geometrical and conformational factors have been identified to be responsible of the activity of all compounds against R39 DD-peptidase, and of some compounds against PBP2a from MRSA. The activity of lipophilic β-lactams (such as **4** and **5**) could be related to the specificity of PBP2a which process only cell-wall precursors bearing a pentaglycine strand attached to a lysine residue of the stem peptide. The *bis*-2-oxoazetidinyl macrocycles which feature branches of different lengths for connecting the two four-membered rings are the most active ones against PBP2a (i.e. compounds **5c**, **5d**, **5f**, **5g**). Due to the occurrence of intramolecular H-bonds inducing geometrical constraints, the so-called non-symmetrical dimers **5** look like screws. Their pitch of screw, depending on the macrocycle size with the optimum for 28-membered cycles, combined with their high conformational adaptability could probably explain why, for instance, the compounds **5c** and **5g** compared to **5e** are able to slip in, and to adapt the closed conformation of PBP2a active site. In the context of the urgent need

of new antimicrobial agents with activity against MRSA and other resistant pathogens, our work provides an alternative approach for the rational design of active β-lactams.

## 5. Acknowledgements

This work was supported by the Interuniversity Attraction Pole (IAP P6/19 PROFUSA), F.R.S.-FNRS, UCL and ULg (computational facilities). G. D. and J. M.-B. are senior research associates of the F.R.S.-FNRS (Belgium). Ir. Raoul Rozenberg and Dr. Cécile Le Duff have contributed to the structural analysis. Chafia Ouali (University Denis Diderot Paris VII) is thanked for her assistance in the synthesis of some compounds.

## 6. Supplementary Information

Relevant material of the Supplementary Information is added below, *i.e.* experimental procedures, characterization data, protocols of biochemical evaluation, information on computational chemistry, acyl-enzyme modeling, absolute energies and figures of compounds **4** and **5**, stereo view of the third model with Pen, molecule **5f** docked as an acyl-enzyme complex in PBP2a cavity, experiments of temperature coefficients for amide protons and the absolute energies of the precursors, unsaturated bicycles and saturated bicycles in the selected conformations, the absolute energies of the transition state structures.

## 6.1. Experimental Section

**General**. Experiments were performed under argon atmosphere in flame-dried glassware. All solvents, including anhydrous solvents, and reagents were purchased from Acros Organics, Alfa Aesar, Fluka, Sigma-Aldrich or VWR, and used without any further purification. TLC analyses were performed on aluminum plates coated with silica gel $60F_{254}$ (Merck) and visualized with a $KMnO_4$ solution and UV (254 nm) detection, and column chromatography was performed on silica gel (40-63 or 63-200 μm) purchased from Rocc. Melting points (mp) were determined on a Büchi B-540 apparatus calibrated with caffeine, vanillin, and phenacetin. $[\alpha]_D$ was measured on Perkin-Elmer 241 MC or 343 polarimeter, at 20 °C, in $CHCl_3$ or $CH_3OH$. Concentrations are given in g/100 mL. Nuclear magnetic resonance ($^1H$ and $^{13}C$) spectra were recorded at 300 MHz for proton and 75 MHz for carbon (Bruker Avance 300) or 500 MHz for proton and 125 MHz for carbon (Bruker Avance 500) using deuterated chloroform ($CDCl_3$). Chemical shifts are reported in parts per million relative to residual $CHCl_3$ in $CDCl_3$ (7.26 and 77.16 ppm). NMR coupling constants (*J*) are reported in hertz. Infrared (IR) spectra were recorded using FTIR-8400S Shimadzu apparatus. Products were analyzed as thin films deposited on a Se-Zn crystal by evaporation from $CH_2Cl_2$ solutions. High Resolution Mass Spectrometry (HRMS) analyses were performed at the University of Mons Hainaut (Belgium) or at the University College London (UK).

**General procedure for the preparation of bis-acylated compounds 3**. Trifluoroacetic acid (13.57 mmol) was added to **2** (0.68 mmol) dissolved in $CH_2Cl_2$ (7 mL) at 0 °C. The mixture was warmed to rt and stirred for 2 h. Concentration of the reaction solution afforded the crude trifluoroacetate salt

as a viscous oil. Then alkenoyl chloride (1.02 mmol) was added to a stirred solution of the crude trifluoroacetate salt and triethylamine (2.04 mmol) in $CH_2Cl_2$ (5 mL) cooled at 0 °C. The mixture was then warmed to r.t. and stirred overnight. The mixture was then diluted with $CH_2Cl_2$ (25 mL), and sequentially washed with HCl 2 M solution (30 mL), saturated aqueous $NaHCO_3$ (30 mL), and brine (40 mL). After drying over $MgSO_4$ and removing the solvent under reduced pressure, the residue was purified by flash column chromatography (hexane/EtOAc 3/2), to provide **3** as a white solid.

**3a**, **3e** and **3i** are described in previous chapter (Chapter 4, section **4.3**, p120, the compounds are therein named **12a**, **12b** and **12c**).
The isolated yields and the spectral data for **3b-d**, **3f-h** are as follows.

*N-[(3S)-2-oxo-1-(pent-4-enoyl)azetidin-3-yl]hex-5-enamide* (**3b**).
Yield: 83%; mp 101.5-102.2 °C; $[\alpha]_D^{20}$ +16.4 (*c* 2.9, $CHCl_3$); $^1$H NMR (300 MHz, $CDCl_3$, 20 °C): δ=6.38 (d, *J*=7.3 Hz, 1H), 5.89-5.68 (m, 2H), 5.10-4.96 (m, 4H), 4.70 (td, *J*=3.8, 7.0 Hz, 1H), 3.85 (m, 1H), 3.67 (dd, *J*=3.9, 7.4 Hz, 1H), 2.86-2.79 (m, 2H), 2.44-2.37 (m, 2H), 2.26-2.21 (m, 2H), 2.12-2.04 (m, 2H), 1.78-1.68 ppm (m, 2H); $^{13}$C (75 MHz, $CDCl_3$, 20 °C): δ=173.6, 170.6, 164.8, 137.6, 136.5, 115.9, 115.7, 55.9, 44.9, 35.9, 35.0, 33.6, 27.9, 24.2 ppm; IR: ν=3298, 3078-2844, 1798, 1780, 1693, 1652, 1541 $cm^{-1}$; MS (ESI) *m/z* (%): 551 (36) $[2M + Na]^+$, 287 (100) $[M + Na]^+$, 265 (12) $[M + H]^+$; HRMS (ESI): calcd. for $C_{14}H_{20}N_2O_3Na$ $[M + Na]^+$ 287.1372, found 287.1380.

*N-[(3S)-2-oxo-1-(pent-4-enoyl)azetidin-3-yl]hept-6-enamide* (**3c**).

Yield: 85%; mp 98.5-99.7 °C; $[\alpha]_D^{20}$ +15.3 (*c* 3.4, $CHCl_3$); $^1$H NMR (300 MHz, $CDCl_3$, 20 °C): δ=6.09 (d, *J*=7.0 Hz, 1H), 5.90-5.71 (m, 2H), 5.11-4.93 (m, 4H), 4.71 (td, *J*=3.8, 7.0 Hz, 1H), 3.87 (m, 1H), 3.68 (dd, *J*=3.9, 7.4 Hz, 1H), 2.93-2.75 (m, 2H), 2.46-2.39 (m, 2H), 2.27-2.22 (m, 2H), 2.10-2.03 (m, 2H), 1.70-1.60 (m, 2H), 1.47-1.37 ppm (m, 2H); $^{13}$C (75 MHz, $CDCl_3$, 20 °C): δ=173.6, 170.6, 164.7, 138.3, 136.5, 115.9, 115.0, 55.9, 45.1, 36.0, 35.8, 33.5, 28.5, 28.0, 24.8 ppm; IR: ν=3313-3300, 2980-2856, 1798, 1697, 1663, 1641, 1526 $cm^{-1}$; MS (ESI) *m/z* (%): 579 (27) $[2M + Na]^+$, 301 (100) $[M + Na]^+$, 279 (31) $[M + H]^+$; HRMS (ESI): calcd. for $C_{15}H_{22}N_2O_3Na$ $[M + Na]^+$ 301.1528, found 301.1534.

*N-[(3S)-1-(hex-5-enoyl)-2-oxoazetidin-3-yl]pent-4-enamide* (**3d**).

Yield: 85%; mp 95.1-96.3 °C; $[\alpha]_D^{20}$ +17.8 (*c* 3.1, $CHCl_3$); $^1$H NMR (300 MHz, $CDCl_3$, 20 °C): δ=6.41 (br s, 1H), 5.86-5.70 (m, 2H), 5.09-4.95 (m, 4H), 4.70 (td, *J*=3.9, 7.0 Hz, 1H), 3.84 (m, 1H), 3.65 (dd, *J*=3.9, 7.4 Hz, 1H), 2.74-2.69 (td, *J*=2.8, 7.4 Hz, 2H), 2.40-2.29 (m, 4H), 2.14-2.07 (m, 2H), 1.80-1.70 ppm (m, 2H); $^{13}$C (75 MHz, $CDCl_3$, 20 °C): δ=173.0, 171.3, 164.7, 137.7, 136.5, 116.2, 115.5, 55.8, 44.9, 36.0, 35.0, 33.1, 29.2, 23.2 ppm; IR: ν=3300, 3080-2872, 1798, 1778, 1693, 1654, 1537 $cm^{-1}$; MS (ESI) *m/z* (%): 551 (85) $[2M + Na]^+$, 287 (100) $[M + Na]^+$, 265 (21) $[M + H]^+$; HRMS (ESI): calcd. for $C_{14}H_{20}N_2O_3Na$ $[M + Na]^+$ 287.1372, found 287.1367.

*N-[(3S)-1-(hex-5-enoyl)-2-oxoazetidin-3-yl]hept-6-enamide* (**3f**).

Yield: 82%; mp 85.8-86.5 °C; $[\alpha]_D^{20}$ +15.3 (*c* 3.3, $CHCl_3$); $^1$H NMR (300 MHz, $CDCl_3$, 20 °C): δ=6.24 (d, *J*=7.1 Hz, 1H), 5.84-5.70 (m, 2H), 5.06-

4.92 (m, 4H), 4.70 (td, *J*=3.9, 7.0 Hz, 1H), 3.85 (m, 1H), 3.66 (dd, *J*=3.9, 7.4 Hz, 1H), 2.75-2.69 (m, 2H), 2.26-2.21 (m, 2H), 2.15-2.02 (m, 4H), 1.80-1.71 (m, 2H), 1.69-1.59 (m, 2H), 1.46-1.36 ppm (m, 2H); $^{13}$C (75 MHz, $CDCl_3$, 20 °C): δ=173.6, 171.2, 164.7, 138.3, 137.7, 115.5, 115.0, 55.8, 45.0, 36.0, 35.8, 33.5, 33.1, 28.4, 24.8, 23.2 ppm; IR: ν=3296, 3080-2854, 1797, 1780, 1693, 1651, 1537 cm$^{-1}$; MS (ESI) *m/z* (%): 607 (21) $[2M + Na]^+$, 315 (100) $[M + Na]^+$, 293 (24) $[M + H]^+$; HRMS (ESI): calcd. for $C_{16}H_{24}N_2O_3Na$ $[M + Na]^+$ 315.1685, found 315.1684.

*N-[(3S)-1-(hept-6-enoyl)-2-oxoazetidin-3-yl]pent-4-enamide* (**3g**).

Yield: 70%; mp 105.2-106.6 °C; $[\alpha]_D^{20}$ +17.3 (*c* 3.3, $CHCl_3$); $^1$H NMR (300 MHz, $CDCl_3$, 20 °C): δ=6.30 (d, *J*=7.0 Hz, 1H), 5.87-5.71 (m, 2H), 5.10-4.91 (m, 4H), 4.71 (td, *J*=3.9, 7.0 Hz, 1H), 3.85 (m, 1H), 3.65 (dd, *J*=3.9, 7.4 Hz, 1H), 2.75-2.69 (m, 2H), 2.41-2.30 (m, 4H), 2.10-2.03 (m, 2H), 1.72-1.62 (m, 2H), 1.49-1.39 ppm (m, 2H); $^{13}$C (75 MHz, $CDCl_3$, 20 °C): δ=173.0, 171.3, 164.7, 138.5, 136.5, 116.2, 114.8, 55.8, 45.0, 36.5, 35.1, 33.5, 29.2, 28.4, 23.5 ppm; IR: ν=3296, 2978-2852, 1799, 1780, 1691, 1653, 1541 cm$^{-1}$; MS (ESI) *m/z* (%): 579 (53) $[2M + Na]^+$, 301 (100) $[M + Na]^+$, 279 (22) $[M + H]^+$; HRMS (ESI): calcd. for $C_{15}H_{22}N_2O_3Na$ $[M + Na]^+$ 301.1528, found 301.1530.

*N-[(3S)-1-(hept-6-enoyl)-2-oxoazetidin-3-yl]hex-5-enamide* (**3h**).

Yield: 79%; mp 87.1-87.9 °C; $[\alpha]_D^{20}$ +14.1 (*c* 3.0, $CHCl_3$); $^1$H NMR (300 MHz, $CDCl_3$, 20 °C): δ=6.26 (d, *J*=7.0 Hz, 1H), 5.85-5.68 (m, 2H), 5.04-4.91 (m, 4H), 4.70 (td, *J*=3.9, 7.0 Hz, 1H), 3.85 (m, 1H), 3.66 (dd, *J*=3.9, 7.4 Hz, 1H), 2.75-2.69 (m, 2H), 2.26-2.21 (m, 2H), 2.12-2.03 (m, 4H), 1.78-1.62 (m, 4H), 1.49-1.39 ppm (m, 2H); $^{13}$C (75 MHz, $CDCl_3$, 20 °C): δ=173.5,

171.3, 164.8, 138.4, 137.6, 115.7, 114.8, 55.8, 45.0, 36.5, 35.0, 33.5, 33.0, 28.4, 24.2, 23.5 ppm; IR: ν=3296, 3065-2852, 1798, 1780, 1693, 1655, 1535 $cm^{-1}$; MS (ESI) *m/z* (%): 607 (100) $[2M + Na]^+$, 315 (78) $[M + Na]^+$, 293 (11) $[M + H]^+$; HRMS (ESI): calcd. for $C_{16}H_{24}N_2O_3Na$ $[M + Na]^+$ 315.1685, found 315.1693.

**General procedure of RCM for the preparation of bis-acylated compounds 4**.

Grubbs catalyst (second generation) (0.05 equiv) was added to a stirred solution of **3** (1 equiv) in dry $CH_2Cl_2$ (5 mM) and the solution was stirred at reflux under argon for 4 h. Then a second addition of Grubbs catalyst (0.05 equiv) was made and the mixture was additionally stirred at reflux for 20 h. Then the solvent was removed under reduced pressure and the crude product was purified thrice by column chromatography (EtOAc/MeOH 98/2), to provide **4** as pale-brown oil.

**4e** and **4i** are described in previous chapter (Chapter 4, section **4.4**, p128, the compounds are therein named **16b** and **16c**).

The isolated yields and the spectral data for **4b-d**, **4f-h** are as follows.

*Non-symmetrical cyclic dimer* (**4b**).

Yield: 35%; $[\alpha]_D^{20}$ -44.7 (*c* 1.0, $CHCl_3$); $^1$H NMR (500 MHz, $CDCl_3$, 20 °C): δ=7.48-7.35 and 7.11-6.80 (m, 2H), 5.52-5.29 (m, 4H), 5.11-4.71 (m, 2H), 3.97-3.77 (m, 2H), 3.69-3.48 (m, 2H), 3.16-2.64 (m, 4H), 2.50-1.98 (m, 12H), 1.81-1.61 ppm (m, 4H); $^{13}$C (75 MHz, $CDCl_3$, 20 °C): δ=174.0, 173.7, 171.5, 171.2, 165.6, 165.4, 130.8, 130.7, 130.5, 130.2, 129.7, 129.2, 55.3, 45.5, 44.9, 36.0, 35.8, 35.0, 34.1, 31.7, 31.0, 27.4, 27.2, 24.3, 23.9 ppm; IR: ν=3350-3255, 2983-2925, 1796, 1744, 1724, 1720, 1709, 1668, 1537, 1444

$cm^{-1}$; MS (ESI) *m/z* (%): 495 (100) $[M + Na]^+$, 481 (16) $[M + Na - CH_2]^+$, 473 (50) $[M + H]^+$, 459 (8) $[M + H - CH_2]^+$, 445 (11) $[M + H - CO]^+$; HRMS (ESI): calcd. for $C_{24}H_{32}N_4O_6Na$ $[M + Na]^+$ 495.2220, found 495.2221.

*Non-symmetrical cyclic dimer* (**4c**).

Yield: 33%; $[\alpha]_D^{20}$ -10.5 (*c* 2.0, $CHCl_3$); $^1H$ NMR (500 MHz, $CDCl_3$, 20 °C): δ=7.13-6.92 (m, 2H), 5.41-5.34 (m, 4H), 5.01-4.83 (m, 2H), 3.95-3.82 (m, 2H), 3.64-3.53 (m, 2H), 2.93-2.67 (m, 4H), 2.36-2.21 (m, 8H), 2.08-1.99 (m, 4H), 1.62-1.54 (m, 4H), 1.39-1.24 ppm (m, 4H); $^{13}C$ (125 MHz, $CDCl_3$, 20 °C): δ=174.0, 173.9, 171.4, 171.1, 165.5, 165.3, 131.8, 131.3, 130.7, 128.9, 129.8, 128.7, 127.9, 55.6, 55.5, 45.6, 45.2, 36.4, 36.1, 35.9, 35.4, 31.8, 31.7, 29.8, 29.5, 28.9, 28.4, 27.9, 27.4, 26.8, 26.2, 25.1, 24.6, 24.3, 22.4 ppm; IR: ν=3284, 2981, 1780, 1693, 1512 $cm^{-1}$; MS (ESI) *m/z* (%): 523 (100) $[M + Na]^+$; HRMS (ESI): calcd. for $C_{26}H_{36}N_4O_6Na$ $[M + Na]^+$ 523.2533, found 523.2513.

*Non-symmetrical cyclic dimer* (**4d**).

Yield: 21%; $[\alpha]_D^{20}$ -43.0 (*c* 1.1, $CHCl_3$); $^1H$ NMR (500 MHz, $CDCl_3$, 20 °C): δ=7.40-7.30 and 7.21-6.82 (m, 2H), 5.60-5.29 (m, 4H), 5.15-4.83 (m, 2H), 3.92-3.77 (m, 2H), 3.67-3.39 (m, 2H), 3.05-2.55 (m, 4H), 2.44-1.56 ppm (m, 16H); $^{13}C$ (125 MHz, $CDCl_3$, 20 °C): δ=173.6, 173.5, 171.5, 171.3, 165.3, 165.2, 131.0, 130.9, 130.8, 130.5, 130.2, 130.0, 129.0, 55.7, 55.5, 55.4, 55.2, 45.7, 45.3, 44.8, 36.8, 36.4, 35.9, 35.1, 35.0, 34.7, 31.2, 31.0, 28.3, 28.1, 26.1, 26.0, 24.0, 23.1, 23.0, 22.5 ppm; IR: ν=3390-3258, 2962-2858, 1796, 1745, 1734, 1712-1647, 1539, 1437 $cm^{-1}$; MS (ESI) *m/z* (%): 495 (100) $[M + Na]^+$, 481 (17) $[M + Na - CH_2]^+$, 473 (9) $[M + H]^+$, 445 (9) $[M + H - CO]^+$; HRMS (ESI): calcd. for $C_{24}H_{32}N_4O_6Na$ $[M + Na]^+$ 495.2220, found 495.2221.

*Non-symmetrical cyclic dimer* (**4f**).

Yield: 57%; $[\alpha]_D^{20}$ -11.6 (*c* 1.0, $CHCl_3$); $^1H$ NMR (300 MHz, $CDCl_3$, 20 °C): δ=7.24-6.82 (m, 2H), 5.47-5.23 (m, 4H), 4.99-4.65 (m, 2H), 3.93-3.79 (m, 2H), 3.69-3.48 (m, 2H), 2.77-2.56 (m, 4H), 2.34-1.95 (m, 12H), 1.81-1.24 ppm (m, 12H); $^{13}C$ (75 MHz, $CDCl_3$, 20 °C): δ=174.4, 174.2, 171.7, 171.4, 165.5, 165.2, 131.9, 130.8, 129.9, 129.3, 55.3, 55.2, 45.3, 44.8, 36.4, 36.1, 35.9, 35.7, 35.2, 35.1, 31.9, 31.6, 31.4, 31.3, 28.8, 28.3, 26.4, 24.7, 24.3, 22.9, 22.4; IR: ν=3408-3231, 2960-2833, 1789, 1720, 1693, 1674, 1531, 1456 $cm^{-1}$; MS (ESI) *m/z* (%): 551 (100) $[M + Na]^+$, 537 (25) $[M + Na - CH_2]^+$, 529 (9) $[M + H]^+$; HRMS (ESI): calcd. for $C_{28}H_{40}N_4O_6Na$ $[M + Na]^+$ 551.2846, found 551.2851.

*Non-symmetrical cyclic dimer* (**4g**).

Yield: 41%; $[\alpha]_D^{20}$ -3.8 (*c* 3.6, $CHCl_3$); $^1H$ NMR (300 MHz, $CDCl_3$, 20 °C): δ=7.20-6.64 (m, 2H), 5.61-5.35 (m, 4H), 5.14-4.67 (m, 2H), 3.89-3.41 (m, 4H), 3.07-2.20 (m, 12H), 2.14-1.96 (m, 4H), 1.66-1.54 (m, 4H), 1.43-1.24 ppm (m, 4H); $^{13}C$ (75 MHz, $CDCl_3$, 20 °C): δ=173.4, 173.3, 171.9, 171.8, 171.7, 165.2, 132.0, 131.2, 130.7, 129.9, 129.3, 55.6, 55.2, 45.3, 45.0, 36.8, 36.1, 35.3, 31.8, 31.4, 29.8, 28.5, 28.4, 28.2, 28.1, 27.7, 27.6, 23.4, 23.0 ppm; IR: ν=3310, 2924, 1794, 1689, 1529 $cm^{-1}$; MS (ESI) *m/z* (%): 523 (100) $[M + Na]^+$, 509 (42) $[M + Na - CH_2]^+$, 501 (39) $[M + H]^+$, 487 (21) $[M + H - CH_2]^+$, 473 (21) $[M + H - CO]^+$, 459 (8) $[M + H - CH_2 - CO]^+$; HRMS (ESI): calcd. for $C_{26}H_{36}N_4O_6Na$ $[M + Na]^+$ 523.2533, found 523.2533.

*Non-symmetrical cyclic dimer* (**4h**).

Yield: 31%; $[\alpha]_D^{20}$ -5.2 (*c* 1.0, $CHCl_3$); $^1H$ NMR (500 MHz, $CDCl_3$, 20 °C): δ=7.53-7.30 and 7.18-6.57 (m, 2H), 5.49-5.18 (m, 5H), 4.98-4.63 (m, 1H),

3.89-3.75 (m, 2H), 3.68-3.43 (m, 2H), 2.79-2.59 (m, 4H), 2.31-1.96 (m, 12H), 1.87-1.35 ppm (m, 12H); $^{13}$C (75 MHz, $CDCl_3$, 20 °C): δ=173.3, 172.2, 165.7, 131.9, 130.7, 130.5, 130.1, 55.0, 45.4, 36.6, 36.4, 36.2, 34.5, 34.1, 32.0, 31.4, 31.1, 28.1, 27.9, 26.7, 26.1, 23.6, 22.6 ppm; IR: ν=3389-3221, 2986-2885, 1796, 1747, 1720, 1697, 1683, 1539, 1521 $cm^{-1}$; MS (ESI) *m/z* (%): 551 (100) $[M + Na]^+$, 537 (45) $[M + Na - CH_2]^+$, 529 (32) $[M + H]^+$, 515 (13) $[M + H - CH_2]^+$, 501 (23) $[M + H - CO]^+$; HRMS (ESI) calcd. for $C_{28}H_{40}N_4O_6Na$ $[M + Na]^+$ 551.2846, found 551.2826.

**General Procedure for Hydrogenation**.

To a stirred solution of compound obtained by RCM (1 eq.) in methanol (0.03 M) was added 10% Pd/C (0.05 eq.). After being stirred under hydrogen atmosphere (P = 1 atm) for 3 h at room temperature, the mixture was filtered through a short pad of Celite and concentrated under reduced pressure. The residue was purified by column chromatography (EtOAc/MeOH 98/2), to provide products as colourless oils.

**5e** and **5i** are described in previous chapter (Chapter 4, section **4.5**, p130, the compounds are therein named **20b** and **20c**).

The isolated yields and the spectral data for **5b-d**, **5f-h** are as follows.

*Non-symmetrical cyclic dimer* (**5b**).

Yield: 48%; $[\alpha]_D^{20}$ -26.1 (*c* 1.0, $CHCl_3$); $^1$H NMR (500 MHz, $CDCl_3$, 20 °C): δ=7.14-6.92 (m, 2H), 5.03-4.89 (m, 2H), 3.95-3.64 (m, 2H), 3.67-3.56 (m, 2H), 2.92-2.76 (m, 2H), 2.66-2.52 (m, 2H), 2.29-2.18 (m, 4H), 1.80-1.58 (m, 8H), 1.40-1.23 ppm (m, 12H); $^{13}$C (75 MHz, $CDCl_3$, 20 °C): δ=174.2, 174.1, 172.1, 171.8, 165.3, 165.2, 55.5, 45.6, 45.2, 36.2, 35.7, 35.6, 35.4, 27.7, 27.5, 27.4, 27.3, 27.2, 27.1, 26.8, 24.9, 24.5, 24.3, 23.4 ppm; IR: ν=3294,

2924, 1791, 1742, 1720, 1705, 1647, 1533, 1435 $cm^{-1}$; MS (ESI) *m/z* (%): 499 (100) $[M + Na]^+$, 485 (15) $[M + Na - CH_2]^+$, 477 (7) $[M + H]^+$; HRMS (ESI): calcd. for $C_{24}H_{36}N_4O_6Na$ $[M + Na]^+$ 499.2533, found 499.2516.

*Non-symmetrical cyclic dimer* (**5c**).
Yield: 52%; $[\alpha]_D^{20}$ +7.9 (*c* 1.6, $CHCl_3$); $^1H$ NMR (300 MHz, $CDCl_3$, 20 °C): δ=6.85-6.64 (m, 2H), 4.98-4.92 (m, 1H), 4.81-4.76 (m, 1H), 3.98-3.85 (m, 2H), 3.69-3.57 (m, 2H), 2.85-2.54 (m, 4H), 2.27-2.22 (m, 4H), 1.74-1.62 (m, 8H), 1.32-1.27 ppm (m, 16H); $^{13}C$ (75 MHz, $CDCl_3$, 20 °C): δ=174.2, 174.0, 172.1, 171.8, 165.2, 165.1, 55.8, 55.6, 45.7, 45.1, 36.3, 36.0, 35.9, 35.5, 28.6, 28.2, 28.1, 27.7, 27.4, 25.0, 24.2, 23.9 ppm; IR: ν=3287, 2923, 1796, 1726, 1693, 1672, 1535 $cm^{-1}$; MS (ESI) *m/z* (%): 527 (100) $[M + Na]^+$, 505 (11) $[M + H]^+$; HRMS (ESI): calcd. for $C_{26}H_{40}N_4O_6Na$ $[M + Na]^+$ 527.2846, found 527.2864.

*Non-symmetrical cyclic dimer* (**5d**). Yield: 22%; $[\alpha]_D^{20}$ -17.7 (*c* 0.6, $CHCl_3$); $^1H$ NMR (300 MHz, $CDCl_3$, 20 °C): δ=7.09-6.50 (m, 2H), 5.20-4.82 (m, 2H), 3.94-3.84 (m, 2H), 3.68-3.57 (m, 2H), 3.01-2.80 (m, 2H), 2.67-2.49 (m, 2H), 2.32-2.21 (m, 4H), 1.87-1.56 (m, 10H), 1.47-1.26 ppm (m, 10H); $^{13}C$ (125 MHz, $CDCl_3$, 20 °C): δ=174.1, 174.0, 173.9, 173.8, 171.8, 165.3, 165.2, 165.1, 55.7, 55.6, 55.5, 55.4, 45.5, 45.3, 36.1, 35.8, 35.7, 35.6, 35.4, 35.2, 27.7, 27.5, 27.4, 27.3, 27.2, 27.1, 27.0, 27.0, 26.9, 26.8, 26.7, 26.5, 24.6, 24.5, 24.4, 24.3, 24.1, 23.9, 23.8, 23.6, 23.5, 23.3 ppm; IR: ν=3263, 2924, 1796, 1747, 1731, 1718, 1705, 1647, 1541, 1437 $cm^{-1}$; MS (ESI) *m/z* (%): 499 (100) $[M + Na]^+$, 485 (17) $[M + Na - CH_2]^+$, 477 (10) $[M + H]^+$, 449 (7) $[M + H - CO]^+$; HRMS (ESI): calcd. for $C_{24}H_{36}N_4O_6Na$ $[M + Na]^+$ 499.2533, found 499.2518.

*Non-symmetrical cyclic dimer* (**5f**).

Yield: 63%; $[\alpha]_D^{20}$ -17.3 (*c* 1.0, $CHCl_3$); $^1$H NMR (300 MHz, $CDCl_3$, 20 °C): δ=6.99-6.81 (m, 2H), 4.88-4.66 (m, 2H), 3.92-3.80 (m, 2H), 3.68-3.58 (m, 2H), 2.85-2.52 (m, 4H), 2.27-2.18 (m, 4H), 1.76-1.52 (m, 8H), 1.39-1.20 ppm (m, 20H); $^{13}$C (75 MHz, $CDCl_3$, 20 °C): δ=174.2, 171.8, 165.1, 165.0, 55.7, 45.3, 45.2, 36.4, 36.2, 35.8, 35.7, 28.4, 28.3, 28.2, 28.1, 28.0, 27.9, 25.0, 24.9, 23.8 ppm; IR: ν=3369-3258, 2935-2850, 1790, 1745, 1731, 1724, 1710, 1649, 1533, 1456 $cm^{-1}$; MS (ESI) *m/z* (%): 555 (100) $[M + Na]^+$, 541 (27) $[M + Na - CH_2]^+$, 533 (20) $[M + H]^+$; HRMS (ESI): calcd. for $C_{28}H_{44}N_4O_6Na$ $[M + Na]^+$ 555.3159, found 555.3134.

*Non-symmetrical cyclic dimer* (**5g**).

Yield: 60%; $[\alpha]_D^{20}$ -23.9 (*c* 1 in $CHCl_3$); $^1$H NMR (300 MHz, $CDCl_3$, 20 °C): δ=7.08-6.86 (m, 2H), 4.92-4.71 (m, 2H), 3.89-3.83 (m, 4H), 3.73-3.61 (m, 2H), 2.84-2.51 (m, 4H), 2.26-2.21 (m, 4H), 1.77-1.52 (m, 8H), 1.41-1.21 ppm (m, 16H); $^{13}$C (75 MHz, $CDCl_3$, 20 °C): δ=174.2, 174.1, 171.8, 165.2, 55.8, 55.6, 45.3, 45.1, 36.3, 35.9, 35.7, 28.2, 28.1, 28.0, 27.8, 27.7, 25.0, 24.9, 24.7, 24.5, 23.9 ppm; IR: ν=3355, 2938, 1794, 1776, 1716, 1682, 1535 $cm^{-1}$; MS (ESI) *m/z* (%): 527 (100) $[M + Na]^+$, 513 (72) $[M + Na - CH_2]^+$, 505 (14) $[M + H]^+$; HRMS (ESI): calcd. for $C_{26}H_{40}N_4O_6Na$ $[M + Na]^+$ 527.2846, found 527.2874.

*Non-symmetrical cyclic dimer* (**5h**).

Yield: 36%; $[\alpha]_D^{20}$ -18.5 (*c* 0.5, $CHCl_3$); $^1$H NMR (300 MHz, $CDCl_3$, 20 °C): δ=6.61-6.40 (m, 2H), 4.90-4.73 (m, 2H), 3.92-3.84 (m, 2H), 3.69-3.62 (m, 2H), 2.83-2.75 (m, 2H), 2.68-2.53 (m, 2H), 2.30-2.21 (m, 4H), 1.77-1.57 (m, 8H), 1.43-1.20 ppm (m, 20H); $^{13}$C (75 MHz, $CDCl_3$, 20 °C): δ=174.1, 174.0,

171.9, 171.8, 165.0, 55.8, 55.7, 45.3, 36.4, 35.8, 28.3, 28.2, 28.1, 28.0, 27.9, 27.7, 24.9, 24.8, 23.9, 23.8 ppm; IR: ν=3362-3223, 2924-2860, 1794, 1695, 1683, 1535, 1461 $cm^{-1}$; MS (ESI) *m/z* (%): 555 (100) $[M + Na]^+$, 541 (47) $[M + Na - CH_2]^+$, 533 (7) $[M + H]^+$; HRMS (ESI): calcd. for $C_{28}H_{44}N_4O_6Na$ $[M + Na]^+$ 555.3159, found 555.3162.

*N-[(3S)-2-oxo-1-(pent-4-enoyl)azetidin-3-yl]heptanamide* (**6**).

Following the general procedure for the preparation of bis-acylated compounds, **6** was obtained as a white solid. Yield: 80%; mp 115.7-116.5 °C; $[\alpha]_D^{20}$ +18.2 (*c* 1.5, $CHCl_3$); $^1H$ NMR (300 MHz, $CDCl_3$, 20 °C): δ=6.37 (br d, *J*=7.3 Hz, 1H), 5.89-5.75 (m, 1H), 5.10-4.97 (m, 2H), 4.69 (td, *J*=3.8, 6.9 Hz, 1H), 3.85 (m, 1H), 3.67 (dd, *J*=3.8, 7.4 Hz, 1H), 2.88-2.73 (m, 2H), 2.44-2.37 (m, 2H), 2.25-2.19 (m, 2H), 1.65-1.55 (m, 2H), 1.43-1.23 (m, 6H), 0.88-0.84 ppm (m, 3H); $^{13}C$ (75 MHz, $CDCl_3$, 20 °C): δ=173.8, 170.6, 164.8, 136.5, 115.9, 55.9, 45.0, 36.0, 31.6, 28.9, 28.0, 25.3, 22.6, 14.1 ppm; IR: ν=3294-3288, 2951-2867, 1797, 1780, 1693, 1651, 1539 $cm^{-1}$; MS (ESI) *m/z* (%): 303 (31) $[M + Na]^+$, 281 (100) $[M + H]^+$, 253 (17) $[M + H - CO]^+$; HRMS (ESI): calcd. for $C_{15}H_{24}N_2O_3Na$ $[M + Na]^+$ 303.1685, found 303.1681.

**General procedure of CM for the preparation of non-cyclic dimers**.

Grubbs catalyst (second generation) (0.05 equiv) was added to a stirred solution of **6** or **9** (1 equiv) in dry $CH_2Cl_2$ (10 mM) and the solution was stirred at reflux under argon for 4 h. Then a second addition of Grubbs catalyst (0.05 equiv) was made and the mixture was additionally stirred at reflux for 8 h. Then the solvent was removed under reduced pressure and the crude product was purified thrice by column chromatography (hexane/EtOAc 2/8), to provide **7** or **10** as a pale-brown solid.

*N-[(3S)-1-{8-[(3S)-3-heptanamido-2-oxoazetidin-1-yl]-8-oxooct-4-enoyl}-2-oxoazetidin-3-yl]heptanamide* (**7**).

Yield: 77%; mp 135.4-136.2 °C; $[\alpha]_D^{20}$ +3.3 (*c* 1.0, $CHCl_3$); $^1$H NMR (300 MHz, $CDCl_3$, 20 °C): δ=6.63 and 6.53 (2 br d, *J*=7.5 Hz, 2H), 5.46 (m, 2H), 4.94-4.88 (m, 2H), 3.90 (m, 2H), 3.60 (m, 2H), 2.86-2.72 (m, 4H), 2.39-2.33 (m, 4H), 2.25-2.20 (m, 4H), 1.67-1.57 (m, 4H), 1.35-1.28 (m, 12H), 0.89-0.85 ppm (m, 6H); $^{13}$C (75 MHz, $CDCl_3$, 20 °C): δ=173.8, 171.0, 165.2, 129.2, 55.6, 45.5, 36.1, 36.0, 31.6, 29.0, 27.1, 25.4, 22.6, 14.1 ppm; IR: ν=3310, 2920, 1798, 1724, 1688, 1666, 1529 cm$^{-1}$; MS (ESI) *m/z* (%): 555 (100) $[M + Na]^+$, 533 (7) $[M + H]^+$; HRMS (ESI): calcd. for $C_{28}H_{44}N_4O_6Na$ $[M + Na]^+$ 555.3159, found 555.3157.

*N-[(3S)-1-{8-[(3S)-3-heptanamido-2-oxoazetidin-1-yl]-8-oxooctanoyl}-2-oxoazetidin-3-yl]heptanamide* (**8**).

Following the general procedure for hydrogenation, compound **8** was obtained as a pale-brown solid. Yield: 60%; mp 145.8-146.4 °C; $[\alpha]_D^{20}$ +6.4 (*c* 2.0, $CHCl_3$); $^1$H NMR (300 MHz, $CDCl_3$, 20 °C): δ=6.70-6.56 (m, 2H), 4.85-4.78 (m, 2H), 3.90-3.84 (m, 2H), 3.65-3.60 (m, 2H), 2.76-2.63 (m, 4H), 2.26-2.19 (m, 4H), 1.65-1.56 (m, 8H), 1.36-1.27 (m, 16H), 0.88-0.84 ppm (m, 6H); $^{13}$C (75 MHz, $CDCl_3$, 20 °C): δ=174.0, 171.5, 165.0, 55.7, 45.2, 36.3, 36.0, 31.6, 29.0, 28.5, 25.4, 23.9, 22.6, 14.1 ppm; IR: ν=3283, 2930, 1789, 1697, 1650, 1547 cm$^{-1}$; MS (ESI) *m/z* (%): 557 (100) $[M + Na]^+$; HRMS (ESI): calcd. for $C_{28}H_{46}N_4O_6Na$ 557.3315, found 557.3323.

*tert-butyl N-[(3S)-2-oxo-1-pentanoylazetidin-3-yl]carbamate*.

To a stirred solution of **1** (553 mg, 2.97 mmol) in dry $CH_2Cl_2$ (25 mL) were added pyridine (0.48 mL, 5.94 mmol) and valeroyl chloride (0.71 mL, 5.94 mmol). The mixture was stirred for 12 h at rt and then diluted with $CH_2Cl_2$

(30 mL) and the organic layer was washed with HCl 2 M solution (50 mL), saturated aqueous $NaHCO_3$ (50 mL), and brine (50 mL). After drying over $MgSO_4$ and removing the solvent under reduced pressure, the residue was purified by flash column chromatography (hexane/EtOAc 4/1), to provide the product as a white solid (321 mg, 40%). mp 114.8-115.3 °C; $[\alpha]_D^{20}$ +10.1 (*c* 1.0, $CHCl_3$); $^1$H NMR (300 MHz, $CDCl_3$, 20 °C): δ =5.17 (br d, *J*=7.5Hz, 1H), 4.68 and 4.45 (2 br s, 1H, rotamers), 3.86 (m, 1H), 3.64 (dd, *J*=3.8, 7.4 Hz, 1H), 2.72 (m, 2H), 1.64 (m, 2H), 1.43-1.33 (m, 11H), 0.91 ppm (t, *J*=7.4Hz, 3H); $^{13}$C (75 MHz, $CDCl_3$, 20 °C): δ=171.5, 165.1, 154.7, 81.2, 56.6, 45.6, 36.5, 28.3, 26.1, 22.4, 13.9 ppm; IR: ν=3362, 2976-2933, 1797, 1780, 1688, 1537 $cm^{-1}$; MS (ESI) *m/z* (%): 293 (100) $[M + Na]^+$, 279 (8) $[M + H]^+$; HRMS (ESI): calcd. for $C_{13}H_{21}N_2O_4$ $[M - H]^+$ 269.1501, found 269.1494.

*N-[(3S)-2-oxo-1-pentanoylazetidin-3-yl]hept-6-enamide* (**9**).

Following the general procedure for the preparation of bis-acylated compounds, starting from tert-butyl N-[(3S)-2-oxo-1-pentanoylazetidin-3-yl]carbamate, compound **9** was obtained as a white solid. Yield: 89%; mp 101.0-101.9 °C; $[\alpha]_D^{20}$ +15.8 (*c* 1.0, $CHCl_3$); $^1$H NMR (300 MHz, $CDCl_3$, 20 °C): δ=6.21 (br d, *J*=7.0 Hz, 1H), 5.84-5.70 (m, 1H), 5.02-4.93 (m, 2H), 4.71 (td, *J*=3.8, 6.8 Hz, 1H), 3.85 (m, 1H), 3.66 (dd, *J*=3.9, 7.4 Hz, 1H), 2.74-2.68 (m, 2H), 2.24 (t, *J*=7.6 Hz, 2H), 2.09-2.02 (m, 2H), 1.69-1.59 (m, 4H), 1.46-1.31 (m, 4H), 0.91 ppm (t, *J*=7.3 Hz, 3H); $^{13}$C (75 MHz, $CDCl_3$, 20 °C): δ=173.6, 171.5, 164.7, 138.3, 115.0, 55.8, 45.0, 36.4, 35.8, 33.5, 28.5, 26.2, 24.8, 22.4, 13.9 ppm; IR: ν=3282, 2959-2923, 1780, 1728, 1718, 1693, 1655, 1537 $cm^{-1}$; MS (ESI) *m/z* (%): 303 (100) $[M + Na]^+$, 281 (65) $[M + H]^+$, 253 (22) $[M + H - CO]^+$; HRMS (ESI): calcd. for $C_{15}H_{24}N_2O_3Na$ $[M + Na]^+$ 303.1685, found 303.1670.

*N,N'-bis[(3S)-2-oxo-1-pentanoylazetidin-3-yl]dodec-6-enediamide* (**10**).

Following the general procedure for CM, compound **10** was obtained as a pale-brown solid. Yield: 74%; mp 146.1-146.8 °C; $[\alpha]_D^{20}$ +5.7 (*c* 1.0, $CHCl_3$); $^1$H NMR (300 MHz, $CDCl_3$, 20 °C): δ=7.03-6.54 (m, 2H), 5.34 (m, 2H), 4.70 (m, 2H), 3.87-3.82 (m, 2H), 3.67-3.63 (m, 2H), 2.73-2.68 (m, 4H), 2.25-2.20 (m, 4H), 2.00 (m, 4H), 1.72-1.58 (m, 8H), 1.43-1.24 (m, 8H), 0.91 ppm (t, *J*=7.4 Hz, 6H); $^{13}$C (75 MHz, $CDCl_3$, 20 °C): δ=174.1, 174.0, 171.6, 165.0, 164.8, 131.3, 130.5, 130.1, 55.8, 44.9, 36.4, 35.9, 34.3, 32.0, 28.7, 26.2, 24.7, 22.4, 13.9 ppm; IR: ν=3292, 2962-2868, 1796, 1693, 1676, 1656, 1537 $cm^{-1}$; MS (ESI) *m/z* (%): 555 (100) $[M + Na]^+$, 541 (57) $[M + Na - CH_2]^+$; HRMS (ESI): calcd. for $C_{28}H_{44}N_4O_6Na$ $[M + Na]^+$ 555.3159, found 555.3160.

*N,N'-bis[(3S)-2-oxo-1-pentanoylazetidin-3-yl]dodecanediamide* (**11**).

Following the general procedure for hydrogenation, compound **11** was obtained as a pale-brown solid. Yield: 82%; mp 165.4-166.3 °C; $[\alpha]_D^{20}$ +12.9 (*c* 1.0, $CHCl_3$); $^1$H NMR (300 MHz, $CDCl_3$, 20 °C): δ=6.70-6.53 (m, 2H), 4.73-4.67 (m, 2H), 3.86-3.82 (m, 2H), 3.67-3.63 (m, 2H), 2.72-2.67 (m, 4H), 2.24-2.19 (m, 4H), 1.68-1.58 (m, 8H), 1.42-1.26 (m, 16H), 0.91 ppm (t, *J*=7.3 Hz, 6H); $^{13}$C (75 MHz, $CDCl_3$, 20 °C): δ=174.1, 171.6, 165.0, 55.8, 44.9, 36.4, 35.9, 35.8, 29.1, 29.0, 28.8, 27.8, 26.2, 25.3, 25.2, 22.3, 13.9 ppm; IR: ν=3300, 2930-2849, 1780, 1730, 1693, 1654, 1539 $cm^{-1}$; MS (ESI) *m/z* (%): 557 (100) $[M + Na]^+$, 541 (70) $[M + Na - CH_2]^+$; HRMS (ESI): calcd. for $C_{28}H_{46}N_4O_6Na$ $[M + Na]^+$ 557.3315, found 557.3314.

**Computational chemistry.** All the calculations have been performed with the Gaussian03 suite of programs.[16] The B3LYP/6-31G(d) optimization of the dimers has been made with redundant internal coordinates in order to ensure a rapid convergence of each component of the gradient lower than 2.10-6 a.u. For the localization of the TS at the RHF/MINI-1' level, 3N-6 variables of the Z-matrix have been used. The eigenvector components associated to the negative eigenvalue of the Hessian matrix well combine the variables describing the pseudo 8-membered ring of the H transfer from Ser49 to the nitrogen of the β-lactam.

**Acyl-enzymes modeling**. The crystal structure of R39 complexed with a monobactam (unpublished results) was used as a template to model the acyl-enzyme between R39 and compound **5e**. The interactions made by the compound amide group with Asn300 side chain on one side, and with the backbone carbonyl of Thr413 on the other side were preserved. The remaining dihedral angles were adapted to avoid steric clashes between the compound and the protein. A similar procedure was used to model the acyl-enzyme between PBP2a and **5e**.

**Assay with resistant PBPs**. Purified PBP5 from *Enterococcus faecium* D63r and PBP2a from methicillin-resistant *Staphylococcus aureus* ATCC 43300 were used as target proteins to test inhibitory activity of synthesized β-lactams. Each of the purified PBPs (2.5 μM) were first incubated with 1 mM potential inhibitor in 100 mM phosphate buffer, 0.01% Triton X-100,[17] pH 7, for 4 h at 30 °C. Then, 25 μM fluorescein-labeled ampicillin was added to detect the residual penicillin binding activity (RA). The samples were further incubated for 30 min at 37 °C in a total volume of 20 μL. Denaturation buffer was added (0.1 M Tris/HCl, pH 6.8, containing 25%

glycerol, 2% SDS, 20% β-mercaptoethanol and 0.02% bromophenol blue) and the samples were heated to 100 °C for 1 min. The samples were then loaded onto a 10% SDS-acrylamide gel (10 x 7 cm) and electrophoresis was performed for 45 min at 180 V (12 mA). Detection and quantification of the RAs were done with Molecular Image FX equipment and Quantity One software (BioRad, Hercules, CA, USA). Three independent experiments were carried out for each inhibitor.

**Assay with R39**. All assays with R39 have been done in microtiter plates 96-wells (Brand, Wertheim, Germany). 20 mM of the tested compounds have been solved in DMF. Finally 7.5 µL of the solution have been used in the assay. The final concentration of the compounds in the assays was 100 µM. The final concentration of DMF in the assays was 0.25%. R39 (3.5 nM) was incubated in the presence of the potential inhibitors in 10 mM sodium phosphate buffer (pH 7.2) with 100 mM NaCl, 100 mM D-alanine, 0.01 mg/ml BSA and 0.01% Triton for 60 min at 25 °C. This preincubation was realized, in order to detect also slow binding inhibitors. After the preincubation the residual activity RA of R39 was determined by observing the hydrolysis of the thiolester S2d substrate (*i.e.* N-benzoyl-D-Alanyl-thioglycolate), in the presence of DTNB, catalyzed by the non-inhibited enzyme. The initial rate of hydrolysis of 1 mM S2d in the presence of 1 mM DTNB was determined by monitoring the increase of absorbance at 412 nm (DTNB: $\varepsilon[\Delta\varepsilon] = 13600\ M^{-1}\ s^{-1}$) using a microplate absorbance reader (Power Wave X, Biotek Instruments, Winooski, U.S.A.). The rate of spontaneous hydrolysis of S2d in the presence of the inhibitors was also determined in absence of R39. All assays have been done three times. The determination of RA of R39 in absence of inhibitors has been done six times on each plate. In order to detect false positives which could be slow binding non-competitive

promiscuous inhibitors, the assays have been done in the presence of 0.01% Triton-X-100.[17,18]

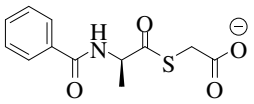

**Figure 7**. N-benzoyl-D-alanyl-thioglycolate (S2d).

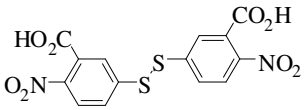

**Figure 8**. 5-(3-Carboxy-4-nitrophenyl)disulfanyl-2-nitrobenzoic acid (DTNB).

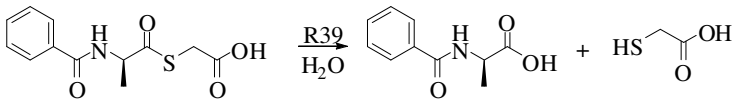


**Scheme 4**. Hydrolysis of the thiolester S2d substrate by R39.

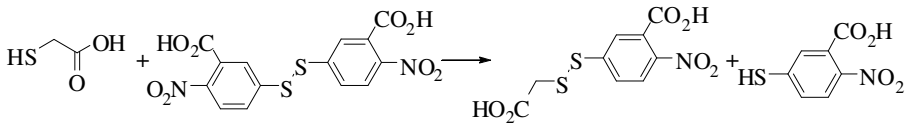

**Scheme 5**. Formed thiol reacts with DTNB, affording 2-nitro-5-thiobenzoate, which ionizes in water at neutral and alkaline pH. This ion has a yellow color and is quantified by measuring the absorbance.

## 6.2. Absolute energies

**Table 4**

Absolute energies of the precursors in the selected conformations.

| Cmpd | Absolute Energy of Open Precursors (a.u.) | |
|---|---|---|
| | *i* | *ii* |
| **3a** | -841.345666490 | -841.344443521 |
| **3b** | -880.656567829 | -880.653009341 |
| **3c** | -919.971821898 | -919.970354436 |
| **3d** | -880.656474399 | -880.655707513 |
| **3e** | -919.971291898 | -919.968972012 |
| **3f** | -959.284718263 | -959.283092592 |
| **3g** | -919.971522432 | -919.970387861 |
| **3h** | -959.285225983 | -959.283693496 |
| **3i** | -998.596454880 | -998.595138399 |

**Table 4** (continued)

| Cmpd | Absolute Energy of Open Precursors (a.u.) | |
|---|---|---|
| | *iii* | *iv* |
| **3a** | -841.353210506 | -841.352690676 |
| **3b** | -880.663916481 | -880.661489845 |
| **3c** | -919.979335270 | -919.978698126 |
| **3d** | -880.664624120 | -880.664457265 |
| **3e** | -919.978967831 | -919.977524714 |
| **3f** | -959.292076753 | -959.291873437 |
| **3g** | -919.979169246 | -919.979055387 |
| **3h** | -959.292508879 | -959.292301476 |
| **3i** | -998.604239590 | -998.603651658 |

**Table 5**

Absolute energies of HH and HT unsaturated and saturated dimers.

| Unsaturated Dimer | Absolute Energy of HH Unsaturated Dimer (a.u.) | Absolute Energy of HT Unsaturated Dimer (a.u.) |
|---|---|---|
| **4b** | -1604.15438264 | -1604.14594029 |
| **4c** | -1682.76433472 | -1682.78664441 |
| **4d** | -1604.12946450 | -1604.15983383 |
| **4e** | -1682.78001976 | -1682.79530381 |
| **4f** | -1761.40880740 | -1761.39708436 |
| **4g** | -1682.75924146 | -1682.78188747 |
| **4h** | -1761.39571506 | -1761.39276448 |
| **4i** | -1840.03971085 | -1840.03584304 |

**Table 5** (continued)

| Saturated Dimer | Absolute Energy of HH Saturated Dimer (a.u.) | Absolute Energy of HT Saturated Dimer (a.u.) |
|---|---|---|
| **5b** | -1606.61653396 | -1606.60549081 |
| **5c** | -1685.22705340 | -1685.24077746 |
| **5d** | -1606.59401209 | -1606.61375676 |
| **5e** | -1685.23800902 | -1685.25186658 |
| **5f** | -1763.86072030 | -1763.84755629 |
| **5g** | -1685.21531345 | -1685.23860424 |
| **5h** | -1763.85536192 | -1763.85467780 |
| **5i** | -1842.49592968 | -1842.49350722 |

**Table 6**

Absolute and relative energies of the precursors of linear dimers in the selected conformations.

| Geometry | Absolute Energy of **6** (a.u.) | Relative Energy of **6** (kcal/mol) |
|---|---|---|
| *i* | -921.208638229 | 4.93 |
| *ii* | -921.207482127 | 5.66 |
| *iii* | -921.216498978 | 0.00 |
| *iv* | -921.215812176 | 0.43 |

**Table 6** (continued)

| Geometry | Absolute Energy of **9** (a.u.) | Relative Energy of **9** (kcal/mol) |
|---|---|---|
| *i* | -921.209144878 | 4.56 |
| *ii* | -921.207458348 | 5.62 |
| *iii* | -921.216415416 | 0.00 |
| *iv* | -921.216085773 | 0.21 |

**Table 7**

Absolute, relative energies and heat of formation of linear dimers **7** and **10**.

| Cmpd | Absolute Energy (a.u.) | Relative Energy (kcal/mol) | Heat of Formation (kcal/mol) |
|---|---|---|---|
| **7** | -1763.84693322 | 0.00 | 0.15 |
| **10** | -1763.84628580 | 0.41 | 0.45 |

The heats of formation of the dimers have been calculated with respect to the most stable conformation of their respective open precursor which is the *iii* conformation.

### 6.3. Stereo view of compound 5e in the model of R39 active site

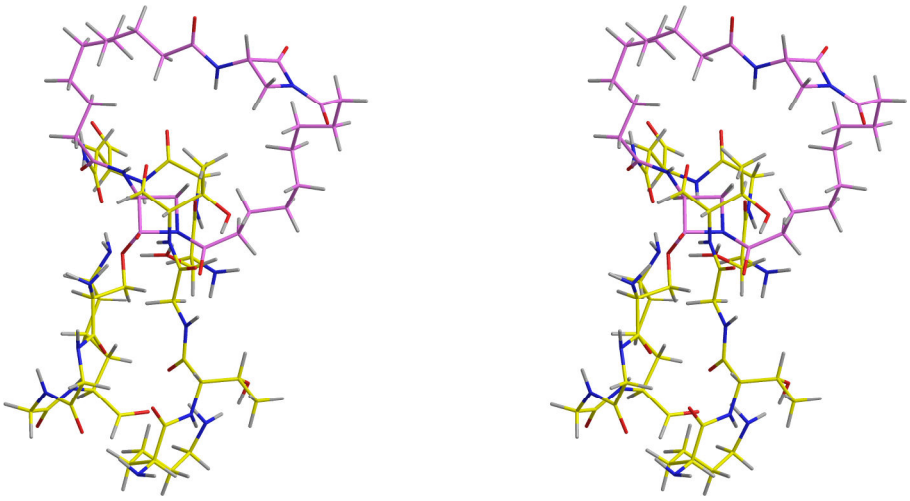

Legend: C of **5e** are purple, others in yellow, H are in grey, O in red, N in blue.

## 6.4. Molecule 5f docked as an acyl-enzyme complex in PBP2a cavity

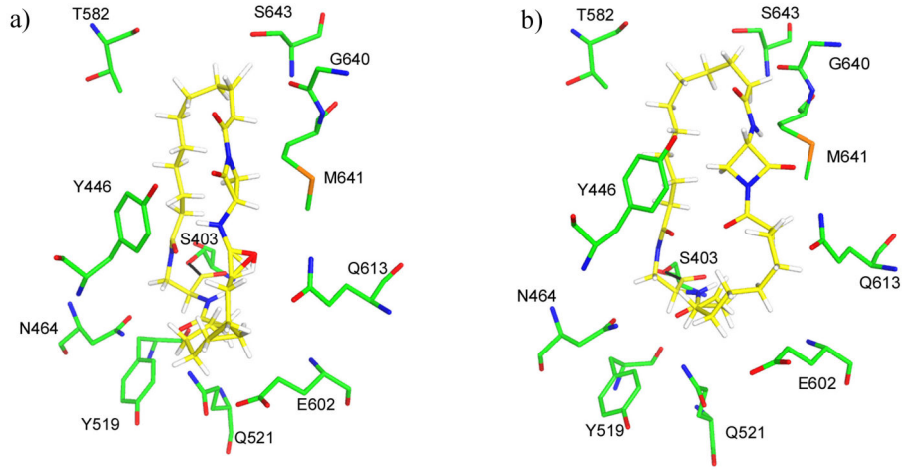


Acyl-enzyme complexes between **5f** and PBP2a. a) **5f**, HH conformer b) **5f**, HT conformer.

Legend: Residues surrounding the alkyl chain of the macrocycle at the bottom of the active site are highlighted with carbon atoms coloured green, nitrogen blue and oxygen red. The carbon atoms of **5f** are coloured yellow and hydrogen white. The active serine 403 is behind the ligand and the covalent bond between the serine and the ligand is coloured black.

The flexibility of the macrocycle **5f** of both HH and HT isomers allows its docking in the active site as acyl-enzymes. The docking highlights the possibility for the whole macrocycle to completely fill the active cavity with the closed lactam cycle sandwiched between Tyr446 and Met641. The figures show the macrocycle lying between a series of residues, especially Glu602 and Gln613 at the entrance of the cavity, without making hydrogen bonds with these residues. The important catalytic residues of the conserved motifs (Ser403, Lys406, Ser462 and Lys597) lie behind the macrocycle and are not shown on the figures.

A modification of the geometry has been applied to dock this molecule into PBP2a. Starting from these two different geometries, a reoptimization at the B3LYP/6-31G(d) level leads to two other local minima with relative energies of 4.56 kcal and 5.16 kcal ( below).

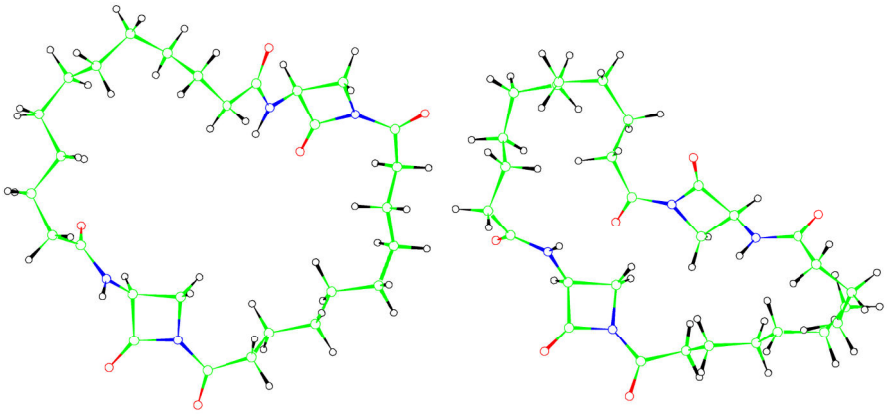

HH ΔE = 4.56 HT ΔE = 5.16

### 6.5. Experiments of temperature coefficients for amide protons

Temperature coefficients of the NH chemical shifts were recorded at 500 MHz in 1,1,2,2-tetrachloroethane-$d_2$ by heating at 10°C intervals from 298 to 358 K.

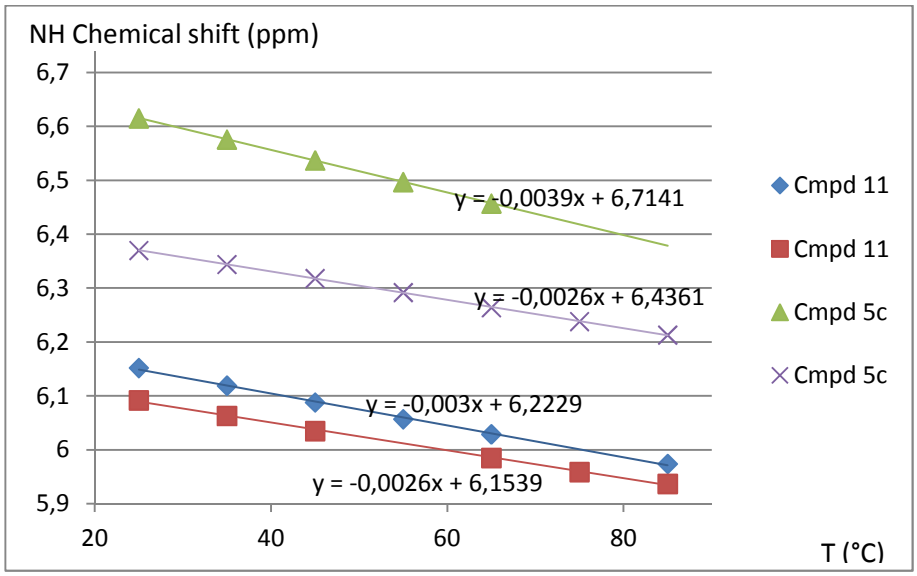


The temperature coefficients of the two amide protons of compound **11** are -3.0 and -2.6 ppb/°C.

The temperature coefficients of the two amide protons of compound **5c** are -2.6 and -3.9 ppb/°C.

In non-competitive solvents, intramolecular hydrogen-bonded amide protons typically exhibit a relatively large temperature dependence of the chemical shift relative to free amide protons which exhibit a small temperature dependence of the chemical shift.[19]

We can observe two different evolutions for the NH of the compound **5c**, it could be explained by the presence of one intramolecular hydrogen-bonded amide proton since the second amide proton is not involved in an intramolecular H bond.

### 6.6. Figures of dimers 4 and 5

Relative energies are given in kcal/mol.

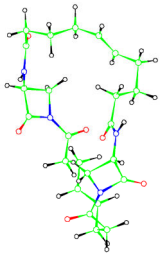

**4b** HH ΔE = 3.42

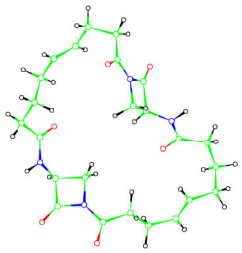

**4b** HT ΔE = 8.72

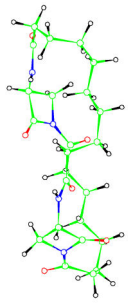

**5b** HH ΔE = 0.00

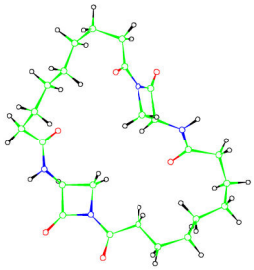

**5b** HT ΔE = 6.93

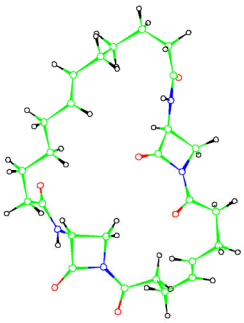

**4c** HH ΔE = 19.43

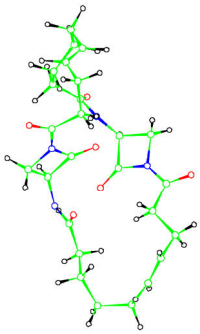

**4c** HT ΔE = 5.43

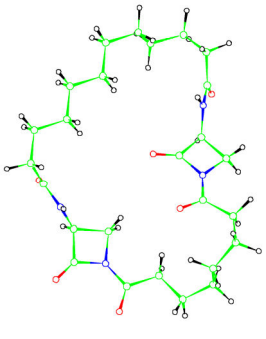

**5c** HH ΔE = 15.57

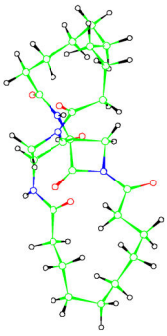

**5c** HT ΔE = 6.96

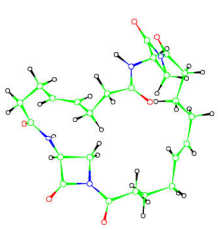

**4d** HH ΔE = 19.06

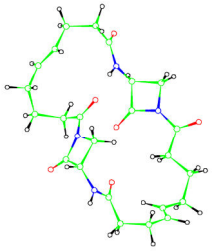

**4d** HT ΔE = 0.00

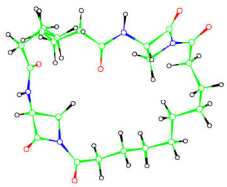

**5d** HH ΔE = 16.02

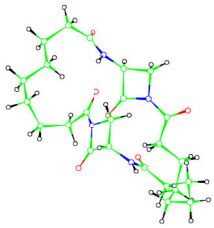

**5d** HT ΔE = 1.74

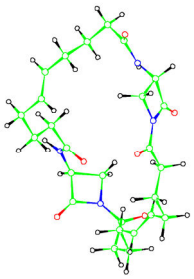

**4e** HH ΔE = 9.59

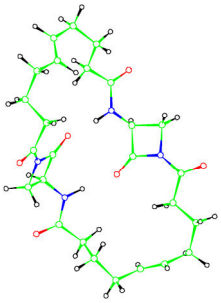

**4e** HT ΔE = 0.00

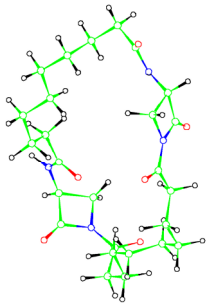

**5e** HH ΔE = 8.70

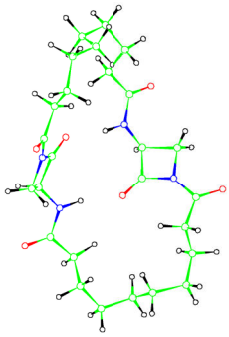

**5e** HT ΔE = 0.00

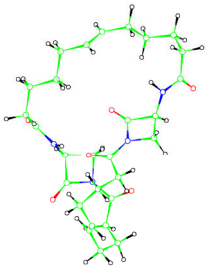

**4f** HH ΔE = 0.00

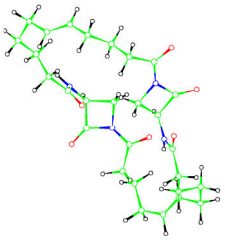

**4f** HT ΔE = 7.36

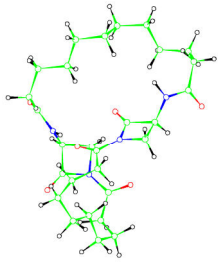

**5f** HH ΔE = 0.00

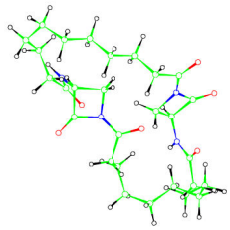

**5f** HT ΔE = 8.26

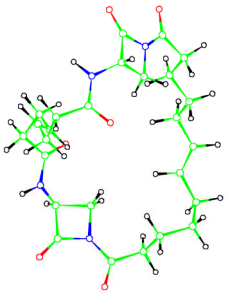

**4g** HH ΔE = 22.63

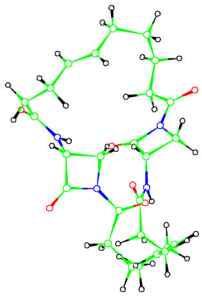

**4g** HT ΔE = 8.42

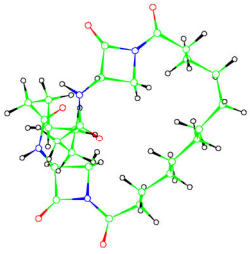

**5g** HH ΔE = 22.94

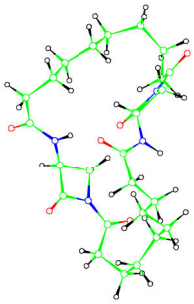

**5g** HT ΔE = 8.32

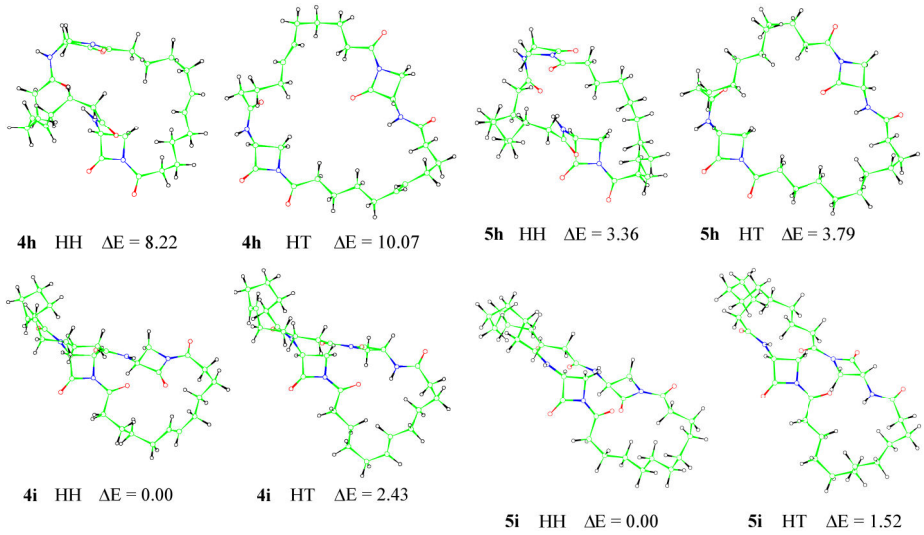


## 7. References and notes

[1] (a) Walsh, C. *Nature* **2000**, *406*, 775-781; (b) Hubschwerlen, C. in *Comprehensive Medicinal Chemistry*, 2nd ed. (Eds: J. B. Taylor, D. J. Triggle), Elsevier, Oxford, UK, **2007**, chapter 7.17, pp. 479-517.

[2] Zapun, A.; Contreras-Martel, C.; Vernet, T. *FEMS Microbiol. Rev.* **2008**, *32*, 361-385.

[3] (a) Hartman, B. J.; Tomasz, A. *J. Bacteriol.* **1984**, *158*, 513-516; (b) Utsui, Y.; Yokota, T. *Antimicrob. Agents Chemother.* **1985**, *28*, 397-403; (c) Lim, D.; Strynadka, N. C. *Nat. Struct. Biol.* **2002**, *9*, 870-876.

[4] (a) Sliwa, A.; Dive, G.; Habib Jiwan, J.-L.; Marchand-Brynaert, J. *Tetrahedron* **2010**, *66*, 9519-9527; b) Sliwa, A.; Marchand-Brynaert, J.; Luhmer, M. *Magn. Reson. Chem.* **2011**, in press.

[5] (a) Sauvage, E.; Herman, R.; Petrella, S.; Duez, C.; Bouillenne, F.; Frère, J.-M.; Charlier, P. *J. Biol. Chem.* **2005**, *280*, 31249-31256; (b)

Sauvage, E.; Powell, A. J.; Heilemann, J.; Josephine, H. R.; Charlier, P.; Davies, C.; Pratt, R. F. *J. Mol. Biol.* **2008**, *381*, 383-393.

[6] Sauvage, E.; Kerff, F.; Fonzé, E.; Herman, R.; Schoot, B.; Marquette, J.-P.; Taburet, Y.; Prevost, D.; Dumas, J.; Leonard, G.; Stefanic, P.; Coyette, J.; Charlier, P. *Cell. Mol. Life Sci.* **2002**, *59*, 1223-1232.

[7] Hong, S. H.; Sanders, D. P.; Lee, C. W.; Grubbs, R. H. *J. Am. Chem. Soc.* **2005**, *127*, 17160-17161.

[8] (a) Schwyzer, R.; Hurlimann, C.; Coenzyle, C. *Helv. Chim. Acta* **1954**, *37*, 155-166; (b) Adam, M.; Damblon, C.; Jamin, M.; Zorzi, W.; Dusart, V.; Galleni, M.; el Kharroubi, A.; Piras, G.; Spratt, B. G.; Keck, W.; Coyette, J.; Ghuysen, J.-M.; Nguyen-Disteche, M.; Frère, J.-M. *Biochem. J.* **1991**, *279*, 601-604.

[9] Lakaye, B.; Damblon, C.; Jamin, M.; Galleni, M.; Lepage, S.; Joris, B.; Marchand-Brynaert, J.; Frydrych, C.; Frère, J.-M. *Biochem. J.* **1994**, *300*, 141-145.

[10] Becke, A. D. *J. Chem. Phys.* **1993**, *98*, 5648-5653.

[11] Francl, M. M.; Pietro, W. J.; Hehre, W. J.; Binkley, J. S.; DeFrees, D. J.; Pople, J. A.; Gordon, M. S. *J. Chem. Phys.* **1982**, *77*, 3654-3666.

[12] (a) Tatewaki, H.; Huzinaga, S. *J. Comp. Chem.* **1980**, *1*, 205-228; (b) Dive, G.; Dehareng, D.; Ghuysen, J. M. *Theor. Chim. Acta* **1993**, *85*, 409-421.

[13] Nicola, G.; Tomberg, J.; Pratt, R. F.; Nicholas, R. A.; Davies, C. *Biochemistry* **2010**, *49*, 8094-8104.

[14] (a) Moreillon, P. *CMI* **2008**, *14* (Suppl. 3), 32-41; (b) Henry, X.; Amoroso, A.; Coyette, J.; Joris, B. *Antimicrob. Agents Chemother.* **2010**, *54*, 953-955.

[15] Bissantz, C.; Kuhn, B.; Stahl, M. *J. Med. Chem.* **2010**, *53*, 5061-5084.

[16] Frisch, M. J.; Trucks, G. W.; Schlegel, H. B.; Scuseria, G. E.; Robb, M. A.; Cheeseman, J. R.; Montgomery, J. A., Jr.; Vreven, T.; Kudin, K. N.; Burant, J. C.; Millam, J. M.; Iyengar, S. S.; Tomasi, J.; Barone, V.; Mennucci, B.; Cossi, M.; Scalmani, G.; Rega, N.; Petersson, G. A.; Nakatsuji, H.; Hada, M.; Ehara, M.; Toyota, K.; Fukuda, R.; Hasegawa, J.; Ishida, M.; Nakajima, T.; Honda, Y.; Kitao, O.; Nakai, H.; Klene, M.; Li, X.; Knox, J. E.; Hratchian, H. P.; Cross, J. B.; Adamo, C.; Jaramillo, J.; Gomperts, R.; Stratmann, R. E.; Yazyev, O.; Austin, A. J.; Cammi, R.; Pomelli, C.; Ochterski, J. W.; Ayala, P. Y.; Morokuma, K.; Voth, G. A.; Salvador, P.; Dannenberg, J. J.; Zakrzewski, V. G.; Dapprich, S.; Daniels, A. D.; Strain, M. C.; Farkas, O.; Malick, D. K.; Rabuck, A. D.; Raghavachari, K.; Foresman, J. B.; Ortiz, J. V.; Cui, Q.; Baboul, A. G.; Clifford, S.; Cioslowski, J.; Stefanov, B. B.; Liu, G.; Liashenko, A.; Piskorz, P.; Komaromi, I.; Martin, R. L.; Fox, D. J.; Keith, T.; Al-Laham, M. A.; Peng, C. Y.; Nanayakkara, A.; Challacombe, M.; Gill, P. M. W.; Johnson, B.; Chen, W.; Wong, M. W.; Gonzalez, C.; Pople, J. A. *Gaussian 03*, *Revision D.02*; Gaussian: Wallingford CT, 2004.

[17] Feng, B. Y.; Shoichet, B. K. *Nat. Protoc.* **2006**, *1*, 550-553.

[18] Shoichet, B. K. *Drug Discovery Today* **2006**, *11*, 607-615.

[19] Chakraborty, T. K.; Ghosh, A.; Nagaraj, R.; Sankar, A. R.; Kunwar, A. C. *Tetrahedron* **2001**, *57*, 9169-9175 and references therein.

# *Chapter 7 - Bis-alkyl derivatives*

The paper was accepted in *Chemistry - An Asian Journal*.

***Title***

12- to 22-Membered bridged β-lactams as potential Penicillin Binding Proteins inhibitors.

***Authors***

Aline Sliwa,[a] Georges Dive[b,*] and Jacqueline Marchand-Brynaert[a,*]

***Affiliations***

[a] Prof. Dr. J. Marchand-Brynaert, Ir. A. Sliwa
Institute of Condensed Matter and Nanosciences (IMCN)
Molecules, Solids and Reactivity (MOST)
Université catholique de Louvain
Bâtiment Lavoisier, Place Louis Pasteur L4.01.02
1348 Louvain-la-Neuve, Belgium
Phone: +32 (0)10 47 27 40
Fax: +32 (0)10 47 41 68
E-mail: jacqueline.marchand@uclouvain.be

[b] Dr. G. Dive
Centre d'ingénierie des Protéines (CIP)
Université de Liège
Bâtiment B6, Allée de la Chimie
4000 Sart-Tilman (Liège), Belgium

Phone: +32 (0)43 66 34 99
Fax: +32 (0)43 66 33 64
E-mail: gdive@ulg.ac.be

***Keywords***

Ab initio calculations; β-Lactams; Macrocycles; Ring Closing Metathesis; Serine-enzyme inhibition

***Abstract***

As potential inhibitors of Penicillin Binding Proteins (PBPs), we focused our research on the synthesis of non-traditional 1,3-bridged β-lactam embedded into macrocycles. 12- to 22-Membered bicyclic β-lactams were synthesized by RCM reaction of *bis*-ω-alkenyl-3(S)-amino-azetidinone precursors. The reactivity of 1,3-bridged β-lactams was estimated by the determination of the energy barrier of a concerted nucleophilic attack and lactam ring-opening process, using *ab initio* calculations. The results predict that 16-membered cycles should be the more reactive. Biochemical evaluations against R39 DD-peptidase and two resistant PBPs, namely PBP2a and PBP5, revealed indeed the inhibition effect of compound **4d** featuring a 16-membered bridge and the N-Boc chain at C(3) position of β-lactam ring. Surprisingly, the corresponding bicycle **12d** with the V side-chain at C(3) was inactive. Very elaborate reactivity models of the R39 active site have been built that allowed to explain these results.

## 1. Introduction

The introduction of penicillins to the therapeutic arsenal, in the early 40's, is the starting point of the antibiotic era which allowed to save millions men from potentially fatal infectious diseases. However, since the initial use of penicillins as chemotherapeutic agents, phenomena of bacterial resistance were reported.[1] Due to the antibiotic pressure, the occurrence of resistant bacteria increases, leading to a worrisome situation about antibiotics efficiency, so worrying that the World Health Organization decided to dedicate the World Health Day 2011 to microbial resistance.

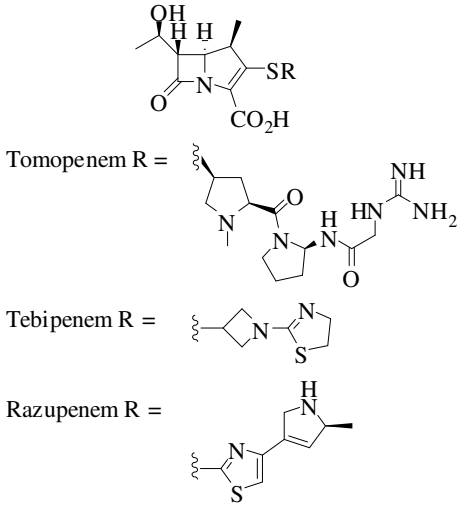


**Figure 1**. Examples of Carbapenems in development.

Despite the discovery of several other classes of antibiotics, the so-called β-lactam class (exemplified nowadays with cephalosporins, carbapenems and penems)[2] still remain the most prescribed one. Initially the activity of β-lactam antibiotics (*i.e.* penicillins) has been attributed to the strain of the four-membered ring and the twisted amide bond of the 2-

azetidinone function. Therefore the search of novel β-lactam antibiotics has been extensively focused on strained 1,4-fused bicyclic structures, intended to improve the so-called "acylating power" of the β-lactam ring versus the target serine-peptidases (*i.e.* bacterial DD-peptidases).[3] Tebipenem, tomopenem or razupenem, (**Figure 1**) three carbapenems in phase II clinical studies, represent examples of this strategy.[4]

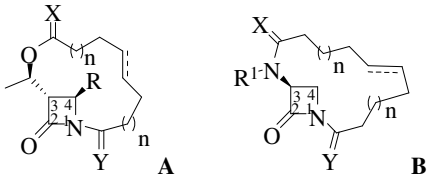


R = H, n-Pr, OAc
$R^1$ = H, Me, $COR^2$
X = Y = O ; X = Y = H,H ; X = O and Y = H,H

**Figure 2**. 1,3-bridged bicyclic β-lactam compounds.

However this traditional model of reactivity seems to be over-evaluated, as there is still no clear relationship between structural characteristics and biological activity. An alternative model of reactivity has been proposed by our group some years ago, based on 1,3-bridged, planar β-lactam motifs embedded into macrocycles. The aim was to possibly decrease the activation barrier of the 2-azetidinone N-C(O) bond cleavage by increasing the conformational adaptability that would be involved in the atoms reorganization during the formation of an acyl-enzyme intermediate.[5] A first series of compounds **A** (**Figure 2**), structurally related to carbapenems, has been previously reported and evaluated against bacterial enzymes with a mitigated success attributed to an inadequate configuration of the C(3) chiral center. To further explore our hypothesis, we decided to synthesize the series of compounds **B** (**Figure 2**) structurally related to

cephalosporins and penicillins, with an amino substituent and inversion of configuration at C(3). Since the nucleophilic attack by serine enzymes occurs normally on the α-face of the β-lactam, the macrocycle of **B** surrounding the β-face would not hamper the serine enzyme processing.

The RCM (Ring Closing Metathesis) reaction was chosen as the key step for the formation of the bridging macrocycles. The precursors are chiral azetidin-2-ones **C** with ω-alkenoyl or ω-alkenyl chains on the positions N(1) and C(3)-N. The starting chirons **D**, derivatives of (S)-3-aminoazetidin-2-one, come from L-serine.

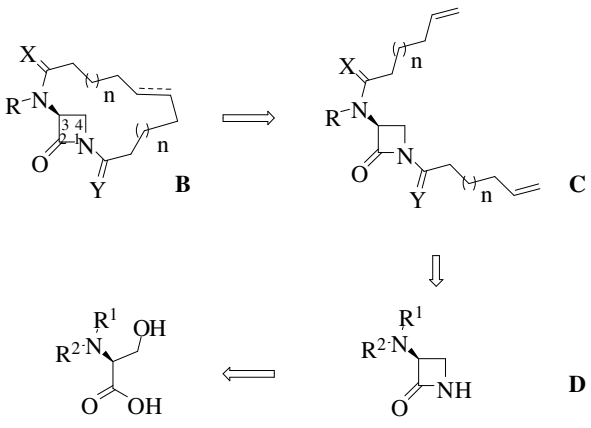


X = Y = O ; R = H, Me, Boc ;
($R^1$, $R^2$) = (Boc, H), (Boc, Me)

X = Y = H,H ; R = Boc, $PhOCH_2CO$ ;
($R^1$, $R^2$) = (Boc, H), ($PhOCH_2CO$, H)

**Scheme 1**. Retrosynthetic strategy.

First we tried to synthesize the bicyclic family **B** with *bis*-acylated chains (X = Y = O). But unexpectedly, when applying the RCM reaction to the *bis*-acylated precursors **C** (X = Y = O, **Scheme 1**), we recovered

exclusively cyclodimers, except in one case (R = Boc; n = 2).[6] Due to the presence of amide and imide functions in the precursors **C**, the conformers leading to the desired cyclizations are strongly disfavoured. This should not be the case for the *bis*-alkylated precursors (X = Y = H,H). Therefore, we kept the same retrosynthetic strategy to synthesize the 1,3-bridged bicyclic β-lactam compounds **B** with *bis*-alkylated chains (X = Y = H,H).

In this article we describe the successful synthesis of target molecules **B** belonging to the *bis*-alkylated family (X = Y = H,H). All these compounds were investigated from a theoretical point of view, and their reactivity into a model of Penicillin Binding Protein (PBP) cavity was studied. Theoretical predictions could be experimentally confirmed by in vitro evaluations against R39 D,D-peptidase,[7] the commonly used model of bacterial enzymes, and against two resistant PBPs, namely PBP2a from *Staphylococcus aureus*[8] and PBP5 from *Enterococcus faecium*.[9]

## 2. Results and Discussion

### 2.1. Synthesis

The first series of *bis*-alkylated bicycles **B** synthesized was the Boc family (X = Y = H,H ; R = Boc). The starting material is the known (S)-3-(tertbutyloxycarbonyl)amino-2-azetidinone **1**, readily prepared from the commercially available Boc-L-serine, as previously described.[6]

ω-Alkenyl bromides of various lengths were used to access various sizes of bicycles. All the ω-alkenyl bromides used are commercially available reagents. The *bis*-alkyl derivatives **2a-f** were synthesized in one

step, with moderate yields, by using 2 equivalents of NaH and 2.2 equivalents of ω-alkenyl bromides (step (a) of **Scheme 2**). Other strong bases were tested (namely LiHMDS, KOH in presence of $Bu_4NHSO_4$ and NaI), without improvement of yields. The use of an excess of base led to racemisation of the *bis*-alkyl derivatives **2**. The *bis*-alkyl derivative **2** with n = 2 was not obtained, probably because HBr elimination occurred from 1-butenyl bromide. With these precursors in hands, we could validate the RCM strategy: using second generation Grubbs' catalyst, the macrocycles **3b-f** were readily formed and isolated in good yields after chromatographic purification (step (b) of **Scheme 2**) leading to 12- to 22-membered rings. The *bis*-alkyl derivative **2a** did not cyclize, the expected 8-membered ring bicycle being too small. Catalytic hydrogenation led to the corresponding saturated macrocycles **4b-f** with high yields (step (c) of **Scheme 2**).

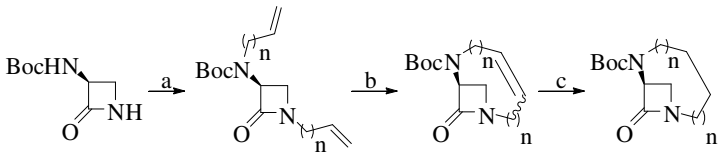


**1**

**2a**, n = 1 (50%)
**2b**, n = 3 (41%)
**2c**, n = 4 (43%)
**2d**, n = 5 (39%)
**2e**, n = 6 (46%)
**2f**, n = 8 (35%)

**3b**, n = 3 (66%)
**3c**, n = 4 (64%)
**3d**, n = 5 (90%)
**3e**, n = 6 (76%)
3f , n = 8 (72%)

**4b**, n = 3 (84%)
**4c**, n = 4 (83%)
**4d**, n = 5 (98%)
**4e**, n = 6 (67%)
**4f**, n = 8 (60%)

**Scheme 2**. Synthesis of bis-alkylated azetidinones **2** and RCM reaction: a) NaH, Br-$(CH_2)_n$-CH=$CH_2$, DMF, 0 °C to 20 °C, 12 h; b) Grubbs II catalyst (2 x 5 mol%), DCM, 40 °C, 12 h; c) $H_2$, Pd-C catalyst, MeOH, 20 °C, 3 h.

Since the N-unprotected derivatives **B** (X = Y = H,H ; R = H) were desirable for biological evaluation and/or further derivatization with penicillin's side-chain, we attempted to remove the Boc group from the precursors **2**, and bicycles **3** and **4**. Several conditions were tested (TFA in

DCM, HCl 2 M solution, CAN in refluxing ACN,[10] TMSCl in presence of NaI[11]) without success; in all cases the β-lactam degradation was observed (IR, NMR analyses).

We tried to replace the Boc protecting group by the penicillin V side-chain (V = $PhOCH_2CO$) *in situ*, by direct acylation (with phenoxyacetyl chloride and TEA or DIEA) of the crude mixtures resulting from the treatment of **2**, **3** and **4** under the above mentioned deprotection conditions. Here again, the results were disappointing with the recovery of untractable mixtures. Hence to access the *bis*-alkylated bicycles **B** with the V side-chain (X = Y = H,H ; R = $PhOCH_2CO$) we re-started the total synthesis from L-serine (**Scheme 3**).

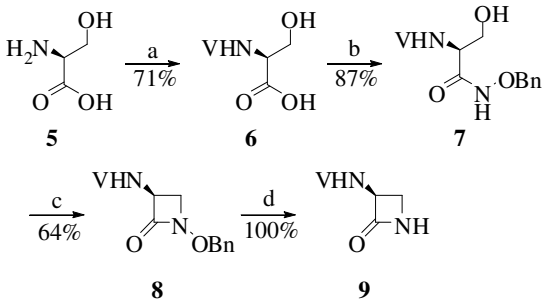


**Scheme 3**. Synthesis of chiron **9**: a) phenoxyacetyl chloride, saturated $NaHCO_3$, $CH_3CN$, rt, 12 h; b) DCC, $NH_2OBn$, THF, 0 °C to rt, 12 h; c) $PPh_3$, $CCl_4$, TEA, $CH_3CN$, 0 °C to rt, 12 h; d) $H_2$, Raney-Ni, MeOH/EtOAc, rt, 12 h.

L-serine **5** was acylated under Schotten-Baumann conditions into (S)-3-hydroxy-2-(2-phenoxyacetamido)propanoic acid **6** in 71% yield. This compound was converted to the corresponding hydroxamate **7**, using O-benzylhydroxylamine and DCC, in 87% yield. Intramolecular cyclization *via* the method proposed by Miller et al.,[12] afforded the β-lactam **8** in 64% yield.

Subsequent hydrogenation in the presence of Raney nickel gave the desired chiron **9** in quantitative yield.

Similarly to the Boc family, the *bis*-alkyl derivatives **10** were synthesized in one step, from **9** in moderate yields. Under conditions of RCM reaction, the precursors **10b-d** (but not **10a**) cyclized into bicycles **11b-d** in good yields, affording 12- to 16-membered rings. Catalytic hydrogenation led to the saturated bicycles **12b-d**. (**Scheme 4**)

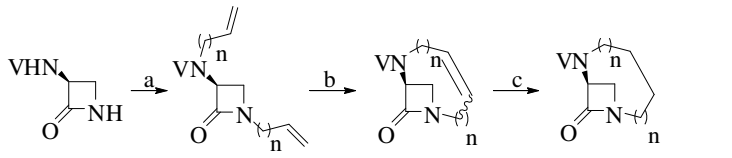


**9**

**10a**, n = 1 (55%)
**10b**, n = 3 (22%)
**10c**, n = 4 (43%)
**10d**, n = 5 (30%)

**11b**, n = 3 (59%)
**11c**, n = 4 (47%)
**11d**, n = 5 (67%)

**12b**, n = 3 (90%)
**12c**, n = 4 (91%)
**12d**, n = 5 (93%)

**Scheme 4**. Synthesis of bis-alkylated azetidinones **10** and RCM reaction: a) NaH, Br-$(CH_2)_n$-CH=$CH_2$, DMF, 0 °C to 20 °C, 12 h; b) Grubbs II catalyst (2 x 5 mol%), DCM, 40 °C, 12 h; c) $H_2$, Pd-C catalyst, MeOH, 20 °C, 3 h.

All precursors (**2**, **10**) and bicycles (**3**-**4**, **11**-**12**) were characterized by IR, NMR and MS (see Experimental). In particular, MS was useful to detect the possible occurrence of side-products issued from (cyclo)oligomerizations and/or double bond migrations (in precursors) leading *in fine* to cyclic products with the formal extrusion of one $CH_2$ unit. Only the 18- and 22-membered ring bicycles, *i.e.* compounds **3e-f**, and consequently **4e-f**, were contaminated with a small amount of lower homologues (respectively 17- and 21-membered ring bicycles).

The NMR patterns confirmed our hypothesis that 1,3-bridged β-lactams embedded into large rings are endowed with a certain conformational adaptability, as discussed in the next section.

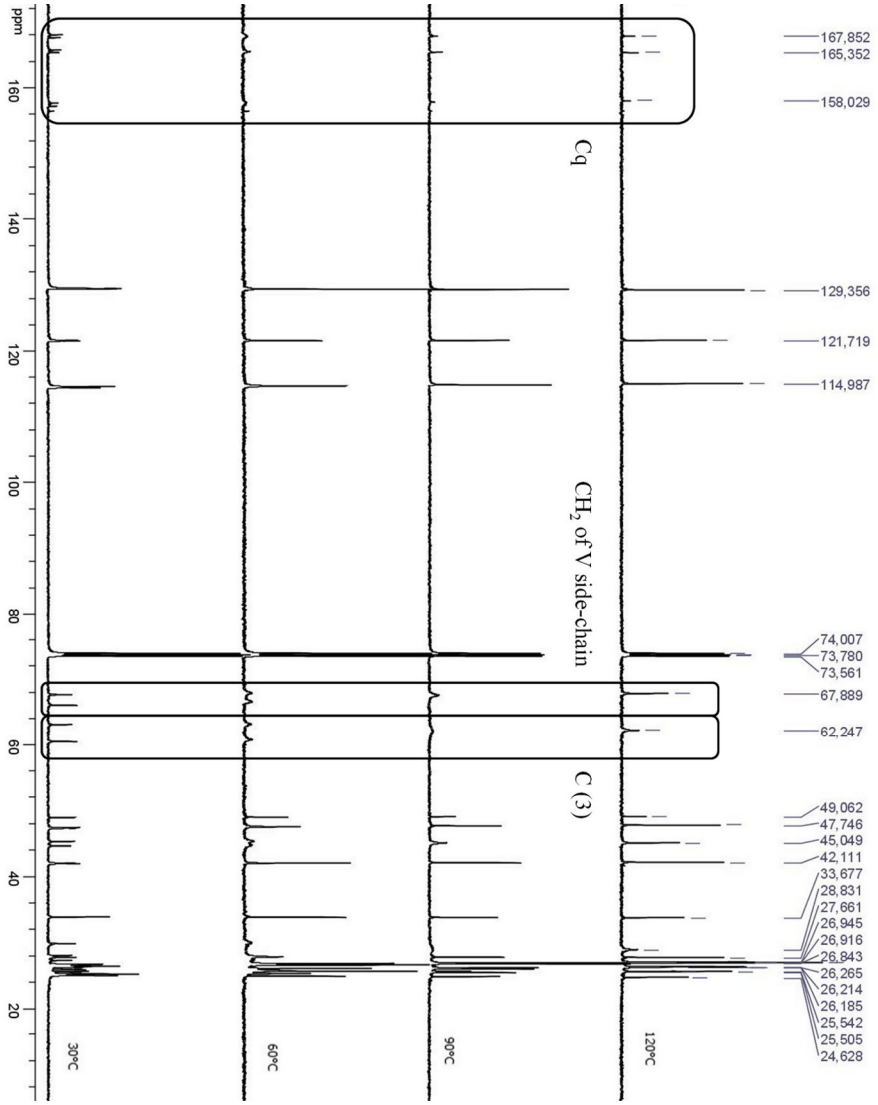


**Figure 3**. $^{13}C$ NMR spectra of compound **12d** recorded at 125 MHz in 1,1,2,2-tetrachloroethane-$d_2$.

## 2.2. Computational chemistry: Conformational study - heat of formation

A lot of conformers can exist for the monocyclic molecules **2** and **10** and also for the bicyclic molecules **3**, **4**, **11** and **12**. In solution, the coexistence of conformers for these compounds was experimentally detected by NMR spectroscopy. For example, in **Figure 3** are presented the $^{13}C$ NMR spectra of compound **12d** recorded in 1,1,2,2-tetrachloroethane-$d_2$ at different temperatures. At 30 °C, a lot of signals are visible because some carbons give rise to signal splitting into several peaks. Rising the temperature to 120 °C leads to signals coalescence and thus allows the structural assignment. The quaternary carbons (Cq) at 167.8 (C=O), 165.3 (C=O) and 158.0 (PhO) ppm at 120 °C appeared as multiple signals at 30 °C. The methylene peak of the V side-chain at 67.9 ppm at 120 °C presented two distinct signals at 30 °C. The C(3) carbon of the β-lactam ring at 62.2 ppm at 120 °C gave two very spaced signals at 30 °C. Similar NMR studies recorded for compounds **10d** and **11d** can be found in Supporting Information (p286).

The geometry of all the molecules has been fully optimized at the RHF level using the minimal basis set MINI-1'.[13]

In the case of *bis*-alkylated precursors **2**, **10** (X = Y = H,H), the molecules are conformationally less constrained than the *bis*-acylated compounds (X = Y = O),[6] as the carbonyls are replaced by methylene groups which can accommodate more conformations. Depending on the nature of the N-substituent (Boc or V), a great number of local minima could be trapped.

Two conformations « *i* » and « *ii* » of the bridging cycle (of compounds **3**, **11** and **4**, **12**) have been located with respect to the β-lactam ring for all the studied compounds. The conformation « *i* » expands the cycle to the right upper corner of the β-lactam C(4); in the conformation « *ii* », the cycle is more orientated to the carbonyl C(2) of the β-lactam. For each conformation, the carbonyl of the side-chain (Boc or V) can rise above the 4-membered ring (« a » conformation) or below (« b » conformation) (**Figure 4**). For all the unsaturated compounds **3**, **11**, the trans configuration of the substituted ethylene has been considered.

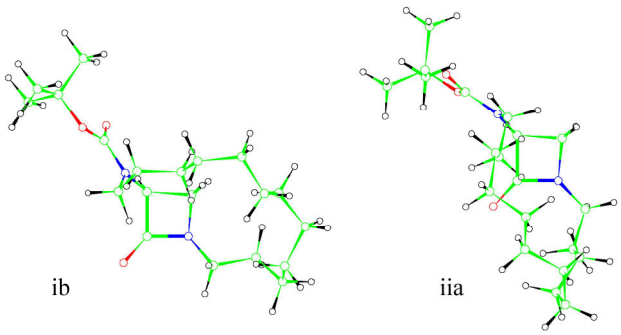


**Figure 4**. Conformers *i*b and *ii*a of compound **4d**.

The heat of formation of **3** and **11** has been computed with respect to the open precursor with the same conformation as the one of the corresponding cyclized molecule. For Boc as well for V side-chains, the 4 conformations lie in the same range of stability, the relative energies being less than 8 kcal/mole in the case of *ii* conformations often more stable than the *i* ones (**Table 1**). The size of the cycle has a significant impact on the conformations for the smallest (12-membered cycle) and the largest ones (22-membered cycle). For the compounds **3b** and **11b**, only the

conformation *i* can be trapped. In the **3f** molecule, the ring is so large that it expands on both sides of the β-lactam in a pseudo *i* conformation only.

Since the *bis*-alkylated precursors **2** and **10** are highly flexible, their cyclization can easily lead to the desired compounds **3** and **11**. Similar reaction was not possible with the *bis*-acylated precursors.[6]

**Table 1**

Relative energies of the precursors/bicycles in the selected conformations and respective heat of formation resulting from the cyclization.

| Precursor | Product | Geometry | Relative Energy of Precursors (kcal/mol) | | Relative Energy of Bicycles (kcal/mol) | |
|---|---|---|---|---|---|---|
| | | | *i* | *ii* | *i* | *ii* |
| **2b** | **3b** | a | 1.39 | | 0.31 | |
| | | b | 0 | | 0 | |
| **2c** | **3c** | a | 2.16 | 0.44 | 2.84 | 0.29 |
| | | b | 2.17 | 0.00 | 3.23 | 0.00 |
| **2d** | **3d** | a | 2.95 | 0.94 | 2.66 | 0.00 |
| | | b | 3.01 | 0.00 | 1.93 | 0.18 |
| **2e** | **3e** | a | 2.95 | 2.92 | 7.83 | 0.00 |
| | | b | 2.95 | 0.00 | 7.66 | 0.27 |
| **2f** | **3f** | a | 0.01 | | 0.33 | |
| | | b | 0.00 | | 0.00 | |
| **10b** | **11b** | a | 0.10 | | 0.00 | |
| | | b | 0.00 | | 0.58 | |
| **10c** | **11c** | a | 2.47 | 0.96 | 1.88 | 1.11 |
| | | b | 2.99 | 0.00 | 0.00 | 0.22 |
| **10d** | **11d** | a | 3.79 | 2.54 | 1.45 | 0.68 |
| | | b | 3.49 | 0.00 | 0.99 | 0.00 |

**Table 1** (continued)

| Precursor | Product | Geometry | Heat of Formation of Bicycles (kcal/mol) | |
|---|---|---|---|---|
| | | | *i* | *ii* |
| **2b** | **3b** | a | 6.54 | |
| | | b | 7.61 | |
| **2c** | **3c** | a | 5.66 | 4.83 |
| | | b | 6.05 | 4.98 |
| **2d** | **3d** | a | 8.30 | 7.64 |
| | | b | 7.50 | 8.76 |
| **2e** | **3e** | a | 11.50 | 3.69 |
| | | b | 11.32 | 6.88 |
| **2f** | **3f** | a | 5.67 | |
| | | b | 5.37 | |
| **10b** | **11b** | a | 6.47 | |
| | | b | 7.14 | |
| **10c** | **11c** | a | 4.19 | 4.92 |
| | | b | 1.78 | 4.99 |
| **10d** | **11d** | a | 7.94 | 8.42 |
| | | b | 7.78 | 10.28 |

### 2.3. Reactivity versus serine enzyme models

The reactivity of the bridged molecules has been studied using a simple model of PBP cavity (**Figure 5**) at the RHF/MINI-1' level. (**Table 2**)

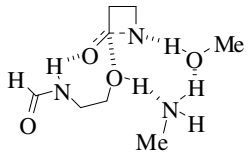


**Figure 5**. Model of concerted nucleophilic attack on the β-lactam ring.

In this model, the β-lactam ring opening occurs *via* a concerted process: the nucleophilic serine is mimicked by 2-(formyl)amino-1-ethanol, in interaction with methylamine working as a proton relay to methanol which, *in fine*, transfers the proton to the β-lactam nitrogen.[14] The formamide moiety mimicks the oxyanion hole stabilization. At the transition state (TS), this pseudo 8-membered ring is described by the reaction coordinate associated to the negative curvature of the energy second derivative matrix.

**Table 2**

Activation energy of concerted nucleophilic attack (MINI-1').

| Unsaturated Compound | Saturated Compound | Geometry | ΔE of Unsaturated Compound (kcal/mol) | | ΔE of Saturated Compound (kcal/mol) | |
|---|---|---|---|---|---|---|
| | | | *i* | *ii* | *i* | *ii* |
| **3b** | **4b** | a | 27.86 | | 28.37 | |
| | | b | 27.18 | | 31.78 | |
| **3c** | **4c** | a | 22.79 | 25.12 | 25.15 | 26.31 |
| | | b | 20.89 | 23.21 | 21.86 | 25.28 |
| **3d** | **4d** | a | 18.90 | 20.47 | 19.48 | 23.76 |
| | | b | 16.86 | 20.55 | 17.96 | 22.41 |
| **3e** | **4e** | a | 20.84 | 19.66 | 20.19 | 20.55 |
| | | b | 19.13 | 17.71 | 19.17 | 18.43 |
| **3f** | **4f** | a | 28.82 | | 28.80 | |
| | | b | 28.62 | | 28.86 | |
| **11b** | **12b** | a | 21.96 | | 23.42 | |
| | | b | 26.36 | | 30.87 | |
| **11c** | **12c** | a | 26.87 | 25.35 | 29.36 | 24.53 |
| | | b | 23.95 | 22.99 | 23.11 | 21.14 |
| **11d** | **12d** | a | 21.47 | 18.95 | 21.22 | 19.82 |
| | | b | 15.53 | 18.95 | 16.52 | 18.38 |
| PenG | | | 9.33 | | | |

The results obtained with Boc and V side-chains present some common features concerning the lowest energy barriers: the optimum size of the cycle is a 16-membered ring (*i.e.* **3d**-**4d** and **11d**-**12d**) while the shorter and the bigger ones enhance the energy barrier calculated with the model. In most of the cases, the activation energy is also higher for the saturated cycle with respect to the corresponding unsaturated one (with the trans configuration at the C=C bond).

### 2.4. Inhibition of R39, PBP2a and PBP5

All products were evaluated for their potential inhibition effect on bacterial serine enzymes. R39 from *Actinomadura* is a model serine-enzyme of low molecular weight D,D-peptidases, usually considered for a preliminary screening of penicillin-like compounds. R39 and the tested β-lactam (100 μM) were incubated (1 h, 25 °C). Then the enzyme residual activity (RA) was determined by observing the hydrolysis of the thioester S2d substrate[15] in the presence of DTNB for labeling the formed thiol, and reading at 412 nm. The results are given in **Table 3** as percentages (%) of residual activity (RA). The activity in the absence of inhibitor is set at 100% and therefore low values indicate a very active compound since the bacterial enzyme has been inhibited by the tested compound and consequently cannot hydrolyze its substrate. A tested compound is considered as a "hit" (*i.e.* potential inhibitor) for a RA < 80%.

**Table 3**

Evaluation of bis-alkylated azetidinones against R39 D,D-peptidase, PBP5 and PBP2a.

| Entry | Compound | n | R39 RA [%] | PBP5 RA [%] | PBP2a RA [%] |
|---|---|---|---|---|---|
| 1 | **2a** | 1 | 101 ± 4 | 81 | 96 |
| 2 | **2b** | 3 | >100 | 94 | 71 |
| 3 | **2c** | 4 | 97 ± 11 | 69 | 68 |
| 4 | **2d** | 5 | 80 ± 4 | 80 | 59 |
| 5 | **2e** | 6 | 97 ± 2 | 100 | 95 |
| 6 | **2f** | 8 | 101 ± 1 | 100 | 100 |
| 7 | **10a** | 1 | 103 ± 8 | 100 | 96 |
| 8 | **10b** | 3 | 97 ± 3 | 90 | 95 |
| 9 | **10c** | 4 | 101 ± 1 | 100 | 98 |
| 10 | **10d** | 5 | 100 ± 4 | 96 | 91 |
| 11 | **3b** | 3 | >100 | 68 | 53 |
| 12 | **3c** | 4 | 103 ± 9 | 78 | 96 |
| 13 | **3d** | 5 | 83 ± 4 | 74 | 58 |
| 14 | **3e** | 6 | 98 ± 1 | 99 | 96 |
| 15 | **3f** | 8 | 97 ± 3 | 72 | 69 |
| 16 | **11b** | 3 | 102 ± 4 | 95 | 89 |
| 17 | **11c** | 4 | 101 ± 3 | 100 | 97 |
| 18 | **11d** | 5 | 104 ± 4 | 100 | 93 |
| 19 | **4b** | 3 | >100 | 96 | 98 |
| 20 | **4c** | 4 | 96 ± 11 | 89 | 88 |
| 21 | **4d** | 5 | 52 ± 3 | 61 | 61 |
| 22 | **4e** | 6 | 95 ± 1 | 100 | 89 |
| 23 | **4f** | 8 | 96 ± 1 | 86 | 90 |
| 24 | **12b** | 3 | 101 ± 3 | 100 | 97 |
| 25 | **12c** | 4 | 97 ± 4 | 100 | 100 |
| 26 | **12d** | 5 | 105 ± 9 | 99 | 100 |

All the compounds were also evaluated against two high-molecular-weight D,D-peptidases responsible for bacterial resistance to β-lactam antibiotics: PBP2a from methicillin-resistant *S. aureus* and PBP5 from *E.*

*faecium.* The tested β-lactams (1 mM) were incubated with the PBPs (4h, 30 °C), then fluorescein-labelled ampicillin was added to detect the residual activity. This reagent is an inhibitor forming a stable acyl-enzyme intermediate. After denaturation, and SDS-PAGE separation of the acylated enzyme from the reagent band, fluorescence was measured. The fluorescence intensity is proportional to the residual active protein, *i.e.* protein non acylated by the tested compound.

Interestingly, the lowest residual activities occur for Boc molecules with the saturated (**4d**, entry 21) and unsaturated (**3d**, entry 13) 16-membered cycles, and their open precursor (**2d**, entry 4). Some activities on PBP2a are also observed for other compounds of the Boc family (entries 2, 3, 11, 15). By opposite, none of the V side-chain molecules has a significant activity on the R39 DD-peptidase, nor on PBP2a and PBP5. Only the saturated 16-membered cycle of the Boc family (**4d**) has a high activity on the R39 DD-peptidase. In order to understand this phenomenon, more elaborate reactivity models of the active site have been built.

### 2.5. Building of the models

The R39 active site is constituted by the three conserved motifs found in PBP and β-lactamases, as highlighted from the X-ray data.[7] The first motif connects Ser49 (nucleophilic serine) and Lys52 by Asn50 and Met51. Remarkably, the conformation of the backbone is stabilized by a hydrogen bond between the carbonyl of Ser49 backbone and the NH of Lys52 allowing the lysine residue extension in such a way that the amino group Nζ lies in the vicinity of Oγ of Ser49. The second motif is formed by

Ser298, Asn299 and Asn300. Ser298 is in connection with the amino group of Lys52 residue. Due to the turn in the conformations of both Asn299 and Asn300, the NH of Asn300 interacts with the ligand carbonyl side-chain. The third motif is formed by Lys410, Thr411, Gly412 and Thr413. Several interactions stabilize its conformation. The carbonyl backbone of Thr413 makes a hydrogen bond with the NH ligand side-chain. The NH backbone of Thr413 interacts with the oxyanion of the ligand, while the amino group of Lys410 side-chain and OH group of Thr411 stabilize the carboxylic group of the penicillin-type antibiotics. Gly416 starts the β4 sheet with Val417 and Ser418 parallel to the β3 one. The bottom of the cavity is delimited by Gly348, Leu349, Ser350 and Arg351 on one hand and by Ala146, Tyr147 and Ser148 on the other hand. As depicted on the 2D drawing (**Figure 6**), side-chains of Arg351, Leu349 and Tyr147 could interact with the side-chain of the ligand. They could also give rise to a steric hindrance with some part of the ligand.

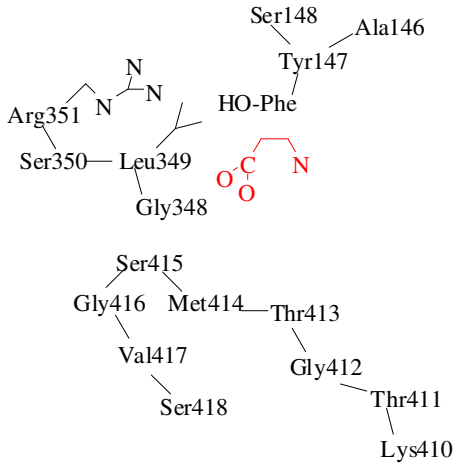


**Figure 6**. Bottom of R39 cavity. The fragment in red is a part of the ligand bearing a side-chain on C(3).

Three models have been built by increase of their complexity in order to locate the transition structure with penicillin bearing a side-chain limited to a formamide group (referred to as Pen). The first one contains the 49 to 52 amino acids of the first motif and methanol mimicking Ser298 (82 atoms, 250 basis functions) as in the simple model (**Figure 7a**). In the second model, the second motif has been added with the 298 to 300 amino acids (110 atoms, 342 basis functions) (**Figure 7b**). Last, the inclusion of the 410 to 413 amino acids of the third motif constitutes the third model formed by 168 atoms and 508 basis functions (**Figure 7c**, hydrogen atoms have been deleted for clarity). Model 3 with hydrogen atoms and hydrogen bonds is presented in supporting information, p279. For sight of clarity also, the point of view is rotated around the Y axis showing that the motif 3 lies above the β-lactam ring. The aim of these calculations is not, at the present stage, to determine an energy barrier which could be representative of the energy involved in the enzymatic reaction with the complete protein, but to analyze the geometrical constraints due to the models. At a geometric point of view, the position of the thiazolidine ring of penicillin (or the tetrahydrothiazine ring of cephalosporin, results not shown) lies at the entrance of the cavity. This feature could be related to the fact that many DD-peptidases can easily accommodate large β-lactam antibiotics such as the tricyclic carbapenems.[16] A second important geometry constraint is related to the conformation of the third motif which defines the accessible volume above the β-lactam ring.

The three transition state (TS) structures have been located as first order saddle points for which the imaginary frequency well describes the motion of the hydrogen between Ser49 and Lys52, Lys52 and Ser298 and Ser298 to the nitrogen of the β-lactam ring. Remarkably, the three equilibrium structures are nearly superimposable, as well as the simple

model of **Figure 5**, when looking at the 8-membered ring formed by the proton shuttle.

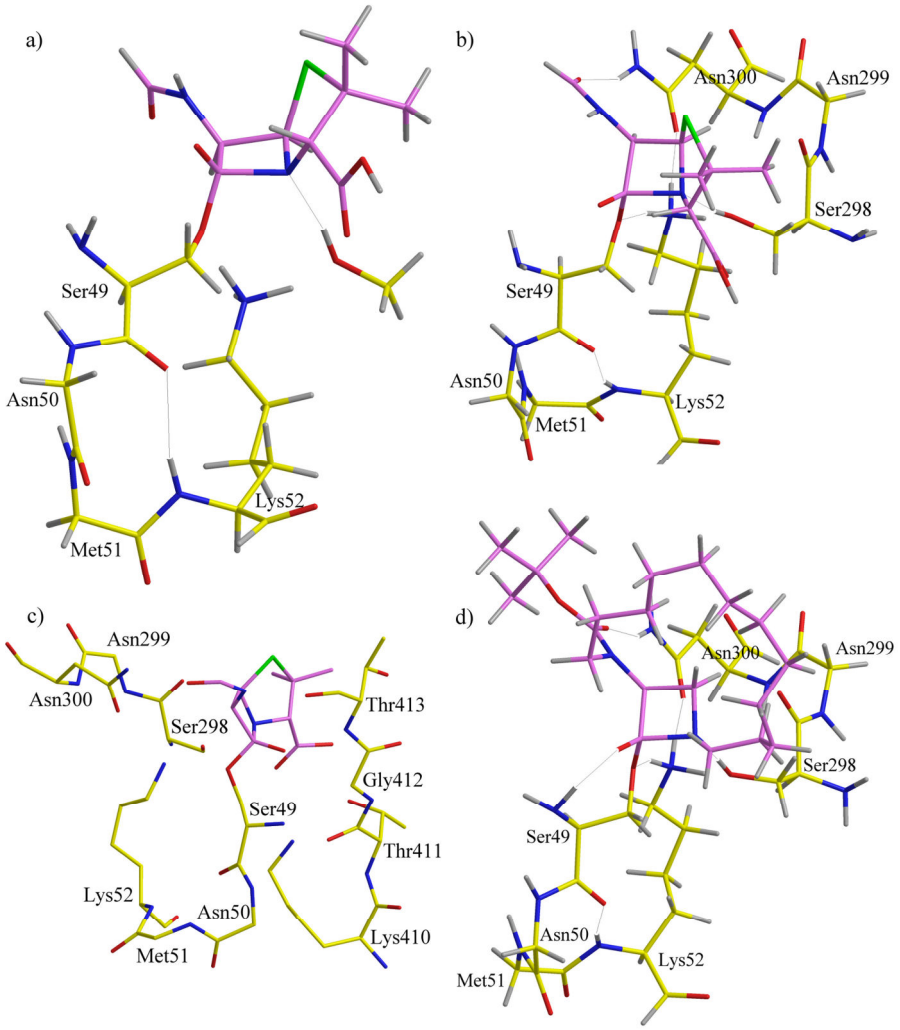


**Figure 7**. a) Pen in the first model. b) Pen in the second model. c) Pen in the third model. d) Compound **4d** in conformation ib in the second model. Legend: C of Pen or **4d** are purple, others in yellow, H are in grey, O in red, N in blue, hydrogen bonds are in thin sticks.

Additional calculations with the **4d** molecule have thus been performed and the transition state structures located for the second (143 atoms, 407 basis functions) and third (201 atoms, 573 basis functions) models, using *i*b and *ii*b conformations as starting geometry. It appears that conformation *ii*b has an important steric hindrance with the third motif and that only conformation *i*b could accommodate the geometry of the active site model (**Figure 7d**).The goodness of fit between this structure and the one obtained with Pen could partially explain the 52% of residual activity observed with **4d** on R39.

One question remains about the lack of activity of **12d**. This molecule can adopt two conformations of the phenoxy side-chain with the *i*b conformation of the bridged cycle differing only by 1.52 kcal. Both of them have been superimposed on the conformation *i*b of **4d** (**Figure 8**). In one conformation, the phenoxy group has a steric hindrance with Tyr147 phenol; on the other, the phenoxy lies in too short contact with Leu349 and Arg351 side-chains. This geometric feature occurring with both conformations could be related to the biological results as **12d** cannot accommodate the active site model geometry while **4d** can do it.

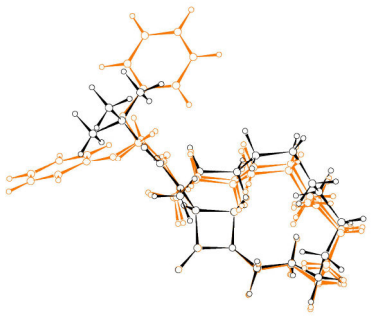

**Figure 8**. Compounds **4d** (black) and **12d** (orange) in conformation *i*b.

## 3. Conclusion

In the *bis*-acylated family previously reported (X = Y = O, **Scheme 1**) cyclodimers were obtained when applying the RCM reaction as key-step for the macrocyclization. In the present work, this synthetic strategy was successful to obtain cyclomonomers with the *bis*-alkylated family (X = Y = H,H) due to the high conformational adaptability of the *bis*-alkylated precursors. 12- to 22-Membered 1,3-bridged β-lactams for the Boc series and 12- to 16-membered bicyclic β-lactams for the V side-chain series were synthesized.

The reactivity of the 1,3-bridged β-lactams in serine enzyme active site highly depends on the ligand conformation explaining why the compounds bearing a V side-chain do not fit with the geometry of the catalytic cavity. This feature has been analyzed using different models of the R39 active site including the three conserved motifs of this enzyme family. Within the synthesized bicycles, **4d** is a good inhibitor of the R39 enzyme (as theoretically predicted), and some compounds also exhibit a significant activity against resistant PBP2a from MRSA. The activity could be related to the flexibility of the bicycles which can accommodate their conformation into the enzyme active site.

The activity of the 1,3-bridged macrocycles deriving from *bis*-ω-alkenyl-3(S)-amino-azetidinone precursors suggests a way to design novel lactam antibiotics with a planar amide bond, and devoid of carboxylic group. Indeed, this acid function only plays a role by stabilizing the conformation of penicillin-like molecules by H-bonds with the residues of the third motif.

## 4. Experimental Section

**General**. Experiments were performed under argon atmosphere in flame-dried glassware. All solvents, including anhydrous solvents, and reagents were purchased from Acros Organics, Alfa Aesar, Fluka, Sigma-Aldrich or VWR, and used without any further purification. TLC analyses were performed on aluminum plates coated with silica gel $60F_{254}$ (Merck) and visualized with a $KMnO_4$ solution and UV (254 nm) detection, and column chromatographies were performed on silica gel (40-63 or 63-200 μm) purchased from Rocc. Melting points (mp) were determined on a Büchi B-540 apparatus calibrated with caffeine, vanillin, and phenacetin. $[\alpha]_D$ was measured on Perkin-Elmer 241 MC polarimeter, at 20 °C. Concentrations are given in g/100 mL. Nuclear magnetic resonance ($^1H$ and $^{13}C$) spectra were recorded at 300 MHz for proton and 75 MHz for carbon (Bruker Avance 300) or 500 MHz for proton and 125 MHz for carbon (Bruker Avance 500). Chemical shifts are reported in parts per million relative to residual solvent peak from the deuterated solvent or relative to peak of TMS. NMR coupling constants (*J*) are reported in hertz. Infrared (IR) spectra were recorded using FTIR-8400S Shimadzu apparatus. Products were analyzed as thin films deposited on an Se-Zn crystal by evaporation from $CH_2Cl_2$ solutions. Low resolution mass spectra were obtained using a ThermoFinnigan LCQ Quantum spectrometer or using a FinniganMat TSQ7000. High Resolution Mass Spectrometry (HRMS) analyses were performed at the University College London (UK). Originally, structural data for compounds **2a**-**c**, **2e**-**f**, **3b**-**c**, **3e**-**f**, **4b**-**c**, **4e**-**f**, **10a**-**c**, **11b**-**c**, **12b**-**c** were in the Supporting Information, here they were added directly to the experimental section.

*Bis-alkyl precursor* (**2d**).

NaH (60% dispersion in oil, 279 mg, 6.98 mmol) was added to a stirred solution of **1** (0.65 g, 3.49 mmol) in dry DMF (41 mL) at 0 °C. Alkyl bromide (1.17 mL, 7.68 mmol) was added after 30 min and the mixture was then slowly warmed to r.t. and stirred overnight. The mixture was quenched with water (30 mL) at 0 °C and then the medium diluted with brine (50 mL). The resulting mixture was extracted with EtOAc (3x30 mL) and the organic layers were washed with brine (70 mL). After drying over $MgSO_4$ and removing the solvent under reduced pressure, the residue was purified by flash column chromatography (hexane/EtOAc 4/1) to provide **2d** as a pale-yellow oil (515 mg, 39%). $R_f$=0.63 (hexane/EtOAc 3/2); $[\alpha]_D^{20}$ +3.0 (*c* 1.7, $CH_3OH$); $^1$H NMR (300 MHz, $CDCl_3$, 20 °C): δ=5.84-5.71 (m, 2H), 5.01-4.90 (m, 4H + 0.4H, rotamer), 4.52 (br s, 0.6H, rotamer), 3.46-3.43 (m, 1H), 3.26-3.08 (m, 5H), 2.07-2.00 (m, 4H), 1.57-1.24 ppm (m, 21H); $^{13}$C (125 MHz, $CDCl_3$, 20 °C): δ=167.1, 154.7, 138.9, 138.7, 114.7, 114.5, 80.9, 80.5, 63.2, 62.9, 47.9, 47.1, 46.7, 41.7, 33.8, 33.7, 29.6, 29.0, 28.7, 28.5, 27.5, 26.5, 26.4 ppm; IR: ν=2974-2856, 1753, 1693, 1639, 1456 $cm^{-1}$; MS (ESI) *m/z* (%): 779 (12) $[2M + Na]^+$, 401 (100) $[M + Na]^+$; HRMS (ESI): calcd. for $C_{22}H_{38}N_2O_3Na$ $[M + Na]^+$ 401.2780, found 401.2778.

*tert-butyl N-[(3S)-2-oxo-1-(prop-2-en-1-yl)azetidin-3-yl]-N-(prop-2-en-1-yl)carbamate* (**2a**).

Prepared by the same procedure as described for **2d**. Yield: 50%; $R_f$=0.31 (hexane/EtOAc 3/2); $[\alpha]_D^{20}$ -12.5 (*c* 4.2, $CHCl_3$); $^1$H NMR (500 MHz, $CDCl_3$, 20 °C): δ=5.84-5.68 (m, 2H), 5.23-5.11 (m, 4H), 5.02 and 4.52 (2 br s, 1H, rotamers), 4.00-3.59 (m, 4H), 3.43-3.41 (m, 1H), 3.31 (br s, 1H), 1.44 ppm (s, 9H); $^{13}$C (125 MHz, $CDCl_3$, 20 °C): δ=166.9, 154.6, 134.6-134.2

(rotamers), 131.5, 118.8, 117.0-116.6 (rotamers), 81.3-81.2 (rotamers), 63.0, 50.0-49.3 (rotamers), 47.4-46.6 (rotamers), 44.5, 28.4 ppm; IR: ν=2976-2932, 1759, 1693, 1645, 1452 $cm^{-1}$; MS (ESI) *m/z* (%): 555 (100) $[2M + Na]^+$, 289 (28) $[M + Na]^+$, 267 (10) $[M + H]^+$, 211 (26) $[M + H - C_4H_8]^+$; HRMS (ESI): calcd. for $C_{14}H_{22}N_2O_3Na$ $[M + Na]^+$ 289.1528, found 289.1525.

*tert-butyl N-[(3S)-2-oxo-1-(pent-4-en-1-yl)azetidin-3-yl]-N-(pent-4-en-1-yl)carbamate* (**2b**).

Prepared by the same procedure as described for **2d**. Yield: 41%; $R_f$=0.53 (hexane/EtOAc 3/2); $[\alpha]_D^{20}$ +4.7 (*c* 1.1, $CH_3OH$); $^1H$ NMR (300 MHz, $CDCl_3$, 20 °C): δ=5.84-5.70 (m, 2H), 5.06-4.93 (m, 4H + 0.5H, rotamer), 4.53 (br s, 0.5H, rotamer), 3.47-3.44 (m, 1H), 3.37-3.00 (m, 5H), 2.11-1.99 (m, 4H), 1.67-1.60 (m, 4H), 1.44 ppm (s, 9H); $^{13}C$ (75 MHz, $CDCl_3$, 20 °C): δ=167.1, 154.7, 137.9, 137.3, 115.7, 115.2, 80.9-80.6 (rotamers), 63.2-63.1 (rotamers), 47.8-47.5-47.0-46.4 (rotamers), 41.3, 31.2, 31.1, 28.4, 26.8 ppm; IR: ν=2976-2930, 1755, 1693, 1641, 1454 $cm^{-1}$; MS (ESI) *m/z* (%): 345 (100) $[M + Na]^+$, 294 (11) $[M + Na - CO]^+$, 267 (48) $[M + H - C_4H_8]^+$; HRMS (ESI): calcd. for $C_{18}H_{30}N_2O_3Na$ $[M + Na]^+$ 345.2154, found 345.2146.

*tert-butyl N-(hex-5-en-1-yl)-N-[(3S)-1-(hex-5-en-1-yl)-2-oxoazetidin-3-yl]carbamate* (**2c**).

Prepared by the same procedure as described for **2d**. Yield: 43%; $R_f$=0.50 (hexane/EtOAc 3/2); $[\alpha]_D^{20}$ +4.1 (*c* 1.6, $CH_3OH$); $^1H$ NMR (300 MHz, $CDCl_3$, 20 °C): δ=5.84-5.69 (m, 2H), 5.03-4.91 (m, 4H + 0.5H, rotamer), 4.52 (br s, 0.5H, rotamer), 3.46-3.43 (m, 1H), 3.36-3.02 (m, 5H), 2.10-2.01

(m, 4H), 1.56-1.32 ppm (m, 17H); $^{13}$C (75 MHz, $CDCl_3$, 20 °C): δ=167.1, 154.8, 138.6, 138.2, 115.1, 114.8, 80.9-80.6 (rotamers), 63.2-63.1 (rotamers), 47.8-47.1 (rotamers), 41.6, 33.4, 33.3, 28.4, 27.0, 26.3, 26.1 ppm; IR: ν=2924-2854, 1759, 1697, 1641, 1458 cm$^{-1}$; MS (ESI) *m/z* (%): 373 (100) $[M + Na]^+$; HRMS (ESI): calcd. for $C_{20}H_{34}N_2O_3Na$ $[M + Na]^+$ 373.2467, found 373.2474.

*tert-butyl N-(oct-7-en-1-yl)-N-[(3S)-1-(oct-7-en-1-yl)-2-oxoazetidin-3-yl]carbamate* (**2e**).

Prepared by the same procedure as described for **2d**. Yield: 46%; $R_f$=0.48 (hexane/EtOAc 7/3); $[\alpha]_D^{20}$ +9.8 (*c* 1.1, $CHCl_3$); $^1$H NMR (300 MHz, $CDCl_3$, 20 °C): δ=5.85-5.71 (m, 2H), 5.00-4.90 (m, 4H + 0.3H, rotamer), 4.52 (br s, 0.7H, rotamer), 3.46-3.43 (m, 1H), 3.34-3.02 (m, 5H), 2.08-1.97 (m, 4H), 1.64-1.22 ppm (m, 25H); $^{13}$C (75 MHz, $CDCl_3$, 20 °C): δ 167.1, 154.8, 139.1, 138.9, 114.5, 114.4, 80.7, 80.5, 63.1, 62.9, 47.9, 47.1, 41.8, 33.8, 33.7, 29.0, 28.9, 28.8, 28.7, 28.5, 27.6, 27.0, 26.8 ppm; IR: ν=2976-2854, 1761, 1693, 1641, 1456 cm$^{-1}$; MS (ESI) *m/z* (%): 835 (50) $[2M + Na]^+$, 429 (100) $[M + Na]^+$, 351 (56) $[M + H - C_4H_8]^+$; HRMS (ESI): calcd. for $C_{24}H_{42}N_2O_3Na$ $[M + Na]^+$ 429.3093, found 429.3104.

*tert-butyl N-(dec-9-en-1-yl)-N-[(3S)-1-(dec-9-en-1-yl)-2-oxoazetidin-3-yl]carbamate* (**2f**).

Prepared by the same procedure as described for **2d**. Yield: 35%; $R_f$=0.53 (hexane/EtOAc 7/3); $[\alpha]_D^{20}$ +8.4 (*c* 1.3, $CHCl_3$); $^1$H NMR (300 MHz, $CDCl_3$, 20 °C): δ=5.86-5.72 (m, 2H), 5.00-4.89 (m, 4H + 0.4H, rotamer), 4.52 (br s, 0.6H, rotamer), 3.46-3.42 (m, 1H), 3.36-3.01 (m, 5H), 2.05-1.99 (m, 4H), 1.60-1.20 ppm (m, 33H); $^{13}$C (75 MHz, $CDCl_3$, 20 °C): δ=167.1, 154.8,

139.3, 139.2, 114.3, 114.2, 80.7, 80.4, 63.1, 62.9, 47.9, 47.7, 47.2, 46.8, 41.8, 33.9, 29.5, 29.4, 29.3, 29.2, 29.1, 29.0, 28.4, 27.6, 27.1, 26.9 ppm; IR: ν=2976-2852, 1759, 1697, 1641, 1464 $cm^{-1}$; MS (ESI) *m/z* (%): 485 (100) $[M + Na]^+$, 429 (15) $[M + Na - C_4H_8]^+$, 407 (44) $[M + H - C_4H_8]^+$; HRMS (ESI): calcd. for $C_{28}H_{50}N_2O_3Na$ $[M + Na]^+$ 485.3719, found 485.3713.

*Unsaturated bicycle* (**3d**).

Grubbs catalyst (second generation) (56 mg, 66.09 μmol) was added to a stirred solution of **2d** (0.50 g, 1.32 mmol) in dry $CH_2Cl_2$ (264 mL) and the solution was stirred at reflux under argon for 4 h. Then a second addition of Grubbs catalyst (56 mg, 66.09 μmol) was made and the mixture was additionally stirred at reflux for 20 h. Then the solvent was removed under reduced pressure and the crude product was purified thrice by column chromatography (hexane/EtOAc 4/1), to provide **3d** as a pale-brown solid (416 mg, 90%). $R_f$=0.43 (hexane/EtOAc 3/2); m.p. 90.1-90.9 °C; $[\alpha]_D^{20}$ -24.4 (*c* 1.2, $CHCl_3$); $^1H$ NMR (500 MHz, $CDCl_3$, 20 °C): δ=5.51 (br s, 0.6H, rotamer), 5.34-5.18 (m, 2H + 0.4H, rotamer), 3.73-3.67 (m, 1H), 3.42-3.35 (m, 1H), 3.25-2.93 (m, 3H), 2.81-2.76 (m, 1H), 2.13-1.94 (m, 4H), 1.69-1.17 ppm (m, 21H); $^{13}C$ (125 MHz, $CDCl_3$, 20 °C): δ=167.6, 167.4, 155.1, 154.3, 131.9, 131.7, 130.4, 130.2, 80.6, 80.3, 62.5, 61.9, 46.9, 45.4, 45.1, 41.2, 41.0, 40.8, 32.2, 30.5, 28.8, 28.4, 28.1, 27.9, 27.2, 27.1, 26.9, 26.7, 26.2, 26.1, 25.1, 25.0, 24.8, 24.5 ppm; IR: ν=2924-2852, 1755, 1697, 1454 $cm^{-1}$; MS (ESI) *m/z* (%): 373 (100) $[M + Na]^+$, 317 (23) $[M + Na - C_4H_8]^+$, 295 (25) $[M + H - C_4H_8]^+$; HRMS (ESI): calcd. for $C_{20}H_{34}N_2O_3Na$ $[M + Na]^+$ 373.2467, found 373.2455.

*tert-butyl 12-oxo-1,10-diazabicyclo[9.1.1]tridec-5-ene-10-carboxylate* (**3b**).

Prepared by the same procedure as described for **3d**. Yield: 66%; $R_f$=0.25 (hexane/EtOAc 1/1); m.p. 82.4-83.2 °C; $[\alpha]_D^{20}$ -49.7 (*c* 2.6, $CHCl_3$); $^1$H NMR (300 MHz, $CDCl_3$, 20 °C): δ=5.57-5.36 (m, 2H+ 0.7H, rotamer), 5.17 (br s, 0.3H, rotamer), 3.78-3.69 (m, 1H), 3.38-2.82 (m, 5H), 2.36-1.85 (m, 4H), 1.77-1.51 (m, 4H), 1.43 ppm (s, 9H); $^{13}$C (75 MHz, $CDCl_3$, 20 °C): δ=166.7, 166.4, 155.2, 154.6, 132.9, 132.5, 129.4, 129.2, 80.5, 80.2, 62.7, 62.0, 46.5, 43.3, 43.1, 40.9, 40.6, 32.7, 29.1, 29.0, 28.4, 27.3, 26.4, 26.1, 26.0 ppm; IR: ν=2922-2825, 1753, 1691, 1483 $cm^{-1}$; MS (ESI) *m/z* (%): 317 (100) $[M + Na]^+$, 266 (15) $[M + Na - CO]^+$, 261 (13) $[M + Na - C_4H_8]^+$; HRMS (ESI): calcd. for $C_{16}H_{26}N_2O_3Na$ $[M + Na]^+$ 317.1841, found 317.1832.

*tert-butyl (13S)-14-oxo-1,12-diazabicyclo[11.1.1]pentadec-6-ene-12-carboxylate* (**3c**).

Prepared by the same procedure as described for **3d**. Yield: 64%; $R_f$=0.34 (hexane/EtOAc 3/2); m.p. 84.6-87.5 °C; $[\alpha]_D^{20}$ -17.0 (*c* 4.5, $CHCl_3$); $^1$H NMR (300 MHz, $CDCl_3$, 20 °C): δ=5.62-5.48 (m, 1H), 5.37-4.96 (m, 2H), 3.72-2.99 (m, 5H), 2.89-2.61 (m, 1H), 2.33-1.24 ppm (m, 21H); $^{13}$C (75 MHz, $CDCl_3$, 20 °C): δ=166.6, 166.0, 155.1, 154.4, 131.7, 131.5, 131.4, 80.5, 80.4, 62.4, 62.0, 49.8, 49.3, 44.8, 44.3, 41.9, 41.8, 41.1, 31.5, 30.4, 29.2, 28.5, 28.1, 28.0, 27.7, 26.8, 25.5, 25.3 ppm; IR: ν=2924-2825, 1739 1454 $cm^{-1}$; MS (ESI) *m/z* (%): 345 (100) $[M + Na]^+$, 289 (32) $[M + Na - C_4H_8]^+$, 267 (16) $[M + H - C_4H_8]^+$; HRMS (ESI): calcd. for $C_{18}H_{30}N_2O_3Na$ $[M + Na]^+$ 345.2154, found 345.2154.

*tert-butyl 18-oxo-1,16-diazabicyclo[15.1.1]nonadec-8-ene-16-carboxylate* (**3e**).

Prepared by the same procedure as described for **3d**. Yield: 76%; $R_f$=0.43 (hexane/EtOAc 3/2); $[\alpha]_D^{20}$ -13.0 (*c* 1.0, $CHCl_3$); $^1$H NMR (300 MHz, $CDCl_3$, 20 °C): δ=5.51-4.98 (m, 3H), 3.72-3.52 (m, 1H), 3.50-3.35 (m, 1H), 3.34-2.96 (m, 3H), 2.93-2.73 (m, 1H), 2.12-1.91 (m, 4H), 1.78-1.16 ppm (m, 25H); $^{13}$C (125 MHz, $CDCl_3$, 20 °C): δ=167.5, 166.7, 166.4, 155.1, 154.4, 131.5, 131.2, 131.1, 130.9, 130.7, 130.1, 80.4, 62.9, 62.3, 62.1, 48.6, 48.2, 47.2, 46.4, 45.5, 45.3, 45.2, 45.0, 42.0, 41.8, 41.7, 41.4, 32.6, 31.7, 31.4, 31.3, 30.9, 30.6, 30.0, 29.8, 29.5, 29.4, 29.2, 28.8, 28.6, 28.4, 28.2, 28.0, 27.6, 27.5, 27.3, 27.1, 26.8, 26.5, 26.3, 25.9, 25.7 ppm; IR: ν=2976-2851, 1755, 1693, 1456 cm$^{-1}$; MS (ESI) *m/z* (%): 401 (51) $[M + Na]^+$, 387 (15) $[M + Na - CH_2]^+$, 323 (100) $[M + H - C_4H_8]^+$, 309 (16) $[M + H - C_4H_8 - CH_2]^+$; HRMS (ESI): calcd. for $C_{22}H_{38}N_2O_3Na$ $[M + Na]^+$ 401.2780, found 401.2758.

*tert-butyl 22-oxo-1,20-diazabicyclo[19.1.1]tricos-10-ene-20-carboxylate* (**3f**).

Prepared by the same procedure as described for **3d**. Yield: 72%; $R_f$=0.45 (hexane/EtOAc 3/2); $[\alpha]_D^{20}$ +1.5 (*c* 1.0, $CHCl_3$); $^1$H NMR (300 MHz, $CDCl_3$, 20 °C): δ=5.39-4.89 (m, 3H), 3.67-3.36 (m, 2H), 3.30-3.07 (m, 3H), 3.02-2.76 (m, 1H), 2.06-1.92 (m, 4H), 1.73-1.17 ppm (m, 33H); $^{13}$C (125 MHz, $CDCl_3$, 20 °C): δ=167.0, 166.8, 155.1, 154.5, 131.3, 131.0, 130.9, 130.8, 130.2, 130.1, 80.4, 63.0, 62.3, 48.2, 47.6, 47.3, 45.8, 45.5, 45.3, 41.8, 41.6, 41.4, 32.6, 32.4, 32.0, ,31.9, 31.8, 30.3, 30.0, 29.5, 29.4, 29.3, 29.1, 29.0, 28.9, 28.8, 28.6, 28.4, 27.9, 27.6, 27.4, 26.9, 26.7 ppm; IR: ν=2922-2852, 1761, 1697, 1464 cm$^{-1}$; MS (ESI) *m/z* (%): 457 (100) $[M + Na]^+$, 443 (13)

$[M + Na - CH_2]^+$, 379 (27) $[M + H - C_4H_8]^+$; HRMS (ESI): calcd. for $C_{26}H_{46}N_2O_3Na$ $[M + Na]^+$ 457.3406, found 457.3396.

*Saturated bicycle* (**4d**).

To a stirred solution of **3d** (110 mg, 0.31 mmol) in methanol (10 mL) was added 10% Pd/C (10 mg). After being stirred under hydrogen atmosphere (P = 1 atm) for 3 h at room temperature, the mixture was filtered through a short pad of Celite and concentrated under reduced pressure. The residue was purified by column chromatography (hexane/EtOAc 4/1), to provide **4d** as a white solid (108 mg, 98%). $R_f$=0.48 (hexane/EtOAc 3/2); m.p. 55.4-56.2 °C; $[\alpha]_D^{20}$ -24.9 (*c* 1.0, $CHCl_3$); $^1$H NMR (500 MHz, $CDCl_3$, 20 °C): δ=5.44 (br s, 0.6H, rotamer), 5.18 (br s, 0.4H, rotamer), 3.68 (br s, 1H), 3.43 (br s, 1H), 3.26-2.99 (m, 3H), 2.84-2.79 (m, 1H), 1.75-1.69 (m, 1H), 1.59-1.20 ppm (m, 28H); $^{13}$C (125 MHz, $CDCl_3$, 20 °C): δ=167.4, 167.1, 155.2, 155.1, 80.5, 62.6, 62.1, 48.0, 47.7, 45.1, 41.9, 29.1, 28.5, 28.2, 26.9, 26.8, 26.6, 26.5, 26.0, 25.4 ppm; IR: ν=2924-2854, 1757, 1697, 1458 $cm^{-1}$; MS (ESI) *m/z* (%): 375 (100) $[M + Na]^+$, 319 (10) $[M + Na - C_4H_8]^+$, 297 (26) $[M + H - C_4H_8]^+$; HRMS (ESI): calcd. for $C_{20}H_{36}N_2O_3Na$ $[M + Na]^+$ 375.2624, found 375.2621.

*tert-butyl 12-oxo-1,10-diazabicyclo[9.1.1]tridecane-10-carboxylate* (**4b**).

Prepared by the same procedure as described for **4d**. Yield: 84%; $R_f$=0.45 (hexane/EtOAc 1/1); m.p. 105.7-106.5 °C; $[\alpha]_D^{20}$ -35.5 (*c* 1, $CHCl_3$); $^1$H NMR (300 MHz, $CDCl_3$, 20 °C): δ=5.31 (br d, *J*=3.8 Hz, 0.6H, rotamer), 5.12 (br d, *J*=2.8 Hz, 0.3H, rotamer), 3.71-3.64 (m, 1H), 3.52-3.27 (m, 4H), 2.78 (dd, *J*=7.6 and 14.3 Hz, 1H), 1.72-1.34 ppm (m, 21H); $^{13}$C (75 MHz, $CDCl_3$, 20 °C): δ=166.9, 166.6, 155.4, 154.6, 80.5, 80.4, 62.9, 62.5, 48.8,

48.6, 43.2, 43.0, 42.3, 42.0, 28.5, 27.0, 26.3, 25.4, 25.2, 25.0, 24.3, 24.1, 23.4, 23.3 ppm; IR: ν=2970-2858, 1743, 1693, 1446 $cm^{-1}$; MS (ESI) *m/z* (%): 319 (100) $[M + Na]^+$, 263 (15) $[M + Na - C_4H_8]^+$; HRMS (ESI): calcd. for $C_{16}H_{28}N_2O_3Na$ $[M + Na]^+$ 319.1998, found 319.2006.

*tert-butyl 14-oxo-1,12-diazabicyclo[11.1.1]pentadecane-12-carboxylate* (**4c**).

Prepared by the same procedure as described for **4d**. Yield: 83%; $R_f$=0.40 (hexane/EtOAc 3/2); m.p. 77.4-78.1 °C; $[\alpha]_D^{20}$ -27.0 (*c* 1, $CHCl_3$); $^1H$ NMR (300 MHz, $CDCl_3$, 20 °C): δ=5.54, 5.45, 5.32 and 5.24 (4 br s, 1H), 3.74-3.65 (m, 1H), 3.47-3.44 (m, 1H), 3.27-3.25 (m, 1H), 3.15-3.01 (m, 2H), 2.83-2.78 (m, 1H), 1.88-1.76 (m, 1H), 1.57-1.25 ppm (m, 24H); $^{13}C$ (75 MHz, $CDCl_3$, 20 °C): δ=167.7, 167.3, 155.2, 154.4, 80.6, 80.4, 62.6, 62.0, 47.6, 47.3, 44.0, 43.8, 41.5, 28.4, 27.1, 26.7, 26.4, 26.1, 25.5, 25.4, 25.1, 24.9, 24.5, 24.3, 24.0 ppm; IR: ν=2930-2860, 1749, 1693, 1456 $cm^{-1}$; MS (ESI) *m/z* (%): 347 (100) $[M + Na]^+$, 269 (12) $[M + H - C_4H_8]^+$; HRMS (ESI): calcd. for $C_{18}H_{32}N_2O_3Na$ $[M + Na]^+$ 347.2311, found 347.2318.

*tert-butyl 18-oxo-1,16-diazabicyclo[15.1.1]nonadecane-16-carboxylate* (**4e**).

Prepared by the same procedure as described for **4d**. Yield: 67%; $R_f$=0.43 (hexane/EtOAc 3/2); $[\alpha]_D^{20}$ -8.4 (*c* 1.0, $CHCl_3$); $^1H$ NMR (300 MHz, $CDCl_3$, 20 °C): δ=5.30 and 4.85 (2 br s, 1H, rotamer), 3.72-2.78 (m, 6H), 1.77-1.19 ppm (m, 33H); $^{13}C$ (125 MHz, $CDCl_3$, 20 °C): δ=167.2, 155.0, 154.5, 80.7, 80.4, 63.3, 62.4, 62.1, 48.5, 47.9, 47.7, 47.1, 46.2, 45.6, 45.3, 41.7, 41.4, 29.8, 28.8, 28.4, 28.0, 27.6, 27.4, 27.1, 27.0, 26.9, 26.8, 26.7, 26.6, 26.5, 26.4, 26.2, 26.1, 25.9, 25.8 ppm; IR: ν=2959-2856, 1757, 1697, 1461 $cm^{-1}$; MS (ESI) *m/z* (%): 403 (100) $[M + Na]^+$, 389 (20) $[M + Na - CH_2]^+$, 325 (40)

$[M + H - C_4H_8]^+$; HRMS (ESI): calcd. for $C_{22}H_{40}N_2O_3Na$ $[M + Na]^+$ 403.2937, found 403.2940.

*tert-butyl 22-oxo-1,20-diazabicyclo[19.1.1]tricosane-20-carboxylate* (**4f**).
Prepared by the same procedure as described for **4d**. Yield: 60%; $R_f$=0.45 (hexane/EtOAc 3/2); $[\alpha]_D^{20}$ +6.2 (*c* 1.0, $CHCl_3$); $^1$H NMR (300 MHz, $CDCl_3$, 20 °C): δ=5.18 and 4.71 (2 br s, 1H, rotamer), 3.58-2.89 (m, 6H), 1.71-1.16 ppm (m, 41H); $^{13}$C (125 MHz, $CDCl_3$, 20 °C): δ=167.1, 155.0, 154.6, 80.8, 80.4, 63.2, 62.6, 47.9, 47.2, 47.1, 46.7, 46.0, 41.7, 29.9, 29.1, 28.9, 28.7, 28.6, 28.3, 28.0, 27.7, 27.5, 27.3, 27.1, 26.9, 26.6 ppm; IR: ν=2924-2852, 1761, 1693, 1458 cm$^{-1}$; MS (ESI) *m/z* (%): 459 (100) $[M + Na]^+$, 445 (13) $[M + Na - CH_2]^+$, 381 (31) $[M + H - C_4H_8]^+$; HRMS (ESI): calcd. for $C_{26}H_{48}N_2O_3Na$ $[M + Na]^+$ 459.3563, found 459.3553.

*(2S)-3-hydroxy-2-(2-phenoxyacetamido)propanoic acid* (**6**).
Phenoxyacetyl chloride (6.57 mL, 47.58 mmol) was added to a solution of L-serine (5.00 g, 47.58 mmol) in saturated aqueous $NaHCO_3$ (200 mL) and MeCN (40 mL). The reaction mixture was stirred vigorously overnight at room temperature and the aqueous phase was extracted with diethyl ether (2 x 200 mL). The aqueous solution was acidified to pH 2-3 with HCl 36% and extracted with EtOAc (4 x 200 mL). The organic layer was dried over $MgSO_4$ and concentrated under reduced pressure. The crude product was solubilized in a minimum of EtOAc and hexane was added until the apparition of a precipitate. After 5-6h the suspension was filtered, washed with hexane and dried under reduced pressure to provide **6** as a white solid (8.08 g, 71%). m.p. 130.1-130.9 °C; $[\alpha]_D^{20}$ +30.4 (*c* 1.1, $(CH_3)_2CO$); $^1$H NMR (300 MHz, $(CD_3)_2CO$, 20 °C): δ=7.62-7.60 (br d, *J*=6.5 Hz, 1H), 7.35-7.30 (m, 2H), 7.04-6.98 (m, 3H), 4.65-4.60 (m, 1H), 4.55 (s, 2H), 4.06-

4.00 (dd, *J*=4.1, 11.1 Hz, 1H), 3.95-3.90 ppm (dd, *J*=3.6, 11.1 Hz, 1H); $^{13}$C (75 MHz, $(CD_3)_2CO$, 20 °C): δ=171.7, 168.6, 158.7, 130.5 (2C), 122.5, 115.7 (2C), 68.0, 62.7, 55.0 ppm; IR: ν=3393-3060, 2754-2469, 1731, 1643, 1539, 1495 cm$^{-1}$; MS (ESI) *m/z* (%): 262 (100) $[M + Na]^+$, 240 (38) $[M + H]^+$, 222 (52) $[M + H - H_2O]^+$, HRMS (CI): calcd. for $C_{11}H_{14}NO_5$ $[M + H]^+$ 240.08720, found 240.08649.

*(2S)-N-(benzyloxy)-3-hydroxy-2-(2-phenoxyacetamido)propanamide* (**7**).
A solution of *N*,*N*-dicyclohexylcarbodiimide (DCC) (2.72 g, 13.17 mmol) in THF (10 mL) was added dropwise, at 0 °C, into a well-stirred solution of **6** (3.00 g, 12.54 mmol) and *O*-(phenylmethyl)hydroxylamine (1.46 mL, 12.54 mmol) in THF (120 mL). The reaction mixture was stirred for 1 h at 0 °C and overnight at room temperature. The obtained white precipitate (DCU) was separated by filtration and the resulting clear reaction mixture was concentrated under reduced pressure. After addition of $Et_2O$ (100 mL), the precipitate was filtered, washed with $Et_2O$ and dried under reduced pressure to provide **7** as a white solid (3.76 g, 87%). $R_f$=0.30 ($CH_2Cl_2$/MeOH 95/5); m.p. 145.0-145.7 °C; $[\alpha]_D^{20}$ -1.5 (*c* 1.0, $(CH_3)_2SO$); $^1$H NMR (300 MHz, $(CD_3)_2SO$, 20 °C): δ=11.33 (br s, 1H), 8.01 (br d, *J*=7.9 Hz, 1H), 7.39-7.28 (m, 7H), 6.99-6.95 (m, 3H), 5.08 (br s, 1H), 4.78 (s, 2H), 4.55 (s, 2H), 4.23-4.29 (m, 1H), 3.59 ppm (br d, *J*=5.5 Hz, 2H); $^{13}$C (75 MHz, $(CD_3)_2SO$, 20 °C): δ=167.6, 166.7, 152.7, 135.8, 129.5 (2C), 128.9 (2C), 128.3 (3C), 121.2, 114.7 (2C), 76.9, 66.6, 61.4, 52.8 ppm; IR: ν=3313-2999, 1650, 1556, 1499 cm$^{-1}$; MS (ESI) *m/z* (%): 367 (100) $[M + Na]^+$, 345 (30) $[M + H]^+$, 222 (12) $[M + H - NH_2OBn]^+$; HRMS (CI): calcd. for $C_{18}H_{21}N_2O_5$ $[M + H]^+$ 345.14505, found 345.14649.

*N-[(3S)-1-(benzyloxy)-2-oxoazetidin-3-yl]-2-phenoxyacetamide* (**8**).

A solution of $PPh_3$ (2.09 g, 7.98 mmol) in dry MeCN (35 mL) was added dropwise, at 0 °C and under Ar atmosphere, to a stirred solution of **7** (2.50 g, 7.26 mmol) in dry $CH_3CN$ (20 mL), containing $CCl_4$ (0.77 mL, 7.98 mmol) and anhydrous triethylamine (1.52 mL, 10.89 mmol). The resultant reaction mixture was stirred for 2 h at 0 °C and overnight at room temperature. After completion of the reaction, the obtained white precipitate ($OPPh_3$) was separated by filtration and the resulting clear reaction mixture concentrated under reduced pressure. The residue was dissolved with EtOAc (50 mL), washed with a saturated $NH_4Cl$ solution (2x40 mL) and brine (40 mL). After drying over $MgSO_4$ and removing the solvent under reduced pressure, the residue was purified by flash column chromatography (hexane/EtOAc 1/1), to provide **8** as a white solid (1.51 g, 64%). $R_f$=0.41 (hexane/EtOAc 4/6); m.p. 138.8-139.4 °C; $[\alpha]_D^{20}$ -6.2 (*c* 1.0, $(CH_3)_2CO$); $^1H$ NMR (300 MHz, $(CD_3)_2CO$, 20 °C): δ=8.19 (br d, *J*=7.0 Hz, 1H), 7.49-7.28 (m, 7H), 7.01-6.96 (m, 3H), 4.98 (s, 2H), 4.91-4.85 (m, 1H), 4.53 (br d, *J*=1.4 Hz, 2H), 3.72-3.69 (m, 1H), 3.53 ppm (dd, *J*=2.4, 4.3 Hz, 1H); $^{13}C$ (75 MHz, $(CD_3)_2CO$, 20 °C): δ 169.1, 163.4, 158.7, 136.5, 130.4 (2C), 130.0 (2C), 129.5, 129.3 (2C), 122.4, 115.6 (2C), 77.9, 67.9, 52.6, 52.4 ppm; IR: ν=3363-3193, 1776, 1677, 1598, 1531, 1495 $cm^{-1}$; MS (ESI) *m/z* (%): 365 (8) $[M + K]^+$, 349 (100) $[M + Na]^+$, 327 (10) $[M + H]^+$; HRMS (ESI): calcd. for $C_{18}H_{18}N_2O_4Na$ $[M + Na]^+$ 349.1164, found 349.1151.

*N-[(3S)-2-oxoazetidin-3-yl]-2-phenoxyacetamide* (**9**).

Compound **8** (1.00 g, 3.06 mmol) dissolved in methanol (18 mL) and EtOAc (18 mL) was placed under $H_2$ (1 atm) at rt in the presence of Raney-Ni (50% in water) catalyst for 12 h. Then the mixture was filtered through a pad of Celite and concentrated under reduced pressure to provide **9** as a white solid

(0.67 g, 100%), which was used without further purification. $R_f$=0.42 (EtOAc/MeOH 95/5); m.p. 155.7-156.6 °C; $[\alpha]_D^{20}$ -19.1 (*c* 1.0, $CH_3OH$); $^1H$ NMR (500 MHz, $CD_3OD$, 20 °C): δ=7.32-7.28 (m, 2H), 7.01-6.97 (m, 3H), 5.04 (dd, *J*=2.7, 5.4 Hz, 1H), 4.54 (br d, *J*=1.2 Hz, 2H), 3.58-3.56 (m, 1H), 3.39 ppm (dd, *J*=2.6, 5.5 Hz, 1H); $^{13}C$ (125 MHz, $CD_3OD$, 20 °C): δ=171.5, 170.8, 159.2, 130.6 (2C), 122.9, 115.9 (2C), 68.1, 57.8, 44.1 ppm; IR: ν=3281-3020, 1776, 1703, 1664, 1628, 1556, 1498 $cm^{-1}$; MS (ESI) *m/z* (%): 243 (100) $[M + Na]^+$; HRMS (CI): calcd. for $C_{11}H_{13}N_2O_3$ $[M + H]^+$ 221.09262, found 221.09253.

*Bis-alkyl precursor* (**10d**).

Prepared by the same procedure as described for **2d**. Yield: 30%; $R_f$=0.47 (hexane/EtOAc 1/1); $[\alpha]_D^{20}$ +3.1 (*c* 1.0, $CHCl_3$); $^1H$ NMR (500 MHz, $C_2D_2Cl_4$, 20 °C): δ=7.33 (t, *J*=7.7 Hz, 2H), 7.03 (t, *J*=7.3 Hz, 1H), 6.93 (br d, *J*=8.0 Hz, 2H), 5.84-5.75 (m, 2H), 5.12-4.95 (m, 4H + 0.3H, rotamer), 4.76-4.62 (m, 2H + 0.7H, rotamer), 3.53-3.10 (m, 6H), 2.07-2.03 (m, 4H), 1.71-1.52 (m, 4H), 1.44-1.25 ppm (m, 8H); $^{13}C$ (125 MHz, $C_2D_2Cl_4$, 90 °C): δ=167.9, 165.1, 157.9, 138.3, 129.4, 121.7, 114.8, 114.4, 67.6, 62.9, 46.8, 41.9, 33.2, 28.3, 28.2, 27.1, 26.3, 26.1 ppm; IR: ν=3003-2854, 1748, 1668, 1599, 1587, 1497 $cm^{-1}$; MS (ESI) *m/z* (%): 435 (100) $[M + Na]^+$, 413 (6) $[M + H]^+$, 288 (10); HRMS (ESI): calcd. for $C_{25}H_{36}N_2O_3Na$ $[M + Na]^+$ 435.2624, found 435.2625.

*N-[(3S)-2-oxo-1-(prop-2-en-1-yl)azetidin-3-yl]-2-phenoxy-N-(prop-2-en-1-yl)acetamide* (**10a**).

Prepared by the same procedure as described for **2d**. Yield: 55%; $R_f$=0.39 (hexane/EtOAc 3/7); $[\alpha]_D^{20}$ -16.9 (*c* 1.3, $CHCl_3$); $^1H$ NMR (300 MHz,

$(CD_3)_2CO$, 20 °C): δ=7.27 (t, *J*=7.9 Hz, 2H), 6.97-6.92 (m, 3H), 5.89-5.76 (m, 2H), 5.43-4.76 (m, 7H), 4.41-4.00 (m, 2H), 3.89-3.74 (m, 2H), 3.64 and 3.46 ppm (2 br s, 2H, rotamers); $^{13}C$ (75 MHz, $CDCl_3$, 20 °C): δ=168.7, 165.9, 157.9, 133.2, 131.4, 129.7, 121.8, 119.5, 118.9, 118.0, 117.5, 114.7, 68.1, 67.1, 63.7, 62.9, 50.0, 46.9, 46.5, 45.9, 44.6 ppm; IR: ν=2908-3068, 1751, 1734, 1672, 1599, 1589, 1495 $cm^{-1}$; MS (ESI) *m/z* (%): 323 (100) $[M + Na]^+$; HRMS (ESI): calcd. for $C_{17}H_{20}N_2O_3Na$ $[M + Na]^+$ 323.1372, found 323.1631.

*N-[(3S)-2-oxo-1-(pent-4-en-1-yl)azetidin-3-yl]-N-(pent-4-en-1-yl)-2-phenoxyacetamide* (**10b**).

Prepared by the same procedure as described for **2d**. Yield: 22%; $R_f$=0.32 (hexane/EtOAc 1/1); $[\alpha]_D^{20}$ +2.8 (*c* 1.1, $CHCl_3$); $^1H$ NMR (300 MHz, $CDCl_3$, 20 °C): δ=7.32-7.27 (m, 2H), 7.02-6.92 (m, 3H), 5.85-5.70 (m, 2H), 5.23 (br s, 0.3H, rotamer), 5.07-4.94 (m, 4H), 4.81-4.61 (m, 2H + 0.7H, rotamer), 3.56-3.13 (m, 6H), 2.16-1.99 (m, 4H), 1.85-1.61 ppm (m, 4H); $^{13}C$ (125 MHz, $CD_2Cl_2$, 20 °C): δ=168.2, 166.0, 158.4, 138.2, 137.9, 137.5, 129.9, 122.0, 121.8, 115.9, 115.7, 115.4, 115.1, 114.9, 68.2, 67.1, 63.7, 63.2, 49.2, 47.7, 47.5, 46.4, 44.2, 41.5, 34.3, 31.5, 31.3, 31.0, 29.3, 27.6, 27.0, 26.0, 25.4 ppm; IR: ν=3072-2850, 1751, 1661, 1599, 1587, 1495 $cm^{-1}$; MS (ESI) *m/z* (%): 379 (100) $[M + Na]^+$, 260 (18); HRMS (ESI): calcd. for $C_{21}H_{28}N_2O_3Na$ $[M + Na]^+$ 379.1998, found 379.2002.

*N-(hex-5-en-1-yl)-N-[(3S)-1-(hex-5-en-1-yl)-2-oxoazetidin-3-yl]-2-phenoxyacetamide* (**10c**).

Prepared by the same procedure as described for **2d**. Yield: 43%; $R_f$=0.52 (hexane/EtOAc 1/1); $[\alpha]_D^{20}$ +3.7 (*c* 1.7, $CHCl_3$); $^1H$ NMR (300 MHz,

$CD_2Cl_2$, 20 °C): δ=7.32-7.28 (m, 2H), 6.99 (t, *J*=7.3 Hz, 1H), 6.91 (br d, *J*=8.3 Hz, 2H), 5.85-5.76 (m, 2H), 5.15 (br s, 0.4H, rotamer), 5.04-4.93 (m, 4H), 4.76-4.63 (m, 2H + 0.6H, rotamer), 3.53-3.12 (m, 6H), 2.11-2.02 (m, 4H), 1.72-1.52 (m, 4H), 1.46-1.32 ppm (m, 4H); $^{13}C$ (75 MHz, $CDCl_3$, 20 °C): δ=168.3, 168.1, 165.8, 165.3, 158.0, 157.5, 138.5, 138.3, 138.0, 129.8, 129.7, 121.9, 121.8, 115.3, 115.1, 114.7, 114.5, 68.3, 67.3, 63.7, 62.8, 49.1, 48.0, 47.5, 46.7, 44.5, 41.8, 34.0, 33.3, 29.6, 27.9, 26.9, 26.5, 26.3, 26.0, 25.7, 25.0 ppm; IR: ν=3074-2856, 1751, 1666, 1599, 1589, 1497 $cm^{-1}$; MS (ESI) *m/z* (%): 791 (67) $[2M + Na]^+$, 407 (100) $[M + Na]^+$, 274 (66); HRMS (ESI): calcd. for $C_{23}H_{32}N_2O_3Na$ $[M + Na]^+$ 407.2311, found 407.2315.

*Unsaturated bicycle* (**11d**).

Prepared by the same procedure as described for **3d**. Yield: 67%; $R_f$=0.42 (hexane/EtOAc 3/7); m.p. 86.7-87.3 °C; $[\alpha]_D^{20}$ -2.8 (*c* 1.9, $CHCl_3$); $^1H$ NMR (500 MHz, $C_2D_2Cl_4$, 20 °C): δ=7.34-7.30 (m, 2H), 7.02 (t, *J*=7.3 Hz, 1H), 6.93-6.91 (m, 2H), 5.84-5.74 (m, 0.4H, rotamer), 5.37-5.16 (m, 2H + 0.6H, rotamer), 4.79-4.62 (m, 2H), 3.72-3.66 (m, 1H), 3.55-3.08 (m, 4H), 2.88-2.66 (m, 1H), 2.16-1.85 (m, 4H), 1.73-1.19 ppm (m, 12H); $^{13}C$ (125 MHz, $C_2D_2Cl_4$, 120 °C): δ=167.8, 165.5, 158.0, 131.8, 131.1, 130.3, 130.1, 129.4, 121.7, 115.0, 67.9, 62.3, 49.1, 47.1, 46.7, 45.2, 44.2, 41.8, 33.7, 31.7, 31.5, 31.3, 30.5, 28.4, 28.2, 28.0, 27.8, 27.4, 27.2, 27.1, 26.5, 26.1, 25.5, 25.2, 24.6 ppm; IR: ν=3003-2853, 1740, 1664, 1497 $cm^{-1}$; MS (ESI) *m/z* (%): 407 (100) $[M + Na]^+$, 385 (89) $[M + H]^+$, 357 (21) $[M + H - CO]^+$; HRMS (ESI): calcd. for $C_{23}H_{32}N_2O_3Na$ $[M + Na]^+$ 407.2311, found 407.2322.

*(1S)-10-(2-phenoxyacetyl)-1,10-diazabicyclo[9.1.1]tridec-5-en-12-one* (**11b**).

Prepared by the same procedure as described for **3d**. Yield: 59%; $R_f$=0.47 (hexane/EtOAc 1/1); m.p. 127.7-128.4 °C; $[\alpha]_D^{20}$ -6.9 (*c* 1.8, $CHCl_3$); $^1$H NMR (300 MHz, $CDCl_3$, 20 °C): δ=7.33-7.26 (m, 2H), 7.01-6.89 (m, 3H), 5.87-5.80 (m, 0.5H, rotamer), 5.65-5.35 (m, 2H), 5.25-5.18 (m, 0.5H, rotamer), 4.81-4.59 (m, 2H), 3.90-2.83 (m, 6H), 2.46-1.36 ppm (m, 8H); $^{13}$C (75 MHz, $CDCl_3$, 20 °C): δ=168.3, 168.0, 165.7, 165.1, 158.1, 157.4, 133.1, 132.6, 129.7, 129.6, 129.3, 128.8, 121.9, 121.7, 114.8, 114.5, 68.0, 66.5, 64.1, 63.6, 60.1, 46.1, 45.7, 45.6, 43.5, 43.4, 40.9, 40.7, 32.8, 32.7, 31.9, 29.1, 28.9, 27.3, 26.1, 25.8 ppm; IR: ν=3001-2927, 1740, 1670, 1434 $cm^{-1}$; MS (ESI) *m/z* (%): 351 (100) $[M + Na]^+$, 329 (64) $[M + H]^+$, 301 (8) $[M + H - CO]^+$; HRMS (ESI): calcd. for $C_{19}H_{24}N_2O_3Na$ $[M + Na]^+$ 351.1685, found 351.1676.

*(1S)-12-(2-phenoxyacetyl)-1,12-diazabicyclo[11.1.1]pentadec-6-en-14-one* (**11c**).

Prepared by the same procedure as described for **3d**. Yield: 47%; $R_f$=0.47 (hexane/EtOAc 3/7); $[\alpha]_D^{20}$ -4.2 (*c* 1.9, $CHCl_3$); $^1$H NMR (300 MHz, $CDCl_3$, 20 °C, TMS): δ=7.32-7.25 (m, 2H), 7.03-6.89 (m, 3H), 5.65-5.20 (m, 3H), 4.83-4.60 (m, 2H), 3.85-3.10 (m, 5H), 2.90-2.65 (m, 1H), 2.32-1.28 ppm (m, 12H); $^{13}$C (75 MHz, $CDCl_3$, 20 °C): δ=168.2, 168.0, 165.2, 165.1, 158.0, 157.5, 132.3, 131.7, 131.2, 130.9, 129.8, 129.7, 121.9, 121.8, 114.7, 114.5, 68.3, 67.1, 63.4, 61.2, 50.2, 49.2, 46.8, 46.4, 46.0, 43.9, 42.0, 41.7, 31.5, 31.2, 30.4, 29.8, 29.1, 28.9, 26.8, 26.5, 25.8, 25.3 ppm; IR: ν=2856-3005, 1740, 1724, 1670, 1599, 1497 $cm^{-1}$; MS (ESI) *m/z* (%): 379 (46) $[M + Na]^+$,

357 (100) $[M + H]^+$, 329 (19) $[M + H - CO]^+$; HRMS (ESI): calcd. for $C_{21}H_{28}N_2O_3Na$ $[M + Na]^+$ 379.1998, found 379.1987.

*Saturated bicycle* (**12d**).

Prepared by the same procedure as described for **4d**. Yield: 93%; $R_f$=0.33 (hexane/EtOAc 1/1); m.p. 85.2-85.7 °C; $[\alpha]_D^{20}$ -1.0 (*c* 1.7, $CHCl_3$); $^1$H NMR (500 MHz, $C_2D_2Cl_4$, 120 °C): δ=7.40-7.36 (m, 2H), 7.10-7.03 (m, 3H), 5.46 (br s, 1H), 4.83-4.74 (m, 2H), 4.05 (br s, 0.4H, rotamer), 3.81-3.75 (m, 1H), 3.60-3.50 (m, 3H + 0.6H, rotamer), 3.38-3.36 (m, 1H), 2.93-2.89 (m, 1H), 2.03-1.47 ppm (m, 19H); $^{13}$C (125 MHz, $C_2D_2Cl_4$, 120 °C): δ=167.8, 165.3, 158.0, 129.3, 121.7, 115.0, 67.9, 62.2, 49.1, 47.7, 45.0, 42.1, 33.7, 28.8, 27.7, 27.0, 26.9, 26.8, 26.3, 26.2, 26.1, 25.6, 25.5, 24.6 ppm; IR: ν=3028-2856, 1740, 1662, 1437 cm$^{-1}$; MS (ESI) *m/z* (%): 409 (100) $[M + Na]^+$, 387 (25) $[M + H]^+$, 359 (7) $[M + H - CO]^+$; HRMS (ESI): calcd. for $C_{23}H_{34}N_2O_3Na$ $[M + Na]^+$ 409.2467, found 409.2439.

*(11S)-10-(2-phenoxyacetyl)-1,10-diazabicyclo[9.1.1]tridecan-12-one* (**12b**).

Prepared by the same procedure as described for **4d**. Yield: 90%; $R_f$=0.36 (hexane/EtOAc 3/7); m.p. 132.1-132.8 °C; $[\alpha]_D^{20}$ -3.4 (*c* 1.8, $CHCl_3$); $^1$H NMR (300 MHz, $CDCl_3$, 20 °C): δ=7.33-7.26 (m, 2H), 7.02-6.90 (m, 3H), 5.70-5.69 (m, 0.5H, rotamer), 5.24-5.20 (m, 0.5H, rotamer), 4.83-4.60 (m, 2H), 3.75-3.31 (m, 5H), 2.88-2.79 (m, 1H), 1.95-1.32 ppm (m, 12H); $^{13}$C (75 MHz, $CDCl_3$, 20 °C): δ=168.4, 168.2, 166.2, 165.6, 158.1, 157.6, 129.8, 129.7, 121.9, 121.8, 114.8, 114.5, 68.2, 66.9, 63.8, 61.1, 48.1, 48.0, 43.1, 41.4, 27.2, 26.5, 25.8, 24.8, 24.5, 24.3, 24.1, 24.0, 23.8, 23.3, 23.1 ppm; IR: ν=2927-2858, 1743, 1668, 1599, 1495 cm$^{-1}$; MS (ESI) *m/z* (%): 353 (57) [M

+ Na]$^+$, 331 (100) [M + H]$^+$; HRMS (ESI): calcd. for $C_{19}H_{26}N_2O_3Na$ [M + Na]$^+$ 353.1841, found 353.1832.

*(13S)-12-(2-phenoxyacetyl)-1,12-diazabicyclo[11.1.1]pentadecan-14-one* (**12c**).

Prepared by the same procedure as described for **4d**. Yield: 91%; $R_f$=0.57 (hexane/EtOAc 3/7); m.p. 94.7-95.3 °C; $[\alpha]_D^{20}$ -2.1 (*c* 2.4, $CHCl_3$); $^1$H NMR (300 MHz, $CDCl_3$, 20 °C): δ=7.33-7.24 (m, 2H), 7.02-6.89 (m, 3H), 5.77-5.75 (m, 0.4H, rotamer), 5.31-5.26 (m, 0.6H, rotamer), 4.83-4.60 (m, 2H), 3.79-3.19 (m, 5H), 2.85-2.77 (m, 1H), 1.92-1.26 ppm (m, 16H); $^{13}$C (75 MHz, $CDCl_3$, 20 °C): δ=168.5, 168.1, 166.3, 166.1, 158.1, 157.5, 129.8, 129.7, 121.9, 121.8, 114.8, 114.5, 68.4, 66.7, 63.8, 60.7, 48.1, 47.5, 44.9, 43.9, 41.8, 41.7, 28.0, 27.0, 25.6, 25.5, 25.4, 25.3, 25.0, 24.8, 24.7, 24.4, 24.2, 23.9 ppm; IR: ν=3011-2858, 1736, 1670, 1599, 1495 cm$^{-1}$; MS (ESI) *m/z* (%): 381 (38) [M + Na]$^+$, 359 (100) [M + H]$^+$, 331 (13) [M + H - CO]$^+$; HRMS (ESI): calcd. for $C_{21}H_{30}N_2O_3Na$ [M + Na]$^+$ 381.2154, found 381.2141.

**Computational chemistry**. All the calculations have been performed with the Gaussian 03 suite of programs.[17] The geometry is optimized by analytical gradient energy minimization. The nature of the located extrema is defined by the inertia of the energy second derivative (Hessian matrix). For the minima, all the eigenvalues are positive; in the case of a first order saddle point as the TS structures, the first eigenvalue is negative and is associated to the imaginary frequency. In the studied models, the related eigenvector components are the geometric variables involved in the H transfer in the pseudo 8 membered ring.

All absolute energies of the precursors, unsaturated bicycles, saturated bicycles, and all the absolute energies of the transition state structures in the simple model, **Figure 5**, computed for the unsaturated bicycles and saturated bicycles in the selected conformations can be found in Supporting Information (p281).

**Assay with resistant PBPs**. Purified PBP5 from *Enterococcus faecium* D63r and PBP2a from methicillin-resistant *Staphylococcus aureus* ATCC 43300 were used as target proteins to test inhibitory activity of synthesized β-lactams. Each of the purified PBPs (2.5 μM) were first incubated with 1 mM potential inhibitor in 100 mM phosphate buffer, 0.01% Triton X-100,[18] pH 7, for 4 h at 30 °C. Then, 25 μM fluorescein-labeled ampicillin[19] was added to detect the residual penicillin binding activity (RA). The samples were further incubated for 30 min at 37 °C in a total volume of 20 μL. Denaturation buffer was added (0.1 M Tris/HCl, pH 6.8, containing 25% glycerol, 2% SDS, 20% β-mercaptoethanol and 0.02% bromophenol blue) and the samples were heated to 100 °C for 1 min. The samples were then loaded onto a 10% SDS-acrylamide gel (10 x 7 cm) and electrophoresis was performed for 45 min at 180 V (12 mA). Detection and quantification of the RAs were done with Molecular Image FX equipment and Quantity One software (BioRad, Hercules, CA, USA). Three independent experiments were carried out for each inhibitor.

**Assay with R39**. All assays with R39 have been done in microtiter plates 96-wells (Brand, Wertheim, Germany). 20 mM of the tested compounds have been solved in DMF. Finally 7.5 μL of the solution have been used in the assay. The final concentration of the compounds in the assays was 100 μM. The final concentration of DMF in the assays was 0.25%. R39 (3.5 nM)

was incubated in the presence of the potential inhibitors in 10 mM sodium phosphate buffer (pH 7.2) with 100 mM NaCl, 100 mM D-alanine, 0.01 mg/ml BSA and 0.01% Triton for 60 min at 25 °C. This preincubation was realized, in order to detect also slow binding inhibitors. After the preincubation the residual activity RA of R39 was determined by observing the hydrolysis of the thioester S2d substrate, in the presence of DTNB, catalyzed by the non-inhibited enzyme. The initial rate of hydrolysis of 1 mM S2d in the presence of 1 mM DTNB was determined by monitoring the increase of absorbance at 412 nm (DTNB: $\varepsilon[\Delta\varepsilon] = 13600\ M^{-1}\ s^{-1}$) using a microplate absorbance reader (Power Wave X, Biotek Instruments, Winooski, U.S.A.). The rate of spontaneous hydrolysis of S2d in the presence of the inhibitors was also determined in absence of R39. All assays have been done three times. The determination of RA of R39 in absence of inhibitors has been done six times on each plate. In order to detect false positives which could be slow binding non-competitive promiscuous inhibitors, the assays have been done in the presence of 0.01% Triton-X-100.[20]

## 5. Acknowledgements

This work was supported by the Interuniversity Attraction Pole (IAP P6/19 PROFUSA), F.R.S.-FNRS, UCL and ULg (computational facilities). G. D. and J. M.-B. are senior research associates of the F.R.S.-FNRS (Belgium). Dr. Astrid Zervosen is acknowledged for the R39 testing and Dr. Ana Amoroso and Olivier Verlaine for the PBP2a and PBP5 testing. Ir. Raoul Rozenberg and Dr. Cécile Le Duff have contributed to the structural analysis.

## 6. Supporting Information

Additionally to structural data for compounds **2a**-**c**, **2e**-**f**, **3b**-**c**, **3e**-**f**, **4b**-**c**, **4e**-**f**, **10a**-**c**, **11b**-**c**, **12b**-**c**, the Supporting Information includes NMR spectra of all new compounds, the figures of Pen in the third model with hydrogen atoms and hydrogen bonds and stereo view of the third model with Pen, the absolute energies of the precursors, unsaturated bicycles and saturated bicycles in the selected conformations, the absolute energies of the transition state structures in the simple model (**Figure 5**) computed for the unsaturated bicycles and saturated bicycles in the selected conformations, and $^{13}C$ NMR spectra of compounds **10d** and **11d** recorded at 125 MHz in 1,1,2,2-tetrachloroethane-$d_2$ at different temperatures.

Relevant material of the Supporting Information is added below, *i.e.* the figures of Pen in the third model with hydrogen atoms and hydrogen bonds and stereo view of the third model with Pen, the absolute energies of the precursors, unsaturated bicycles and saturated bicycles in the selected conformations, the absolute energies of the transition state structures in the simple model (**Figure 5**) computed for the unsaturated bicycles and saturated bicycles in the selected conformations, and $^{13}C$ NMR spectra of compounds **10d** and **11d** recorded at 125 MHz in 1,1,2,2-tetrachloroethane-$d_2$ at different temperatures.

### 6.1. Stereo view of the third model with Pen

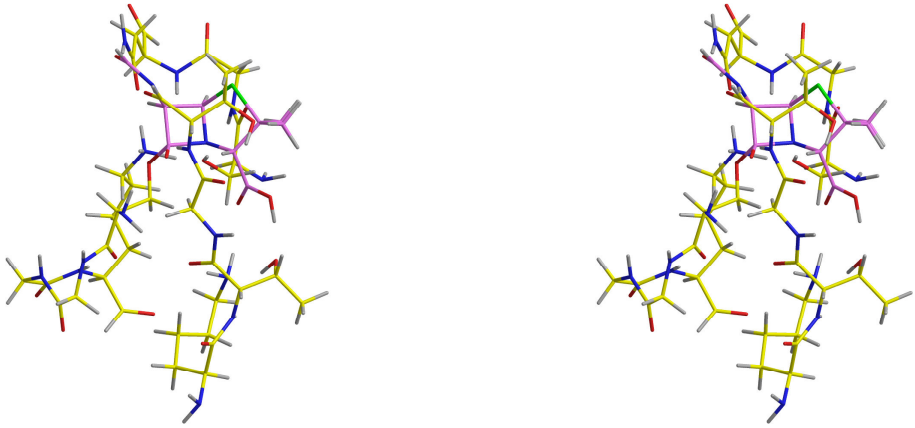

**Figure 9**

Legend: C of Pen are purple, others in yellow, H are in grey, O in red, N in blue.

### 6.2. Pen in the third model with hydrogen atoms and hydrogen bonds

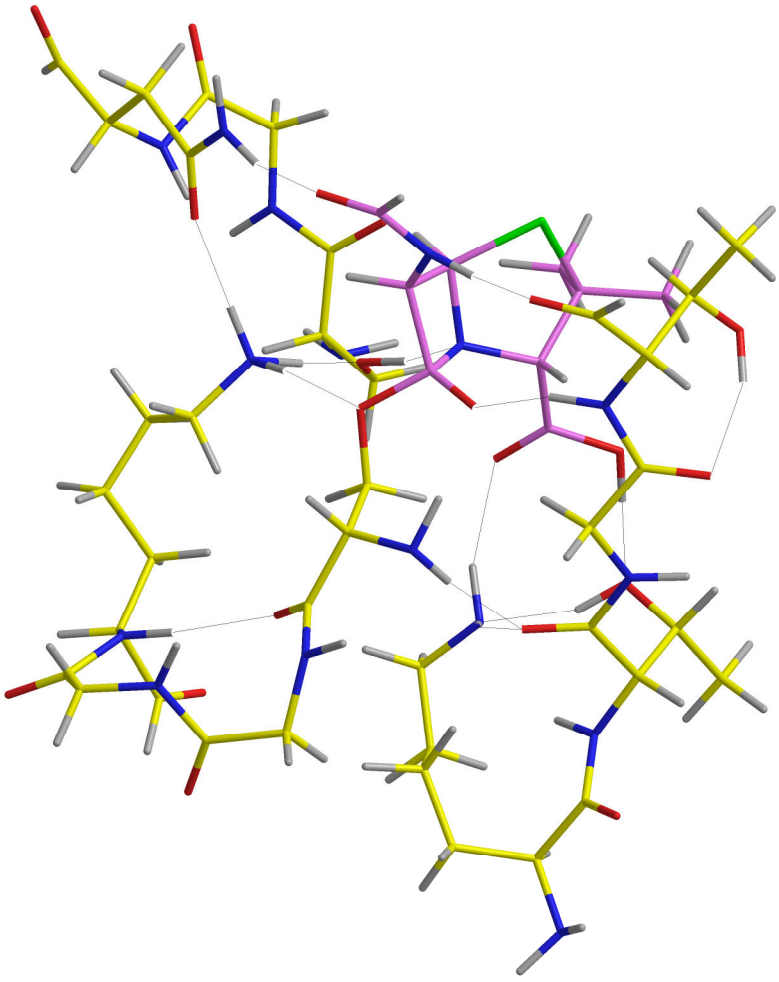

**Figure 10**

Legend: C of Pen are purple, others in yellow, H are in grey, O in red, N in blue.

## 6.3. Absolute energies of the precursors, unsaturated bicycles and saturated bicycles in the selected conformations

**Table 4**

| Precursor | Unsaturated Bicycle | Geometry | Absolute Energy of Precursors (a.u.) | |
|---|---|---|---|---|
| | | | *i* | *ii* |
| **2b** | **3b** | a | -1025.41459608 | |
| | | b | -1025.41680594 | |
| **2c** | **3c** | a | -1102.95781219 | -1102.96054731 |
| | | b | -1102.95779563 | -1102.96124697 |
| **2d** | **3d** | a | -1180.50332292 | -1180.50652038 |
| | | b | -1180.50322571 | -1180.50802245 |
| **2e** | **3e** | a | -1258.05108883 | -1258.05112969 |
| | | b | -1258.05107656 | -1258.05578360 |
| **2f** | **3f** | a | -1413.14432534 | |
| | | b | -1413.14433688 | |
| **10b** | **11b** | a | -1137.00780866 | |
| | | b | -1137.00797131 | |
| **10c** | **11c** | a | -1214.55193630 | -1214.55434404 |
| | | b | -1214.55110676 | -1214.55586836 |
| **10d** | **11d** | a | -1292.09683293 | -1292.09882421 |
| | | b | -1292.09730802 | -1292.10286951 |

**Table 4** (continued)

| Precursor | Unsaturated Bicycle | Geometry | Absolute Energy of Unsaturated Bicycles (a.u.) | |
|---|---|---|---|---|
| | | | *i* | *ii* |
| **2b** | **3b** | a | -947.917540781 | |
| | | b | -947.918039747 | |
| **2c** | **3c** | a | -1025.46216311 | -1025.46622074 |
| | | b | -1025.46152842 | -1025.46668293 |
| **2d** | **3d** | a | -1103.00347057 | -1103.00771074 |
| | | b | -1103.00463621 | -1103.00742688 |
| **2e** | **3e** | a | -1180.54613861 | -1180.55861844 |
| | | b | -1180.54641176 | -1180.55819032 |
| **2f** | **3f** | a | -1335.64866302 | |
| | | b | -1335.64918136 | |
| **10b** | **11b** | a | -1059.51087693 | |
| | | b | -1059.50995858 | |
| **10c** | **11c** | a | -1137.05863676 | -1137.05986889 |
| | | b | -1137.06163515 | -1137.06128715 |
| **10d** | **11d** | a | -1214.59755676 | -1214.59877554 |
| | | b | -1214.59827603 | -1214.59985976 |

**Table 4** (continued)

| Saturated Bicycle | Geometry | Absolute Energy of Saturated Bicycles (a.u.) | |
|---|---|---|---|
| | | *i* | *ii* |
| **4b** | a | -949.118167603 | |
| | b | -949.118473279 | |
| **4c** | a | -1026.66576579 | -1026.66964604 |
| | b | -1026.66560999 | -1026.66993933 |
| **4d** | a | -1104.20406865 | -1104.21268925 |
| | b | -1104.20444900 | -1104.21269400 |
| **4e** | a | -1181.75298536 | -1181.75770921 |
| | b | -1181.75345343 | -1181.75718892 |
| **4f** | a | -1336.84956815 | |
| | b | -1336.85012875 | |
| **12b** | a | -1060.71230229 | |
| | b | -1060.71057616 | |
| **12c** | a | -1138.26197438 | -1138.26430158 |
| | b | -1138.26269730 | -1138.26337318 |
| **12d** | a | -1215.79681594 | -1215.79955742 |
| | b | -1215.79749965 | -1215.80114833 |

### 6.4. Absolute energies of the transition state structures in the simple model (Figure 5) computed for the unsaturated bicycles and saturated bicycles in the selected conformations

**Table 5**

| Unsaturated Bicycle | Saturated Bicycle | Geometry | Absolute Energy of Transition State of Unsaturated Bicycles (a.u.) | |
|---|---|---|---|---|
| | | | *i* | *ii* |
| **3b** | **4b** | a | -1476.31616831 | |
| | | b | -1476.31775785 | |
| **3c** | **4c** | a | -1553.86887196 | -1553.86922442 |
| | | b | -1553.87125985 | -1553.87272150 |
| **3d** | **4d** | a | -1631.41638151 | -1631.41811686 |
| | | b | -1631.42080250 | -1631.41770045 |
| **3e** | **4e** | a | -1708.95595438 | -1708.97030995 |
| | | b | -1708.95894947 | -1708.97299114 |
| **3f** | **4f** | a | -1864.04575537 | |
| | | b | -1864.04660361 | |
| **11b** | **12b** | a | -1587.91890973 | |
| | | b | -1587.91098184 | |
| **11c** | **12c** | a | -1665.45884587 | -1665.46251502 |
| | | b | -1665.46649664 | -1665.46767432 |
| **11d** | **12d** | a | -1743.00636462 | -1743.01160133 |
| | | b | -1743.01655071 | -1743.01269207 |

**Table 5** (continued)

| Unsaturated Bicycle | Saturated Bicycle | Geometry | Absolute Energy of Transition State of Saturated Bicycles (a.u.) | |
|---|---|---|---|---|
| | | | *i* | *ii* |
| **3b** | **4b** | a | -1477.51598160 | |
| | | b | -1477.51085237 | |
| **3c** | **4c** | a | -1555.06870812 | -1555.07074802 |
| | | b | -1555.07381019 | -1555.07267871 |
| **3d** | **4d** | a | -1632.61606004 | -1632.61786417 |
| | | b | -1632.61886408 | -1632.62001218 |
| **3e** | **4e** | a | -1710.16384544 | -1710.16798503 |
| | | b | -1710.16593341 | -1710.17084346 |
| **3f** | **4f** | a | -1865.24670602 | |
| | | b | -1865.24716622 | |
| **11b** | **12b** | a | -1589.11800355 | |
| | | b | -1589.10440493 | |
| **11c** | **12c** | a | -1666.65820714 | -1666.66823219 |
| | | b | -1666.66889480 | -1666.67271153 |
| **11d** | **12d** | a | -1744.20602116 | -1744.21099469 |
| | | b | -1744.21419702 | -1744.21487699 |

### 6.5. $^{13}$C NMR spectra of compound 10d recorded at 125 MHz in 1,1,2,2-tetrachloroethane-$d_2$ at different temperatures

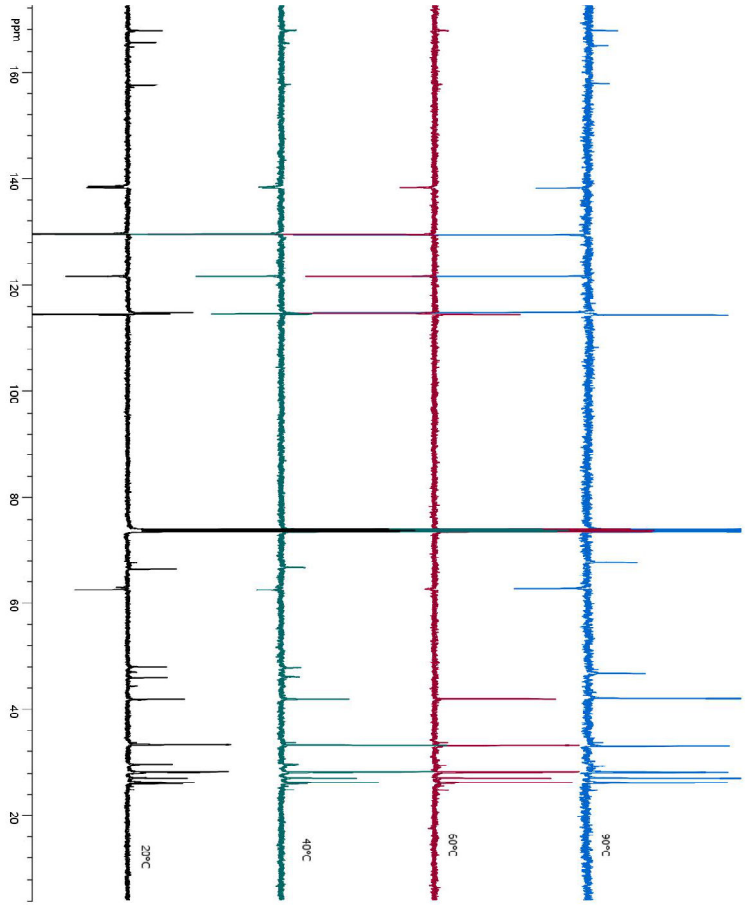


**Figure 11**

**6.6. $^{13}$C NMR spectra of compound 11d recorded at 125 MHz in 1,1,2,2-tetrachloroethane-$d_2$ at different temperatures**

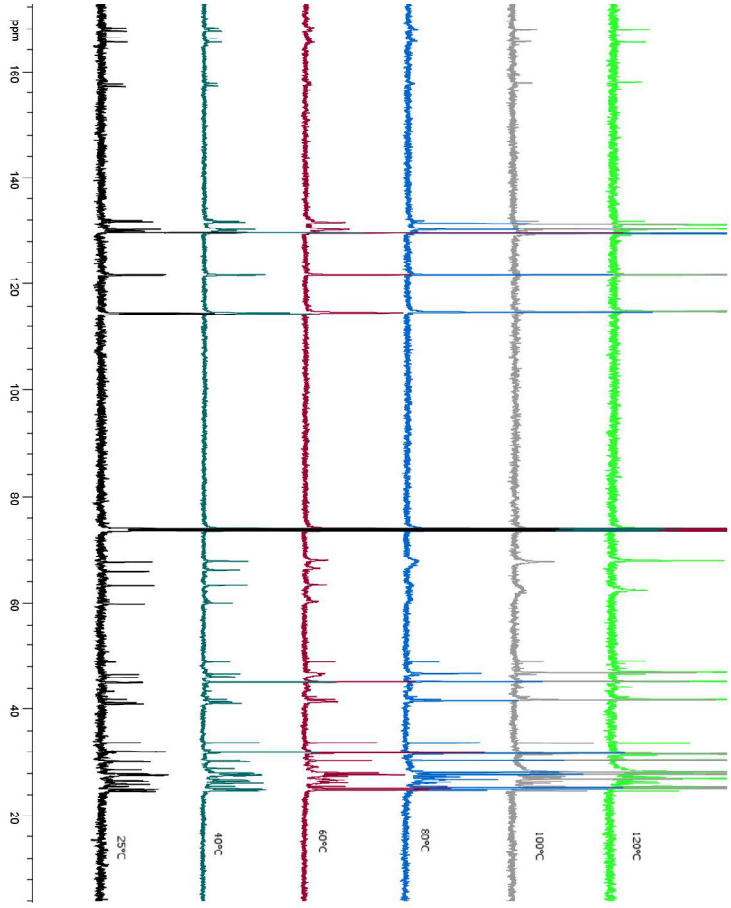


**Figure 12**

## 7. References and notes


[1] (a) Abraham, E. P.; Chain, E. *Nature* **1940**, *146*, 837; (b) Walsh, C. *Nature* **2000**, *406*, 775-781; (c) Livermore, D. M. *J. Antimicrob. Chemother.* **2009**, *64 (suppl 1)*, i29-i36; d) French, G. L. *Int. J. Antimicrob. Agents* **2010***, 36S3*, S3-S7.

[2] Hubschwerlen, C. in *Comprehensive Medicinal Chemistry*, 2nd ed. (Eds: J. B. Taylor, D. J. Triggle), Elsevier, Oxford, UK, **2007**, chapter 7.17, pp. 479-517.

[3] (a) Strominger, J. L. *Antibiotics* **1967**, *1*, 705-713; (b) Woodward, R. B. in *The Chemistry of Penicillin* (Eds. H. T. Clarke, J. R. Johnson et R. Robinson), Princeton University Press, Princeton, New Jersey, **1949**, pp. 440-454; (c) Alcaide, B.; Aragoncillo, C.; Almendros, P. in *Comprehensive Heterocyclic Chemistry III* (Ed.: C. Stevens), Elsevier, Oxford, **2008**, vol. 2, chapter 2.02, pp. 111-171; (d) Marchand-Brynaert, J.; Brulé C. in *Comprehensive Heterocyclic Chemistry III* (Ed.: C. Stevens), Elsevier, Oxford, **2008**, vol. 2, chapter 2.03, pp. 173-237.

[4] (a) Bassetti, M.; Nicolini, L.; Esposito, S.; Righi, E.; Viscoli, C. *Curr. Med. Chem.* **2009**, *16*, 564-575; (b) Llarrull, L. I.; Testero, S. A.; Fisher, J. F.; Mobashery, S. *Curr. Opin. Microbiol.* **2010**, *13*, 551-557; (c) Bassetti, M.; Ginocchio, F.; Mikulska, M. *Critical Care* **2011**, 15, 215.

[5] (a) Urbach, A.; Dive, G.; Marchand-Brynaert, J. *Eur. J. Org. Chem.* **2009**, *11*, 1757-1770; (b) Urbach, A.; Dive, G.; Tinant, B.; Duval, V.; Marchand-Brynaert, J. *Eur. J. Med. Chem.* **2009**, *44*, 2071-2080.

[6] (a) Sliwa, A.; Dive, G.; Habib Jiwan, J.-L.; Marchand-Brynaert, J. *Tetrahedron* **2010**, *66*, 9519-9527 and references therein; b) Sliwa,

A.; Marchand-Brynaert, J.; Luhmer, M. *Magn. Reson. Chem.* **2011**, in press.

[7] (a) Sauvage, E.; Herman, R.; Petrella, S.; Duez, C.; Bouillenne, F.; Frère, J.-M.; Charlier, P. *J. Biol. Chem.* **2005**, *280*, 31249-31256; (b) Sauvage, E.; Powell, A. J.; Heilemann, J.; Josephine, H. R.; Charlier, P.; Davies, C.; Pratt, R. F. *J. Mol. Biol.* **2008**, *381*, 383-393.

[8] Lim, D.; Strynadka, N. C. *Nat. Struct. Biol.* **2002**, *9*, 870-876.

[9] Sauvage, E.; Kerff, F.; Fonzé, E.; Herman, R.; Schoot, B.; Marquette, J.-P.; Taburet, Y.; Prevost, D.; Dumas, J.; Leonard, G.; Stefanic, P.; Coyette, J.; Charlier, P. *Cell. Mol. Life Sci.* **2002**, *59*, 1223-1232.

[10] Hwu, J. R.; Jain, M. L.; Tsay, S.-C.; Hakimelahi, G. H. *Tet. Lett.* **1996**, *37*, 2035-2038.

[11] Olah, G. A.; Narang, S. C.; Gupta, B. G. B.; Malhotra, R. *J. Org. Chem*. **1979**, *44*, 1247-1251.

[12] Miller, M. J.; Mattingly, P. G.; Morrison, M. A.; Kerwin, J. F., Jr. *J. Am. Chem. Soc.* **1980**, *102*, 7026-7032.

[13] (a) Tatewaki, H.; Huzinaga, S. *J. Comp. Chem.* **1980**, *1*, 205-228; (b) Dive, G.; Dehareng, D.; Ghuysen, J. M. *Theor. Chim. Acta* **1993**, *85*, 409-421.

[14] Dive, G.; Dehareng, D. *Int. J. Quant. Chem.* **1999**, *73*, 161-174.

[15] *N*-benzoyl-D-alanyl-thioglycolate (S2d). (a) Schwyzer, R.; Hurlimann, C.; Coenzyle, C. *Helv. Chim. Acta* **1954**, *37*, 155-166; (b) Adam, M.; Damblon, C.; Jamin, M.; Zorzi, W.; Dusart, V.; Galleni, M.; el Kharroubi, A.; Piras, G.; Spratt, B. G.; Keck, W.; Coyette, J.; Ghuysen, J.-M.; Nguyen-Disteche, M.; Frère, J.-M. *Biochem. J.* **1991**, *279*, 601-604.

[16] Sader, H. S.; Gales, A. C. *Drugs* **2001**, *61*, 553-564.

[17] Frisch, M. J.; Trucks, G. W.; Schlegel, H. B.; Scuseria, G. E.; Robb, M. A.; Cheeseman, J. R.; Montgomery, J. A., Jr.; Vreven, T.; Kudin, K. N.; Burant, J. C.; Millam, J. M.; Iyengar, S. S.; Tomasi, J.; Barone, V.; Mennucci, B.; Cossi, M.; Scalmani, G.; Rega, N.; Petersson, G. A.; Nakatsuji, H.; Hada, M.; Ehara, M.; Toyota, K.; Fukuda, R.; Hasegawa, J.; Ishida, M.; Nakajima, T.; Honda, Y.; Kitao, O.; Nakai, H.; Klene, M.; Li, X.; Knox, J. E.; Hratchian, H. P.; Cross, J. B.; Adamo, C.; Jaramillo, J.; Gomperts, R.; Stratmann, R. E.; Yazyev, O.; Austin, A. J.; Cammi, R.; Pomelli, C.; Ochterski, J. W.; Ayala, P. Y.; Morokuma, K.; Voth, G. A.; Salvador, P.; Dannenberg, J. J.; Zakrzewski, V. G.; Dapprich, S.; Daniels, A. D.; Strain, M. C.; Farkas, O.; Malick, D. K.; Rabuck, A. D.; Raghavachari, K.; Foresman, J. B.; Ortiz, J. V.; Cui, Q.; Baboul, A. G.; Clifford, S.; Cioslowski, J.; Stefanov, B. B.; Liu, G.; Liashenko, A.; Piskorz, P.; Komaromi, I.; Martin, R. L.; Fox, D. J.; Keith, T.; Al-Laham, M. A.; Peng, C. Y.; Nanayakkara, A.; Challacombe, M.; Gill, P. M. W.; Johnson, B.; Chen, W.; Wong, M. W.; Gonzalez, C.; Pople, J. A. *Gaussian 03*, *Revision D.02*; Gaussian: Wallingford CT, 2004.

[18] Feng, B. Y.; Shoichet, B. K. *Nat. Protoc.* **2006**, *1*, 550-553.

[19] Lakaye, B.; Damblon, C.; Jamin, M.; Galleni, M.; Lepage, S.; Joris, B.; Marchand-Brynaert, J.; Frydrych, C.; Frère, J.-M. *Biochem. J.* **1994**, *300*, 141-145.

[20] Zervosen, A.; Lu, W.-P.; Chen, Z.; White, R. E.; Demuth, T. P., Jr.; Frère, J.-M. *Antimicrob. Agents Chemother.* **2004**, *48*, 961-969.

# *Chapter 8 - Attempts to synthesize mixed precursors*

## 1. Introduction

In the last chapter, we have seen that 1,3-bridged bicyclic β-lactams from *bis*-alkylated precursors **A** were easily obtained, while the RCM reaction was not as conclusive with *bis*-acylated precursors **B** (**Figure 1**).

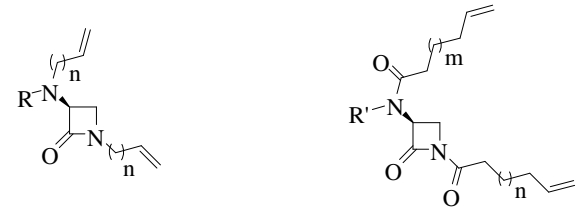

**A** **B**

R = Boc, $PhOCH_2CO$ R' = Boc, Me, H

**Figure 1**. Precursors **A** and **B**.

In the *bis*-acylated precursors **B**, due to the accumulation of amide and imide functions, the conformers leading to the desired cyclizations are strongly disfavoured. To avoid this accumulation of amide and imide functions, mixed precursors could be synthesized, *i.e.* chiral azetidin-2-ones equipped with one ω-alkenoyl chain and one ω-alkenyl chain on the positions N(1) and C(3)-N, giving precursors **C** and **D** (**Figure 2**).

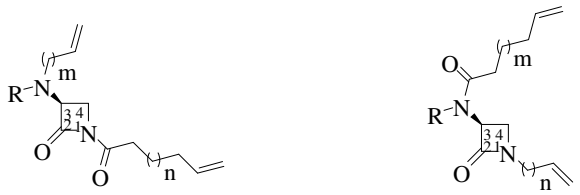

**C** R = COR', H, Me, ... **D**

**Figure 2**. Precursors **C** and **D**.

These precursors should be conformationally less constrained than precursors **B** and should probably allow the desired monocyclizations.

## 2. N(1) position acylated and C(3)-N position alkylated

Some tests have already been done to synthesize the mixed precursors. Starting from the mono acylated compound **1**, several attempts were performed to alkylate the C(3)-N position in the presence of a strong base (LiHMDS in THF, NaH in DMF, KOH in presence of $Bu_4NHSO_4$ and NaI in THF[1]). These only led to degradation of the starting material (**Scheme 1**).

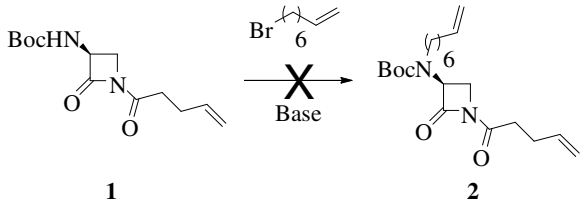


**1** **2**

**Scheme 1**. Attempts to alkylate compound **2**.

From the mono acylated compound **1**, we also tried to apply the following two-step sequence: the Boc protecting group was removed with trifluoroacetic acetic acid and then we attempted to alkylate the free amine function with 8-bromooct-1-ene to afford compound **4** (**Scheme 2**).

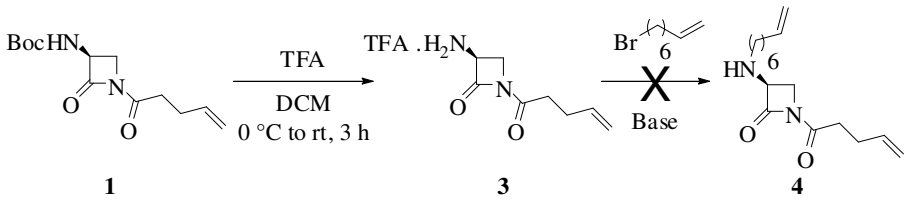


**1** **3** **4**

**Scheme 2**. Attempts to synthesize compound **4**.

Several bases were tested: TEA in DCM, $K_2CO_3$ in $CH_3CN$,[2] KOH in presence of $Bu_4NHSO_4$ and NaI in THF, $LiOH.H_2O$ with molecular sieve in DMF,[3] $CsOH.H_2O$ with molecular sieve in DMF,[4] DBU in toluene.[5] Unfortunately, all these conditions led to degradation of the β-lactam ring.

These problems of degradation could be due to two factors. In presence of a strong base, side-reactions could occur because of the enolizable character of the proton alpha to the carbonyl of the acyl chain. Another problem could be a low reactivity of the used electrophiles, and then the deprotonated carbamate or the free amine function of compounds **1** and **3** respectively could be acylated by another β-lactam compound, leading to degradation of the β-lactam ring. Enolization of H(3) leading to the opening of the four-membered ring could not be excluded too.

Allyl bromide, a more reactive ω-alkenyl bromide was tested but without success, leading to degradation of the starting material. Mitsunobu reaction was also evaluated but again without success, the starting material being predominantly recovered (**Scheme 3**).

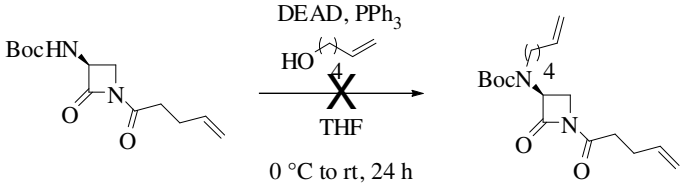


**1** **5**

**Scheme 3**. Attempt to alkylate compound **5**.

## 3. N(1) position protected

As another strategy, we tried to firstly functionalize the C(3)-N position. Therefore, we had to protect the N(1) position, and we employed a TBS protecting group.[6] Chiron **6** was silylated at the N(1) position in presence of Hünig's base, affording **7** in 84% yield (**Scheme 4**).

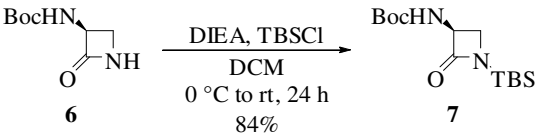


**6** **7**

**Scheme 4**. N-silylation of β-lactam **6**.

The compound **7** was then acylated at C(3)-N position with pentenoyl chloride using LiHMDS as a base at -78 °C. Only two assays were necessary, *i.e.* 30 min and 1 h between the additions of LiHMDS and 4-pentenoyl chloride, to determine that the second condition allowed the access to compound **8** in 85% yield (**Scheme 5**).

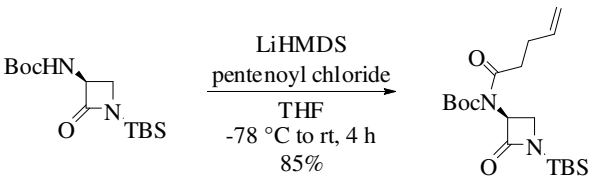


**7** **8**

**Scheme 5**. Acylation of compound **7**.

The removal of the TBS protecting group was performed with a fluorinated reagent. Three compounds were tested, *i.e.* KF,[7] $CsF$[6] and $NH_4F$,[8] the best result being obtained with $NH_4F$, which afforded **9** in 88% yield (**Scheme 6**).

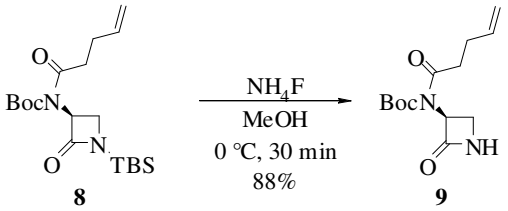


**8** **9**

**Scheme 6**. Deprotection of compound **8**.

Then several attempts were performed to alkylate the N(1) position in the presence of a strong base: LiHMDS in THF, NaH in DMF, KOH in presence of $Bu_4NHSO_4$ and NaI in THF. These conditions only led to the degradation of the starting material (**Scheme 7**).

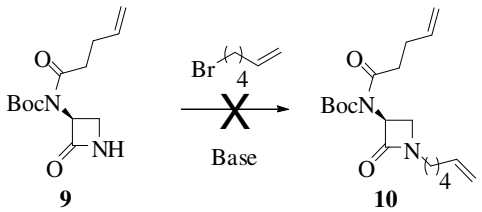


**9** **10**

**Scheme 7**. Attempts to alkylate compound **10**.

The problem could be the same as previously described for the failure of the alkylation of the mono-acylated compounds **1** and **3**.

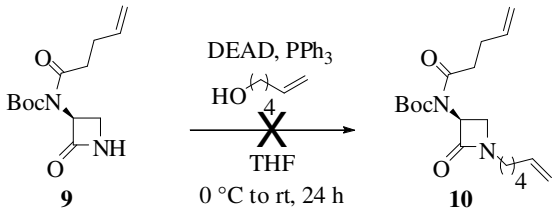


**Scheme 8**. Attempt to alkylate compound **10**.

Mitsunobu reaction was also tried but also without success, the starting material being predominantly recovered (**Scheme 8**).

Then, we tried to alkylate the compound **7** at the C(3)-N position (**Scheme 9**).

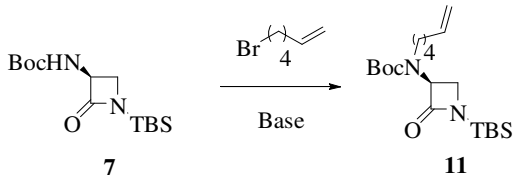


**Scheme 9**. Alkylation of compound **7**.

The different attempts are reported in **Table 1**: the results are mainly the recovery of starting material or deprotected and *bis*-alkylated compound.

**Table 1**

Alkylation of compound **7** to compound **11**.

| Base (1 eq) (Solvent) | T (°C) | Time with base | Results |
|---|---|---|---|
| LiHMDS (THF) | -78 | 30 min | Starting material |
| LiHMDS (THF) | -20 | 30 min | Starting material |
| KHMDS (THF) | -78 | 50 min | Degradation, Deprotection, Deprotection and *bis*-alkylation |
| NaH (DMF) | 0 | 30 min | Degradation, Deprotection and *bis*-alkylation |
| LiHMDS (DMF) | 0 | 5 min | Starting material, Degradation, Deprotection |
| LiHMDS (DMF) | 0 | 15 min | Starting material, Deprotection and *bis*-alkylation, **11** (17%) |

More trials would be necessary to enhance the formation of the desired compound **11**, by finding the adequate base and temperature to allow the desired reaction but not the deprotection of TBDMS and subsequent *bis*-alkylation.

## 4. N(1) position silylated

Since the compound **8** (**Scheme 5**), which is acylated at C(3)-N position and protected with a silyl compound at N(1) position, was easily obtained, we expected to synthesize another type of mixed compound with an acyl chain and a silyl chain to obtain precursors **E** and **F** (**Figure 3**).

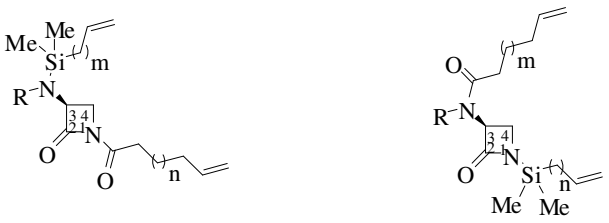


**E** R = COR', H **F**

**Figure 3**. Precursors **E** and **F**.

From the starting materials **1** and **3**, we tried to silylate the C(3)-N position with the commercially available 5-hexenyldimethylchlorosilane using LiHMDS and TEA respectively, but recovered only degradation products (**Scheme 10**).

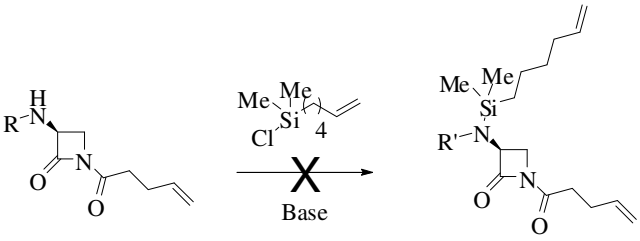


**1** R = Boc
**3** R = H.TFA

**12**
R' = Boc, H

**Scheme 10**. Attempts to synthesize compound **12**.

Treatment of chiron **6** with TEA or DIEA and commercially available allylchlorodimethylsilane and 5-hexenyldimethylchlorosilane afforded the corresponding compound **13a** in 35% and **13b** in 40% yield respectively (**Scheme 11**). The problem encountered is the low stability of compounds **13**. The purification by column chromatography partially degraded the silylated compounds.

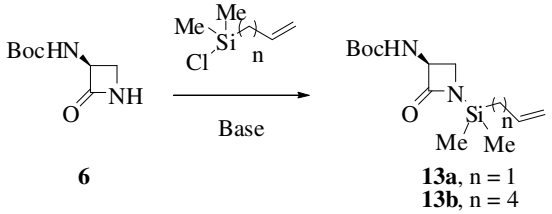


**6** **13a**, n = 1 **13b**, n = 4

**Scheme 11**. Synthesis of compounds **13**.

In order to enhance the stability of the silylated compounds at N(1) position, the geminal methyl groups on silicium could be changed by more bulky groups.

## 5. N(1) position alkylated

When the *bis*-alkyl compounds were synthesized, we were also looking for mono-alkyl compounds. By treatment of chiron **6** with bromo octene in the presence of KOH, $Bu_4NHSO_4$ and NaI, compound **14** was obtained in 25% yield. With the same conditions as for the *bis*-alkylation but with one equivalent of NaH, compound **14** was obtained in 28% yield together with the *bis*-alkyl compound (**Scheme 12**).

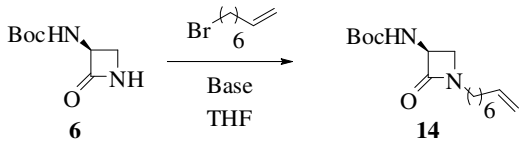


**6** **14**

**Scheme 12**. Alkylation of β-lactam **6**.

Other bases, like potassium *tert*-butanolate[9] for example, have to be tested to enhance the obtention of mono-alkyl compound.

## 6. Conclusion

The attempts to N-alkylate compounds which have been previously N-acylated, only led to degradation of the starting material. The problem could be due to the strong bases, which enable different side-reactions. The problem could result also from low reactivity of the alkenyl bromides.

To avoid the potential problem of low reactivity of the alkenyl bromide, a reductive amination could be tried with the commercially available 4-pentenal to afford the compound **15** from the deprotected mono-acylated compound **3**, for instance with Borch conditions[10] (**Scheme 13**).

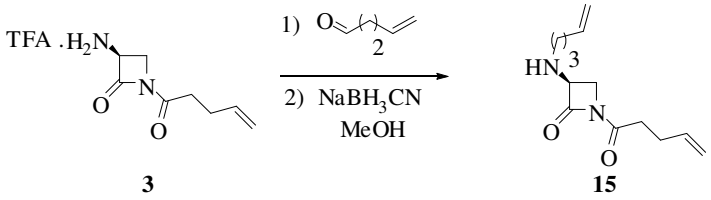


**Scheme 13**. Reductive amination with 4-pentenal.

For the mono-alkylation of chiron **6**, other conditions and bases have to be tested in order to increase the rate of the mono-alkylation instead of di-alkylation.

## 7. Experimental Section

Experiments were performed under argon atmosphere in flame-dried glassware. All solvents, including anhydrous solvents, and reagents were purchased from Acros Organics, Alfa Aesar, Fluka, Sigma-Aldrich or VWR, and used without any further purification. TLC analyses were performed on

aluminium plates coated with silica gel $60F_{254}$ (Merck) and visualized with a $KMnO_4$ solution and UV (254 nm) detection and column chromatography was performed on silica gel (40-63 or 63-200 μm) purchased from Rocc. Melting points (mp) were determined on a Büchi B-540 apparatus calibrated with caffeine, vanillin, and phenacetin. $[\alpha]_D$ were measured on a Perkin-Elmer 241 MC or 343 polarimeter, at 20 °C, in $CHCl_3$. Concentrations are given in g/100 mL. Nuclear magnetic resonance ($^1H$ and $^{13}C$) spectra were recorded at 300 MHz for proton and 75 MHz for carbon (Bruker Avance 300) or 500 MHz for proton and 125 MHz for carbon (Bruker Avance 500) using deuterated chloroform ($CDCl_3$). Chemical shifts are reported in ppm relative to residual $CHCl_3$ in $CDCl_3$ (7.26 and 77.16 ppm). NMR coupling constants (*J*) are reported in Hertz. Infrared (IR) spectra were recorded using a FTIR-8400S Shimadzu apparatus. Products were analyzed as thin films deposited on a Se-Zn crystal by evaporation from $CH_2Cl_2$ solutions. Low resolution mass spectra were obtained using a ThermoFinnigan LCQ Quantum spectrometer or using a FinniganMat TSQ7000. High Resolution Mass Spectrometry (HRMS) analyses were performed at the University College London (UK).

*(S)-tert-butyl 1-(tert-butyldimethylsilyl)-2-oxoazetidin-3-ylcarbamate* (**7**).

A modified procedure from literature was used.[6,8]

To a stirred solution of chiron **6** (400 mg, 2.15 mmol) in dry $CH_2Cl_2$ (12 mL) at 0 °C were added *tert*-butyldimethylsilylchloride (372 mg, 2.47 mmol) and N-N'-diisopropylethylamine (0.56 mL, 3.22 mmol). The mixture was then warmed to rt and stirred additionally for 20 h. The mixture was then diluted with $CH_2Cl_2$ (20 mL), and sequentially washed with water (30 mL) and brine (30 mL). After drying over $MgSO_4$ and removing the solvent under reduced pressure, the residue was purified by flash column chromatography

(hexane/EtOAc 4/1), to provide **7** as a gummy solid (542 mg, 84%). $R_f$=0.33 (hexane/EtOAc 7/3); $[\alpha]_D^{20}$ +19.6 (*c* 1.6, $CHCl_3$); $^1$H NMR (300 MHz, $CDCl_3$): δ=5.32-5.12 (br s, 1H, N*H*-Boc), 4.97-4.80 (br s, 1H, C*H* β-lactam), 3.54-3.46 (m, 1H, C$H_2$ β-lactam), 3.16-3.10 (m, 1H, C$H_2$ β-lactam), 1.43 (s, 9H, 3C$H_3$ Boc), 0.95 (s, 9H, 3C$H_3$ TBS), 0.22 ppm (s, 6H, Si-(C$H_3$)$_2$); $^{13}$C (75 MHz, $CDCl_3$): δ=172.3 (*C*=O β-lactam), 154.9 (*C*=O Boc), 80.3 (*C*quat Boc), 59.0 (*C*H β-lactam), 47.6 (*C*$H_2$ β-lactam), 28.4 (3*C*$H_3$ Boc), 26.1 (3*C*$H_3$ TBS), 18.6 (*C*quat TBS), -6.0 (Si-(*C*$H_3$)$_2$) ppm; IR: ν= 2999-2924, 1747, 1724, 1712, 1691, 1517 cm$^{-1}$; MS (ESI) *m/z*: 623 $[2M + Na]^+$, 323 $[M + Na]^+$, 245 $[M + H - C_4H_8]^+$.

*(S)-tert-butyl 1-(tert-butyldimethylsilyl)-2-oxoazetidin-3-yl(pent-4-enoyl) carbamate* (**8**).

A stirred solution of β-lactam **7** (100 mg, 0.33 mmol) in anhydrous THF (3 mL) was cooled to -78 °C. LiHMDS 1N in hexane (0.33 mL, 0.33 mmol) was slowly added and the mixture was stirred for 1 h. 4-Pentenoyl chloride (40 μL, 0.37 mmol) was then added by syringe and the mixture was stirred for another 30 minutes. The mixture was then warmed to rt over 3 h and then quenched with saturated $NH_4Cl$ (8 mL). The resulting mixture was extracted with EtOAc (2 x 10 mL) and the organic layers were washed with a saturated aqueous $NaHCO_3$ (20 mL) and brine (20 mL). After drying over $MgSO_4$ and removing the solvent under reduced pressure, the residue was purified by flash column chromatography (hexane/EtOAc 9/1), to provide **8** as a pale-yellow oil (108 mg, 85%). $R_f$=0.25 (hexane/EtOAc 9/1); $^1$H NMR (300 MHz, $CDCl_3$): δ=5.90-5.74 (m, 1H, C*H*=$CH_2$), 5.65-5.58 (m, 1H, C*H* β-lactam), 5.10-4.93 (m, 2H, CH=C$H_2$), 3.45-3.34 (m, 2H, C$H_2$ β-lactam), 2.97-2.87 (m, 2H, C$H_2$-C=O acyl chain), 2.43-2.32 (m, 2H, C$H_2$-CH=$CH_2$), 1.51 (s, 9H, 3C$H_3$ Boc), 0.95 (s, 9H, 3C$H_3$ TBS), 0.26 (s, 3H, Si-C$H_3$), 0.21

ppm (s, 3H, Si-C*H*$_3$); $^{13}$C (75 MHz, $CDCl_3$): δ=174.9 (*C*=O acyl chain), 172.1 (*C*=O β-lactam), 152.0 (*C*=O Boc), 137.2 (*C*H=$CH_2$), 115.5 (CH=*C*$H_2$), 84.7 (*C*quat Boc), 59.5 (*C*H β-lactam), 44.5 (*C*$H_2$ β-lactam), 37.8 (*C*$H_2$-C=O acyl chain), 29.2 (*C*$H_2$-CH=$CH_2$), 28.1 (3*C*$H_3$ Boc), 26.1 (3*C*$H_3$ TBS), 18.9 (*C*quat TBS), -5.9 (Si-*C*$H_3$), -6.1 (Si-*C*$H_3$) ppm; IR: ν=2978-2860, 1755, 1738, 1697, 1641, 1464 cm$^{-1}$; MS (ESI) *m*/*z*: 787 [2M + Na]$^+$, 405 [M + Na]$^+$, 383 [M + H]$^+$, 327 [M + H - $C_4H_8$]$^+$, 283 [M + H - $CO_2$ - $C_4H_8$]$^+$.

*(S)-tert-butyl 2-oxoazetidin-3-yl(pent-4-enoyl)carbamate* (**9**).

A modified procedure from literature was used.[8]

To a stirred solution of β-lactam **8** (108 mg, 0.28 mmol) in methanol (4 mL) at 0 °C was added ammonium fluoride (14 mg, 0.34 mmol) and the mixture was stirred for 30 min. After removing the solvent under reduced pressure, the residue was purified by column chromatography (hexane/EtOAc 3/2), to provide **9** as a colorless oil (66 mg, 88%). $R_f$=0.33 (hexane/EtOAc 1/1); $[\alpha]_D^{20}$ -22.4 (*c* 1.1, $CHCl_3$); $^1$H NMR (300 MHz, $CDCl_3$): δ=6.06-5.97 (br s, 1H, N*H* β-lactam), 5.90-5.75 (m, 1H, C*H*=$CH_2$), 5.73-5.67 (dd, *J*=3.1, 5.7 Hz, 2H, C*H* β-lactam), 5.09-4.93 (m, 2H, CH=C*H*$_2$), 3.56-3.49 (m, 1H, C*H*$_2$ β-lactam), 3.46-3.41 (dd, *J*=3.2, 4.8 Hz, 1H, C*H*$_2$ β-lactam), 3.00-2.90 (m, 2H, C*H*$_2$-C=O acyl chain), 2.42-2.32 (m, 2H, C*H*$_2$-CH=$CH_2$), 1.53 ppm (s, 9H, 3C*H*$_3$ Boc); $^{13}$C (75 MHz, $CDCl_3$): δ=175.1 (*C*=O acyl chain), 168.3 (*C*=O β-lactam), 151.8 (*C*=O Boc), 137.1 (*C*H=$CH_2$), 115.5 (CH=*C*$H_2$), 85.2 (*C*quat Boc), 59.4 (*C*H β-lactam), 42.6 (*C*$H_2$ β-lactam), 37.7 (*C*$H_2$-C=O acyl chain), 29.0 (*C*$H_2$-CH=$CH_2$), 27.9 (3*C*$H_3$ Boc) ppm; IR: ν=3305, 2991-2906, 1763, 1738, 1693 cm$^{-1}$; MS (ESI) *m*/*z*: 559 [2M + Na]$^+$, 291 [M + Na]$^+$, 169

$[M + H - CO_2 - C_4H_8]^+$; HRMS (ESI): calcd. for $C_{13}H_{20}N_2O_4Na$ $[M + Na]^+$ 291.1321, found 291.1320.

*(S)-tert-butyl 1-(tert-butyldimethylsilyl)-2-oxoazetidin-3-yl(hex-5-enyl) carbamate* (**11**).

A stirred solution of β-lactam **7** (81 mg, 0.27 mmol) in anhydrous DMF (2 mL) was cooled to 0 °C. LiHMDS 1N in hexane (0.27 mL, 0.27 mmol) was added and the mixture was stirred for 15 min. 6-bromohex-1-ene (72 μL, 0.54 mmol) was then added by syringe and the mixture was then slowly warmed to r.t. and stirred overnight. The mixture was quenched with saturated $NH_4Cl$ (5 mL) and then the medium diluted with water (10 mL). The resulting mixture was extracted with EtOAc (3 x 10 mL) and the organic layers were washed with brine (30 mL). After drying over $MgSO_4$ and removing the solvent under reduced pressure, the residue was purified by flash column chromatography (hexane/EtOAc 9/1), to provide **11** as a pale-yellow oil (18 mg, 17%). $R_f$=0.53 (hexane/EtOAc 4/1); $[\alpha]_D^{20}$ +15.2 (*c* 1.4, $CHCl_3$); $^1$H NMR (300 MHz, $CDCl_3$): δ=5.85-5.70 (m, 1H, C*H*=$CH_2$), 5.16-4.89 (m, 2H + 0.5H, rotamer, CH=C$H_2$ and C*H* β-lactam), 4.72 (br s, 0.5H, rotamer, C*H* β-lactam), 3.47-3.37 (m, 1H, C$H_2$ β-lactam), 3.35-3.12 (m, 3H, C$H_2$ β-lactam and Boc-N-C$H_2$), 2.10-2.00 (m, 2H, C$H_2$-CH=$CH_2$), 1.70-1.31 (m, 13H, 3C$H_3$ Boc and 2C$H_2$ alkyl chain), 0.95 (s, 9H, 3C$H_3$ TBS), 0.23 ppm (br s, 6H, Si-(C$H_3$)$_2$); $^{13}$C (125 MHz, $CDCl_3$): δ=172.5 (*C*=O β-lactam), 154.8 (*C*=O Boc), 138.7 (*C*H=$CH_2$), 114.7 (CH=*C*$H_2$), 80.9-80.4 (rotamers) (*C*quat Boc), 64.8 (*C*H β-lactam), 47.3-46.4-46.0-45.4 (2C rotamers) (*C*$H_2$ β-lactam and Boc-N-*C*$H_2$), 33.5 (*C*$H_2$-CH=$CH_2$), 28.5 (3*C*$H_3$ Boc), 26.2 (2C) (2*C*$H_2$ alkyl chain), 26.1 (3*C*$H_3$ TBS), 18.7 (*C*quat TBS), -6.0 (Si-(*C*$H_3$)$_2$) ppm; IR: ν=3012-2852, 1751, 1734, 1709, 1699, 1456 cm$^{-1}$; MS

(APCI) *m/z*: 383 $[M + H]^+$, 327 $[M + H - C_4H_8]^+$, 283 $[M + H - CO_2 - C_4H_8]^+$.

*(S)-tert-butyl 1-(allyldimethylsilyl)-2-oxoazetidin-3-ylcarbamate* (**13a**).

A modified procedure from literature was used.[6,8]

To a stirred solution of chiron **6** (100 mg, 0.54 mmol) in dry $CH_2Cl_2$ (3 mL) at 0 °C were added allylchlorodimethylsilane (97 μL, 0.64 mmol) and triethylamine (89 μL, 0.64 mmol). The mixture was then warmed to rt and stirred additionally for 20 h. The mixture was then diluted with $CH_2Cl_2$ (10 mL), and washed with water (10 mL). After drying over $MgSO_4$ and removing the solvent under reduced pressure, the residue was purified by flash column chromatography (hexane/EtOAc 4/1), to provide **13a** as a colourless solid (53 mg, 35%). $R_f$=0.48 (hexane/EtOAc 4/1); mp 173.3-173.8 °C; $[\alpha]_D^{20}$ +14.0 (*c* 1.1, $CHCl_3$); $^1$H NMR (300 MHz, $CDCl_3$): δ=5.82-5.66 (m, 1H, C*H*=$CH_2$), 5.28 (br s, 1H, Boc-N*H*), 4.97-4.81 (br s, 3H, CH=C$H_2$ and C*H* β-lactam), 3.50-3.42 (m, 1H, C$H_2$ β-lactam), 3.15-3.07 (m, 1H, C$H_2$ β-lactam), 1.77-1.71 (d, *J*=8.1 Hz, 2H, C$H_2$-CH=$CH_2$), 1.41 (s, 9H, 3C$H_3$ Boc), 0.25 ppm (s, 6H, Si-(C$H_3$)$_2$); $^{13}$C (75 MHz, $CDCl_3$): δ=172.3 (*C*=O β-lactam), 154.9 (*C*=O Boc), 132.7 (*C*H=$CH_2$), 115.0 (CH=*C*$H_2$), 80.3 (*C*quat Boc), 59.1 (*C*H β-lactam), 46.5 (*C*$H_2$ β-lactam), 28.4 (3*C*$H_3$ Boc), 22.9 (*C*$H_2$-CH=$CH_2$), -3.4 (Si-(*C*$H_3$)$_2$) ppm; IR: ν=3348, 3035-2914, 1749, 1728, 1714, 1697, 1533 cm$^{-1}$;MS (APCI) *m/z*: 285 $[M + H]^+$, 229 $[M + H - C_4H_8]^+$.

*(S)-tert-butyl 1-(hex-5-enyldimethylsilyl)-2-oxoazetidin-3-ylcarbamate* (**13b**).

Prepared by the same procedure as described for **13a**. Yield: 40%; $R_f$=0.64 (hexane/EtOAc 3/2); $[\alpha]_D^{20}$ +11.2 (*c* 1.1, $CHCl_3$); $^1$H NMR (300 MHz, $CDCl_3$): δ=5.82-5.73 (m, 1H, C*H*=$CH_2$), 5.23-5.17 (m, 1H, Boc-N*H*), 5.00-

4.90 (m, 2H, CH=C$H_2$), 4.86 (br s, 1H, C$H$ β-lactam), 3.48-3.42 (m, 1H, C$H_2$ β-lactam), 3.11-3.06 (m, 1H, C$H_2$ β-lactam), 2.07-2.01 (m, 2H, C$H_2$-CH=$CH_2$), 1.48-1.30 (m, 13H, 3C$H_3$ Boc and 2C$H_2$ alkyl chain), 0.75-0.70 (m, 2H, Si-C$H_2$), 0.23 ppm (s, 6H, Si-(C$H_3$)$_2$); $^{13}$C (75 MHz, $CDCl_3$): δ=172.2 (*C*=O β-lactam), 154.9 (*C*=O Boc), 138.9 (*C*H=$CH_2$), 114.5 (CH=*C*$H_2$), 80.3 (*C*quat Boc), 59.0 (*C*H β-lactam), 46.4 (*C*$H_2$ β-lactam), 33.4 (*C*$H_2$-CH=$CH_2$), 32.4 (*C*$H_2$-$CH_2$-CH=$CH_2$), 28.4 (3*C*$H_3$ Boc), 22.5 (Si-$CH_2$-*C*$H_2$), 15.0 (Si-*C*$H_2$), -3.0 (Si-(*C*$H_3$)$_2$) ppm; IR: ν=2986-2916, 1747, 1733, 1695, 1539, 1413 cm$^{-1}$;MS (ESI) *m*/*z*: 349 [M + Na]$^+$, 271 [M + H - $C_4H_8$]$^+$.

*(S)-tert-butyl 1-(oct-7-enyl)-2-oxoazetidin-3-ylcarbamate* (**14**).

NaH (60% dispersion in oil, 21 mg, 0.54 mmol) was added to a stirred solution of **6** (100 mg, 0.54 mmol) in dry DMF (7 mL) at 0 °C. Alkyl bromide (90 μL, 0.59 mmol) was added after 30 min and the mixture was then slowly warmed to r.t. and stirred overnight. The mixture was quenched with water (10 mL) at 0 °C and then the medium diluted with brine (10 mL). The resulting mixture was extracted with EtOAc (3 x 20 mL) and the organic layers were washed with brine (60 mL). After drying over $MgSO_4$ and removing the solvent under reduced pressure, the residue was purified by flash column chromatography (hexane/EtOAc 3/2) to provide **14** as a white solid (44 mg, 28%). $R_f$=0.38 (hexane/EtOAc 1/1); mp 79.9-80.8 °C; $[\alpha]_D^{20}$ +18.2 (*c* 1.1, $CHCl_3$); $^1$H NMR (300 MHz, $CDCl_3$): δ=5.85-5.70 (m, 1H, C*H*=$CH_2$), 5.28-5.19 (br d, *J*=6.7 Hz, 1H, Boc-N*H*), 5.01-4.88 (m, 2H, CH=C$H_2$), 4.76 (br s, 1H, C*H* β-lactam), 3.55-3.48 (m, 1H, C$H_2$ β-lactam), 3.24-3.14 (m, 3H, C$H_2$ β-lactam and C$H_2$-N-C=O alkyl chain), 2.07-1.97 (m, 2H, C$H_2$-CH=$CH_2$), 1.57-1.20 ppm (m, 17H, 3C$H_3$ Boc and 4C$H_2$ alkyl chain); $^{13}$C (75 MHz, $CDCl_3$): δ=166.8 (*C*=O β-lactam), 155.0 (*C*=O Boc),

138.9 (*C*H=$CH_2$), 114.5 (CH=*C*$H_2$), 80.4 (*C*quat Boc), 57.1 (*C*H β-lactam), 49.1 (*C*$H_2$ β-lactam), 41.9 (*C*$H_2$-N-C=O alkyl chain), 33.7 (C*H*$_2$-CH=$CH_2$), 28.8 (*C*$H_2$ alkyl chain), 28.7 (*C*$H_2$ alkyl chain), 28.4 (3*C*$H_3$ Boc), 27.5 (*C*$H_2$ alkyl chain), 26.9 (*C*$H_2$ alkyl chain) ppm; IR: ν=3344-3315, 2951-2848, 1755, 1707, 1693, 1641, 1523, 1456 $cm^{-1}$; MS (ESI) *m/z*: 319 $[M + Na]^+$, 263 $[M + Na - C_4H_8]^+$, 241 $[M + H - C_4H_8]^+$.

## 8. References and notes


[1] Desroy, N.; Robert-Peillard, F.; Toueg, J.; Duboc, R.; Hénaut, C.; Rager, M.-N.; Savignac, M.; Genêt, J.-P. *Eur. J. Org. Chem.* **2004**, 4840-4849.

[2] Takahata, H.; Banba, Y.; Ouchi, H.; Nemoto, H.; Kato, A.; Adachi, I. *J. Org. Chem.* **2003**, *68*, 3603-3607.

[3] Cho, J. H.; Kim, B. M. *Tetrahedron Lett.* **2002**, *43*, 1273-1276.

[4] Salvatore, R. N.; Nagle, A. S.; Schmidt, S. E.; Jung, K. W. *Org. Lett.* **1999**, *1*, 1893-1896.

[5] Couty, F.; Prim, D. *Tetrahedron: Asymmetry* **2002**, *13*, 2619-2624.

[6] Baldwin, J. E.; Adlington, R. M.; Gollins, D. W.; Schofield, C. J. *Tetrahedron* **1990**, *46*, 4733-4748.

[7] Kozawa, Y.; Mori, M. *J. Org. Chem.* **2003**, *68*, 3064-3067.

[8] Padova, A.; Roberts, S. M.; Donati, D.; Marchioro, C.; Perboni, A. *Tetrahedron* **1996**, *52*, 263-270.

[9] Kaura, A. C.; Maycock, C. D.; Stoodley, R. J.; Beagley, B.; Pritchard, R. G. *J. Chem. Soc. Perkin Trans 1* **1988**, 2259-2269.

[10] Borch, R. F.; Bernstein, M. D.; Durst, H. D. *J. Am. Chem. Soc.* **1971**, *93*, 2897-2904.

# *Chapter 9 - Conclusions and perspectives*

## 1. Conclusions

The chosen synthetic strategy, *i.e.* the ring-closing metathesis reaction as the key-step for the preparation of 1,3-bridged bicyclic β-lactams on the positions N(1) and C(3)-N, was successful for the synthesis of 1,3-bridged macrocycles **A** deriving from *bis*-ω-alkenyl-3(S)-amino-azetidinone precursors **B**. 12- to 22-Membered 1,3-bridged β-lactams bearing the Boc side-chain and 12- to 16-membered bicyclic β-lactams bearing the V side-chain were synthesized from the corresponding derivatives of L-serine **D** (**Scheme 1**).

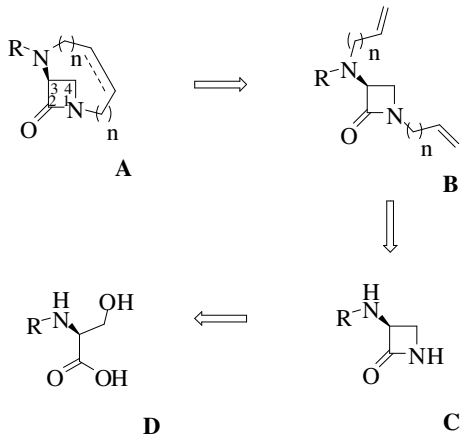


R = Boc ; n = 3, 4, 5, 6, 8
R = $PhOCH_2CO$ ; n = 3, 4, 5

**Scheme 1**. General retrosynthetic strategy.

The same synthetic strategy employed to synthesize bicyclic β-lactams from *bis*-ω-alkenoyl-3(S)-amino-azetidinone precursors **E** was mainly unsuccessful, although it allowed the discovery of interesting unexpected compounds.

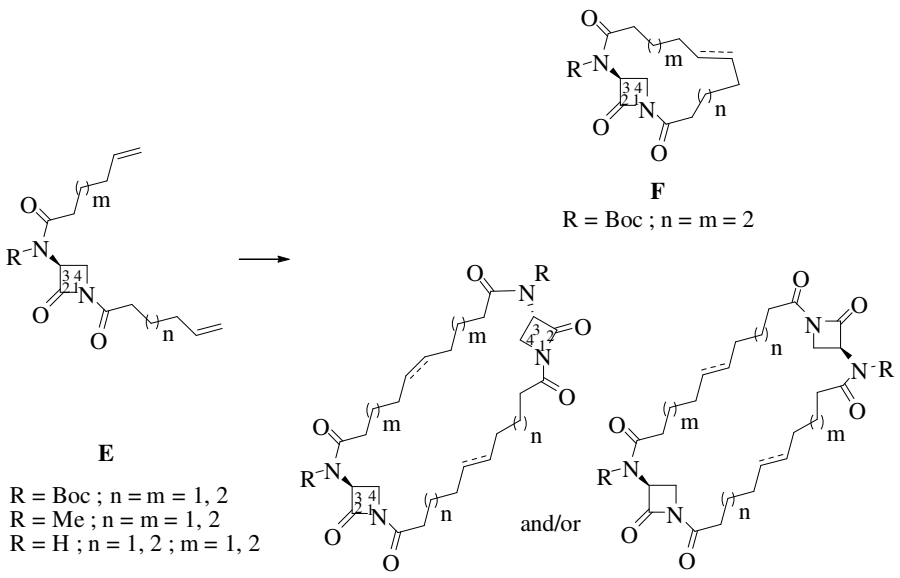


**Scheme 2**. Synthesis of macrocycles **G** and **F** from precursors **E**.

In fact by applying ring closing metathesis reaction on precursors **E**, the desired cyclomonomer **F** was obtained in a single case as a minor product (R = Boc and n = 2), while cyclodimers **G** were the preferred outcome (**Scheme 2**). Several parameters, such as the choice of the catalyst, the solvent, the temperature, the concentration, the use of Lewis acid $Ti(OiPr)_4$ and the reaction time were investigated but without success.

For these two families, *i.e. bis*-alkyl **B** and *bis*-acyl **E** precursors, we could notice that the efficiency of the RCM reaction depends mainly on intrinsic structural parameters and not on experimental conditions. The almost exclusive formation of macrocyclic dimers instead of cyclic

monomers deriving of *bis*-acyl precursors **E** was studied by *ab initio* calculations performed by Dr. G. Dive. The experimental results were in good agreement with the computed heats of formation of cyclomonomers and cyclodimers. In fact, due to the presence of amide and imide functions in the precursors **E**, the conformers leading to the desired cyclizations are strongly disfavoured.

Even if the synthetic strategy employed was only partially successful, RCM reaction allowed to synthesize rapidly 1,3-bridged bicyclic β-lactams on the positions N(1) and C(3)-N from 12- to 22-membered ring. 28- and 32-Membered cyclodimers were also obtained, and even if they were "unwanted" products, these compounds revealed to be very promising, regarding their inhibition potential against PBPs.

All products were evaluated for their potential inhibition effect on bacterial serine enzymes. Firstly, they were tested against R39 D,D-peptidase,[1] which is a commonly used model for bacterial serine-enzymes. All the compounds were also evaluated against two high-molecular-weight D,D-peptidases responsible for bacterial resistance to β-lactam antibiotics: PBP2a from methicillin-resistant *Staphylococcus aureus*[2] (MRSA) and PBP5 from *Enterococcus faecium.*[3]

Concerning the *bis*-alkyl derivatives, none of the V side-chain molecules has a significant activity on R39, PBP2a or PBP5. The lowest residual activities (corresponding to the highest inhibition activities) on R39 occurred for Boc molecules with the saturated and unsaturated 16-membered cycles (**A**, R = Boc, n = 5, **Scheme 1**), and their open precursor (**B**, R = Boc, n = 5, **Scheme 1**). The reactivity of the bridged molecules, using a simple

model of PBP cavity to mimic the nucleophilic β-lactam ring-opening (**Figure 1**), was theoretically evaluated and the lowest energy barriers were calculated for the 16-membered ring bicycles **A** (n = 5, **Scheme 1**) of both series (Boc and V side-chains).

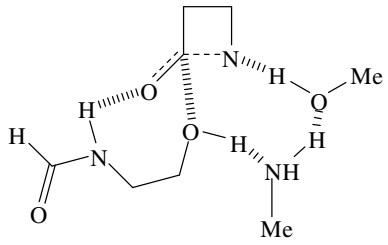


**Figure 1**. Model of concerted nucleophilic attack on the β-lactam ring.

To understand the experimental difference of activity between Boc and V derivatives of 16-membered 1,3-bridged bicyclic β-lactams, different models of the R39 active site including one to three conserved motifs of this DD-peptidase family have been built. The reactivity of the 1,3-bridged β-lactams in serine enzyme active site highly depends on the ligand conformation explaining why the compounds bearing a V side-chain do not fit with the geometry of the catalytic cavity.

Concerning the *bis*-acyl derivatives, all cyclic dimers **G** with R = H (**Scheme 2**) were good inhibitors of R39, even better inhibitors than their respective precursors (**E**, R = H, **Scheme 2**). As shown in the model of the R39 active site including the three conserved motifs, one β-lactam fits into the catalytic cavity since the long acyl chains of the macrocycle and the second β-lactam expand outside of the active site. Some of these compounds exhibit also a modest to high activity against PBP2a. In these cyclic dimers (R = H), depending of the size of the macrocycle, because of the presence of

intramolecular H bonds inducing geometrical constraints, some dimers look like screws. Additionally to their conformational flexibility, this particular feature could explain why some compounds are able to slip into the closed conformation of PBP2a active site, and hence display an inhibition capacity.

The model of reactivity proposed, based on 1,3-bridged, planar β-lactam motifs embedded into macrocycles with increased conformational adaptability is validated since some macrocycles **A** and cyclodimers **G** exhibit really promising activities against PBPs. All these compounds are devoid of the carboxylic function, usually present in β-lactam antibiotics. Our study clearly shows that slight changes in the conformation of the potential inhibitors could lead to very different activities in the active site of the PBPs since they could more or less accommodate to the amino acids of the active site.

## 2. Perspectives

### 2.1. Cyclodimers

With the strategy employed, the isolated cyclodimers are most probably a mixture of head-head (HH) and head-tail (HT) isomers. Since some of these compounds exhibit a good activity against PBP2a, it would be interesting to pursue the study on these compounds, as example by determining which isomer is the most active one. The head-head and head-tail isomers could be synthesized selectively. The head-head cyclodimer **K** (**Scheme 3**), could be obtained from mono-acylated compounds **H** previously synthesized. Cross-metathesis of products **H** would give the non-cyclic dimer **I**. Then, the Boc protecting group would be removed with

trifluoroacetic acid and the free amine function acylated with the alkenoyl chlorides affording compounds **J**. Cross-metathesis of products **J** would give the head-head cyclic dimer **K**.

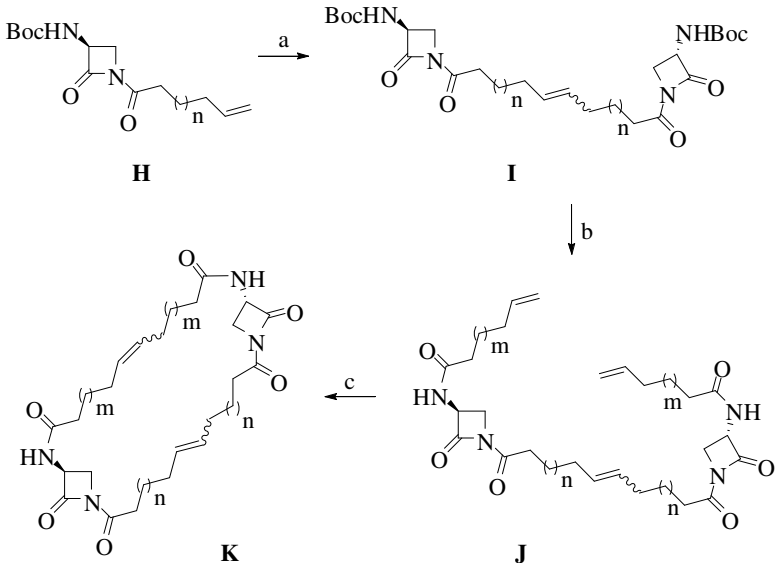


**Scheme 3**. Synthesis of dimers **K**. Reagents and conditions: (a) Grubbs II catalyst (5 mol%), DCM, 40 °C; (b) TFA, $CH_2Cl_2$, 0 °C to rt; (c) alkenoyl chloride, TEA, $CH_2Cl_2$, 0 °C to rt; (c) Grubbs II catalyst (5 mol%), DCM, 40 °C.

An inherent problem of the cyclic dimers is their low solubility in a biological (aqueous) environment. In order to enhance their solubility, diols could be inserted at the carbon-carbon double-bond position, or oxygen could be inserted in the acyl chain.

To pursue the study on this family of compounds, representative inhibitors **G** (**Scheme 2**) with high activity against R39 (*i.e.* compounds with R = H) are currently tested in order to obtain crystal structures of acyl-enzyme complexes. These crystal structures would allow to observe the

interactions occurring between our compounds and the active site of R39, and also would confirm if the predicted conformation of cyclodimers, *i.e.* the carbonyl of the amide on position C(3)-N rising below the 4-membered ring and the chain of the macrocycle expanding to the right upper corner C(4) of the processed β-lactam to allow the interaction with the NH of Asn300 amino acid residue, is concordant with experimental observations.

To estimate the potential acylating power of the synthesized compounds, an elaborate model of R39 active site representing the three conserved motifs of the PBPs family has been built by computational chemistry. PBP2a shares with R39 the three conserved motifs so this model of reactivity could also be applied, but differences are to be found at the entry, since PBP2a present a "closed" conformation, and at the bottom of the respective cavities. In order to explore the geometrical constraints of the PBP2a active site, a dedicated model will be build in the future.

### 2.2. Change of the side chain

The reactivity of the 1,3-bridged β-lactams **A** (**Scheme 1**) in serine enzyme active site highly depends on the side-chain (R) conformation. A direct perspective could be the synthesis of bicycles of type **A** but without side-chain (**Scheme 4**) to avoid this problem of ligand conformation. The removing of the Boc protecting group on compounds **A** and **B** (**Scheme 1**) led to the degradation of the β-lactam ring. Therefore another chiron, bearing another side-chain than Boc or V, which could be easily removed, must be synthesized (**Scheme 4**). The chosen protecting group should not be deprotected under the same conditions than Boc, nor by hydrogenation.

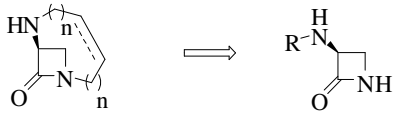


R ≠ $PhOCH_2CO$, Boc

**Scheme 4**. Retrosynthetic strategy for 1,3-bridged β-lactams **A** without side-chain.

The phthalimide group is a commonly used protecting group for the amine function of monocyclic β-lactam rings. The phthalimide-L-serine compound **3** could be synthesized from L-serine **2** using phthalic anhydride **1**.[4] Then the same synthetic strategy would be applied as previously, *i.e.* coupling reaction would afford the corresponding hydroxamate subsequently cyclized and hydrogenated to give the β-lactam **4** (**Scheme 5**).

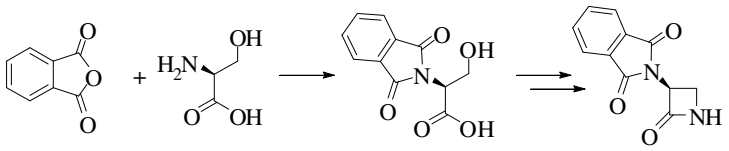


**1** **2** **3** **4**

**Scheme 5**. Synthesis of compound **4**.

After the alkylation at N(1) position, the phthalimide could be deprotected with hydrazine, affording the free amine function which, could subsequently be alkylated, affording the desired bicyclic β-lactam without side-chain after the RCM reaction.

Instead of the second alkylation, the C(3)-N position could be acylated, leading to mixed precursor, *i.e.* N(1)-alkylated and C(3)-N acylated.

### 2.3. Click cyclizations

Instead of the RCM reaction as a key-step for the cyclization, we could use as an example the 1,3-dipolar cycloaddition between an azide and an alkyne to form a triazole. The highly regioselective variant developed by Meldal[5] and Sharpless[6] groups to generate the 1,4-disubstitution catalyzed by copper (I) is often associated with the term click chemistry. This reaction occurs under mild conditions and is compatible with the β-lactam ring since it has been successfully used in presence of azetidinones.[7] 1,2,3-Triazole are not incompatible with biological activities, since this moiety is present in β-lactam antibiotics such as Tazobactam[8] and Cefatrizine[9] (**Figure 2**).

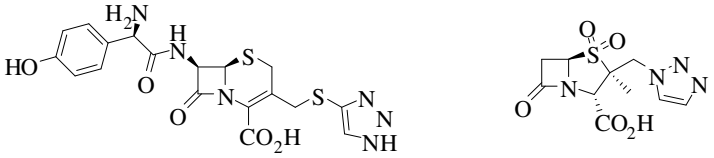

Cefatrizine Tazobactam

**Figure 2**. Structures of cefatrizine and tazobactam.

As an example, precursors **L** could lead to bridged β-lactams **M** (**Scheme 6**).

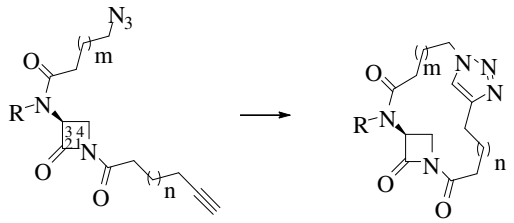

**L** **M**

**Scheme 6**. Precursors **L** and **M**.

In this proposed strategy, the chiron β-lactam could be acylated at the N(1) position with 5-hexynoyl chloride (prepared from commercially available 5-hexynoic acid, **Scheme 6**, n = 1). Then the C(3)-N position could be acylated with commercially available 4-bromobutyryl chloride (**Scheme 6**, n = 1), followed by $SN_2$ reaction with sodium azide to afford the azide.

### 2.4. Non β-lactam ring

Instead of the β-lactam moiety, which revealed sometimes to be difficult to manipulate (see the degradation of the azetidinone in multiple reactions), a 5-membered ring, such as a pyrrolidinone, pyrazolidinone or isoxazolidinone moiety may be used as the acylating function of serine enzymes (**Figure 3**).

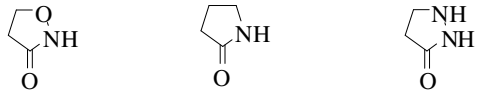

3-isoxazolidinone 2-pyrrolidinone 3-pyrazolidinone

**Figure 3**. Isoxazolidinone, pyrrolidinone and pyrazolidinone moiety.

Such 5-membered rings have been already tested as analogues of β-lactam antibiotics[10] with some success. LY186826 (**Figure 4**) is an example of fused bicyclic pyrazolidinone presenting an antibacterial activity.[11] Lactivicin (**Figure 4**) is an example of natural non-β-lactam antibiotic that inhibit PBPs.[12]

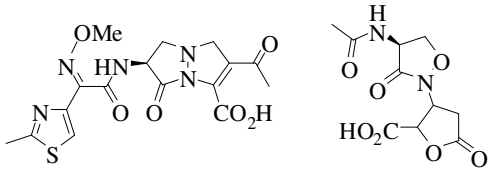


**Figure 4**. Structures of LY186826 and lactivicin.

Studies have shown that single γ-lactams ring could react reversibly with serine peptidases,[13] but Lactivicin reacts irreversibly with PBPs, most probably due to the fact that a stable acyl enzyme is the result of a subsequent opening of the lactone after the initial opening of cycloserine.[14]

Bridged bicyclic non-β-lactams (**Scheme 7**) should be of interest, with the initial strategy developed in the laboratory (planar amide and conformational adaptability), and the presence of the second cycle would prevent the reversible reaction with PBPs. The three 5-membered rings described above, with an amino substituent on the alpha position of the carbonyl, analogues of the β-lactams **C** (**Scheme 1**), could be used as new chirons, *i.e.* L-cycloserine,[15,12,10] (S)-3-amino-2-pyrrolidone[16,10] and (S)-4-amino-3-pyrazolidinone.[17,10]

The same synthetic strategy, *i.e.* RCM as key-step for the macrocyclization, from 5-membered ring chiron equipped with ω-alkenoyl and ω-alkenyl chains, could be used to the formation of the bicycle (**Scheme 7**).

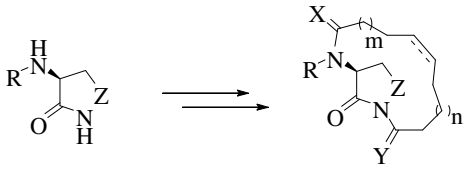


**Scheme 7**. 1,4-bridged macrocycles from 5-membered ring chirons.

## 3. References and notes

[1] (a) Sauvage, E.; Herman, R.; Petrella, S.; Duez, C.; Bouillenne, F.; Frère, J. M.; Charlier, P. *J. Biol. Chem.* **2005**, *280*, 31249-31256; (b) Sauvage, E.; Powell, A. J.; Heilemann, J.; Josephine, H. R.; Charlier, P.; Davies, C.; Pratt, R. F. *J. Mol. Biol.* **2008**, *381*, 383-393.

[2] Lim, D.; Strynadka, N. C. *Nat. Struct. Biol.* **2002**, *9*, 870-876.

[3] Sauvage, E.; Kerff, F.; Fonzé, E.; Herman, R.; Schoot, B.; Marquette, J.-P.; Taburet, Y.; Prevost, D.; Dumas, J.; Leonard, G.; Stefanic, P.; Coyette, J.; Charlier, P. *Cell. Mol. Life Sci.* **2002**, *59*, 1223-1232.

[4] Sheehan, J. C.; Goodman, M.; Hess, G. P. *J. Am. Chem. Soc.* **1956**, *78*, 1367-1369

[5] Tornoe, W. C.; Christensen C.; Meldal, M. *J. Org. Chem.* **2002**, *67*, 3057-3064.

[6] Rostovtsev, V. V.; Green, L. G.; Fokin, V. V.; Sharpless, K. B. *Angew. Chem. Int. Ed.* **2002**, *41*, 2596-2599.

[7] (a) Vatmurge, N. S.; Hazra, B. G.; Pore, V. S.; Shirazi, F.; Deshpande, M. V.; Kadreppa, S.; Chattopadhyay, S.; Gonnade, R. G.

*Org. Biomol. Chem.* **2008**, *6*, 3823-3830; (b) Vatmurge, N. S.; Hazra, B. G.; Pore, V. S.; Shirazi, F.; Chavan, P. S.; Deshpande, M. V. *Bioorg. Med. Chem. Lett.* **2008**, 18, 2043-2047; (c) Palomo, C.; Aizpurua, J. M.; Balentová, E.; Azcune, I.; Santos, J. I.; Jiménez-Barbero, J.; Cañada, J.; Miranda, J. I. *Org. Lett.* **2008**, 10, 2227-2230.

[8] Aronoff, S. C.; Jacobs, M. R.; Johenning, S.; Yamabe, S. *Antimicrob. Agents Chemother.* **1984**, *26*, 580-582.

[9] Leitner, F.; Buck, R. E.; Misiek, M.; Pursiano, T. A.; Price, K. E. *Antimicrob. Agents Chemother.* **1975**, *7*, 298-305.

[10] Baldwin, J. E.; Lynch, G. P.; Pitlik, J. *J. Antibiot.* **1991**, *44*, 1-24.

[11] Allen, N. E.; Hobbs, J. N., Jr.; Preston, D. A.; Turner, J. R.; Wu, C. Y. E. *J. Antibiot.* **1990**, *43*, 92-99.

[12] Harada, T.; Tsubotani, S.; Hida, T., Koyama, K.; Kondo, M.; Ono, H. *Tetrahedron* **1988**, *44*, 6589-6606.

[13] Westwood, N. J.; Claridge, T. D. W.; Edwards, P. N.; Schofield, C. J. *Bioorg. Med. Chem. Lett.* **1997**, *7*, 2973-2978.

[14] (a) Macheboeuf, P.; Fischer, D. S.; Brown, T., Jr.; Zervosen, A.; Luxen, A.; Joris, B.; Dessen, A.; Schofield, C. J. *Nat. Chem. Biol.* **2007**, *3*, 565-569; (b) Brown, T., Jr.; Charlier, P.; Herman, R.; Schofield, C. J.; Sauvage, E. *J. Med. Chem.* **2010**, *53*, 5890-5894.

[15] Stammer, C. H.; Wilson, A. N.; Spencer, C. F.; Bachelor, F. W.; Holly, F. W.; Folkers K. *J. Am. Chem. Soc.* **1957**, *79*, 3236-3240.

[16] Jones, C. F. R.; Crockett, A. K. *Tetrahedron Lett.* **1993**, *34*, 7459-7462.

[17] Holmes, R. E.; Neel, D. A. *Tetrahedron Lett.* **1990**, *31*, 5567-5570.

## *Appendix - Computational Chemistry*

The first quantum chemistry calculations on atoms and very small molecules started in the 1960's when computers began accessible. Meanwhile, most of the energy calculations have been made by molecular mechanics models. In such a framework, a molecule is described as a building of small entities which have been parametrized from experience. The most explicit example is a protein for which the relative energy can be computed as a sum of energy of their amino acids. The energy function is a sum of several terms as deviations of distances, valence angles and dihedral angles from their equilibrium values as the C-C bond length defined in ethane. By definition, this method could not describe transient species as transition state structures.

Quantum chemistry is based on quantum mechanics. As the electrons are very small, the Heisenberg principle shows that only the product of their mass by velocity can be known and not their values separately. During 20 years, the formalism has been developed to allow the explicit calculation of the absolute energy of a molecule at a given geometry. Most of the present methods remains lied to two approximations: the first one is the model of the independent electron in the field of all the other ones. To estimate this field, the energy has to be calculated and thus the procedure will be iterative. The second one is the basis set expansion corresponding to the domain where electrons can move. As an infinite domain cannot be computed, a set of functions derived from atomic orbitals is used to calculate their linear combinations which define the orthogonal molecular orbitals.

The analytical first derivative of the absolute energy has been available in the seventy years and the second one in the eighties. By minimizing the first derivative of the total energy, equilibrium structures can be located on the energy hypersurface which dimension is defined by the number of degrees of freedom (interatomic distances, valence and dihedral angles). These structures can be characterized as minima or first order saddle points (transition state structures) or higher ones by the curvature expressed by the first eigenvalue(s) of the diagonalized Hessian matrix (second derivatives of the energy). The associated eigenvector describes the geometry components which are involved in a transition state structure.

The density functional theory (DFT methods) attempts to limitate the effect of the independent electron model by an approach of the energy via the total electronic density. Today, with extensive basis sets and elaborate functionals, the numerical calculations are in very good accordance with experiences as well in spectroscopies as thermochemistry.

In the present work, several numerical approaches have been applied. For the geometry optimisation corresponding to the location of several conformers and transition state structures, all the calculations have been performed at the Hatree-Fock level with the minimal basis set MINI-1 of Huzinaga or using the DFT functional B3LYP with the extended basis set 6-31G(d) with additional polarization functions on heavy atoms. For the docking of several molecules into the active site of the protein as R39 DD-peptidase and PBP2a, a molecular mechanics function has been used to minimize the energy of the Michaelis complex.